Targeting strategies for glucocorticoid administration to alveolar macrophages

Ludmila Pinheiro Do Nascimento

université PARIS-SACLAY

NNT : 2019SACLS215

Thèse de doctorat

UNIVERSITÉ PARIS SUD
Comprendre le monde, construire l'avenir

Stratégies de ciblage des macrophages alvéolaires pour l'administration de glucocorticoïdes

Thèse de doctorat de l'Université Paris-Saclay
préparée à l'Université Paris-Sud

École doctorale n°569 Innovation thérapeutique : du fondamental à l'appliqué (ITFA)
Spécialité de doctorat: Pharmacotechnie et biopharmacie

Thèse présentée et soutenue à Châtenay-Malabry, le 15 Juillet 2019, par

Ludmila Pinheiro do Nascimento

Composition du Jury :

Pierre Chaminade Professeur, Université Paris-Sud (Lip(Sys) EA7357)	Président
Karim Amighi Professeur, Université Libre de Bruxelles	Rapporteur
Sandrine Marchand Professeur, Université de Poitiers	Rapporteur
Franceline Reynaud MCU, Université Fédérale du Rio de Janeiro (UFRJ)	Examinateur
Elise Lepeltier MCU, Université d'Angers	Examinateur
Elias Fattal Professeur, Université Paris-Sud (Institut Galien Paris-Sud, IGPS)	Directeur de thèse
Nicolas Tsapis Directeur de Recherches CNRS, Université Paris-Sud (IGPS)	Co-Directeur de thèse

Remerciements

Je voudrais tout d'abord adresser toute ma gratitude à mes directeurs de thèse, Elias Fattal et Nicolas Tsapis. Elias, qui a accepté de m'encadrer dès le premier contact et qui m'a accordé sa confiance, je vous remercie pour votre patience, implication et amitié, vos conseils et soutien pendant ces années. Nicolas, qui a été plusieurs fois le sauveur de mes problèmes en laboratoire, je vous remercie aussi pour toujours avoir été disponible pour m'aider et m'écouter, avec votre patience qui m'a rassurée et m'a donné la force de ne jamais abandonner une expérience quand quelque chose n'allait pas. A vous deux, ma gratitude pour tous les enseignements que je garderai toute ma vie, ainsi que le soutien émotionnel indispensable pendant ces années. Ce travail n'a été possible que grâce à votre dédicace et confiance.

J'adresse mes sincères remerciements à tous les professeurs, intervenants et toutes les personnes qui ont consacré du temps pour discuter et m'aider durant mon doctorat. Un grand merci spécialement à Sonia Abreu, Pierre Chaminade, Catherine Cailleau, Juliette Vergnaud, Laurence Moine, Hervé Hillaireau, Didier Desmaëlle, Claire Gueutin, Stéphanie Denis, Valérie Nicolas, Claire Boulogne, Audrey Solgadi et Bastien Prost.

J'aimerais remercier en particulier Franceline, une amie que j'ai retrouvée en France dix ans après l'avoir connue à Porto Alegre. Merci pour la compagnie ces derniers années et pour avoir toujours été une personne aimable à qui je sais que je peux faire confiance, dans les bons et mauvais moments.

Je tiens à remercier tous mes collègues de l'Institut Galien, en particulier Barbara, Renato, Federica, Céline, Caroline, Maud, Clélia, Serra, Balthazar, Sophie, Marion, Mathilde, Alexandre, Mujeeb et Rosana, qui ont été toujours disponibles pour m'aider et discuter avec moi sur mon sujet de thèse. Je ne vais jamais oublier mes collègues brésiliens qui ont partagé au moins un an de leur doctorat avec moi : Simone, Cassiana, Sarah, Guilherme, Gabriela, Henrique et Lucas, vous avez rendu mon adaptation beaucoup plus facile.

A mes amies Tatiane, Barbara, Marianna, Renata, Eloisa, et plusieurs autres amis que je pourrais dire qui « sont la famille que la France m'a donnée », pour avoir toujours été présents avec moi pendant ces années.

Je tiens également à remercier mes amis du Brésil Paula, Marco, Alexandre, Simone, Ana, Luis, Dimara, Jaqueline et tous les autres que la distance n'a jamais permis de nous séparer.

Enfin, j'adresse mes plus sincères remerciements à ma famille : mes parents, Ana Maria et Jurandyr, mes frères, Vladimir et Yuri, mes belles-sœurs Fernanda et Gisele, mon neveu Eduardo. Vous m'avez accompagnée, aidée, soutenue et encouragée tout au long de la préparation de cette thèse, même à distance. Vous êtes toujours dans mon cœur.

Table de matières

Abréviations

AC	Alveolar cell pellet
ACN	Acetonitrile
ACO	Asthma-COPD overlap
AF	Alveolar particle fraction
AM	Alveolar macrophages
AP-1	Activator protein 1
ASM	Airway smooth muscle
ATCC	American Type Culture Collection
AUC	Area under the curve
BALF	Bronchoalveolar lavage fluid
BDP	Beclomethasone dipropionate
BP	Budesonide palmitate
BPCO/COPD	Bronchopneumopathie chronique obstructive/ chronic obstructive pulmonary disease
BSA	Bovine serum albumin
Bud	Budesonide
CBA	Cytometric Beads Array
$CDCl_3$	Deuterated chloroform
cGCR	Cytosolic glucocorticoid receptors
CINC-1	Cytokine-induced neutrophil chemoattractant-1
CO_2	Carbon dioxide
CZT	Crizotinib
DDS	Drug delivery systems
DFZ	Deflazacort
DLPC	Dilauroylphosphatidyl choline
DLS	Dynamic light scattering
DMEM	Dulbecco's Modified Eagle's Medium
DMSO	Dimethylsulfoxyde
DPI	Dry powder inhaler
DPPC	1,2-dipalmitoyl-*sn*-glycero-3-phosphatidylcholine
DSPE-mPEG	(1,2-Distearoyl-sn-Glycero-3-Phosphoethanolamine-N-(methoxy(polyethylene glycol)-2000) (ammonium salt))
DXM	Dexamethasone
DXP	Dexamethasone palmitate
EDA	Ethylenediamine
EE	Emulsion evaporation
EF	Emitted fraction
ELSD	Evaporative light-scattering detector
eNOS	Endothelial nitric oxide synthase
FBS	Fetal bovine serum
FP	Fluticasone propionate
FPF	Fine particle fraction

GC	Glucocorticoids
GCR or GR	Glucocorticoid receptor
GMCSF	Granulocyte-macrophage colony-stimulating factor
GRAS	Generally recognized as safe
HÁ	Hyaluronic acid
HCl	Hydrochloric acid
HPLC	High-performance liquid chromatography
ICS	Inhaled corticosteroids
IL-5	Interleukin 5
IL-6	Interleukin 6
IL-10	Interleukin 10
LA	Lipoic acid
LABA	Long-acting $beta_2$-agonists
LC-MS/MS	Liquid chromatography-tandem mass spectrometry
LNP	Lipid nanoparticles
LOQ	Lower limit of quantification
LPP	Large porous particle
LPS	Lipopolysaccharides
mAb	Monoclonal antibodies
MAP	Mucoadhesive particles
MCP-1	Monocyte chemoattractant protein 1
MF	Mometasone furoate
$MgSO_4$	Magnesium sulfate
MMAD	Mass median aerodynamic diameter
MPP	Mucus penetrating particles
MPS	Methylprednisolone
MR	Mannose receptor
MSLI	Multi-stage liquid impinger
MTT	(3-(4,5-dimethylthiazol-2-yl)-2,5-diphenyltetrazolium bromide)
Mw	Molecular weight
NaCl	Sodium chloride
$NaHCO_3$	Sodium bicarbonate
NC	Nanocapsules
NF-kB	Nuclear factor kB
NLC	Nanostructured lipid carriers
NMR	Nuclear magnetic resonance
NO	Nitric oxide
NP	Nanoprecipitation
OCS	Oral corticosteroid
PAA	Polyacrylic acid
PAM	Polyacrylamide
PBS	Phosphate-buffered saline
PCL	Polycaprolactone
PCS	Photon correlation spectroscopy
PdI	Polydispersity index
PE	Phycoerythrin

PEG	Polyethylene glycol
PGA	Polyglycolide
PHEA	α,β-poly(*N*-2-hydroxyethyl)-D,L-aspartamide
PLA	Polylactide
PLA-TPGS	Polylactide-tocopheryl polyethylene glycol 1000 succinate
PLGA	Poly (lactide co-glycolide)
PMAA	Poly (methacrylic acid)
pMDI	Pressurized metered dose inhaler
PMLA	Poly (malic acid)
PMMA	Poly (methyl methacrylate)
PNPs	Polymer nanoparticles
POE	Polyorthoester
PVA	Poly (vinyl alcohol)
PVP	Poly (N-vinyl pyrrolidone)
SEM	Scanning electron microscopy
SLN	Solid lipid nanoparticle
SP-A	Surfactant protein A
SPIONs	Superparamagnetic iron oxide nanoparticles
TEM	Transmission electron microscopy
TNFα	Tumor necrosis factor α
TSLP	Thymic stromal lymphopoietin
UV	Ultraviolet

INTRODUCTION GENERALE

Introduction générale

Cette thèse a eu pour objectif de développer et d'évaluer une forme pharmaceutique permettant de vectoriser un glucocorticoïde, le budesonide, vers les macrophages alvéolaires. En prenant en compte les difficultés rencontrées par les patients au cours de maladies pulmonaires inflammatoires telles que l'asthme et la bronchopneumopathie chronique obstructive (BPCO, ou COPD en anglais), nous proposons une stratégie de formulation qui se découpe en quatre parties: 1) la synthèse d'une prodrogue lipidique du budésonide, le palmitate de budésonide, visant à augmenter sa lipophilie et à prolonger sa rétention dans le tissu pulmonaire; 2) l'utilisation de lipides PEGylés qui permet de former en présence de palmitate de budésonide des nanoparticules capables de diffuser au travers du mucus souvent abondant chez les patients atteints de BPCO; 3) la formulation de microparticules Troyennes pour faciliter le dépôt des nanoparticules directement au niveau des alvéoles pulmonaires; et 4) la mannosylation des nanoparticules dont le récepteur est présent à la surface des nanoparticules afin d'assurer un ciblage cellulaire.

Le manuscrit a été divisé en deux grandes parties. Dans la première partie, nous présentons une revue de la littérature relative aux deux pathologies pulmonaires d'intérêt, l'asthme et la BPCO, les traitements actuellement disponibles, les cibles suggérées pour la thérapie pharmacologique et les possibilités d'utiliser des nanotechnologies pour améliorer ces traitements. La deuxième partie présente la description des travaux expérimentaux développés ainsi que les résultats obtenus qui sont divisés en 2 chapitres rédigés sous la forme d'articles scientifiques.

Le premier chapitre des travaux expérimentaux décrit le développement et l'évaluation *in vitro* et *in vivo* des nanoparticules et des microparticules troyennes. Ainsi, des nanoparticules PEGylées ont été formulées et caractérisées par des analyses physico-chimiques et des études de pénétration cellulaire et d'efficacité *in vitro* sur des macrophages activés. Ces nanoparticules ont ensuite été encapsulées dans des microparticules Troyennes qui ont fait l'objet d'analyses de propriétés aérodynamiques. Une étude *in vivo* chez le rat sain a été réalisée suite à l'administration intratrachéale des microparticules et l'évaluation de la pharmacocinétique, pulmonaire et plasmatique ainsi que de la biodistribution de la prodrogue de budésonide et de sa forme libre.

Le chapitre 2 aborde la formulation, la caractérisation et l'évaluation *in vitro* de nanoparticules mannosylées. Un lipide mannosylé, DSPE-PEG-Man, a été synthétisé puis utilisé dans la formulation des nanoparticules, qui ont également été caractérisées sur le plan physico-chimique. Des études *in vitro* d'internalisation cellulaire ont été réalisées en comparant des nanoparticules PEGylées et mannosylées, démontrant que la présence de mannose à la surface des nanoparticules favorise une augmentation considérable de l'internalisation cellulaire.

Le manuscrit s'achève par une conclusion sur le travail effectué ainsi que les perspectives envisagées pour le futur.

TRAVAUX ANTERIEURS

1 INTRODUCTION

Chronic respiratory diseases affect several million people worldwide and impose an immense health burden. Among most common causes of severe illness and death, around 400 million people are affected by asthma or chronic obstructive pulmonary disease (COPD) (Forum of International Respiratory Societies, 2017). The commonly recommended treatment for these diseases is based on a combined therapy of glucocorticoids and bronchodilators. However, the need of frequent daily administrations and the increase in the resistance to glucocorticoids make treatment not always effective.

The advent of nanotechnology allowed the development of new formulations to improve the release and targeting of drugs to specific tissues and cells, also preventing their loss of activity by degradation. Nanoparticulate systems such as liposomes, lipid nanoparticles, polymer nanoparticles and more recently, Trojan microparticles have been used for the pulmonary release of active substances, prolonging their retention time in the body, with resulting decrease in the number of daily doses. Drug targeting directly to the lungs also allows a reduction of the unwanted side effects commonly seen during the use of glucocorticoids.

In addition to the potential characteristics presented by the nanoparticles, chemical changes can be performed to the drugs already available for the treatment of these diseases, such as the synthesis of prodrugs in the case of glucocorticoids. This approach is based on evidence that some glucocorticoids such as budesonide undergo intracellular esterification in airways, prolonging local tissue binding and efficacy. For instance, budesonide palmitate renders the molecule highly hydrophobic and allows sustained release of active budesonide from the prodrug upon cleavage of the ester bond in a biological medium.

In this review of the literature, we will firstly describe asthma and COPD diseases, their pathophysiology, their inflammatory process as well as the current therapeutic strategy, with special focus on corticosteroids therapy. We will then approach the obstacles to drug delivery and their potential targets. Finally, we will introduce the drug delivery systems that have been proposed for the treatment of asthma and COPD diseases.

2 ASTHMA AND COPD

2.1 Asthma

Asthma is a worldwide disease that touches all age groups with an estimated number of individuals affected around 300 million. The standard methods for evaluating asthma symptoms allow identifying a global prevalence ranging from 1 to 16 % of the population according to the country. There are evidences that the symptoms prevalence has been decreasing in Western Europe and increasing in regions where it was previously low. However, the disease prevalence continue to rise in Africa, Latin America, Eastern Europe and Asia (GINA, 2018). It is also estimated that an additional 100 million persons will be affected by asthma by 2025 (Masoli *et al.*, 2004).

2.1.1 Pathophysiology of Asthma

The problem of asthma makes this disease identified as a priority in government's health strategies of several countries. Asthma cost of treatment, including hospitalisation and pharmaceuticals, is considerable. Nevertheless, several barriers have been recognized hampering the problem of treating asthma, ranging from generic barriers (poverty, lack of education and weak infrastructure), environmental barriers (indoor and outdoor air pollution, tobacco smoking, and occupational exposures) to the inadequate government resources provided for healthcare (Masoli *et al.*, 2004).

Asthma is a heterogeneous disease typically characterized by chronic airway inflammation. The diagnosis is based on the history of respiratory symptoms such as wheeze, shortness of breath, chest tightness and cough that vary over time and intensity, together with variable expiratory airflow limitation (GINA, 2018). To evaluate the severity of the disease, audible wheezing is usually a sign of moderate asthma, whereas no wheezing could be a sign of severe airflow obstruction. Severe asthma include symptoms such as chest toughness, cough (with or without sputum), sensation of air hunger, inability to lie flat, insomnia and severe fatigue (Fergeson *et al.*, 2017).

Figure 1 shows the difference between a normal airway and bronchial asthma. The three common pathophysiological components of obstructive airway diseases are airway inflammation, obstruction and hyperresponsiveness. In asthma, the airway inflammation is primarily eosinophilic and driven by CD4 cells but also neutrophilic or even mixed eosinophilic/neutrophilic inflammatory patterns. The airway obstruction results from bronchospasm, mucosal edema and inflammation, mucus hypersecretion and the formation of mucus plugs. Finally, the airway hyperresponsiveness is an exaggerated bronchoconstrictor response to a wide variety of stimuli and, together with bronchodilator reversibility, is present in almost all patients with asthma (Nakawah *et al.*, 2013).

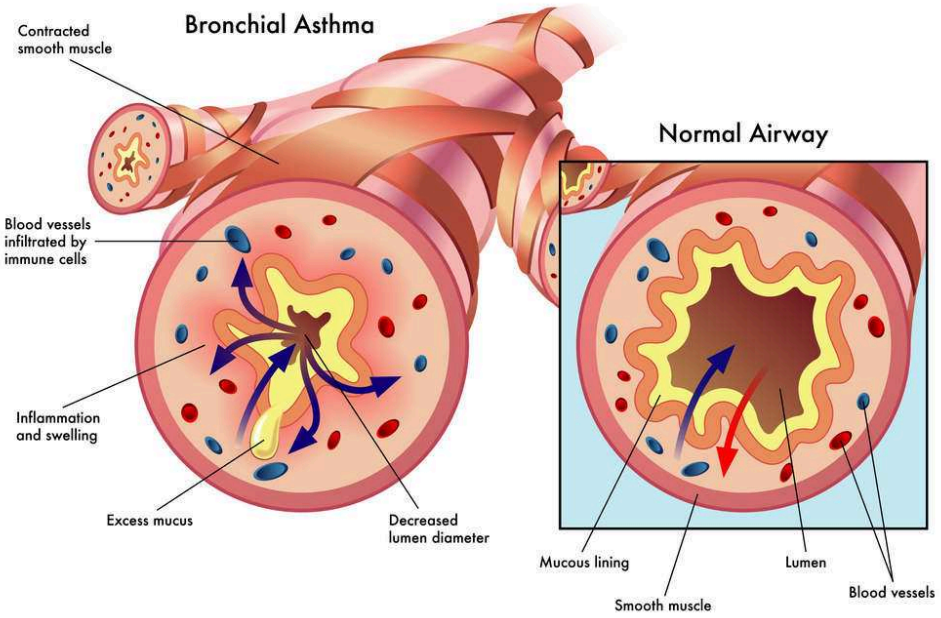

Figure 1: Normal airway versus bronchial asthma (Hildreth, 2017).

Whether asthma is a single disease with variable types or severity or several diseases that have variable airflow obstruction as a common feature is part of a debate. Usually, patients having asthma are classified by a disease phenotype that corresponds to observable clinical, physiological, morphological and biochemical characteristics, as well as responses to different treatments. However, this approach, even if relevant, does not indicate the underlying disease processes. For this reason, Lötvall *et al.* (2011) described a hypothesis dividing asthma syndrome into distinct disease classes with specific mechanisms called “asthma endotypes”. Six endotypes were proposed to be a subtype of a condition defined by a distinct pathophysiological mechanism, summarized in Table 1 (Ishmael, 2011; Meyer *et al.*, 2014; Lötvall *et al.*, 2011).

Table 1. Examples of asthma endotypes (Ishmael, 2011 ; Lötvall *et al.*, 2011).

Endotype	Clinical aspects	Proposed mechanism	Treatment response
Allergic asthma	Childhood onset, sensitization to allergens and allergic rhinitis, airway eosinophilia	T_H2-dominant	Responds to glucocorticoids and omalizumab
Allergic broncopulmonary mycosis (ABPM)	Adulthood, severe mucus production, long duration	Colonization of airways, most frequently *Aspergillus*	Responds to systemic glucocorticoids, antifungal agents, anti-IgE mAb omalizumab
API-positive preschool wheezer*	Childhood, family history of asthma, > 3 episodes per year	T_H2-dominant	Responds to daily inhaled glucocorticoids
Aspirin-sensitive asthma	Adulthood, often after ingestion of a non-steroidal anti-inflammatory (NSAID) medication, chronic/severe rhinosinusitis and nasal polyps	Eicosanoids-related	Responds to antileukotrienes, aspirin desensitization
Exercise-induced bronchospasm	Symptoms start after 5 to 20 minutes of non-stop exercise	Dehydration of airways	Mixed responds to glucocorticoids and bronchodilators
Severe late-onset hypereosinophilic asthma	Late-onset disease, several exacerbations, peripheral blood eosinophilia	Nonatopic, mechanisms still unknown	Commonly dependent on oral glucocorticoids

* API: asthma predictive indices

2.1.2 Inflammatory cells in asthma

During asthma, airways are infiltrated by inflammatory cells that release or activate *in situ* mediators and cytokines, such as mast cells, macrophages, eosinophils, T lymphocytes, dendritic cells, basophils, neutrophils, and platelets. It is also known that structural cells such as airway epithelial cells, smooth muscle cells, endothelial cells, and fibroblasts may play an important role, since they are all able to synthesize and release inflammatory mediators (Barnes *et al.*, 1998; Haley *et al.*, 1998).

Eosinophils are the most prominent inflammatory cells in asthma, but mast cells, lymphocytes, and macrophages play also a major role in the therapeutic care of asthma. It is for example known that the presence of significant numbers of eosinophils in sputum from patients affected by the disease is associated with steroid responsiveness (Sutherland and Martin, 2003). There is also an increase in the number of $CD4^+$ T-cells in the airways with predominance of T helper (T_H) type 2 cells. T_H-2 cells have a central role in allergic inflammation. T_H-2 cells regulation is therefore an area of intense research, due their role in the secretion of IL-4 and IL- 13 cytokines, which control immunoglobulin IgE production by

B-cells, IL-5, which is exclusively responsible for eosinophil differentiation in the bone marrow, and IL-9, which attracts and coordinates the differentiation of mast cells (Barnes, 2011). These cytokines are implicated in eosinophil accumulation, since IL-4 and IL-13 up-regulate adhesion molecules in the capillary endothelium of the bronchial mucosa, resulting in increased adhesion and diapedesis of eosinophils. Once in the tissues, IL-5 extends the survival of eosinophils and activate them for increased release of their basic granular proteins and production of other mediators. In particular, cysteinyl leukotrienes are the most potent natural bronchoconstrictors and proinflammatory mediators, which promote vascular leakage and therefore edema of the lining of the airways (Corrigan, 2012). Histamine and prostaglandins are also released from mainly mast cells and contribute to the bronchomotor tone in asthma (Ichinose, 2009). All these effects probably contribute to airways obstruction.

Figure 2 describes the cycle of chronic inflammation in patients with asthma. Environmental and inflammatory stimuli induce the production of mediators from the airway epithelium, which activates and recruits inflammatory cells. Inflammatory cells infiltrate the lungs and release mediators that increase the inflammatory response in the epithelium, creating a cycle of chronic inflammation. This process causes bronchoconstriction, mucus production and epithelial damage, and it can result in airway remodelling (Ishmael, 2011).

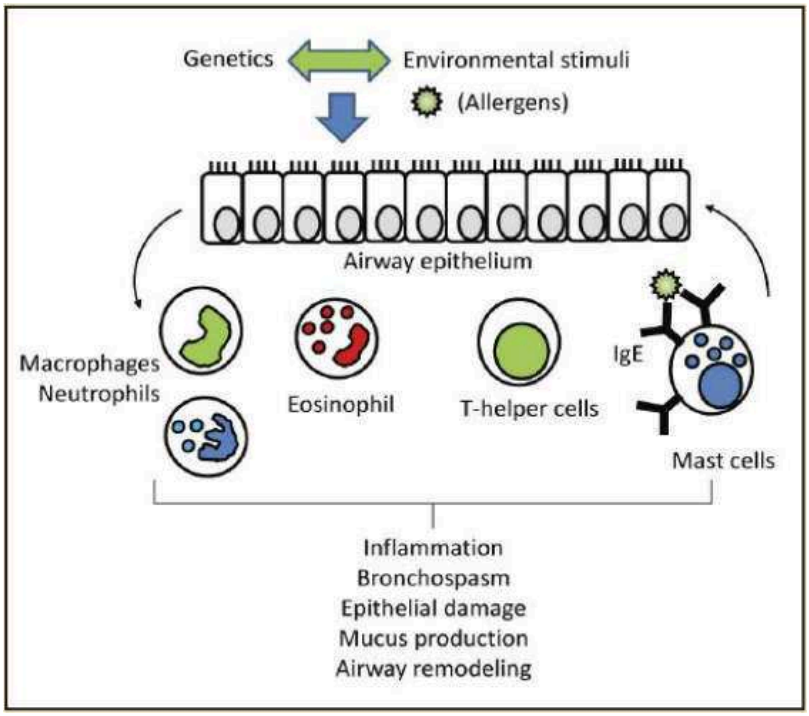

Figure 2. Cycle of chronic inflammation in patients with asthma (Ishmael, 2011).

However, even though eosinophils are predominant in asthma, several studies have shown that increased number of neutrophils in asthmatic airways is a potent source of proinflammatory cytokines released from secretory vesicles, because of their activation. Resistance to corticosteroids treatment, exacerbations of the disease and occupational forms of asthma are found to be associated with increased neutrophils count in peripheral blood and patient's bronchoalveolar lavage fluid (BALF) (Ciepiela et al, 2015).

2.2 Chronic Obstructive Pulmonary Disease (COPD)

COPD is a worldwide important cause of morbidity and mortality being considered the fourth leading cause of death in the world and projected to be the third by 2020. More than 3 million people died of COPD in 2012, representing 6% of all deaths globally. Because of the continued exposure to risks factors and aging of the population, the COPD burden is projected to increase during the next decades (GOLD, 2018).

2.2.1 Pathophysiology of COPD

COPD is a common preventable and treatable disease, characterized by persistent airflow limitation that is usually progressive and associated with an enhanced chronic inflammatory response in the airways and the lungs to harmful particles or gases. Exacerbations and comorbidities contribute to the overall severity in patients. The most common respiratory symptoms include dyspnea (shortness of breath), frequent respiratory infections, chronic cough and/or sputum production (GOLD, 2018). Others comorbidities such as cardiovascular disease, diabetes, hypertension, osteoporosis and psychological disorders are commonly reported (Chatila *et al.*, 2008). The term COPD refers to chronic disorders that disturb airflow, whether the most prominent development of the disease occurs within the airways or within the lung parenchyma. The chronic bronchitis and emphysema are two disorders generally included in this category. The term COPD does not include bronchial asthma although it could be included in this category (Weinberger *et al.*, 2019).

The most common risk factor for COPD includes different types of smoking including tobacco (e.g. cigarettes, pipe, cigar, and water pipe) or marijuana. Other factors are considered to provoke COPD such as outdoor, occupational, and indoor air pollution – the latter resulting from the burning of wood and biomass fuels. Even non-smokers may also develop the disease, since COPD is the result of a complex combination of long-term cumulative exposure to toxic gases and particles with a variety of host factors that are genetics, age and gender, asthma and airway hyper-responsiveness and poor lung growth during childhood (Garlapati and Rampure, 2015; GOLD, 2018). Various population-based

studies suggest COPD also increases twofold the risk of cardiovascular morbidity and mortality. There are also evidences that some bronchodilators, which are commonly used to treat symptoms in COPD, could increase the risk of cardiovascular morbidity and even mortality in COPD patients (Sin and Man, 2005).

Although men have higher prevalence of COPD than women, several studies show that an increased number of women is affected by the disease, mainly related to increase of cigarette smoking in females within the last several decades. Among the risk factors in women, those such occupational exposures (women are more likely than men to be exposed to risks from unregulated 'cottage' industries, such as fish smoking and textile working), non-occupational exposures (Biomass fuel exposure greater because of more domestic responsibilities) and the role of oestrogen and progesterone in the pathogenesis are discussed. Furthermore, women tend to be under-diagnosed, as a result of years of consideration that COPD was a men disease, thereby several times women have been diagnosed wrongly with asthma (Tam *et al.*, 2011; American Lung Association, 2013; Sansores and Ramírez-Venegas, 2016; Jenkins *et al.*, 2017; Camp *et al.*, 2009).

All cigarette smokers have some inflammation in their lungs but those who develop COPD have an enhanced or abnormal response to inhaling toxic agents. This increased response may induce mucus hypersecretion (chronic bronchitis), tissue destruction (emphysema), and disruption of normal repair and defense mechanisms causing small airway inflammation and fibrosis (bronchiolitis). Besides inflammation, there are two other processes involved in the pathogenesis of COPD : an imbalance between proteases and antiproteases and an imbalance between oxidants and antioxidants (oxidative stress) in the lungs (MacNee, 2006).

2.2.2 Inflammatory Process in COPD

Several types of inflammatory cells and inflammatory mediators are involved in COPD, as well as in asthma. In the case of COPD, there is evidence of neutrophil rather than eosinophilic inflammation in larger airways, with an increased number of neutrophils in BALF. Induced sputum shows a characteristic increase in the proportion of neutrophils that is much greater in patients with COPD than in smokers without obstruction (Barnes, 2000; Barnes *et al.*, 2003). In COPD, with the eosinophils playing a minor role, except in the setting of exacerbations, the presence of significant numbers of eosinophils in induced sputum is associated with steroid responsiveness in patients. Neutrophils have been hypothesized to have a significant role in the pathogenesis because of their ability to mediate tissue destruction by the release of elastases (Sutherland and Martin, 2003).

The COPD inflammation is characterized by increased numbers of alveolar macrophages, neutrophils, T lymphocytes (predominantly TC1, TH1, and TH17 cells), and B lymphocytes. Both innate immunity (neutrophils, macrophages, eosinophils, mast cells, natural killer cells, innate lymphoid cells, and dendritic cells) and adaptive immunity (T and B lymphocytes) seem to be involved, but also, there is activation of structural cells, including airway and alveolar epithelial cells, endothelial cells and fibroblasts. Epithelial cells are activated by cigarette smoke and other inhaled irritants to produce inflammatory mediators, including tumour necrosis factor (TNF-α), interleukin (IL-1b, IL-6), granulocyte-macrophage colony-stimulating factor (GMCSF), and CXCL8 (IL-8) (Barnes, 2016).

Inflammatory mechanisms in COPD are shown in Figure 3. Cigarette smoke and other environmental harmful agents activate macrophages and epithelial cells to release chemotactic factors that recruit neutrophils and CD8 cells from the circulation. These cells release factors that activate fibroblasts, resulting in abnormal repair processes and bronchiolar fibrosis. An imbalance between proteases released from neutrophils and macrophages and antiproteases leads to alveolar wall destruction (emphysema). Proteases also cause the release of mucus (MacNee, 2006).

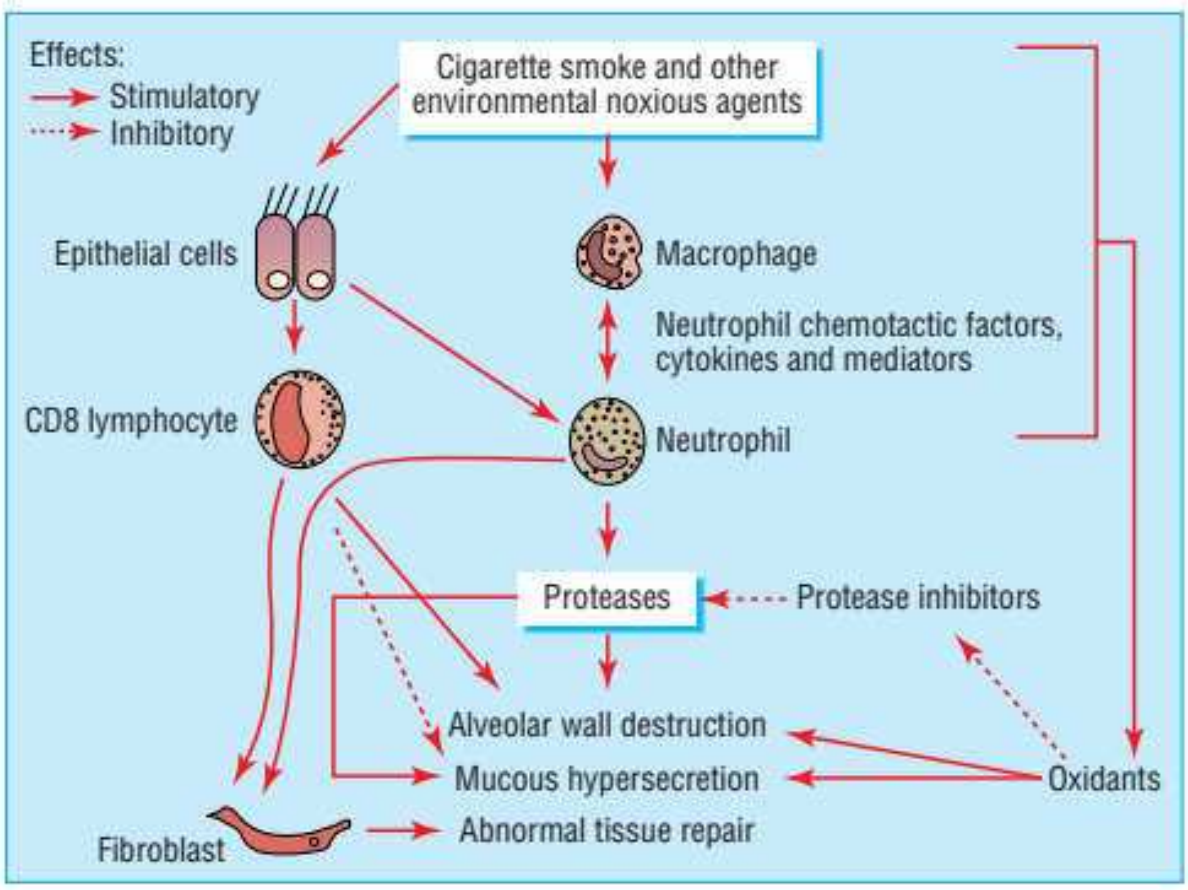

Figure 3. Inflammatory mechanisms in COPD (MacNee, 2006).

Macrophages appear to play a pivotal role in the pathophysiology of COPD, and since they are localised in sites of alveolar wall destruction in patients with emphysema, it is possible to correlate macrophage numbers in the airways and the severity of COPD. Macrophage number is increased in the lungs of patients with COPD as well as in asthma, but their number is greater in COPD, suggesting that they may orchestrate the inflammation of COPD through the release of chemokines that attract neutrophils, monocytes and T-cells, and the release of proteases, particularly MMP-9 (Barnes, 2016; Rovina *et al.*, 2013).

In terms of immune response, the $CD4^+$ T-cells that accumulate in the airways and lungs of patients with COPD are mainly T_H-1 cells. However, there are evidences that T_H-2 cells are also increased in lavage fluid of patients with COPD, and as already mentioned, patients with more severe asthma T_H-1 cells are activated, as well as T_H-2 cells, making the distinction between the T_H-cell response in these two diseases less clear (Barnes, 2011). The proteases are also considered to play an important role in the inflammation, since they can break down connective tissue components, particularly elastin, in lung parenchyma to produce emphysema. Normally, the balance between proteases and endogenous antiproteases may protect against protease-mediated effects. Elastin may be the most important target for these enzymes as there is a loss of elasticity in the lung parenchyma in patients with emphysema and elastin cannot be regenerated in an active form. When compared to healthy patients, smokers with rapid decline in lung function show an increased excretion of desmosine, derived from elastin cross-links, proving the evidence for elastin degradation in COPD (Barnes *et al.*, 2003).

In terms of immunologic response from the description of both diseases asthma and COPD, it is important to establish differences as described in Table 2. One important and key parameter is that in both cases macrophages plays an important role meaning that they could be one of the key cells to target to reduce the inflammation process.

Table 2. Cellular and molecular differences between asthma and COPD.

	Asthma	COPD
Cells	Eosinophils	Neutrophils
	CD4+ T cells	CD8+ T cells
	Macrophages +	Macrophages +++
	Mastocytes	
Mediators	Leukotriene B4	Leukotriene B4
	Histamine	
	IL-4, IL-5, IL-9, IL-13	IL-1b, IL-6, IL-8, TNFα
Response to Steroids	Sensitive	Resistant

2.3 Asthma – COPD Overlap (ACO)

Asthma and COPD are heterogeneous diseases with for each one separated characteristic. However, in many cases, it is difficult to differentiate both. Clinicians give a common description for this, called Asthma – COPD Overlap (ACO), that is characterized by persistent airflow limitation with severe features commonly associated with asthma and others commonly associated with COPD. In the clinical practice, ACO is accordingly identified by the features that it shares with both diseases. Nevertheless, ACO includes manifold different clinical phenotypes and may be caused by a range of different underlying mechanisms (GINA, 2018).

It is known that airway inflammation in asthma differs from that in COPD. Asthma is characterized predominantly by eosinophilic inflammation and inflammation involving type 2 helper T (TH2) lymphocytes, whereas COPD is characterized predominantly by neutrophilic inflammation and inflammation involving CD8 lymphocytes (Table 2). Furthermore, the inflammation seen in asthma affects all structures of the bronchi, occurring mainly in large airways but also in small airways in more severe disease, without damage to the lung parenchyma. On the other hand, COPD predominantly affects the small airways and lung parenchyma, although similar inflammatory changes may also be found in larger airways (Postma and Rabe, 2015; Barnes, 2011; GINA, 2018).

The diagnosis of ACO is based on the comparison of the number of features in favor of each diagnosis. For example, if three or more features of asthma are present, that diagnosis is suggested, with the same approach to COPD. On the other hand, if there are similar numbers of features of asthma and COPD, the diagnosis of ACO should be considered (Yanagisawa and Ichinose, 2018).

A correct diagnosis of ACO is important because it represents a form of airways disease that is associated with a disproportionate number of exacerbations hospital admissions and use of health-care resource. However, from the moment those patients with ACO have been excluded from trial investigating treatments for asthma or COPD, almost no high-quality data exist to define a specific treatment to ACO. Some guidelines recommend for patients with overlap phenotype COPD–asthma the administration of inhaled corticosteroids for the treatment for COPD (Bateman *et al.*, 2015).

3 CURRENT TREATMENTS OF ASTHMA AND COPD

The adequate treatment in asthma and COPD may reduce symptoms and number of exacerbations and improve the quality of life. However, the goal of treatment in asthma is the suppression of inflammation and induction of bronchodilation, while treatment in COPD is aiming to reduce the symptoms, prevent exacerbations and decrease mortality (Cukic *et al.*, 2012).

The pharmacotherapy of asthma has undergone marked changes over the past century, but for the past 50 years, the therapeutics is based primarily on five classes of drugs: β2-agonists, anticholinergics, methylxanthines, cromones, and corticosteroids (Cockcroft, 1999 ; Gross et Barnes, 2017).

The use of bronchodilating agents in asthma can lead to immediate relief of broncho-constriction and dyspnea, activating the β2 adrenergic receptor on airway smooth muscle (β-agonists). For long-term control, the most effective class is corticosteroids, which reduce inflammation and suppress airway constriction and dyspnea. Bronchodilating agents and corticosteroids are typically administered by inhalation in mild to moderate disease, which decrease but does not eliminate side effects. Anticholinergics are considered a secondary class of agents used for controlling bronchospasm, which are antagonists of the muscarinic acetylcholine receptor (Corry *et al.*, 2019). Although bronchoconstriction in COPD patients is considerably lower than in patients with bronchial asthma, bronchodilators remain an important part of the treatment of many patients, principally sympathomimetic agents (β2 agonists), anticholinergic drugs, and methylxanthines (Weinberger *et al.*, 2019). In this report we will focus mainly on bronchodilators and corticosteroids. We will also describe novel use of immunotherapy.

3.1 Bronchodilators

Bronchodilators are central in the treatment of airways disorders. They are the backbone of the current management of COPD and are critical in the symptomatic management of asthma. Bronchodilators work through their direct relaxation effect on airway smooth muscle cells. Nowadays, three major classes of bronchodilators, 2-adrenoceptor (AR) agonists, muscarinic receptor antagonists, and xanthines are available and can be used individually or in combination. The inhaled route is currently preferred to minimize systemic effects (Cazzola *et al.*, 2012).

For COPD, the short-acting beta$_2$-agonists are used, including salbutamol, and fenoterol. They have a rapid onset of action, a bronchodilating effect for 3-6 h and are used on demand. The long-acting beta$_2$-agonists (LABAs), including salmeterol and formoterol, have 12-hour duration of action and are used with a twice-daily dosing regimen for long-term COPD treatment. Unlike salmeterol, formoterol has a

rapid onset of action. Pharmacological characteristics required by novel inhaled LABAs include 24 h bronchodilator effect *in vivo* which would make them suitable for once daily administration (ultra-LABA), high potency and selectivity for beta$_2$-adrenoceptors, rapid onset of action, low oral bioavailability (< 5%) after inhalation, and high systemic clearance (Fuso *et al.*, 2013).

The presence of acute reversibility to bronchodilators does not distinguish asthma from COPD. Patients with either condition can benefit from bronchodilators and should be given a trial to assess their response. Some of them reply with a modification of lung volume displaying less hyperinflation; others improve their forced inspiratory flow and become much more comfortable.

3.2 Corticosteroids

Corticosteroids have been used for decades because of their property to reduce a variety of inflammatory processes, recognized in the late 1940s and early 1950s. They are then largely studied and used in the treatment of lung diseases due to their broad anti-inflammatory and immunosuppressive effects. Corticosteroids and their biologically active synthetic derivatives differ in their metabolic (glucocorticoid) and electrolyte-regulating (mineralocorticoid) activities. However, the term “corticosteroids” is generally used to refer to glucocorticoids (GC). These agents are employed at physiological doses for replacement therapy when endogenous production is impaired. Glucocorticoids potently suppress inflammation, and their use in a variety of inflammatory and autoimmune diseases makes them among the most frequently prescribed classes of drugs (Cockcroft, 1999; Shaikh *et al.*, 2010; Ramamoorthy and Cidlowski, 2016).

Glucocorticoids (cortisol in humans and corticosterone in rodents) are steroid hormones synthesized and released by the adrenal glands in a circadian manner, in response to physiologic reactions and stress. Several modifications in the molecular structure of hydrocortisone influences the potency of steroids and alter some of its pharmacokinetic properties, but all corticosteroids used can bind glucocorticoid receptors and mimic the effects of hydrocortisone. Their physiological effects occur via activation of either glucocorticoid receptor (GR, or GCR) or the mineralocorticoid receptor in target tissues, to alter the expression of corticosteroid-responsive genes. GCR in the cytoplasm of the cell binds to steroid ligands to form hormone-receptor complexes that eventually translocate to the cell nucleus. These complexes bind to specific DNA sequences and alter their expression, being able to induce the transcription of mRNA leading to the synthesis of new proteins (Morris, 1985 ; Ramamoorthy and Cidlowski, 2016 ; Spoelhof and Ray, 2014).

Classical genomic actions are the most important mechanisms of GC action and lead to changes in gene expression. These actions are caused by the passage of GC molecules across the plasma membrane, high affinity binding to inactive cytosolic GC receptors (cGCR), formation of the activated GC / cGCR complex, and translocation of the complex to the nucleus. In "transactivation", the dimerized GCR protein complex binds to the promoter of genes regulated by GC, leading finally to the synthesis by transcriptional activation. In “transrepression” GCR monomers interfere (‘tethering’) with the activity of proinflammatory transcription factors such as activator protein 1 (AP-1) and nuclear factor kB (NF-kB), leading to down-regulation of proinflammatory protein synthesis. Genomic processes require at least 30 minutes before significant changes can be observed at regulatory protein concentrations. Usually, it takes hours to days for changes to occur at the level of cells, tissues, or organs (Spies *et al.*, 2011).

Glucocorticoids can modulate the transcription of a variety of genes, including cytokines and chemokines, receptors, enzymes, adhesion molecules, and inhibitory proteins. This modulation inhibits the transcription of most cytokines and chemokines that are relevant in asthma, including IL-1b ,TNF-α , GM-CSF, IL-3, IL-4, IL-5, IL-6, IL-8, IL-11, IL-12 and IL-13 (Van Der Velden, 1998). Non-genomic mechanisms must also be considered. Glucocorticoids can signal non-genomically through GR to activate endothelial nitric oxide synthase (eNOS) and therefore increase the production of nitric oxide (NO), a presumable anti-inflammatory molecule. GC can also induce the rapid phosphorylation, plasma membrane translocation and extracellular release of the anti-inflammatory molecule, annexin-1 (Keenan et al., 2012).

Another important factor to be considered in the use of GC is the resistance or insensitivity. A few patients with chronical diseases such as asthma and COPD show a poor or absent response even to high doses of glucocorticoids. Several molecular mechanisms are involved in these cases, as genetic susceptibility, defective glucocorticoid receptor binding and translocation, transcription factor activation and others (Barnes et Adcock, 2009).

The development of active corticosteroids such as betamethasone-17- valerate and beclomethasone dipropionate occurred in the early 1970s, and there are several corticosteroids currently available. However, it soon became apparent that long term systemic corticosteroid therapy, unless in very low dose, was associated with serious adverse effects including hypertension, osteoporosis, diabetes, obesity, facial mooning, acne, skin thinning and bruising. Research into safer administration of corticosteroids led to the development and introduction into clinical practice of inhaled beclomethasone dipropionate (BDP) in 1972. Initial reports of uncontrolled studies were enthusiastic

and placebo-controlled studies soon confirmed the great value of this form of therapy. It was further demonstrated that the two most widely favored agents on a worldwide basis would be budesonide and fluticasone propionate (Cockcroft, 1999 ; Crompton, 2006).

Interestingly, the pattern of corticosteroid use in COPD has changed over the last half century. Long-term oral corticosteroid (OCS) use was a fairly common practice in the mid-to-late 20th century, but it is estimated that now the indications are only 4–10 %. In place of OCS, inhaled corticosteroids (ICS) use has been increasing, to improve symptoms and reduce exacerbations (approaching 65 % of the COPD population in some studies). Complications from long-term corticosteroid use are important, but they appear less when corticosteroids are given by the inhaled route (Macintyre and Faarc, 2006).

The efficacy of corticosteroids arises from their anti-inflammatory and immunosuppressive effects. Systemic corticosteroids were first shown to be effective in the treatment of acute asthma in 1956. Since then, numerous studies have confirmed the effectiveness of systemic corticosteroid therapy in managing acute and chronic asthma. Since the mid-1990s, several studies have demonstrated their efficacy in acute exacerbations of COPD (Raissy *et al.*, 2013).

In general, therapies for COPD have a much more limited effect when compared with those for asthma. While inhaled corticosteroids are the base of the pharmacologic management of persistent asthma, inhaled bronchodilators (β2-agonists and anticholinergics) are the therapeutic choice for patients with COPD (Nakawah *et al.*, 2013). Clinical evidence is particularly strong supporting the use of inhaled corticosteroids to prevent exacerbations and oral corticosteroids to reduce the duration and impact of exacerbations (Macintyre and Faarc, 2006).

For the above-mentioned reasons, the combination of LABAs and inhaled steroids was considered useful in both disease conditions. While anticholinergics seem to yield the best results in COPD, some patients with asthma also benefit from their use (Donohue, 2004). Combination with ICS (fluticasone/salmeterol, budesonide/formoterol, beclomethasone/formoterol) appears to provide an additional benefit over the monotherapy, although the extent of this benefit is variable and often not clinically significant in all the endpoints assessed. In patients with COPD, treatment with ICS is associated with increased risk of pneumonia which should be carefully considered when assessing the risk/benefit ratio of ICS/LABA combinations (Fuso *et al.*, 2013).

Corticosteroids can be given by two principal routes of administration either orally or by pulmonary delivery, this latest being today the most popular due to the lower side-effects compared to oral administration.

3.2.1 Oral corticosteroids

Chronic oral glucocorticoid use is common in patients with COPD and asthma. Side effects of chronic use include bruising, muscle weakness, weight gain, sleep disturbances, cataracts, skin changes, and pathologic fractures. OCS administration can also induce psychiatric side effects: mood disorders, anxiety, delirium, and panic disorder (Ericson-Neilsen and Kaye, 2014). It was not until 1958 that the association between successful treatment with OCS and a reduction in eosinophils in the sputum was noted. The subsequent development of inhaled corticosteroids and the recognition that they may be equally effective in the majority of patients with asthma, therefore, led to a decline in the use of OCS, except in the population with severe asthma (Ramsahai et Wark, 2018).

3.2.2 Inhaled corticosteroids

Inhaled corticosteroids are the base of chronic asthma therapy and the understanding that chronic inflammation is also present in COPD provided a rationale for their use also in this disease. Given this, inhaled corticosteroids are widely prescribed in the treatment of COPD and even are used almost as frequently as in asthma. However, it is important to stress out that inhaled or oral corticosteroids fail to reduce cytokine and chemokines in COPD even at high doses, probably because the neutrophilic inflammation in humans is not suppressible by corticosteroids. By contrast, there is a beneficial effect of systemic corticosteroids in treating acute exacerbations of COPD, and this discrepancy between steroid responses in acute versus chronic COPD may relate to differences in the inflammatory response (increased eosinophils) or airway edema in exacerbations (Barnes *et al.*, 2003).

Beclomethasone dipropionate (BDP) was the first ICS introduced in the early 1970s characterized by an enhanced local activity. Subsequently, studies have not only evidenced the efficacy of such treatment but also due to the reduction of adverse effects, a decrease in morbidity and mortality was observed in asthma patients. Six ICSs are available for use in the United States: BDP, flunisolide, budesonide (Bud), fluticasone propionate (FP), mometasone furoate (MF), and ciclesonide (Raissy *et al.*, 2013). A comparison between available ICSs is showed in Table 3 (Derendorf *et al.*, 1998 ; Derendorf *et al.*, 2006 ; GINA, 2018 ; Kelly, 1998 ; Winkler *et al.*, 2004).

Table 3. Comparison between available ICSs and their pharmacokinetics data after inhalation.

Corticosteroid	Chemical formula	Doses (low-medium, µg)	t ½ in plasma (h)	$F_{inhaled}$ (%)*
Beclomethasone dipropionate	$C_{28}H_{37}ClO_7$ 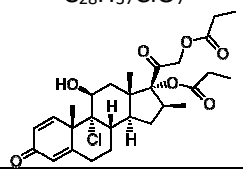	200-1000	0.1	55-60
Flunisolide	$C_{24}H_{31}FO_6$ 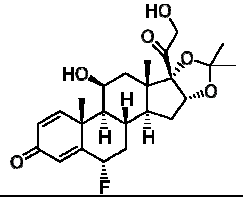	80-320	1.6	20-68
Budesonide	$C_{25}H_{34}O_6$ 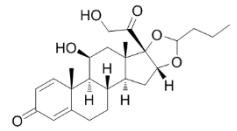	200-800	2.8	18
Fluticasone propionate	$C_{22}H_{27}F_3O_4S$ 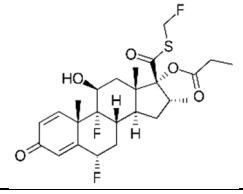	100-500	7.8	17-29
Mometasone furoate	$C_{22}H_{28}Cl_2O_4$ 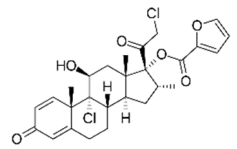	110-440	4.5	11
Ciclesonide	$C_{32}H_{44}O_7$ 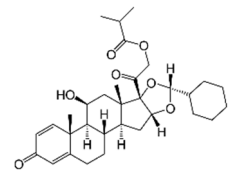	80-320	0.4	52

* $F_{inhaled}$ = bioavailability after inhalation. The results vary according to the device used (DPI/MDI).

A great progress was achieved with ICS permitting their delivery at high concentrations to the whole lungs. Although the safety profile of inhaled corticosteroids was markedly better than that of oral corticosteroid therapy, the total elimination of systemic adverse effects was not confirmed by clinical trials (Lipworth, 1999 ; Tattersfield *et al.*, 2004). Indeed, ICS are partially absorbed from the lungs into the systemic circulation, exposing the patients to adverse effects as osteoporosis, risk of cataracts, glaucoma, skin atrophy, and vascular changes that increase the risk of ecchymoses (Allen *et al.*, 2003).

Figure 4 describes the fate of ICS. To evaluate the ICS systemic bioavailability, the amount of an ICS reaching the systemic circulation is the sum of the drug available after absorption across lung and nasal mucosa, plus the gastrointestinal tract absorption of administrated drug that escapes hepatic first-pass inactivation, and is distinct for each ICS molecule/device (Heffler *et al.*, 2018). Only a fraction of the dose, approximately 10 % to 40 % depending on the delivery device, is retained in the lungs while the rest is absorbed. The swallowed corticosteroid enters the gastrointestinal tract in which it can produce undesired local effects and is then absorbed from the gastrointestinal tract. Fortunately, most of the swallowed dose undergoes first pass inactivation in the liver, and only a small portion of it makes it to the systemic circulation. Part of this orally bioavailable fraction is distributed again in the lungs where it is still active (Allen *et al.*, 2003). Although inhaler devices are designed to deliver drugs locally into the lungs, a very large proportion of the dose (60–90 %) is deposited in the mouth and pharynx and enters the gastrointestinal tract. For all these reasons, corticosteroids themselves have been adapted to substantially reduce the oral uptake. Corticosteroids that are administered orally such as prednisolone, methylprednisolone, and dexamethasone have oral bioavailability greater than 80 %. Beclomethasone dipropionate is also well absorbed from the gut, having an oral bioavailability of 41 %. The development of budesonide represented a significant advance, where the oral bioavailability was reduced to 11 %. But the most recent generation of drugs, fluticasone propionate, ciclesonide, and mometasone furoate, have an oral bioavailability lower than 1 %. Thus essentially all the systemic exposure from these compounds results from lung to blood passage (Biggadike *et al.*, 2004).

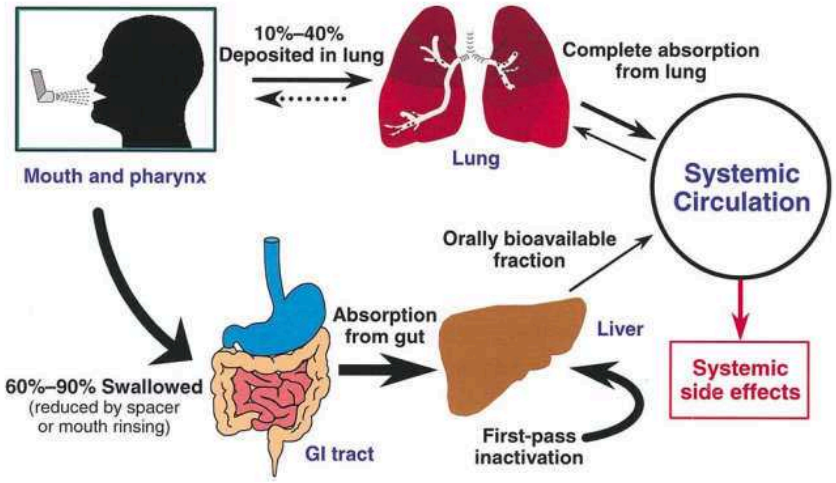

Figure 4. The fate of inhaled corticosteroids (Allen *et al.*, 2003).

As described in Figure 4, another fraction of the ICS appears in the systemic circulation. Due to their high lipophilicity, corticosteroids are passively diffusing across biological membranes. This is the reason why they are transported to the circulation. This ability of passive diffusion is however essential since,

to be efficient, ICS must be able to diffuse across cellular membranes to reach the intracellular corticosteroid receptors (Allen *et al.*, 2003).

Structure-activity relationships have been used to study and select potential GCs modifications to improve lung retention and minimize systemic adverse effects. Typical examples are the so-called nitro-steroids, in which nitric oxide (NO) is associated with GCs by an aliphatic or aromatic linker molecule. NO, which is known to enhance the anti-inflammatory effects of GCs, is slowly released from these drugs. NO-prednisolone (NCX-1015) presents 10-fold stronger anti-inflammatory effects but also fewer adverse effects on the bone compartment compared to conventional prednisolone in murine arthritis models (Strehl et Buttgereit, 2013). Other common strategy is the use of corticosteroid prodrugs. Between the available inhaled corticosteroids until 2003, beclomethasone dipropionate was the only prodrug. Inactive in its native form, it requires metabolization to beclomethasone-17-monopropionate before acquiring activity. However, once activated, beclomethasone-17-monopropionate has one of the highest receptor affinities of any corticosteroid, approximately 13.5-fold greater than dexamethasone, the standard for measuring corticosteroid activity. In the last years, prednisolone and ciclesonide were also approved as prodrugs to respiratory diseases (Chopra *et al.*, 2012).

There are several evidences that budesonide undergoes rapid, extensive and reversible intracellular esterification, probably contributing to its retention and prolonged duration of action. Budesonide oleate, palmitate, linoleate, palmitoleate, and arachidonate were identified as metabolites after bud administration. These fatty acid esters are inactive, however, they are gradually hydrolyzed by intracellular lipases and free budesonide is released. A balance between bud and these pharmacologically inactive lipoidal conjugates is probably established in tissues on repeated exposure to budesonide (Brattsand and Miller-Larsson, 2003 ; Brink *et al*., 2008 ; Edsbäcker and Brattsand, 2002 ; Miller-Larsson *et al.*, 2000 ; Tunek *et al.*, 1997).

3.2.3 Immunotherapy

As previously presented, inhaled corticosteroids are important in managing symptoms and exacerbations in asthma and COPD. However, for patients with severe disease, the efficiency of these drugs is often suboptimal. During the last 30 years, the development of therapeutic antibodies has raised very significantly. This rapid progress has seen biologics becoming an important pillar for treating several diseases particularly, patients with autoimmune and inflammatory diseases (Nixon *et al.*, 2017).

New biologics that target eosinophilic inflammation have been used as adjunctive therapy to corticosteroids and have proven beneficial in the treatment of asthma. Different type of antibodies against Interleukin-5 (IL-5) or its receptor have been designed and all of them are present at different clinical stages or on the market. IL-5 is a proinflammatory cytokine that plays a crucial role in the maturation, recruitment, proliferation and tissue migration of eosinophils (Rothenberg et Hogan, 2006 ; Stirling *et al.*, 2001). IL-5 is also involved in cell survival and prevention of eosinophil apoptosis (Rothenberg and Hogan, 2006).

Two antibodies that antagonize IL-5 Nucala® (mepolizumab) and Cinquair® (reslizumab) are today in clinics. They bind to free IL-5 and block its fixation to the IL-5R α chain of the receptor. A third antibody Fasenra® (benralizumab) has been developed. This antibody binds to the alpha chain of the IL-5 receptor on the eosinophil surface to inhibit their proliferation (Hom and Pisano, 2017). All three antibodies reduce eosinophilic inflammation to various degrees, which has been demonstrated to correlate with reduction in acute exacerbations and improvement in lung function and asthma control in some studies (Nixon *et al.*, 2017). On the contrary of the two other anti-IL-5 antibodies, Benralizumab, by binding to the IL-5R α chain, can block the typical IL-5/IL5R activation pathway. The α chain of IL-5R exclusively binds to IL-5 and its expression is found mainly on eosinophils and basophils in humans. Because of the inhibition of IL-5 pathway, an impact on proliferation and maturation of eosinophil precursors in bone marrow, and on the migration, activation and apoptosis of mature cells at the site of inflammation is found. Benralizumab is also characterized by high affinity for the Fcγ receptor found on cells involved in apoptosis such as natural killers lymphocytes, macrophages and neutrophils. This explains properties of benralizumab to target circulating, as well as tissue-resident eosinophils. This monoclonal antibody induces depletion of eosinophils in circulation, bone marrow and target tissues, which is in contrast with the mechanisms of action of other anti-IL-5 biologics (mepolizumab and reslizumab) which block the activation of eosinophils by neutralizing circulating IL-5 without any impact on resident eosinophils apoptosis (Kupczyk and Kuna, 2018).

These drugs reduce eosinophil numbers and diminish asthma exacerbations in severe asthma and in the same time allow to decrease oral steroid use. Additional monoclonal antibodies targeting both the innate and the adaptive immune pathways are currently under development. These drugs are very expensive but are now available for the treatment of severe asthma, which represents 3–10 % of the population of adults with asthma (Weiss, 2017).

Other monoclonal antibodies has been evaluated in asthma such as anti-TSLP (AMG157/MEDI-9929), which target the cytokine thymic stromal lymphopoietin (TSLP) known to mediate immune reaction in

patients with asthma (Corren *et al.*, 2017). Others examples of targets for antibodies are anti-IgE (omalizumab, ligelizumab), anti-IL-13 (tralokinumab, lebrikizumab), and anti-IL-4Rα (dupilumab) (Bel and Brinke, 2017 ; Gauvreau *et al.*, 2016 ; Korenblat *et al.*, 2017 ; Maltby *et al.*, 2017 ; Nixon *et al.*, 2017 ; Panettieri *et al.*, 2018 ; Vatrella *et al.*, 2014). Omalizumab (Xolair, Genentech) is a recombinant humanized IgG1 monoclonal anti-IgE antibody that binds to the IgE molecule at the same epitope on the Fc region that binds to FcεRI. This design means that omalizumab is not anaphylactogenic, since it cannot interact with IgE that is already bound to cell surfaces and thus cannot induce degranulation of mast cells or basophils. Instead, omalizumab binds to circulating IgE, regardless of allergen specificity, forming small, biologically inert IgE–anti-IgE complexes without activating the complement cascade. A 89 to 99% reduction in free serum IgE (i.e., IgE not bound to omalizumab) occurs soon after the administration of omalizumab, and low levels persist throughout treatment with appropriate doses (Strunk and Bloomberg, 2006).

3.2.4 Devices for particle deposition

The development of the first atomizers devices occurred in the last half 19th century, a time with unprecedented innovation in pharmaceutical aerosol delivery technologies. The introduction of nebulizers, pressurized metered dose inhalers (pMDIs), dry powder inhalers (DPIs), advances in the commercialization of asthma cigarettes, and a number of other delivery technologies dramatically reformulated the practice of delivering drugs to the respiratory tract (Stein and Thiel, 2017).

The choice of correct inhaler devices plays an important role in successful treatment, and many systems have been developed in the last decades. There are two main groups of inhaler devices: pMDI and DPI. Each has its own advantages, disadvantages and limitations in regard to the type of formulation that can be used, the types of drugs, and the amount of respirable dose that can be generated from these devices (Muralidharan *et al.*, 2015; Chorão *et al.*, 2014).

The pMDI was initially used for the administration of the non-selective beta-agonists adrenaline and isoprenaline. However, the epidemic of asthma deaths which occurred in the 1960s led to these drugs being outdated and replaced by the selective short-acting beta-agonist salbutamol, and the first ICS beclomethasone (Crompton, 2006). The pMDI is still the most frequently prescribed device worldwide, but even after repeated training many patients fail to use it correctly. In addition, the correct technique can be lost over time. Although several improvements in pMDIs such as a change in the propellant and actuation have resulted in improvements in lung deposition DPIs are easier to use (Virchow *et al.*, 2008).

DPIs are devices through which a dry powder formulation of an active drug is delivered for local or systemic effect via the pulmonary route. A wide range of DPI devices are currently available on the market to deliver drugs into lungs with the goal to maximize drug delivery with low variability. Successful delivery of drugs into the deep lungs depends both on the powder formulations and the device performance. However, these devices also have limitations such as dependency of drug particle size on flow rate and loss of the metered dose if the patient exhales through the device before inhaling (Islam and Gladki, 2008; Virchow *et al.*, 2008).

Dry powders for inhalation are formulated either as loose agglomerates of micronized drug particles with aerodynamic particle sizes lower than 5 µm or as carrier-based interactive mixtures with micronized drug particles adhered onto the surface of large lactose carriers. For local respiratory drug delivery, a particle aerodynamic size of 2–5 µm yields optimal benefit, whereas for systemic effects particle aerodynamic size of lower than 2 µm is needed for drug deposition in the small peripheral airways. Particles greater than 5 µm may also result in systemic effects due to impaction in the throat (i.e., oropharyngeal delivery) and further oral absorption (Islam and Gladki, 2008). Improvements in using inhalation devices more efficiently, in inhaler design for supporting patient compliance, and advances in inhaler technology to insure drug delivery to the lungs, have the potential to improve asthma and COPD management and control. New and advanced devices are considered being helpful to minimize the most important problems patients have with current DPIs (Virchow *et al.*, 2008).

Although a great emphasis is placed on the proper inhalation technique, most of the patients with both asthma and COPD still mishandle their inhalers. It has been reported that 4-94 % of patients make errors during inhalation. Improper drug inhalation is related to a variety of factors, including the type and number of inhalers used duration of the device usage, patient's level of education, age, sex and obesity. Improper inhaler use results in an inadequate drug intake and its reduced lung deposition, worsening of disease control as well as further compliance, which is poorer than in patients that inhale properly. For these reasons, it has been emphasized that there is a continuous need to control and re-train patients in their inhalation technique (Luczak-Wozniak *et al.*, 2018).

4 OBSTACLES AND TARGETS TO DRUG DELIVERY IN ASTHMA AND COPD

4.1 Obstacles to drug delivery in asthma and COPD

Successful delivery of inhaled particles depends mainly on particle size and particle density, and therefore the mass median aerodynamic diameter. The aerodynamic diameter is defined as the produce of the geometric diameter of the particle/droplet - its actual diameter - by the square root of the particle/droplet density (Colombo *et al.*, 2013 ; Edwards *et al.*, 1997 ; He *et al.*, 2007 ; von Wichert and Seifart, 2005):

$$d_{aer} = d_g\sqrt{\rho}$$

Depending on their aerodynamic diameter, once inhaled particles/droplets will deposit in different regions of the lungs, as described in Figure 5. According to pharmacopoeias, one can define the fine particle fraction (FPF) which corresponds to percentage of the administered dose of the drug actually reaching the lungs, as the dose with aerodynamic diameter below 5 µm divided by the initial dose (Pharmacopoeia E., 2019).

Particle diameter is the primary factor determining pulmonary deposition of aerosols in the various regions of the respiratory tract. The evidence available in the literature confirms that smaller particles delivered to the lungs are deposited in the smaller airways as opposed to the larger airways. There are five different mechanisms by which particle deposition can occur in the lungs: inertial impaction, sedimentation, diffusion, interception (related to particle shape, e.g. elongated particles) and electrostatic precipitation (related to electrostatic charges) (Carvalho *et al.*, 2011).

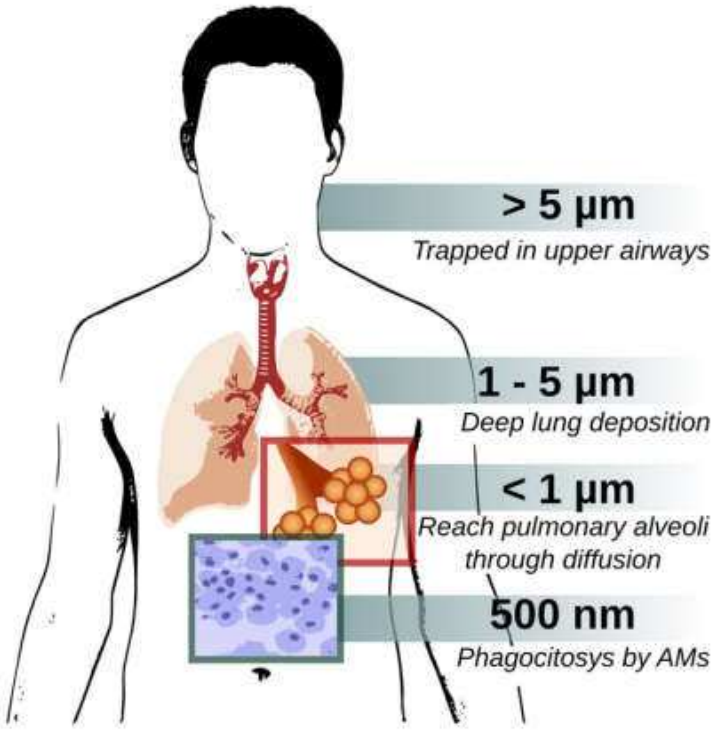

Figure 5. Influence of particle size in lung deposition and phagocytosis by the alveolar macrophages (Costa *et al.*, 2016).

Other factors that affect the deposition of aerosolized drugs are airflow velocity, airway geometry, degree of humidity and the mechanisms of mucociliary clearance. The increase in inspiratory flow reduces the retention time of particles in the airway, therefore, the effects of gravity and Brownian movement will be much smaller. In pathologies such as chronic bronchitis or asthma, which may alter the pulmonary architecture with the appearance of bronchoconstriction, inflammation or accumulation of secretion, deposition of aerosolized drugs is modified. The smaller caliber of the airway increases air velocity, producing turbulence in places where the flow is generally laminar. Airway obstruction also means that air tends to be moved to unobstructed areas and therefore particles also tend to be deposited mostly in healthy lung. In addition, particles may be hygroscopic to a greater or lesser degree. Hygroscopicity means that particles can get bigger or smaller when entering the airway, with the consequent modification in the deposition pattern compared to what is initially expected. A last, a factor to be considered is the mucociliary clearance, where once deposited in the airways, the particles can be carried by the mucociliary system, degraded or absorbed into the systemic circulation or the lymph ducts (Tena and Clará, 2012).

Airway mucus is a complex adhesive and viscoelastic hydrogel composed primarily of water (~95 %), glycoproteins (mucins, ~2–5 % w/v), lipids, DNA, non-mucin proteins, and cell debris. Since mucus

production is a primary defense mechanism for maintaining lung health, the overproduction of mucin (the chief glycoprotein component of mucus) is a related pathological feature in asthma, COPD, lung cancer and cystic fibrosis (Evans and Koo, 2009; Murgia *et al.*, 2018). Mucus gel is composed of highly cross-linked mucin fibers by hydrophobic interactions and disulfides link, creating a dense porous structure (Liu *et al.*, 2015). The highly adhesive nature of mucus is likely due to a high density of negatively charged glycans that contain both strong proton acceptor and donor groups and to hydrophobic naked protein domains that are further coated with lipids (Wang *et al.*, 2008).

Such complex biochemical composition and continuous turnover confer to mucus the defending ability to adsorb a wide range of molecules and particles, including drugs, and other potentially harmful entities like pathogens, toxins, and pollutants. However, the protective function of the mucus also hampers the diffusion of drugs and nanomedicines, which dramatically reduces their efficiency (Murgia *et al.*, 2018; Wu *et al.*, 2018; Taherali *et al.*, 2018). Since the lung provides a reservoir that limits rapid diffusion of molecules away from the site of delivery, proteins, peptides, and small molecules are all readily absorbed across the pulmonary epithelium, at a rate dependent upon the properties of the drug and the route of transport. For small molecules below 1000 Da in molecular weight, physicochemical properties such as lipophilicity, molecular polar surface area, and hydrogen bonding potential appear to control the rate of pulmonary absorption (Gursahani *et al.*, 2009). In numerous pulmonary diseases such as COPD, mucus stagnates and accumulates in the airways, leading to bacterial colonization, airway inflammation, tissue destruction, and, eventually, respiratory failure. Mechanisms of mucociliary dysfunction include aberrant overproduction of mucus, leading to accumulation on the surfaces of the airways (Fernández-Blanco *et al.*, 2018).

Several strategies have been used to modify the surface of nanocarriers for an improved drug delivery to mucosal tissues (Figure 6). Mucoadhesive drug delivery systems provide an increased interaction with the mucus layer and consequently improve the residence time of particles in the targeted mucosal sites, probably because the positively charged particles can bind with negatively charged mucin via electrostatic attraction (Khutoryanskiy, 2018 ; Wu *et al.*, 2018). On the other hand, mucus-penetration strategies mediated by stealth drug nanocarriers which comply with the size and surface chemistry requirements of the mucus barrier have gained growing attention. Thereby, to penetrate mucus, nanocarriers must be small enough to avoid steric obstruction in spite of NPs with larger size are preferred to improve drug loading and release kinetics (Liu *et al.*, 2015). Coating nanoparticles with PEG (PEGylation) is one of the strategies to enhance their penetration through mucus. PEGylation was originally developed to prolong the systemic circulation time of proteins and nanoparticles by protecting their surface from aggregation, opsonization, and phagocytosis (Murgia *et al.*, 2018).

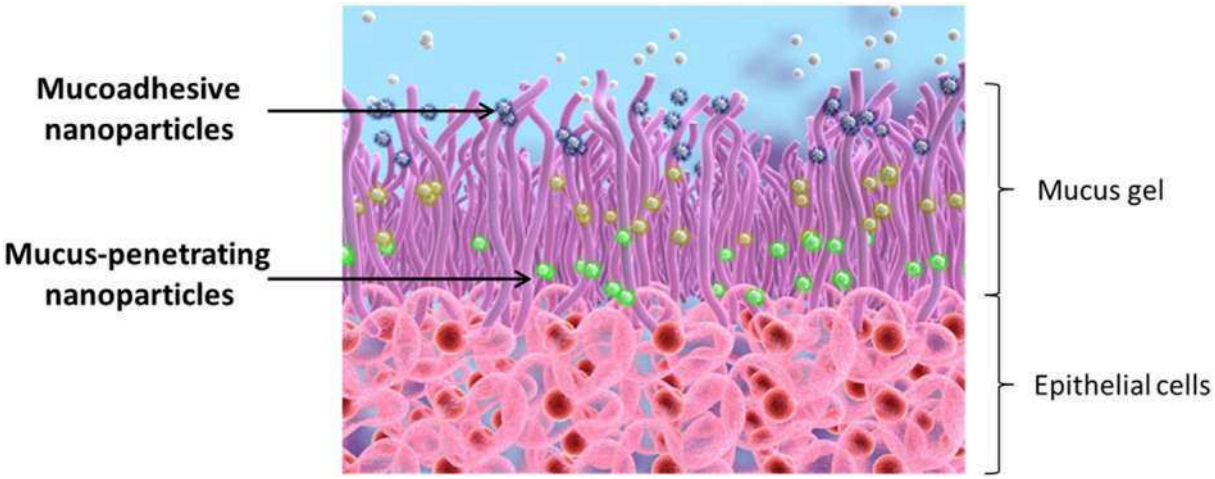

Figure 6. Schematic illustration of nanoparticles penetration through mucus layer (Khutoryanskiy, 2018).

The PEGylated nanoparticles have hydrophilic and near neutrally-charged surfaces that reduce mucoadhesion by preventing hydrophobic or electrostatic interactions, which mimics the ability of pathogenic microorganisms to pass through mucus. Additionally, the molecular weight (Mw) of PEG will define if the nanoparticles can be mucus-penetrating (when Mw is 2,000 Da) or mucoadhesive (when Mw is 10,000 Da) (Khutoryanskiy, 2018). To determine the effect of PEG Mw on the interactions of coated particles with mucus, Wang et col (2008) studied the diffusion rate of NPs modified by different PEG Mw (2, 5 and 10 kDa) and densities (42 %, 65 % and 69 %) of PEG. The results showed that low Mw (e.g. 2 kDa) and high-density (e.g. 65-70 %) PEG coating can facilitate nanoparticle penetration through mucus.

Another potential obstacle to drug delivery in obstructive lung diseases is the evidence of surfactant dysfunctions related to COPD, which might be one of the mechanisms leading to increased airway resistance (Hohlfeld *et al*, 1997). Pulmonary surfactant is a lipid-protein complex essential to reduce surface tension at the air-liquid interface, and lack or dysfunction of this system is associated with severe respiratory pathologies, which are in some cases treated by supplementation with exogenous surfactant materials (Autilio and Pérez-Gil, 2018). There are four types of surfactant-associated proteins, SP-A, SP-B, SP-C and SP-D, among which SP-A and SP-D have important host defense properties, and SP-B and SP-C are intensely hydrophobic and interact with surfactant phospholipids to optimize surface tension reduction function (Devendra and Spragg, 2002). Lower levels of surfactant-associated proteins have been associated to emphysematous changes, and the use of inhaled corticosteroids appears to increase SP levels in the lung (Sims *et al.*, 2008 ; Um *et al.*, 2013).

4.2 Targets to drug delivery in asthma and COPD

In the previous topics, we have discussed the central role of the inflammatory process in asthma and COPD. Even though these diseases have specific characteristics and different local inflammation process, with asthma affecting mainly the larger conducting airways and COPD the small airways and lung parenchyma, they have in common the airway obstruction with recruitment and activation of inflammatory cells, followed by changes in the structural cells of the lung. Both are also characterized by an increased expression of inflammatory proteins including cytokines, chemokines, growth factors, enzymes, receptors and adhesion molecules (Barnes, 2011 ; Caramori and Adcock, 2003).

The knowledge of the role of the macrophages in chronic inflammatory diseases is essential in the development of strategies for targeted delivery. In COPD, there are many evidences that lung macrophages orchestrate inflammation through the release of chemokines that attract neutrophils, monocytes and T cells, with the release of several proteases. By contrast, in asthma, it is possible that alveolar macrophages are inappropriately activated and are implicated in the development and progression of the disease (Pappas *et al.*, 2013). Macrophages also express receptors that activate the cells to produce cytokines, such as mannose receptors, which is recognized as an exclusive transmembrane receptor that binds and internalizes exogenous and endogenous materials (Fujiwara and Kobayashi, 2005 ; Gazi and Martinez-Pomares, 2009 ; Martinez-Pomares, 2012 ; Shepherd *et al.*, 1984 ; Taylor, 2001).

Due to these specific features directly related to the pulmonary pathway, we decided in this introduction to explore the targeting potential of alveolar macrophages and mannose receptors in the glucocorticoid treatment of asthma and COPD.

4.2.1 Macrophages

Macrophages are a major cellular component of the innate immune system and play an important role in the recognition of microbes, particulates, immunogens, and to the regulation of inflammatory responses. In lungs, macrophages react with soluble proteins that bind microbial products in order to remove pathogens and particles and to maintain the sterility of the airway tract (Pappas *et al.*, 2013).

Alveolar macrophages are distinct from the macrophages that reside between the airway epithelium and the blood vessels, which implies that a greater specialization of macrophage populations occurs in the lungs. They are also long-lived, with a turnover rate of only approximately 40 % in 1 year. In the case of lung tissue and peritoneal macrophages, the turnover occurs within a period of 21 days (Barnes, 2004; Hussell and Bell, 2014).

These alveolar macrophages play a critical role in the pathophysiology of COPD and are a major target for anti-inflammatory therapy. Macrophage numbers are markedly increased in the lung and alveolar space of patients with asthma and COPD and are localized close to sites of alveolar destruction. Specifically in the case of COPD, alveolar macrophages appears to be resistant to the anti-inflammatory effects of corticosteroids, and alternative anti-inflammatory therapies that inhibit macrophages are therefore needed (Barnes, 2004; Hussell and Bell, 2014). Figure 7 describes the alveolar macrophage activation and the initiation of inflammation.

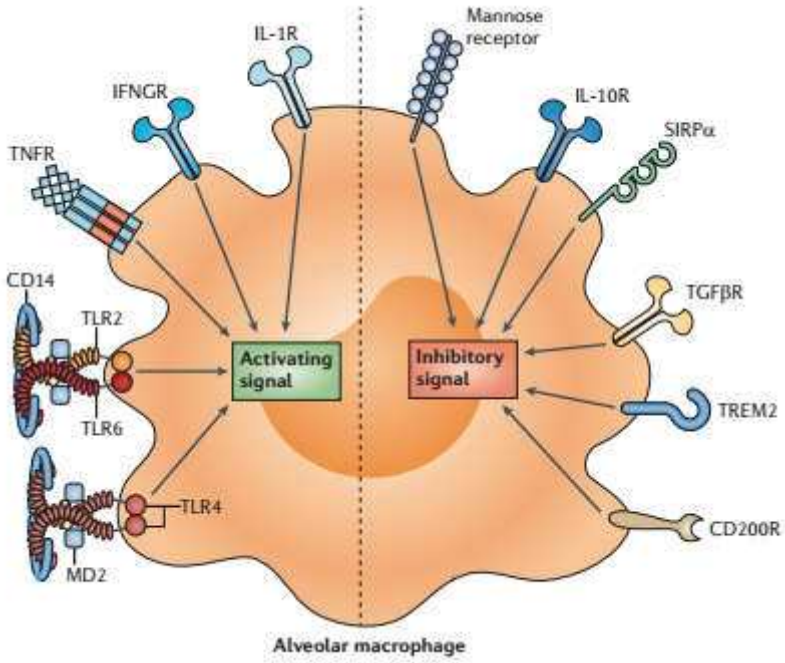

Figure 7. Alveolar macrophage activation and the initiation of inflammation, which involves a complex balancing act between activating and repressing signals (Hussell and Bell, 2014).

The most common and potent drugs used in macrophage mediated diseases treatment often induce unwanted side effects, when applied as a free form, due to the necessity of high doses to induce a satisfactory effect. This could result in their systemic spreading, a lack of bioavailability at the desired sites, and a short half-life. Therefore, the use of drug-loaded nanoparticles represents a good alternative to avoid, or at least decrease, side effects and increase efficacy (Chellat *et al.*, 2005).

4.2.2 Mannose receptor

The mannose receptor (MR, also known as CD206) is a 175 kDa transmembrane protein of the C-type lectin family (carbohydrate-binding) expressed by dendritic cells and macrophages, including alveolar macrophages. MR interacts with glycoproteins and glycolipids that are found on the surface of pathogens, and most of MR is intracellular. Recognition of unopsonized bacteria results in the

suppression of alveolar macrophages in humans, rats, mice and rabbits — an effect that is dependent on the expression of mannose receptors by these cells (Hussell and Bell, 2014; Martinez-Pomares, 2012).

This receptor is exclusively expressed on the surface of alveolar macrophages that can recognize mannose terminal molecules with high affinity. Based on this knowledge, several suitable strategies have been developed for macrophage selective targeting systems. However, the success of macrophage-selective delivery systems is directly connected on the ability to deliver drugs or agents to the intracellular site for the desired pharmacological action. Inadequate specificity for macrophages and poor internalization of drug-carrier conjugates are critical obstacles to their success (Yeeprae *et al.*, 2006).

A study proposed by Wileman *et al.* (1985) showed the mechanistic uptake and transport of mannosylated ligands by alveolar macrophages, following the endocytic pathway taken by mannose-terminated glycoproteins. Soon after entering the cell, these ligands pass through a vesicle which has a density intermediate between that of the plasma membrane and secondary lysosomes. Dissociation of mannose-terminating ligands from the mannose receptor takes place within this compartment, suggesting intravesicular acidification.

Zhang *et al*. (2005) have studied the negative regulatory role of mannose receptors on human alveolar macrophage proinflammatory cytokine release *in vitro*, and the results suggest that these receptors may suppress select proinflammatory cytokine release and may serve to regulate the innate inflammatory responses to infectious challenge in the lungs.

It is known that the efficiency of ligand recognition depends on the ligand–receptor interaction, and multivalent ligands with a “cluster effect” showed higher binding affinity to their counter receptors than monovalent ligand. The drug internalization by alveolar macrophages and consequently an increase in accumulation on lung tissue can be reached using nanosystems with surface modification. In this way, mannose is one of the most common ligands used to decorate the surfaces, once the alveolar macrophages express mannose receptors on its surface (Yeeprae *et al.*, 2006; Costa *et al.*, 2018).

5 NANOPARTICULATE DRUG DELIVERY IN ASTHMA AND COPD

In recent decades, colloidal drug carriers received great attention. Liposomes were the first nanotechnology-based drug delivery system discovered in the 1960s. In 1976, the first controlled release polymer drug delivery system was reported and in 1990 the lipid systems carriers became a new strategy to drug delivery as they entered in clinics. However, new propositions and designs were still made for developing sustained drug delivery and improving carrier characteristics (Wang and Rempel, 2015).

Nanoparticles can be administered via different routes of administration as parenteral, oral, intraocular, transdermal or pulmonary. Aerosol therapy using particulate drug delivery systems (DDS) is becoming a popular method to provide therapies or diagnostic compounds either locally or systemically. This is due to the large alveolar surface area suitable for drug absorption, thickness of the epithelial barrier, extensive vascularization and relatively low proteolytic activity in the alveolar space compared to other sites of administration and the absence of the first passage metabolism. Lung delivery has only been achieved with particles in the micrometer range. Delivery of nanoparticles to the lungs is however an attractive concept because it can support the targeting of different cells and control as well the kinetics of release inducing long term effect (Azarmi *et al.*, 2008). As discussed above, particle size of medically used nanoparticles is nevertheless too small to be suitable for direct pulmonary delivery. This section will approach the possibilities of delivering optimally nanoparticle formulations for deep lung delivery by designing proper carrier delivery systems.

The pharmacokinetics and pharmacodynamics of a drug are highly dependent on its physical and chemical features and are influenced by the type of formulation used to deliver it. Encapsulating drugs into nanoparticulate systems can modulate and improve their performance to an extent not achievable by conventional formulations. For example, these systems can increase drug solubility, protect them from degradation, enhance their epithelial absorption, target the drugs to specific cells/tissues/organs, releasing them in a controlled manner as a response to a specific stimulus, and enhance their uptake by cells (Andrade *et al.*, 2013). Other important factor is that the best place to deposit drugs in the lungs depends on the disease type. In asthma, for example, drug delivery to the upper airways is needed, while for alveolar lung diseases, such as chronic obstructive pulmonary disease (COPD), it is important to have drug deposition in the deep lung rather than the upper airways (Rijt *et al.*, 2014).

Recent advances in nanotechnology open a door for enhancing the efficacy of inhalation treatment of different lung diseases. The application of nanotechnology to the design of drug delivery systems for effective delivery of therapeutics specifically to tissues and cells affected by the disease allows for

enhanced treatment outcomes and prevention of severe adverse side effects upon tissues and cells, including those in the lungs (Kuzmov and Minko, 2015).

5.1 Liposomes

Liposomes are artificial vesicles formed of lipid bilayers basically composed of phospholipids and cholesterol, thus enabling to encapsulate both hydrophilic and hydrophobic drugs. The polar head and hydrophobic tail of phospholipids allow the formation of lipid bilayers, whereas cholesterol rigidifies and stabilizes the liposome membrane. With this lipidic composition, liposomes may modulate drug release (Loira-Pastoriza *et al.*, 2014).

Liposomes offer several advantages for pulmonary drug delivery. They can serve as a solubilization matrix for poorly soluble agents, act as a pulmonary sustained release reservoir, and facilitate intracellular delivery of drugs, specifically to alveolar macrophages. They also show good compatibility with lung surfactant components, low level of local irritation to lung tissue and, by consequence, reduced pulmonary toxicity (Parmar *et al.*, 2010). Indeed, it had already been demonstrated the efficacy and enhanced drug delivery by liposomes (Gonzalez-rothi and Schreier, 1995 ; Khan *et al.*, 2013 ; Parmar *et al.*, 2010 ; Rudokas *et al.*, 2016).

Budesonide was entrapped in several liposome formulations (Chennakesavulu *et al.*, 2018 ; Konduri *et al.*, 2003 ; Parmar *et al.*, 2010). In one of the most interesting study, the authors have developped budesonide encapsulated in sterically stabilized PEGylated liposomes and conventional liposomes for nebulization in an ovalbumin-sensitized mice model mimicking allergic asthma (Konduri *et al.*, 2003). They observed that weekly therapy with budesonide encapsulated in PEGylated liposomes was as effective as daily free budesonide therapy in decreasing lung inflammation and lowering eosinophil peroxidase activity, peripheral blood eosinophils, and total serum IgE levels. Weekly treatments with free budesonide, budesonide encapsulated in conventional liposomes, and empty stealth liposomes did not have comparable effects. However to obtain liposomes within dry powders, mostly freeze-drying was applied. In one study by Parmar *et al.* (2010), liposomes were prepared by lipid film hydration and freeze dried. When analyzed by transmission electron microscopy (TEM), liposomes appeared as bright spheres surrounded by dark thick layer showing large internal aqueous core, while freeze dried liposomes appeared as aggregated particles with lipids on the surface. Drug leakage was significantly less in freeze-dried liposomes compared to aqueous liposomes. The effectiveness of pulmonary delivery of colchicine and budesonide dry powder inhaler liposomes for Idiopathic pulmonary fibrosis was investigated by Chennakesavulu *et al.* (2018). Spherical liposomes with mean size below 100 nm were lyophilized using Mannitol as carrier and cryoprotectant, showing high

entrapment efficiency, a decrease in a number of inflammatory cells and a sustained drug release up to 24 hours.

Liposomes for inhalation were functionnalized with several ligands. Their delivery could improve the pharmacokinetics and increase lung retention (Marqués-Gallego and Kroon, 2014 ; Osman *et al.*, 2018). Exemples of liposome ligands that have been reported in the literature are mannose, chitosan, lectins, peptides, etc (Abu-Dahab *et al.*, 2001; Vyas *et al.*, 2000 ; Vyas *et al.*, 2007 ; Wijagkanalan *et al.*, 2008a ; Zaru *et al.*, 2009). As an exemple, Wijagkanalan *et al.*, (2008b) have demonstrated the efficient targeting of alveolar macrophages by mannosylated liposomes by increasing the mannose residues expressed on the surface of liposomes. They have shown that mannosylated liposomes with a high content of Mannose-C4-Chol exhibit high affinity for mannose receptors resulting in extensive uptake by alveolar macrophages after intratracheal administration.

The influence of liposome formulation on the ability of vesicles to penetrate a pathological mucus model obtained from COPD affected patients was evaluated by De Leo *et al.* (2018). In this study, they compared three different liposomes containing beclomethasone dipropionate: small Unilamellar Liposomes, Pluronic® F127-surface modified liposomes and PEG 2000PE-surface modified liposomes. All liposomes were stable in size both at 37°C and at 4°C, presented diameters in the range of 40-65 nm. Encapsulation efficiency was similar for PEGylated and pluronic-coated liposomes (around 80%), whereas plain liposomes presented results close to 100 %. Cell uptake studies showed a non-significant reduction in the internalization of PEGylated when compared with plain liposomes. Penetration studies of mucus from COPD patients showed that the PEGylated liposomes were the most mucus-penetrating vesicles without any local toxicity.

A different approach proposed by Li *et al.* (2017) was the use of surfactant protein A (SP-A) which has receptors on alveolar macrophages. These authors have firstly developed methylprednisolone (MPS) loaded into functionalized sterically stabilized unilamellar liposomes and then functionalized them through conjugation of surfactant protein A nanobodies. This latest liposome presented particle size of about 100 nm in diameter in average and a polydispersity index of 0.26, with unilamellar spherical morphology confirmed by cryo-TEM. *In vivo* imaging showed a significant lung accumulation of SP-A-coated liposomes. No significant liposome aggregation was observed in other organs, and particles with no active targeting presented little accumulation in lung tissue.

With the aim to evaluate safety and tolerability of liposomes, a study in healthy volunteers was realized by Waldrep *et al.* (2008). Low single doses of BDP dilauroylphosphatidyl choline (DLPC) liposome aerosol (0.56 ± 0.07 mg of BDP) were administered in 4 volunteers, while 6 were exposed to higher

doses (1.29 ± 0.14 mg of BDP). These doses reproduce approximately the dosages of this glucocorticoid used with metered-dose inhalers. Clinical observations, clinical chemistry, spirometry and hematology were monitored, with no adverse events observed.

5.2 Lipid nanoparticles

In 1990, lipid nanoparticles (LNPs) have been introduced as alternative to traditional carriers such as polymeric nanoparticles and liposomes. This new lipid nanoparticle-based formulation was called solid lipid nanoparticles (SLNs) and presented as advantages a high stability *in vivo* as they remained solid at body temperature, improved bioavailability of poorly water-soluble molecules, avoidance of organic solvents in production methods and use of biodegradable physiological lipids which decreases the danger of acute and chronic toxicity. However, potential problems associated with SLNs, such as limited drug loading ability, adjustment of the drug release profile and possible expulsion of the drug during storage were detected, probably due the reduced drug mobility in the solid lipid state compared with the oily phase, thereby enhancing the controlled release of loaded drugs. To avoid or minimize these issues, a second generation of nanostructured lipid carriers (NLCs) was developed starting from 2000. In these particles the matrix is composed not only of one solid lipid, but of a blend of a solid and a liquid lipid (e.g. oil) (Beloqui *et al.*, 2016 ; Garud *et al.*, 2012 ; Müller *et al.*, 2011 ; Müller, *et al.*, 2002 ; Puri *et al.*, 2009).

NLCs, like SLNs, are colloidal particles that typically range in size from 100 to 500 nm. A blend of solid- and liquid-phase lipids, NLCs are generally solid at temperatures above 40°C. They also have the advantage of a lower cost and are easily scaled up, with the use of high-pressure homogenization process. In contrast to the lipid crystal matrix of SLN, the lipid matrix of NLC has an imperfect crystal or amorphous structure, which allows the loading of drugs in both the molecular form and in clustered aggregates. As a result, NLCs show increased drug loading and less pronounced drug expulsion by avoiding a crystalline structure. Encapsulation of drug solutions into lipid nanoparticles can be performed using numerous methods, including high-pressure homogenization, microemulsion formation, emulsification solvent evaporation (precipitation), solvent injection (or solvent displacement), phase inversion, the multiple emulsion technique, ultrasonication, and the membrane contractor technique (Puri *et al.*, 2009). Figure 8 describes the differences between liposomes, SLNs and NLCs (Chuang *et al.*, 2018).

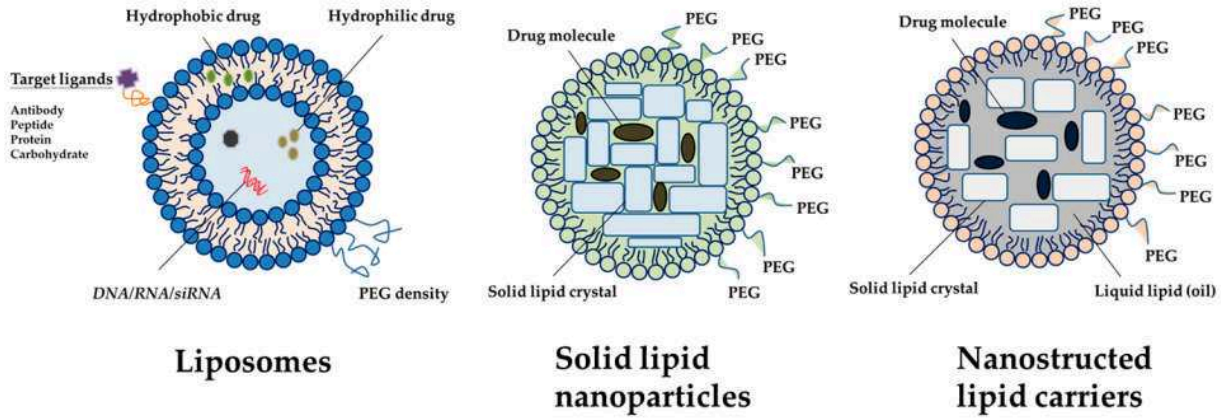

Figure 8: Scheme of different types of lipid nanocarrier systems. Liposomes are typically composed of natural phospholipids, a major component of most biological membranes. Solid lipid nanoparticles are formed by a mixture of solid lipids dispersed in inner cores. Nanostructured lipid carriers are constituted by the mixture of solid lipids and liquid lipids in the cores. PEG: Polyethylene Glycol. (Adapted from Chuang *et al.*, 2018).

Lipid nanoparticles show interesting features concerning therapeutic purposes. They have higher drug loading capacity, higher stability and may not require the use of organic solvents during production, in contrast to liposomes and polymeric NPs. On the other hand, like liposomes and most polymeric NPs, these nanocarriers are biocompatible and can be produced with a size and morphology appropriate to the lung targeting and deposition, thus being considered a viable strategy for pulmonary delivery of drugs. It is also possible to modify the surface NLCs to achieve active targeting of the alveolar macrophages (AMs), using for example mannose as ligand. Their main characteristic is the fact that they are prepared with physiologically well-tolerated lipids, excipients generally recognized as safe (GRAS) status for oral and topical administration, which decreases the cytotoxicity and is a pre-requisite for the introduction of a product to the pharmaceutical market (Costa *et al.*, 2016 ; Costa *et al.*, 2018 ; Severino *et al.*, 2012).

Lipid nanoparticles are also considered as a versatile nanoparticulate delivery system for different routes of administration. Areas of highest interest are oral and topical delivery, subcutaneous, intramuscular and intravenous injections, ocular applications and pulmonary targeting (Müller *et al.*, 2011 ; Müller *et al.*, 2002). Considering pulmonary delivery, an increasing number of lipid nanocarriers have been proposed toward different lung diseases, mostly using lipid nanoparticles in a dry powder form inhalation (Islan *et al.*, 2016 ; Kaczmarek *et al.*, 2017 ; Liu *et al.*, 2008 ; Sahu *et al.*, 2014 ; Varshosaz *et al.*, 2013 ; Zhao *et al.*, 2017).

Concerning GCs, Shah *et al.*, (2013) have developed SLN DPI formulations containing mometasone furoate (MF), a potent synthetic glucocorticoid used in long term management of asthma and COPD.

MF-SLNs prepared by solvent diffusion method and dried using lactose as carrier presented mean particle size of about 225 nm before lyophilization, increasing to 327 nm after this process. *In vitro* drug release was 93 % in 24 hours from SLN. The pulmonary deposition pattern for MF-SLN DPI formulation was compared with conventional MF DPI formulations, showing a delivered dose uniformity of 94 ± 2 %. Compared to conventional DPI formulations, MF-SLN DPI formulations exhibited a controlled release profile, uniformity in drug content/dose and higher pulmonary deposition.

Jaafar-Maalej *et al.* (2011) have proposed beclomethasone dipropionate (BDP) lipid nanoparticles (LN) for administration via the pulmonary route. Solid lipid nanoparticles (SLN) and nanostructured lipid carriers (NLC) prepared by high-shear homogenization method produced lipidic particles in the nanometer size range with narrow particle size distribution (PdI below 0.25). SLN showed particles sizes from 193 to 218 nm, slightly larger than NLC (167-185 nm), while all formulations presented a good colloidal stability as demonstrated by zeta-potential values of in the range -40 mV/-25 mV. High encapsulation efficiency was found with values ranging from 80.46 ± 1.79 % to 89.88 ± 2.64 % for SLN and from 97.23 ± 2.34 % to 99.56 ± 1.81 % for NLC as it was expected because lipids containing fatty acids of different chain lengths (stearic acid C18) form less perfect crystals with many imperfections, providing enough space to accommodate the drugs. *In vitro* drug release indicated for both formulations a sustained drug release, with a pseudo-burst effect at the initial 24 hours followed by a sustained release at a constant rate. Lastly, aerosolization and subsequent cascade impaction measurements were realized, and similar aerodynamic diameters for both LN founded confirm that nanoparticles formulation did not significantly influence the aerosol droplet size. FPF were also similar, proving that SLN and NLC were efficiently nebulized providing aerosols of a suitable particle size for BDP deep lung delivery.

The effects of formulation and processing parameters on particle size of prepared SLNs was evaluated by Esmaeili *et al.* (2016). Budesonide-loaded solid lipid nanoparticles (Bud-SLNs) were optimized and the drug concentration was fixed at 0.5 mg/mL to represent the concentration of commercially available suspension of budesonide (Pulmicort Respules®). Bud-SLNs were prepared using optimized parameters, resulting in spherical particles with size of 176 nm (SEM) and entrapment efficiency of budesonide in SLNs of 97 %. Drug release studies showed a constant rate during 24 h, where nearly all the drug has been released from bulk budesonide during the first 24 h, while still 20 % of the drug has remained in the nanoparticles when loaded on SLNs. Finally, results of aerodynamic behavior indicated an FPF of Bud-SLNs of 19.16 %, significantly higher than the commercial microsuspension (14.22 %), suggesting a possible improvement in lung deposition of the drug.

Like liposomes, new strategies concerning lipid nanoparticles functionalization have been extensively proposed in the last years. Sedaghat *et al.* (2016) have synthetized mannosylated lipopeptides as a method to targeting antigenic peptide and protein vaccines to the mannose receptor. Uptake studies in cells showed significant uptake and/or binding for lipopeptides containing mannose, and the lipopeptide without mannose when compared to the controls. Mannan inhibition assays demonstrated that uptake of the mannosylated and lipopeptides was receptor mediated, with surface plasmon resonance studies confirming high affinity of the mannosylated and lipopeptides vaccine constructs toward the mannose receptor.

Recently, Liu *et al.* (2018) have proposed a budesonide delivery system based on lipid-DNA micelles for the treatment of chronic inflammatory diseases such as asthma. As advantages, this system displays characteristics such as high drug loading, attributed to the interactions between the hydrophobic drugs and the hydrophobic core, and improved biocompatibility by reducing the dose. Additionally, it allows for easy modifications by taking advantage of DNA hybridization to endow ligand-receptor-mediated drug targeting properties, such as folic acid to sites of inflammation. A simple method was developed, where lipid-DNA amphiphile (called UU11mer were two alkyl chains coupled to the first two uracil bases on the 5'-UUTGGCGTCTT-3' sequence). UU11 mer forms micelles at low critical micelle concentration (CMC, 29 µM) and can load budesonide. Micelles with a narrow size distribution and regular shape both before and after budesonide loading were visualized by cryo-TEM, with diameter increasing slightly from 9.0 ± 1.2 nm to 10.3 ± 1.5 nm after budesonide loading. Anti-inflammatory activity was studied by its effect on IL-1β-induced release of IL-8 from hTERT immortalized human airway smooth muscle (ASM) cells. Nanoscale size suggests the non-specific pinocytotic uptake of UU11mer micelles into the cells, which is followed by endosomal escape and the release of budesonide to complex with the glucocorticoid receptors. Results obtained *in vitro* demonstrate that unloaded UU11mer micelles induce a 30 % inhibition of the IL-1β response, indicating some inhibitory effect by micelles themselves. Budesonide solubilized by UU11mer micelles inhibited IL-1β release in a concentration-dependent manner: at concentrations of 3, 30 and 300 nM, the inhibition was 84.7 %, 90.1 % and 92.2 %, respectively.

5.3 Polymer nanoparticles

Polymer nanoparticles (PNPs) are submicron-sized colloidal systems (1 to 1000 nm) used as delivery carriers for drug solubilization, stability, and specific targeting. The term PNP comprises any type of polymer nano-sized particles, but specifically polymer nanospheres and nanocapsules. Polymer nanospheres are matrix particles, particles whose entire mass is solid, serving as carriers for other biologically active molecules which may be either adsorbed at the sphere surface or encapsulated within the matrix. In contrast to polymer nanospheres, polymer nanocapsules are vesicular systems in which the bioactive agents are confined to an aqueous/oily liquid core and surrounded by the polymeric shell in which a drug can also be loaded (Kaur and Singh, 2014 ; Lu *et al.*, 2011). The differences between these carriers are described in Figure 9 (Lu *et al.*, 2011).

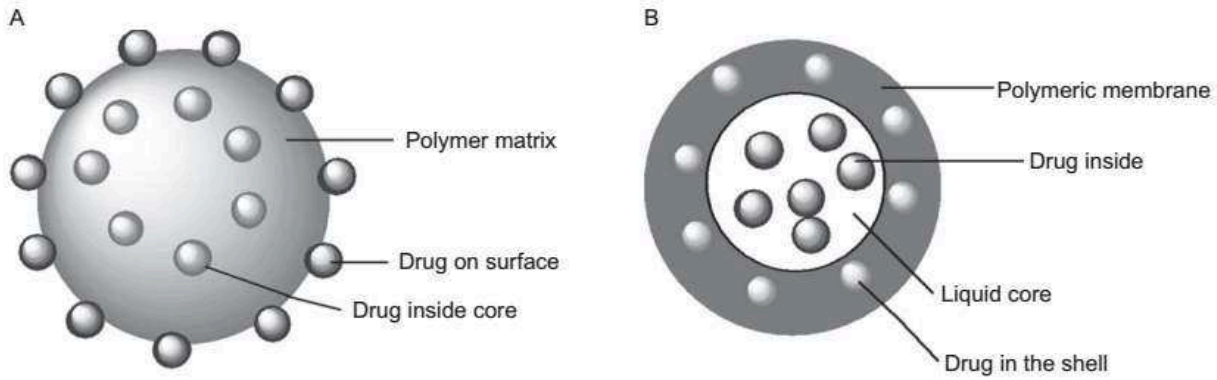

Figure 9. Polymer nanoparticles. A) Polymer nanospheres and B) Polymer nanocapsules (Lu *et al.*, 2011).

Polymers are the main component utilized for PNPs preparation. According to polymer source of origin, two major types of polymers are used for PNPs formulation: natural polymers and synthetic polymers. The most frequently used natural polymers in PNPs formulation are sodium alginate, albumin, chitosan and gelatin. In addition, several safe synthetic polymers are commonly used for PNPs formulation: polylactides (PLA), poly(lactide-*co*-glycolide)s (PLGA), polyglycolides, polyanhydrides, polyorthoesters (POE), polycyanoacrylates, polycaprolactone (PCL), poly(malic acid) (PMLA), polyglutamic acid (PGA), poly (methyl methacrylate) (PMMA), poly (N-vinyl pyrrolidone) (PVP), poly (vinyl alcohol) (PVA), polyacrylamide (PAM), polyethylene glycol (PEG), polyacrylic acid (PAA or Carbomer), and poly(methacrylic acid) (PMAA). The choice of polymer should be also based on biocompatibility and biodegradability characteristics, in order to guarantee the absence of immunogenicity and toxicity (El-Say and El-Sawy, 2017) such as in the case of PLGA polymers as demonstrated (Aragao-Santiago *et al.*, 2016 ; Barillet *et al.*, 2019 ; Grabowski *et al.*, 2016 ; Grabowski *et al.*, 2013 ; Grabowski *et al.*, 2015). PNPs can also be designed to deliver the drug effectively to a

target location and then increase the therapeutic efficacy, minimizing the side effects. As disadvantages, possible non-biodegradability, lability, higher manufacturing costs, toxic residuals solvent as well as low drug loading efficiency and high burst release have been reported (Lu *et al.*, 2011). Several studies have been reported with PNPs and also surface modification to enhance lung drug delivery (Beck-Broichsitter *et al.*, 2017 ; Ishihara *et al.*, 2009 ; Menon *et al.*, 2014 ; Yang *et al.*, 2012 ; Yoo *et al.*, 2013).

With the aim to examine the therapeutic potential of injectable polymeric nanoparticles encapsulating betamethasone phosphate in a murine model of asthma, Matsuo *et al.* (2009) developed PNPs with PLA homopolymers and PEG-PLA block copolymers, diameter around 116 nm and drug loading of 10.7 wt %. Result shows that PNPs have been found to accumulate at the site of airway inflammation and exhibited anti-inflammatory activity. Significant decreases in the number of BAL eosinophils were maintained for 7 days with a single injection of nanoparticles containing 40 µg of betamethasone phosphate.

Vij *et al.* (2016) evaluated the efficacy of a PEGylated immuno-conjugated PLGA-nanoparticle (PINP). As results, PINP with average diameter 344 ± 35 nm and PdI 0.116 show efficacy as PINP mediated non-steroidal anti-inflammatory drug (ibuprofen), with delivery to neutrophils in murine models of obstructive lung diseases, based on its ability to control neutrophilic-inflammation and resulting lung disease.

Yeh and Chen (2017) have proposed core-shell PLGA nanoparticles containing budesonide and theophylline, drugs which are highly hydrophobic and hydrophilic, respectively. They produced by dual capillary electrospray technique core-shell particles with various drug-loaded positions, shell thicknesses and overall particle sizes. The analysis indicated that PLGA polymer with low molecular weight produced lower porosity in the shell matrix, which could prevent the diffusion of release media, leading to the further release rate decrease. However, when drugs were loaded at different locations in a PLGA composite particle, with theophylline loaded in the particle core and budesonide in the particle shell, the drug release resulted in the increase of core-loaded theophylline release. The best control of theophylline released was found when both drugs were loaded in the core and particles having a thick shell.

A quality-by-design (QbD) approach was adopted by Leng *et al.* (2018) to design lipid-polymer hybrid nanoparticles (LPNs) loaded with budesonide. LPNs based on the biodegradable polymer PLGA and the cationic lipid dioleyltrimethylammonium propane (DOTAP) were prepared using a double emulsion solvent evaporation method. QbD was used to define the optimal formulation parameters, and the

theoretical budesonide and DOTAP loadings were identified as critical formulation parameters. The authors found that the particles size is not dependent of critical parameters, in contrast to the zeta potential which was highly dependent on the theoretical DOTAP loading. The results suggests that the LPN surface is covered by DOTAP, the DOTAP loading is saturable and that the interaction between drug and PLGA increases when increasing the initial amount of budesonide. In conclusion, the study shows the importance of systematic formulation design for understanding the effect of formulation parameters on the characteristics of LPNs.

Surface modification of polymeric nanoparticles can also be used to improve targeting delivery. Ruge *et al.* (2016) have synthetized mannosylated PLA-PEG copolymer and produced nanoparticles with a PLGA/PLA core and a PEG shell decorated with mannose residues, with the aim of to increase their uptake by alveolar macrophages due a strong association with SP-A. *In vitro* uptake studies demonstred that the association with SP-A increased nanoparticle uptake by THP-1 macrophages. After intratracheal *in vivo* administration of nanoparticles with or without SP-A, SP-A-coated mannosylated nanoparticles were internalized by alveolar macrophages in greater proportion than SP-A-coated nonmannosylated nanoparticles, indicating that the biomimetic approach might be an efficient strategy to target these cells.

A model of polymeric nanoparticles densely coated with low molecular weight PEG was described by Schuster *et al.* (2013) to minimize the airway muco-adhesion barrier. They found that polymeric nanoparticles up to 200 nm and densely coated with low molecular weight PEG can rapidly diffuse through respiratory mucus. In contrast, PEG coated particles above 500 nm in diameter were sterically immobilized by the mucus mesh. In another study with mucus penetrating polymeric nanoparticles, Popov *et al.* (2016) have encapsulated fluticasone propionate (FP) into PLA-PEG-based MPP (mucus penetrating particles) and PLA-SDS-based MAP (mucoadhesive particles) and evaluated their pulmonary residence by measuring FP levels in mouse lungs over 24 h following intratracheal instillation. The results demonstrated that pulmonary delivery of FP formulated as MPP nanoparticles achieved a higher local exposure in lungs of rodents when compared to free drug and to a MAP formulation with similar particle size. Delivery of FP as MPP also present an improve in the anti-inflammatory effect of FP in a rat lung inflammation model as compared to non-encapsulated FP control.

5.4 Trojan Microparticles

For pharmaceutical applications and to improve their administration (oral, pulmonary and dermal), nanocarriers can be loaded into microparticles. These supramolecular associations can also modulate the kinetic release of drugs entrapped in the nanoparticles.

Microparticles have the important advantage to avoid rapid clearance following administration, increasing drug residence time. However, because of their large size, microparticles are not able to diffuse within tissues. Although they do not induce long-term release, nanoparticles can easily diffuse into a tissue and even penetrate the cells located in these tissues. Unfortunately, nanoparticles are often difficult to manipulate as compared with microparticles, and due to their small sizes they are predominantly exhaled after inhalation (El-Sherbiny *et al.*, 2015 ; Gómez-Gaete *et al.*, 2008). In their dry form, they have the tendency to aggregate and may be unstable in aqueous suspension due to hydrolysis and/or sedimentation. Under such circumstances, a hybrid system, combining the advantages of nanoparticles from the therapeutic point of view with the ease of microparticles manipulation, would be an interesting delivery vehicle for active molecules (Gómez-Gaete *et al.*, 2008).

The first system applying these characteristics was proposed by Tsapis *et al.* (2002), combining the drug release and delivery potential of nanoparticulate systems with the ease of flow, processing, and aerosolization potential of large porous particle (LPP) systems by spray drying solutions of polymeric and nonpolymeric nanoparticles. Once deposited in the lungs (or placed in a physiological or physiological-like environment), they disassociate to yield nanoparticles, with their inherent attractive features for drug delivery. A principal advantage of LPPs over conventional inhaled therapeutic aerosol particles is their aerosolization efficiency, since LPPs have the potential to avoid alveolar macrophage clearance, enabling sustained drug release in the lung.

Trojan particles were developed by Gómez-Gaete *et al.* (2008) to deliver dexamethasone-loaded nanoparticles using excipients such as 1,2-dipalmitoyl-*sn*-glycero-3-phosphatidylcholine (DPPC) and hyaluronic acid (HA). This formulation showed that DPPC-HA microparticles are hollow shells, whereas pure DPPC particles are dense spheres. The addition of HA to the formulation increased the stability of DPPC powders by preventing phospholipids rearrangement upon aging. Additionally, HA leads to an increase of particle size and a decrease of aggregation due to morphological change. The *in vitro* release of dexamethasone showed that the excipient matrix provides protection to encapsulated nanoparticles by slowing drug release.

Superparamagnetic iron oxide nanoparticles (SPIONs)-loaded Trojan microparticles were formulated by Tewes *et al.* (2014), for targeted aerosol delivery to the lung. These microparticles made of SPIONs, PEG, hydroxypropyl-β-cyclodextrin (HPβCD), $(NH_4)_2CO_3$ and magnesium stearate (MgST) were formulated by spray drying and resulted in a mass median aerodynamic diameter (MMAD) of 2.2 ± 0.8 µm. If loaded with a pharmaceutical active ingredient, these particles may be useful for treating localized lung disease such as cancer nodule, since these Trojan particles appeared highly sensitive to the magnetic field.

A summary of the performed studies involving glucocorticoids and lung delivery is shown in Table 4.

Table 4. Summary of published works involving glucocorticoids, lung pathologies and nanotechnology.

Glucocorticoid	Formulation	Study	Results	Reference
Budesonide	Liposomes	Comparison between weekly therapy with aerosolized budesonide encapsulated in stealth or conventional liposomes with daily budesonide therapy in reducing allergic inflammation in asthma. *In vivo* test in ovalbumin-sensitized C57/Black 6 mice.	Weekly therapy was as effective as daily budesonide therapy in decreasing lung inflammation and reducing activity of eosinophil peroxidase, peripheral blood eosinophils, and total serum IgE levels.	Konduri *et al.* (2003)
Budesonide	Liposomes	Pulmonary liposomal delivery system of budesonide prepared by film hydration method and evaluation for sustained release. Liposomes were freeze dried for better shelf life.	Freeze dried liposomes showed better fine particle fraction and drug content over the period of six months at ambient or 2-8°C storage condition compared to aqueous dispersion of liposomes.	Parmar *et al.* (2010)
Budesonide	Liposomes	Dry powder of Liposomes to evaluate the efficacy of pulmonary delivery of colchicine and budesonide for idiopathic pulmonary fibrosis.	Liposomes lyophilized using Mannitol as carrier and cryoprotectant showed high entrapment efficiency around 98 % and sustained drug release up to 24 hours, with prolonged drug retention at targeted site and reduced systemic exposure.	Chennakesavulu *et al.* (2018)
Dexamethasone palmitate	Liposomes	Anti-inflammatory effects of dexamethasone palmitate incorporated in mannosylated liposomes intratracheally administrated were investigated in LPS-induced lung inflammation in rats.	Mannosylated liposomes significantly inhibited TNF, IL-1, and CINC-1 levels, suppressed neutrophil infiltration and myeloperoxidase activity, and inhibited NFB and p38 mitogen-activated protein kinase activation in the lung.	Wijagkanalan *et al.* (2008a)

Beclomethasone dipropionate	Liposomes	Evaluation of the ability of liposome formulation to penetrate a pathological mucus model obtained from COPD affected patients.	The penetration studies of mucus from COPD patients showed that the PEGylated liposomes were the most mucus penetrating vesicles after 27 hours, when compared to small unilamellar liposomes and Pluronic® F127-surface modified liposomes.	De Leo *et al.* (2018)
Methylprednisolone (MPS)	Liposomes	Development of lung-targeting MPS-loaded liposomes by conjugation of surfactant protein A nanobodies (SPANb), to improve the efficacy of the drug payload and also reduce adverse side effects by targeting the desired tissues or lesions.	Liposomes demonstrated good size distribution, morphology and encapsulation efficiency, in addition to reduce lung inflammation and decrease liver and renal toxicity. Besides that, superior performance to treat lung injury in animal models was found when compared with antibody functionalized systems.	Li *et al.* (2017)
Methylprednisolone	Liposomes	Effect of a liposomal formulation of MP on the expression of LPS-induced proinflammatory TNF and antiinflammatory IL-10 in human alveolar macrophages.	Liposomal MP can consistently induce IL-10 and reduce TNF when macrophages are exposed for a prolonged period of time.	Frankenberger *et al.* (2005)
Beclomethasone dipropionate	Liposomes	Tolerance and safety of single doses of beclomethasone dipropionate liposome aerosol in 10 healthy volunteers.	Liposome aqueous aerosol was well tolerated in doses equivalent to those currently administered by MDIs and DPIs for treatment of asthma. No adverse clinical or laboratory events were observed.	Waldrep *et al.* (2008)
Dexamethasone	Liposomes	Study of the prophylactic effect of liposome-entrapped dexamethasone (L-DEX) in an animal acute lung injury LPS model.	Animals pretreatment with L-DEX was significantly more effective than pretreatment with the free drug in reducing lung inflammation and other lung injuries.	Suntres and Shek (2000)

Beclomethasone dipropionate	Nanomicelles	Physicochemical and *in vitro* evaluation of sterically stabilized phospholipid nanomicelles (SSMs) loaded with beclomethasone dipropionate as a carrier for pulmonary delivery.	The maximum solubility of BDP in SSMs was approximately 1300 times its actual solubility. The SSM system controlled the release of BDP and all aerodynamic values of aerosol rehydrated BDP-SSMs were acceptable with a significant level of deposition in the lungs.	Sahib *et al.* (2012)
Beclomethasone dipropionate	Lipid nanoparticles	Beclomethasone dipropionate SLN and NLC for administration via the pulmonary route were developed and characterized in terms of morphology, size, encapsulation efficiency, *in vitro* drug release and aerosol aerodynamic properties.	BDP-loaded LN with high entrapment efficiency were obtained, presenting a diffusion-controlled release from the lipidic matrix. SLN and NLC also showed suitable and aerosol aerodynamic properties for BDP deep lung delivery.	Jaafar-Maalej *et al.* (2011)
Dexamethasone acetate	Solid lipid nanoparticles	Development of SLN for the lung-targeting delivery of dexamethasone acetate by intravenous administration. Physicochemical characterization, *in vitro* and *in vivo* studies in mice were carried out.	*In vitro* drug release profile showed an initial burst release of DXA from DXA-SLNs (68% during the first 2 h), and then the remaining drug was released gradually over the following 48 hours. The concentration of DXA in the lung reached a maximum level at 0.5 h post DXA-SLNs injection, with a 17.8-fold larger area under the curve of DXA-SLNs when compared to that of DXA-solution.	Xiang *et al.* (2007)
Budesonide	Solid lipid nanoparticles	Evaluation of the effects of formulation and processing parameters on particle size of prepared SLNs. SLNs were prepared with different values of drug content, ultrasonication, amplitude, and homogenization time and the data were modelled using artificial neural networks (ANNs).	Small-sized particles of 170–200 nm were found using low drug content with high-amplitude and high-homogenization time. *In vitro* aerosolization performance of Bud-SLNs indicated enhancement in fine particle fraction value, when compared to that of commercial budesonide.	Esmaeili *et al.* (2016)

Fluticasone propionate (FP)	Solid lipid microparticles	Development of two different SLMs using chitosan and alginate such as mucoadhesive polymers. Study of biocompatibility and efficacy compared with the free drug in controlling senescence and inflammatory processes in cigarette smoke extracts.	SLMs showed useful MMAD (3.5–4.0 µM) for pulmonary release of FP to the secondary bronchi, avoiding side effects due to systemic absorption. The SLMs also were well-tolerated by bronchial epithelial cells (16-HBE) and more effective than FP alone to control events associated with lung inflammation.	Amore *et al.* (2017)
Mometasone furoate (MF)	Solid lipid nanoparticles	Dry powder inhaler (DPI) formulations containing MF-SLNs were designed to increase pulmonary deposition, improve pulmonary residence time and respirable fraction. MF-SLNs were characterized for physicochemical parameters, *in vitro* drug release kinetics and *in vitro* pulmonary deposition pattern.	The mean particle size of developed SLNs was found to be 227 nm and 327 nm before and after lyophilization, respectively. *In vitro* drug release was 93 % in 24 hours from SLN. Compared to conventional DPI formulations, MF-SLN DPI formulations exhibited a controlled release profile, uniformity in drug content/dose and higher pulmonary deposition.	Shah *et al.* (2013)
Budesonide	Lipid-polymer hybrid nanoparticles (LPNs)	Quality by design approach to define critical formulation parameters to produce LPNs loaded with budesonide, that could be combined with small interfering RNA (siRNA) for COPD management.	Two critical formulation parameters were identified as the theoretical budesonide and DOTAP loading. These parameters were used to understand the effect of formulation parameters on the characteristics of LPNs.	Leng *et al.* (2018)
Budesonide	Nanosuspension	Production and characterization of a budesonide nanosuspension by high-pressure homogenization for pulmonary delivery. To investigate the aerosolization properties, the nanosuspension was nebulized and afterward analysed on particle size.	Long-term stable budesonide nanosuspension was obtained, without aggregates and particle growth during 1 year. Particle size was about 500-600 nm. The diameter before and after aerosolization did not change, showing the suitability for pulmonary delivery.	Jacobs and Helmut Müller (2002)

Budesonide	Nanosuspension	Formulation of stable and well-dispersible budesonide nanosuspensions by microfluidizer method. Physicochemical characterization, *in vitro* release and *in vivo* lung distribution evaluation.	Bud nanosuspensions measured average particle size around 120 nm. *In vitro* tests showed a deposition distribution with fine particle ratio 82.2 %, indicating that nanosuspensions were better distributed in lung when compared with normal particle and micronized particles. 1 h after inhalation, the drug concentration can reach high levels compared to those found for normal particles and micronized particles.	Zhang and Zhang (2016)
Betamethasone phosphate	Polymeric nanoparticles	Effects of betamethasone disodium phosphate encapsulated in biocompatible, biodegradable nanoparticles (PEG-PLA) on a murine model of asthma, with the aim to improve efficacy and reduce side effects.	Nanoparticles showed accumulation at the site of airway inflammation and exhibited anti-inflammatory activity. Significant decreases in BALF eosinophil number were maintained for 7 days with a single injection containing 40 µg of bethamethasone phosphate.	Matsuo *et al.* (2009)
Fluticasone propionate	Polymeric nanoparticles	Fluticasone propionate (FP) was encapsulated into PLA-based MPP and MAP and evaluated in terms of pulmonary residence by measuring FP levels in mouse lungs over 24 hours following intratracheal instillation.	Pulmonary delivery of FP formulated as MPP achieved a higher local deposition in lungs of rodents when compared to free drug and even when compared to a MAP with similar particle size. Delivery of FP as MPP also showed a significant enhancement of anti-inflammatory effect of FP in a rat lung inflammation model as compared to non-encapsulated FP control.	Popov *et al.* (2016)

Budesonide	Polymeric nanoparticles	Development of core-shell PLGA nanoparticles containing budesonide and theophylline.	PLGA polymer with low molecular weight produced lower porosity in the shell matrix, which could prevent the diffusion of release media, leading to slower release. The best control of theophylline release was found when both drugs were loaded in the core and particles having a thick shell.	Yeh and Chen (2017)
Beclomethasone dipropionate	Polymeric nanoparticles	Formulation of PHEA-PLA/PHEA-PEG2000-PLA nanoparticles and evaluation of their potential as carriers for beclomethasone dipropionate into the lung after aerosolization in mice. *In vivo* biodistribution of BDP and its metabolites was evaluated 3 h post-administration in mice by aerosolization of BDP-loaded NPs or free BDP (control, commercial formulation).	PHEA-PLA/PHEA-PEG2000-PLA nanoparticles size was lower than 200 nm and zeta potential slightly negative. BDP entrapped into NPs reached all analysed lung compartments and detected amounts were comparable to those of control-treated mice. Moreover, the entrapment into NPs protects the drug from the enzymatic hydrolysis.	Craparo *et al.* (2016)
Fluticasone Propionate	Polymeric nanoparticles	Evaluation of PHEA-PLA-PEG2000 nanoparticles as a potential carrier for lung administration of fluticasone propionate.	FP-loaded nanoparticles showed a slightly negative surface charge and nanometric size that are maintained after storage for one year at -20°C and 5°C. FP was slowly released in simulated lung fluid and nanoparticles were biocompatible and did not induce cell necrosis and cell apoptosis on bronchial epithelial cells (16-HBE).	Craparo *et al.* (2017)

Beclomethasone dipropionate	Polymeric nanoparticles	Development of PHEA-PEG2000-EDA-LA micelles as drug delivery systems for beclomethasone dipropionate into the lung.	BDP-loaded micelles presented adequate chemical-physical characteristics for pulmonary administration such as mean size of about 200 nm, positive surface charge and spherical shape. Moreover, they showed higher biocompatibility in comparison with the commercial formulation (control) and are able to increase cell uptake of BDP of about 44 wt % compared to control on 16-HBE cells.	Triolo *et al.* (2017)
betamethasone disodium 21-phosphate	Polymeric nanoparticles	Design of polymeric nanoparticles with various sustained profiles of drug release and prolonged circulation by blending PLA/PLGA homopolymers and PEG-block-PLA/PLGA copolymers encapsulating betamethasone disodium 21-phosphate.	Nanoparticles uptake by macrophage-like cells decreased with nanoparticles of higher PEG content, and nanoparticles of PEG-PLGA block copolymers were taken up earlier than those of PEG-PLA block copolymers after incubation with serum. Nanoparticles of smaller size with higher PEG content provided prolonged blood circulation, and nanoparticles of PEG-PLA block copolymers remained longer in circulation than those of PEG-PLGA block copolymers.	Ishihara *et al.* (2009)
Deflazacort	Polymeric nanoparticles	Anti-inflammatory effect of PCL deflazacort nanocapsules (NC-DFZ) and possible improvement of epithelial barrier function for the treatment of pulmonary diseases.	NC with a mean size around 200 nm, slightly negative zeta potential, and low PdI did not showed cytotoxic effects. NC-DFZ reduced the LPS mediated secretion of IL-8. *In vitro* dissolution testing revealed controlled release of DFZ from nanocapsules, which may explain the improved effect of DFZ on the cells.	Rigo *et al.* (2017)

6 CONCLUSIONS

Despite advances in asthma and COPD management, these diseases remain as a major public health problem worldwide, with increasing morbidity and mortality. As previously exposed in this introduction, the available treatments still present low adhesion by the patients, due mainly to the large number of side effects presented, a need for several daily applications and a difficulty in the correct use of the inhaler devices, which may lead to the delivery of inadequate doses to the patient.

In this chapter, after presenting a review of the state of the art in treating asthma and COPD, we have been able to design, propose and demonstrate the value of the use of nanovectors to deliver anti-inflammatory drugs, particularly GCs.

The experimental works of this thesis presented in the following chapters proposed the development of nanoparticulate systems that allow to improve the residence time of the drug in lung tissues, the penetration of the particles by the pulmonary mucus, the deposition of the particles in the deeper lung regions and a targeting to alveolar macrophages, key effector cells of the innate immune response. To achieve these goals, we described and tested four development strategies, respectively: synthesis of a prodrug of budesonide, budesonide palmitate; use of a PEGylated lipid in the formulation of the nanoparticles; development of Trojan microparticles; and mannosylation of nanoparticles for vectorization to the mannose receptors, present on the surface of the alveolar macrophages.

7 REFERENCES

Abu-Dahab R., Schäfer U. F., Lehr C.-M. « Lectin-functionalized liposomes for pulmonary drug delivery: effect of nebulization on stability and bioadhesion ». *Eur. J. Pharm. Sci.* [En ligne]. 1 août 2001. Vol. 14, n°1, p. 37-46. Disponible sur : < https://doi.org/10.1016/S0928-0987(01)00147-6 > (consulté le 16 mars 2019)

Allen D. B., Bielory L., Derendorf H., Dluhy R., Colice G. L., Szefler S. J. « Inhaled corticosteroids: past lessons and future issues. » *J. Allergy Clin. Immunol.* [En ligne]. 2003. Vol. 112, p. S1-S40. Disponible sur : < https://doi.org/10.1067/mai.2003.1707 >

Amore E., Ferraro M., Manca M. L., Gjomarkaj M., Giammona G., Pace E., Bondì M. L. « Mucoadhesive solid lipid microparticles for controlled release of a corticosteroid in the chronic obstructive pulmonary disease treatment ». *Nanomedicine* [En ligne]. 2017. Vol. 12, n°19, p. 2287-2302. Disponible sur : < https://doi.org/10.2217/nnm-2017-0072 >

Andrade F., Rafael D., Videira M., Ferreira D., Sosnik A., Sarmento B. « Nanotechnology and pulmonary delivery to overcome resistance in infectious diseases ». *Adv. Drug Deliv. Rev.* [En ligne]. 2013. Vol. 65, p. 1816-1827. Disponible sur : < https://doi.org/10.1016/j.addr.2013.07.020 >

Aragao-Santiago L., Hillaireau H., Grabowski N., Mura S., Nascimento T. L., Dufort S., Coll J. L., Tsapis N., Fattal E. « Compared in vivo toxicity in mice of lung delivered biodegradable and non-biodegradable nanoparticles ». *Nanotoxicology* [En ligne]. 2016. Vol. 10, n°3, p. 292-302. Disponible sur : < https://doi.org/10.3109/17435390.2015.1054908 >

Autilio C., Pérez-Gil J. « Understanding the principle biophysics concepts of pulmonary surfactant in health and disease ». *Arch. Dis. Child. - Fetal Neonatal Ed.* [En ligne]. 11 février 2018. Vol. 14 decembe, p. F1-F9. Disponible sur : < https://doi.org/10.1136/archdischild-2018-315413 >

Azarmi S., Roa W. H., Löbenberg R. « Targeted delivery of nanoparticles for the treatment of lung diseases ». *Adv. Drug Deliv. Rev.* [En ligne]. 2008. Vol. 60, n°8, p. 863-875. Disponible sur : < https://doi.org/10.1016/j.addr.2007.11.006 >

Barillet S., Fattal E., Mura S., Tsapis N., Pallardy M., Hillaireau H., Kerdine-Römer S. « Immunotoxicity of poly (lactic-co-glycolic acid) nanoparticles: influence of surface properties on dendritic cell activation ». *Nanotoxicology* [En ligne]. 2019. Vol. Feb 14, p. 1-17. Disponible sur : < https://doi.org/10.1080/17435390.2018.1564078 >

Barnes P. « Mechanisms in COPD: Differences From Asthma ». *CHEST J.* [En ligne]. 2000. Vol. 117, p. 10S-14S. Disponible sur : < https://doi.org/10.1378/chest.117.2 >

Barnes P. J. « Similarities and differences in inflammatory mechanisms of asthma and COPD ». *Breathe* [En ligne]. 2011. Vol. 7, n°3, p. 229-238. Disponible sur : < https://doi.org/10.1183/20734735.026410 >

Barnes P. J. « Inflammatory mechanisms in patients with chronic obstructive pulmonary disease ». *J. Allergy Clin. Immunol.* [En ligne]. 1 juillet 2016. Vol. 138, n°1, p. 16-27. Disponible sur : < https://doi.org/10.1016/J.JACI.2016.05.011 > (consulté le 11 juillet 2018)

Barnes P. J. « Alveolar Macrophages as Orchestrators of COPD ». *COPD J. Chronic Obstr. Pulm. Dis.* [En ligne]. 2004. Vol. 1, n°1, p. 59-70. Disponible sur : < https://doi.org/10.1081/COPD-120028701 >

Barnes P. J., Adcock I. M. « Glucocorticoid resistance in inflammatory diseases ». *Lancet* [En ligne]. 30 mai 2009. Vol. 373, n°9678, p. 1905-1917. Disponible sur : < https://doi.org/10.1016/S0140-

6736(09)60326-3 > (consulté le 10 décembre 2018)

Barnes P. J., Chung K. F., Page C. P. « Inflammatory mediators of asthma: an update. » *Pharmacol. Rev.* 1998. Vol. 50, n°4, p. 515-596.

Barnes P. J., Shapiro S. D., Pauwels R. A. « Chronic obstructive pulmonary disease: Molecular and cellular mechanisms ». *Eur. Respir. J.* [En ligne]. 2003. Vol. 22, n°4, p. 672-688. Disponible sur : < https://doi.org/10.1183/09031936.03.00040703 >

Bateman E. D., Reddel H. K., Van Zyl-Smit R. N., Agusti A. « The asthma-COPD overlap syndrome: Towards a revised taxonomy of chronic airways diseases? ». *Lancet Respir. Med.* [En ligne]. 2015. Vol. 3, n°9, p. 719-728. Disponible sur : < https://doi.org/10.1016/S2213-2600(15)00254-4 >

Beck-Broichsitter M., Bohr A., Ruge C. A. « Poloxamer-Decorated Polymer Nanoparticles for Lung Surfactant Compatibility ». *Mol. Pharm.* [En ligne]. 2 octobre 2017. Vol. 14, n°10, p. 3464-3472. Disponible sur : < https://doi.org/10.1021/acs.molpharmaceut.7b00477 >

Bel E. H., Ten Brinke A. « New Anti-Eosinophil Drugs for Asthma and COPD: Targeting the Trait! ». *Chest* [En ligne]. 2017. Vol. 152, n°6, p. 1276-1282. Disponible sur : < https://doi.org/10.1016/j.chest.2017.05.019 >

Beloqui A., Solinís M. Á., Rodríguez-Gascón A., Almeida A. J., Préat V. « Nanostructured lipid carriers: Promising drug delivery systems for future clinics ». *Nanomedicine Nanotechnology, Biol. Med.* [En ligne]. 1 janvier 2016. Vol. 12, n°1, p. 143-161. Disponible sur : < https://doi.org/10.1016/J.NANO.2015.09.004 > (consulté le 5 février 2019)

Biggadike K., Uings I., Farrow S. N. « Designing Corticosteroid Drugs for Pulmonary Selectivity ». *Proc. the. Am. Thorac. Soc.* [En ligne]. 2004. Vol. 1, p. 352-355. Disponible sur : < https://doi.org/10.1513/pats.200409-048TA >

Brattsand R., Miller-Larsson A. « The Role of Intracellular Esterification in Budesonide Once-Daily Dosing and Airway Selectivity ». *Clin. Ther.* [En ligne]. 2003. Vol. 25, n°SUPPL. C, p. 28-41. Disponible sur : < https://doi.org/10.1016/S0149-2918(03)80304-1 >

Brink K. I. M. Van den, Boorsma M., Staal-Van Den Brekel A. J., Edsbäcker S., Wouters E. F., Thorsson L. « Evidence of the in vivo esterification of budesonide in human airways ». *Br. J. Clin. Pharmacol.* [En ligne]. 2008. Vol. 66, n°1, p. 27-35. Disponible sur : < https://doi.org/10.1111/j.1365-2125.2008.03164.x >

Camp P. G., O'Donnell D. E., Postma D. S. « Chronic Obstructive Pulmonary Disease in Men and Women: Myths and Reality ». *Proc. Am. Thorac. Soc.* [En ligne]. 2009. Vol. 6, n°6, p. 535-538. Disponible sur : < https://doi.org/10.1513/pats.200904-018DS >

Caramori G., Adcock I. « Pharmacology of airway inflammation in asthma and COPD ». *Pulm. Pharmacol. Ther.* [En ligne]. 2003. Vol. 16, n°5, p. 247-277. Disponible sur : < https://doi.org/10.1016/S1094-5539(03)00070-1 >

Carvalho T. C., Peters J. I., Williams R. O. « Influence of particle size on regional lung deposition – What evidence is there? ». *Int. J. Pharm.* [En ligne]. 15 mars 2011. Vol. 406, n°1-2, p. 1-10. Disponible sur : < https://doi.org/10.1016/J.IJPHARM.2010.12.040 > (consulté le 31 octobre 2018)

Cazzola M., Page C. P., Calzetta L., Matera M. G. « Pharmacology and Therapeutics of Bronchodilators ». *Pharmacol. Rev.* 2012. Vol. 64, n°3, p. 450-504.

Chatila W. M., Thomashow B. M., Minai O. A., Criner G. J., Make B. J. « Comorbidities in Chronic

Obstructive Pulmonary Disease ». *Proc. Am. Thorac. Soc.* [En ligne]. 2008. Vol. 5, n°4, p. 549-555. Disponible sur : < https://doi.org/10.1513/pats.200709-148ET >

Chellat F., Merhi Y., Moreau A., Yahia L. H. « Therapeutic potential of nanoparticulate systems for macrophage targeting ». *Biomaterials* [En ligne]. 2005. Vol. 26, p. 7260-7275. Disponible sur : < https://doi.org/10.1016/j.biomaterials.2005.05.044 >

Chennakesavulu S., Mishra A., Sudheer A., Sowmya C., Suryaprakash Reddy C., Bhargav E. « Pulmonary delivery of liposomal dry powder inhaler formulation for effective treatment of idiopathic pulmonary fibrosis ». *Asian J. Pharm. Sci.* [En ligne]. 1 janvier 2018. Vol. 13, n°1, p. 91-100. Disponible sur : < https://doi.org/10.1016/J.AJPS.2017.08.005 > (consulté le 4 février 2019)

Chopra D., Bhandari B., Wardhan N. « Ciclesonide-a novel corticosteroid for the management of asthma ». *Curr. Clin. Pharmacol.* 2012. Vol. 7, n°2, p. 73-77.

Chorão P., Pereira A. M., Fonseca J. A. « Inhaler devices in asthma and COPD – An assessment of inhaler technique and patient preferences ». *Respir. Med.* [En ligne]. 1 juillet 2014. Vol. 108, n°7, p. 968-975. Disponible sur : < https://doi.org/10.1016/J.RMED.2014.04.019 > (consulté le 10 octobre 2018)

Chuang S.-Y., Lin C.-H., Huang T.-H., Fang J.-Y. « Lipid-Based Nanoparticles as a Potential Delivery Approach in the Treatment of Rheumatoid Arthritis ». *Nanomaterials* [En ligne]. 2018. Vol. 8, n°42, p. 1-16. Disponible sur : < https://doi.org/10.3390/nano8010042 >

Ciepiela O., Ostafin M., Demkow U. « Neutrophils in asthma-A review ». *Respir. Physiol. Neurobiol.* [En ligne]. 2015. Vol. 209, p. 13-16. Disponible sur : < https://doi.org/10.1016/j.resp.2014.12.004 >

Cockcroft D. W. « Pharmacologic Therapy for Asthma : Overview and Historical Perspective ». *J. Clin. Pharmacol.* 1999. Vol. 39, p. 216-222.

Colombo P., Traini D., Buttini F. *Inhalation drug delivery: Techniques and Products*. [s.l.] : [s.n.], 2013. Wiley-Blackwell:Oxford p.

Corren J., Parnes J. R., Wang L., Mo M., Roseti S. L., Griffiths J. M., Van der Merwe R. « Tezepelumab in Adults with Uncontrolled Asthma ». *N. Engl. J. Med.* [En ligne]. 2017. Vol. 377, n°10, p. 936-946. Disponible sur : < https://doi.org/10.1056/nejmoa1704064 >

Corrigan C. « Mechanisms of asthma ». *Medicine (Baltimore).* [En ligne]. 1 mai 2012. Vol. 40, n°5, p. 223-227. Disponible sur : < https://doi.org/10.1016/J.MPMED.2012.02.007 > (consulté le 11 octobre 2018)

Corry D. B., Kheradmand F., Luong A., Pandit L. « Immunological Mechanisms of Airway Diseases and Pathways to Therapy ». *Clin. Immunol.* [En ligne]. 1 janvier 2019. p. 571-584.e1. Disponible sur : < https://doi.org/10.1016/B978-0-7020-6896-6.00041-7 > (consulté le 11 juillet 2018)

Costa A., Pinheiro M., Magalhães J., Ribeiro R., Seabra V., Reis S., Sarmento B. « The formulation of nanomedicines for treating tuberculosis ». *Adv. Drug Deliv. Rev.* [En ligne]. 1 juillet 2016. Vol. 102, p. 102-115. Disponible sur : < https://doi.org/10.1016/J.ADDR.2016.04.012 > (consulté le 31 janvier 2019)

Costa A., Sarmento B., Seabra V. « Mannose-functionalized solid lipid nanoparticles are effective in targeting alveolar macrophages ». *Eur. J. Pharm. Sci.* [En ligne]. 1 mars 2018. Vol. 114, p. 103-113. Disponible sur : < https://doi.org/10.1016/J.EJPS.2017.12.006 > (consulté le 11 juillet 2018)

Craparo E. F., Ferraro M., Pace E., Bondì M. L., Giammona G., Cavallaro G. « Polyaspartamide-Based Nanoparticles Loaded with Fluticasone Propionate and the In Vitro Evaluation towards Cigarette

Smoke Effects ». *Nanomater. (Basel, Switzerland)* [En ligne]. 13 août 2017. Vol. 7, n°8, p. 222. Disponible sur : < https://doi.org/10.3390/nano7080222 >

Craparo E. F., Di Gioia S., Trapani A., Cellamare S., Belgiovine G., Mandracchia D., Giammona G., Cavallaro G., Conese M. « Realization of polyaspartamide-based nanoparticles and in vivo lung biodistribution evaluation of a loaded glucocorticoid after aerosolization in mice ». *Int. J. Pharm.* [En ligne]. 20 août 2016. Vol. 510, n°1, p. 263-270. Disponible sur : < https://doi.org/10.1016/J.IJPHARM.2016.06.042 > (consulté le 29 mars 2019)

Crompton G. « A brief history of inhaled asthma therapy over the last fifty years ». *Prim. Care Respir. J.* [En ligne]. 1 décembre 2006. Vol. 15, n°6, p. 326-331. Disponible sur : < https://doi.org/10.1016/J.PCRJ.2006.09.002 > (consulté le 31 octobre 2018)

Cukic V., Lovre V., Dragisic D., Ustamujic A. « Asthma and Chronic Obstructive Pulmonary Disease (COPD) - Differences and Similarities ». *Mater. Socio Medica* [En ligne]. 2012. Vol. 24, n°2, p. 100-105. Disponible sur : < https://doi.org/10.5455/msm.2012.24.100-105 >

Derendorf H., Hochhaus G., Meibohm B., Möllmann H., Barth J. « Pharmacokinetics and pharmacodynamics of inhaled corticosteroids ». *J. Allergy Clin. Immunol.* [En ligne]. avril 1998. Vol. 101, n°4, p. S440-S446. Disponible sur : < https://doi.org/10.1016/S0091-6749(98)70156-3 > (consulté le 16 mars 2016)

Derendorf H., Nave R., Drollmann A., Cerasoli F., Wurst W. « Relevance of pharmacokinetics and pharmacodynamics of inhaled corticosteroids to asthma ». *Eur. Respir. J.* [En ligne]. 1 novembre 2006. Vol. 28, n°5, p. 1042 LP - 1050. Disponible sur : < https://doi.org/10.1183/09031936.00074905 >

Devendra G., Spragg R. G. « Lung surfactant in subacute pulmonary disease ». *Respir. Res.* [En ligne]. 2002. Vol. 3, n°19, p. 1-4. Disponible sur : < https://doi.org/10.1186/rr168 >

Donohue J. F. « Therapeutic Responses in Asthma and COPD ». *Chest* [En ligne]. 2004. Vol. 126, n°2, p. 125S-137S. Disponible sur : < https://doi.org/10.1378/chest.126.2 >

Edsbäcker S., Brattsand R. « Budesonide fatty-acid esterification: a novel mechanism prolonging binding to airway tissue. Review of available data ». *Ann. Allergy, Asthma Immunol.* [En ligne]. 1 juin 2002. Vol. 88, n°6, p. 609-616. Disponible sur : < https://doi.org/10.1016/S1081-1206(10)61893-5 > (consulté le 11 octobre 2017)

Edwards D. A., Hanes J., Caponetti G., Hrkach J., Ben-Jebria A., Eskew M. Lou, Mintzes J., Deaver D., Lotan N., Langer R. « Large Porous Particles for Pulmonary Drug Delivery ». *Science (80-.).* [En ligne]. 20 juin 1997. Vol. 276, n°5320, p. 1868-1872. Disponible sur : < https://doi.org/10.1126/science.276.5320.1868 >

El-Say K. M., El-Sawy H. S. « Polymeric nanoparticles: Promising platform for drug delivery ». *Int. J. Pharm.* [En ligne]. 7 août 2017. Vol. 528, n°1-2, p. 675-691. Disponible sur : < https://doi.org/10.1016/J.IJPHARM.2017.06.052 > (consulté le 5 février 2019)

El-Sherbiny I. M., El-Baz N. M., Yacoub M. H. « Inhaled nano- and microparticles for drug delivery ». *Glob. Cardiol. Sci. Pract.* [En ligne]. 31 mars 2015. Vol. 2015, p. 1-14. Disponible sur : < https://doi.org/10.5339/gcsp.2015.2 >

Ericson-Neilsen W., Kaye A. D. « Steroids : Pharmacology , Complications , and Practice Delivery Issues ». *Ochsner J.* 2014. Vol. 14, n°2, p. 203-207.

Esmaeili M., Aghajani M., Abbasalipourkabir R., Amani A. « Budesonide-loaded solid lipid nanoparticles

for pulmonary delivery: preparation, optimization, and aerodynamic behavior ». *Artif. Cells, Nanomedicine, Biotechnol.* [En ligne]. 2016. Vol. 44, n°8, p. 1964-1971. Disponible sur : < https://doi.org/10.3109/21691401.2015.1129614 >

Evans C. M., Koo J. S. « Airway mucus: The good, the bad, the sticky ». *Pharmacol. Ther.* [En ligne]. 1 mars 2009. Vol. 121, n°3, p. 332-348. Disponible sur : < https://doi.org/10.1016/J.PHARMTHERA.2008.11.001 > (consulté le 17 octobre 2018)

Fergeson J. E., Patel S. S., Lockey R. F. « Acute asthma, prognosis, and treatment ». *J. Allergy Clin. Immunol.* [En ligne]. 1 février 2017. Vol. 139, n°2, p. 438-447. Disponible sur : < https://doi.org/10.1016/J.JACI.2016.06.054 > (consulté le 10 juillet 2018)

Fernández-Blanco J. A., Fakih D., Arike L., Rodriguez-Pineiro A., Martínez-Abad B., Skansebo E., Jackson S., Root J., Singh D., McCrae C., M. Evans C., Åstrand A., Ermund A., Hansson G. « Attached stratified mucus separates bacteria from the epithelial cells in COPD lungs ». *JCI Insight* [En ligne]. 6 septembre 2018. Vol. 3, n°17, p. 1-18. Disponible sur : < https://doi.org/10.1172/jci.insight.120994 >

Forum of International Respiratory Societies. *The Global Impact of Respiratory Disease* [En ligne]. [s.l.] : [s.n.], 2017. 1-43 p. Disponible sur : < http://www.who.int/gard/publications/The_Global_Impact_of_Respiratory_Disease.pdf >ISBN : 9781849840873.

Frankenberger M., Häussinger K., Ziegler-Heitbrock L. « Liposomal methylprednisolone differentially regulates the expression of TNF and IL-10 in human alveolar macrophages ». *Int. Immunopharmacol.* [En ligne]. 1 février 2005. Vol. 5, n°2, p. 289-299. Disponible sur : < https://doi.org/10.1016/J.INTIMP.2004.09.033 > (consulté le 15 mars 2019)

Fujiwara N., Kobayashi K. « Macrophages in Inflammation ». *Curr. Drug Target -Inflammation Allergy* [En ligne]. 2005. Vol. 4, n°3, p. 281-286. Disponible sur : < https://doi.org/10.2174/1568010054022024 >

Fuso L., Mores N., Valente S., Malerba M., Montuschi P. « Long-Acting Beta-Agonists and their Association with Inhaled Corticosteroids in COPD ». *Curr. Med. Chem.* 2013. Vol. 20, n°12, p. 1477-1495.

Garlapati V., Rampure D. M. « A study of COPD in non-smokers ». *J. Sci.* [En ligne]. 2015. Vol. 5, n°12, p. 1242-1248. Disponible sur : < https://doi.org/10.4102/sajs.vl07il/2.593 >

Garud A., Singh D., Garud N. « Solid Lipid Nanoparticles (SLN): Method, Characterization and Applications ». *Int. Curr. Pharm. J.* [En ligne]. 2012. Vol. 1, n°11, p. 384-393. Disponible sur : < https://doi.org/10.3329/icpj.v1i11.12065 >

Gauvreau G. M., Arm J. P., Boulet L. P., Leigh R., Cockcroft D. W., Davis B. E., Mayers I., FitzGerald J. M., Dahlen B., Killian K. J., Laviolette M., Carlsten C., Lazarinis N., Watson R. M., Milot J., Swystun V., Bowen M., Hui L., Lantz A. S., Meiser K., Maahs S., Lowe P. J., Skerjanec A., Drollmann A., O'Byrne P. M. « Efficacy and safety of multiple doses of QGE031 (ligelizumab) versus omalizumab and placebo in inhibiting allergen-induced early asthmatic responses ». *J. Allergy Clin. Immunol.* [En ligne]. 2016. Vol. 138, n°4, p. 1051-1059. Disponible sur : < https://doi.org/10.1016/j.jaci.2016.02.027 >

Gazi U., Martinez-Pomares L. « Influence of the mannose receptor in host immune responses ». *Immunobiology* [En ligne]. 2009. Vol. 214, n°7, p. 554-561. Disponible sur : < https://doi.org/10.1016/j.imbio.2008.11.004 >

GINA. « GLOBAL STRATEGY FOR Global Strategy for Asthma Management and Prevention ». 2018.

p. 1-162.

GOLD. « Pocket guide to COPD diagnosis, management and prevention: a guide for health care professionals ». *Glob. Initiat. Chronic Obstr. Lung Dis. Inc* [En ligne]. 2018. Vol. 1, n°1, p. 3-14. Disponible sur : < https://doi.org/http://dx.doi.org/10.1164/rccm.201701-0218PP >

Gómez-Gaete C., Fattal E., Silva L., Besnard M., Tsapis N. « Dexamethasone acetate encapsulation into Trojan particles ». *J. Control. Release* [En ligne]. 2008. Vol. 128, p. 41-49. Disponible sur : < https://doi.org/10.1016/j.jconrel.2008.02.008 >

Gonzalez-rothi R. J., Schreier H. « Pulmonary Delivery of Liposome-Encapsulated Drugs in Asthma Therapy ». *Clin. Immunother.* 1995. Vol. 4, n°5, p. 331-337.

Grabowski N., Hillaireau H., Vergnaud J., Nicolas V., Tsapis N., Kerdine-Römer S., Fattal E. « Surface-Modified Biodegradable Nanoparticles' Impact on Cytotoxicity and Inflammation Response on a Co-Culture of Lung Epithelial Cells and Human-Like Macrophages ». *Journal of Biomedical Nanotechnology* [En ligne]. [s.l.] : [s.n.], 2016. 135-146 p. Disponible sur : < https://doi.org/10.1166/jbn.2016.2126 >

Grabowski N., Hillaireau H., Vergnaud J., Santiago L. A., Kerdine-Romer S., Pallardy M., Tsapis N., Fattal E. « Toxicity of surface-modified PLGA nanoparticles toward lung alveolar epithelial cells ». *Int. J. Pharm.* [En ligne]. 2013. Vol. 454, n°2, p. 686-694. Disponible sur : < https://doi.org/10.1016/j.ijpharm.2013.05.025 >

Grabowski N., Hillaireau H., Vergnaud J., Tsapis N., Pallardy M., Kerdine-Römer S., Fattal E. « Surface coating mediates the toxicity of polymeric nanoparticles towards human-like macrophages ». *Int. J. Pharm.* [En ligne]. 2015. Vol. 482, n°1-2, p. 75-83. Disponible sur : < https://doi.org/10.1016/j.ijpharm.2014.11.042 >

Gross N. J., Barnes P. J. « New Therapies for Asthma and Chronic Obstructive Pulmonary Disease ». *Am. J. Respir. Crit. Care Med.* [En ligne]. 2017. Vol. 195, n°2, p. 159-166. Disponible sur : < https://doi.org/10.1164/rccm.201610-2074pp >

Gursahani H., Riggs-sauthier J., Pfeiffer J., Lechuga-ballesteros D. « Absorption of Polyethylene Glycol (PEG) Polymers : The Effect of PEG Size on Permeability ». *J. Pharm. Sci.* [En ligne]. 2009. Vol. 98, n°8, p. 2847-2856. Disponible sur : < https://doi.org/10.1002/jps >

Haley K. J., Sunday M. E., Wiggs B. R., Kozakewich H. P., Reilly J. J., Mentzer S. J., Sugarbaker D. J., Doerschuk C. M., Drazen J. M. « Inflammatory cell distribution within and along asthmatic airways ». *Am. J. Respir. Crit. Care Med.* [En ligne]. 1998. Vol. 158, n°2, p. 565-572. Disponible sur : < https://doi.org/10.1164/ajrccm.158.2.9705036 >

He L., Gao Y., Lin Y., Katsumi H., Fujita T., Yamamoto A. « Improvement of pulmonary absorption of insulin and other water-soluble compounds by polyamines in rats ». *J. Control. Release* [En ligne]. 2007. Vol. 122, n°1, p. 94-101. Disponible sur : < https://doi.org/https://doi.org/10.1016/j.jconrel.2007.06.017 >

Heffler E., Nascimento L., Madeira G., Ferrando M. « Inhaled Corticosteroids Safety and Adverse Effects in Patients with Asthma ». *J. Allergy Clin. Immunol. Pract.* [En ligne]. 2018. Vol. 6, n°3, p. 776-781. Disponible sur : < https://doi.org/10.1016/j.jaip.2018.01.025 >

Hildreth C. « Cynata Ramping Up Asthma Program ». [s.l.] : [s.n.], 2017. Disponible sur : < https://bioinformant.com/cynata-ramping-asthma-program/ >

Hohlfeld J., Fabel H., Hamm H. « The role of pulmonary surfactant in obstructive airway disease ». *Eur.*

Respir. J. [En ligne]. 1 mars 1997. Vol. 10, p. 482-491. Disponible sur : < https://doi.org/10.1183/09031936.97.10020482 >

Hom, S. and Pisano, M. « Reslizumab (Cinqair): An Interleukin-5 Antagonist for Severe Asthma of the Eosinophilic Phenotype. » *P & T : a peer-reviewed journal for formulary management* vol. 42(9), (2017): 564-568.

Hussell T., Bell T. J. « Alveolar macrophages : plasticity in a tissue-specific context ». *Nat. Publ. Gr.* [En ligne]. 2014. n°January, p. 1-13. Disponible sur : < https://doi.org/10.1038/nri3600 >

Ichinose M. « Differences of Inflammatory Mechanisms in Asthma and COPD ». *Allergol. Int.* [En ligne]. 1 janvier 2009. Vol. 58, n°3, p. 307-313. Disponible sur : < https://doi.org/10.2332/ALLERGOLINT.09-RAI-0106 > (consulté le 28 août 2018)

Ishihara T., Kubota T., Choi T., Takahashi M., Ayano E., Kanazawa H., Higaki M. « Polymeric nanoparticles encapsulating betamethasone phosphate with different release profiles and stealthiness ». *Int. J. Pharm.* [En ligne]. 22 juin 2009. Vol. 375, n°1-2, p. 148-154. Disponible sur : < https://doi.org/10.1016/J.IJPHARM.2009.04.001 > (consulté le 5 février 2019)

Ishmael F. T. « The inflammatory response in the Pathogenesis of Asthma ». *J. Am. Osteopath. Assoc.* [En ligne]. 2011. Vol. 111, n°11_suppl_7, p. S11-S17. Disponible sur : < http://dx.doi.org/ >

Islam N., Gladki E. « Dry powder inhalers (DPIs)—A review of device reliability and innovation ». *Int. J. Pharm.* [En ligne]. 2008. Vol. 360, n°1, p. 1-11. Disponible sur : < https://doi.org/10.1016/j.ijpharm.2008.04.044 > (consulté le 8 juin 2017)

Islan G. A., Tornello P. C., Abraham G. A., Duran N., Castro G. R. « Smart lipid nanoparticles containing levofloxacin and DNase for lung delivery. Design and characterization ». *Colloids Surfaces B Biointerfaces* [En ligne]. 2016. Vol. Jul 1, n°143, p. 168-176. Disponible sur : < https://doi.org/10.1016/j.colsurfb.2016.03.040 >

Jaafar-Maalej C., Andrieu V., Elaissari A., Fessi H. « Beclomethasone-Loaded Lipidic Nanocarriers for Pulmonary Drug Delivery: Preparation, Characterization and <I>In Vitro</I> Drug Release ». *J. Nanosci. Nanotechnol.* [En ligne]. 2011. Vol. 11, n°3, p. 1841-1851. Disponible sur : < https://doi.org/10.1166/jnn.2011.3119 >

Jacobs C., Helmut Müller R. « Production and Characterization of a Budesonide Nanosuspension for Pulmonary Administration ». *Pharm. Res.* [En ligne]. 1 mars 2002. Vol. 19, n°2, p. 189-194. Disponible sur : < https://doi.org/10.1023/A:1014276917363 >

Jenkins C. R., Chapman K. R., Donohue J. F., Roche N., Tsiligianni I., Han M. K. « Improving the Management of COPD in Women ». *Chest* [En ligne]. 1 mars 2017. Vol. 151, n°3, p. 686-696. Disponible sur : < https://doi.org/10.1016/J.CHEST.2016.10.031 > (consulté le 2 août 2018)

Kaczmarek J. C., Patel A. K., Kauffman K. J., Fenton O. S., Webber M. J., Heartlein M. W., DeRosa F., Anderson D. G. « Polymer-Lipid Nanoparticles for Systemic Delivery of mRNA to the Lungs ». *Angew. Chemie Int. Ed. English* [En ligne]. 2017. Vol. 55, n°44, p. 13808-13812. Disponible sur : < https://doi.org/10.1002/anie.201608450.Polymer-Lipid >

Kaur I. P., Singh H. « Nanostructured drug delivery for better management of tuberculosis ». *J. Control. Release* [En ligne]. 28 juin 2014. Vol. 184, p. 36-50. Disponible sur : < https://doi.org/10.1016/J.JCONREL.2014.04.009 > (consulté le 31 janvier 2019)

Keenan C. R., Salem S., Fietz E. R., Gualano R. C., Stewart A. G. « Glucocorticoid-resistant asthma and

novel anti-inflammatory drugs ». *Drug Discov. Today* [En ligne]. 1 septembre 2012. Vol. 17, n°17-18, p. 1031-1038. Disponible sur : < https://doi.org/10.1016/J.DRUDIS.2012.05.011 > (consulté le 10 décembre 2018)

Kelly H. W. « Comparison of Inhaled Corticosteroids ». *Ann. Pharmacother.* [En ligne]. 1 février 1998. Vol. 32, n°2, p. 220-232. Disponible sur : < https://doi.org/10.1345/aph.17014 >

Khan I., Elhissi A., Shah M., Alhnan M. A., Ahmed W. « Liposome-based carrier systems and devices used for pulmonary drug delivery ». *Biomater. Med. Tribol.* [En ligne]. 1 janvier 2013. p. 395-443. Disponible sur : < https://doi.org/10.1533/9780857092205.395 > (consulté le 4 février 2019)

Khutoryanskiy V. V. « Beyond PEGylation: Alternative surface-modification of nanoparticles with mucus-inert biomaterials ». *Adv. Drug Deliv. Rev.* [En ligne]. 15 janvier 2018. Vol. 124, p. 140-149. Disponible sur : < https://doi.org/10.1016/J.ADDR.2017.07.015 > (consulté le 25 juillet 2018)

Konduri K. S., Nandedkar S., Düzgünes N., Suzara V., Artwohl J., Bunte R., Gangadharam P. R. J. « Efficacy of liposomal budesonide in experimental asthma ». *J. Allergy Clin. Immunol.* [En ligne]. 2003. Vol. 111, n°2, p. 321-327. Disponible sur : < https://doi.org/10.1067/mai.2003.104 >

Korenblat P., Kerwin E., Leshchenko I., Yen K., Holweg C. T. J., Anzures-Cabrera J., Martin C., Putnam W. S., Governale L., Olsson J., Matthews J. G. « Efficacy and safety of lebrikizumab in adult patients with mild-to-moderate asthma not receiving inhaled corticosteroids ». *Respir. Med.* [En ligne]. 2017. Vol. 134, n°October 2017, p. 143-149. Disponible sur : < https://doi.org/10.1016/j.rmed.2017.12.006 >

Kupczyk M., Kuna P. « Benralizumab: an anti-IL-5 receptor α monoclonal antibody in the treatment of asthma ». *Immunotherapy* [En ligne]. 2018. Vol. 10, n°5, p. 349-359. Disponible sur : < https://doi.org/10.2217/imt-2017-0161 >

Kuzmov A., Minko T. « Nanotechnology approaches for inhalation treatment of lung diseases. » *J. Control. Release* [En ligne]. 10 décembre 2015. Vol. 219, p. 500-18. Disponible sur : < https://doi.org/10.1016/j.jconrel.2015.07.024 > (consulté le 12 mai 2016)

Leng D., Thanki K., Fattal E., Foged C., Yang M. « Engineering of budesonide-loaded lipid-polymer hybrid nanoparticles using a quality-by-design approach ». *Int. J. Pharm.* [En ligne]. 2018. Vol. 548, n°2, p. 740-746. Disponible sur : < https://doi.org/https://doi.org/10.1016/j.ijpharm.2017.08.094 >

De Leo V., Ruscigno S., Trapani A., Di Gioia S., Milano F., Mandracchia D., Comparelli R., Castellani S., Agostiano A., Trapani G., Catucci L., Conese M. « Preparation of drug-loaded small unilamellar liposomes and evaluation of their potential for the treatment of chronic respiratory diseases ». *Int. J. Pharm.* [En ligne]. 10 juillet 2018. Vol. 545, n°1-2, p. 378-388. Disponible sur : < https://doi.org/10.1016/J.IJPHARM.2018.04.030 > (consulté le 15 mars 2019)

Li N., Weng D., Wang S. M., Zhang Y., Chen S. S., Yin Z. F., Zhai J., Scoble J., Williams C. C., Chen T., Qiu H., Wu Q., Zhao M. M., Lu L. Q., Mulet X., Li H. P. « Surfactant protein-A nanobody-conjugated liposomes loaded with methylprednisolone increase lung-targeting specificity and therapeutic effect for acute lung injury ». *Drug Deliv.* [En ligne]. 2017. Vol. 24, n°1, p. 1770-1781. Disponible sur : < https://doi.org/10.1080/10717544.2017.1402217 >

Lipworth B. J. « Systemic Adverse Effects of Inhaled Corticosteroid Therapy: a systematic review and meta-analysis ». *Arch. Intern. Med.* 1999. Vol. 159, p. 941-955.

Liu J., Gong T., Fu H., Wang C., Wang X., Chen Q., Zhang Q., He Q., Zhang Z. « Solid lipid nanoparticles for pulmonary delivery of insulin ». *Int. J. Pharm.* [En ligne]. 2008. Disponible sur : <

https://doi.org/10.1016/j.ijpharm.2008.01.008 >

Liu M., Zhang J., Shan W., Huang Y. « Developments of mucus penetrating nanoparticles ». *Asian J. Pharm. Sci.* [En ligne]. 2015. Vol. 10, n°4, p. 275-282. Disponible sur : < https://doi.org/10.1016/j.ajps.2014.12.007 >

Liu Y., Bos I. S. T., Oenema T. A., Meurs H., Maarsingh H., Hirsch A. K. H. « Delivery system for budesonide based on lipid-DNA ». *Eur. J. Pharm. Biopharm.* [En ligne]. 1 septembre 2018. Vol. 130, p. 123-127. Disponible sur : < https://doi.org/10.1016/J.EJPB.2018.06.012 > (consulté le 16 mars 2019)

Loira-Pastoriza C., Todoroff J., Vanbever R. « Delivery strategies for sustained drug release in the lungs ». *Adv. Drug Deliv. Rev.* [En ligne]. 2014. Vol. 75, p. 81-91. Disponible sur : < https://doi.org/10.1016/j.addr.2014.05.017 >

Lötvall J., Akdis C. A., Bacharier L. B., Bjermer L., Casale T. B., Custovic A., Lemanske R. F., Wardlaw A. J., Wenzel S. E., Greenberger P. A. « Asthma endotypes: A new approach to classification of disease entities within the asthma syndrome ». *J. Allergy Clin. Immunol.* [En ligne]. 2011. Vol. 127, n°2, p. 355-360. Disponible sur : < https://doi.org/10.1016/j.jaci.2010.11.037 >

Lu X., Wu D., Li Z.-J., Chen G.-Q. *Polymer Nanoparticles I . Definition and General Ingredients of Polymer Nanoparticles* [En ligne]. 1re éd.[s.l.] : Elsevier Inc., 2011. 299-323 p. Disponible sur : < https://doi.org/10.1016/B978-0-12-416020-0.00007-3 >ISBN : 9780124160200.

Luczak-Wozniak K., Dabrowska M., Domagala I., Miszczuk M., Lubanski W., Leszczynski A., Krenke R. « Mishandling of pMDI and DPI inhalers in asthma and COPD – Repetitive and non-repetitive errors ». *Pulm. Pharmacol. Ther.* [En ligne]. 2018. Vol. 51, p. 65-72. Disponible sur : < https://doi.org/10.1016/j.pupt.2018.06.002 >

Macintyre N. R., Faarc M. « Corticosteroid Therapy and Chronic Obstructive Pulmonary Disease Introduction The Rationale for Corticosteroids in COPD Corticosteroid Risks for Patients With COPD The Evidence Base for Clinical Efficacy of Corticosteroids in COPD Recommendations Summary ». *Respir. Care* [En ligne]. 2006. Vol. 51, n°3, p. 289-296. Disponible sur : < http://www.rcjournal.com/contents/03.06/03.06.0289.pdf >

MacNee W. « Pathology, pathogenesis, and pathophysiology ». *Bmj* [En ligne]. 2006. Vol. 332, n°7551, p. 1202-1204. Disponible sur : < https://doi.org/10.1136/bmj.332.7551.1202 >

Maltby S., Gibson P. G., Powell H., McDonald V. M. « Omalizumab Treatment Response in a Population With Severe Allergic Asthma and Overlapping COPD ». *Chest* [En ligne]. 1 janvier 2017. Vol. 151, n°1, p. 78-89. Disponible sur : < https://doi.org/10.1016/J.CHEST.2016.09.035 > (consulté le 10 juillet 2018)

Marqués-Gallego P., Kroon A. I. P. M. « Ligation Strategies for Targeting Liposomal Nanocarriers ». *Biomed Res. Int.* 2014. Vol. 2014, p. 12 pages.

Martinez-Pomares L. « The mannose receptor ». *J. Leukoc. Biol.* 2012. Vol. 92, n°December, p. 1177-1186.

Masoli M., Fabian D., Holt S., Beasley R. « The global burden of asthma: Executive summary of the GINA Dissemination Committee Report ». *Allergy Eur. J. Allergy Clin. Immunol.* [En ligne]. 2004. Vol. 59, n°5, p. 469-478. Disponible sur : < https://doi.org/10.1111/j.1398-9995.2004.00526.x >

Matsuo Y., Ishihara T., Ishizaki J., Miyamoto K., Higaki M., Yamashita N. « Effect of betamethasone phosphate loaded polymeric nanoparticles on a murine asthma model ». *Cell. Immunol.* [En ligne]. 1 janvier 2009. Vol. 260, n°1, p. 33-38. Disponible sur : <

https://doi.org/10.1016/J.CELLIMM.2009.07.004 > (consulté le 5 février 2019)

Menon J. U., Ravikumar P., Pise A., Gyawali D., Hsia C. C. W., Nguyen K. T. « Polymeric nanoparticles for pulmonary protein and DNA delivery ». *Acta Biomater.* [En ligne]. 1 juin 2014. Vol. 10, n°6, p. 2643-2652. Disponible sur : < https://doi.org/10.1016/J.ACTBIO.2014.01.033 > (consulté le 10 février 2019)

Meyer N., Dallinga J. W., Nuss S. J., Moonen E. J. C., Berkel J. J. B. N. Van, Akdis C., Schooten F. J. Van, Menz G. « Defining adult asthma endotypes by clinical features and patterns of volatile organic compounds in exhaled air ». *Respir. Res.* 2014. Vol. 15, n°136, p. 1-9.

Miller-Larsson A., Jansson P., Runstrom A., Brattsand R. « Prolonged airway activity and improved selectivity of budesonide possibly due to esterification ». *Am. J. Respir. Crit. Care Med.* [En ligne]. 2000. Vol. 162, n°4 I, p. 1455-1461. Disponible sur : < https://doi.org/10.1164/ajrccm.162.4.9806112 >

Morris H. G. « Mechanisms of action and therapeutic role of corticosteroids in asthma ». *J. Allergy Clin. Immunol.* [En ligne]. 1 janvier 1985. Vol. 75, n°1, p. 1-13. Disponible sur : < https://doi.org/10.1016/0091-6749(85)90002-8 > (consulté le 10 décembre 2018)

Müller R. H., Shegokar R., Keck C. M. « 20 Years of Lipid Nanoparticles (SLN & NLC): Present State of Development & Industrial Applications ». *Curr. Drug Discov. Technol.* 2011. Vol. 8, n°3, p. 207-227.

Müller R., Radtke M., Wissing S. A. « Nanostructured lipid matrices for improved microencapsulation of drugs ». *Int. J. Pharm.* 2002. Vol. 242, p. 121-128.

Muppidi K., Wang J., Betageri G., Pumerantz A. S. « PEGylated Liposome Encapsulation Increases the Lung Tissue Concentration of Vancomycin ». *Antimicrob. Agents Chemother.* 2011. Vol. 55, n°10, p. 4537-4542.

Muralidharan P., Hayes D., Mansour H. M. « Dry powder inhalers in COPD, lung inflammation and pulmonary infections ». *Expert Opin. Drug Deliv.* [En ligne]. 3 juin 2015. Vol. 12, n°6, p. 947-962. Disponible sur : < https://doi.org/10.1517/17425247.2015.977783 >

Murgia X., Loretz B., Hartwig O., Hittinger M., Lehr C.-M. « The role of mucus on drug transport and its potential to affect therapeutic outcomes ». *Adv. Drug Deliv. Rev.* [En ligne]. 15 janvier 2018. Vol. 124, p. 82-97. Disponible sur : < https://doi.org/10.1016/J.ADDR.2017.10.009 > (consulté le 25 juillet 2018)

Nakawah M. O., Hawkins C., Barbandi F. « Asthma, Chronic Obstructive Pulmonary Disease (COPD), and the Overlap Syndrome ». *J. Am. Board Fam. Med.* [En ligne]. 2013. Vol. 26, n°4, p. 470-477. Disponible sur : < https://doi.org/10.3122/jabfm.2013.04.120256 >

Nixon J., Newbold P., Mustelin T., Anderson Gary P., Kolbeck R. « Monoclonal antibody therapy for the treatment of asthma and chronic obstructive pulmonary disease with eosinophilic inflammation ». *Pharmacol. Ther.* [En ligne]. 1 janvier 2017. Vol. 169, p. 57-77. Disponible sur : < https://doi.org/10.1016/J.PHARMTHERA.2016.10.016 > (consulté le 3 décembre 2018)

Osman N., Kaneko K., Carini V., Saleem I. « Carriers for the targeted delivery of aerosolized macromolecules for pulmonary pathologies ». *Expert Opin. Drug Deliv.* [En ligne]. 2018. Vol. 15, n°8, p. 821-834. Disponible sur : < https://doi.org/10.1080/17425247.2018.1502267 >

Panettieri R. A., Wang M., Braddock M., Bowen K., Colice G. « Tralokinumab for the treatment of severe, uncontrolled asthma: The ATMOSPHERE clinical development program ». *Immunotherapy* [En ligne]. 2018. Vol. 10, n°6, p. 473-490. Disponible sur : < https://doi.org/10.2217/imt-2017-0191 >

Pappas K., Papaioannou A. I., Kostikas K., Tzanakis N. « The role of macrophages in obstructive airways

disease: Chronic obstructive pulmonary disease and asthma ». *Cytokine* [En ligne]. 2013. Vol. 64, n°3, p. 613-625. Disponible sur : < https://doi.org/10.1016/j.cyto.2013.09.010 >

Parmar J. J., Singh D. J., Hegde D. D., Lohade A. A., Soni P. S., Samad A., Menon M. D. « Development and Evaluation of Inhalational Liposomal System of Budesonide for Better Management of Asthma ». *Indian J. Pharm. Sci.* 2010. Vol. 72, n°August, p. 442-448.

Pharmacopoeia E. *Non enrobés inhalation: évaluation aérodynamique des particules*. [s.l.] : [s.n.], 2019.

Popov A., Schopf L., Bourassa J., Chen H. « Enhanced pulmonary delivery of fluticasone propionate in rodents by mucus-penetrating nanoparticles ». *Int. J. Pharm.* [En ligne]. 11 avril 2016. Vol. 502, n°1-2, p. 188-197. Disponible sur : < https://doi.org/10.1016/J.IJPHARM.2016.02.031 > (consulté le 20 septembre 2017)

Postma D. S., Rabe K. F. « The Asthma–COPD Overlap Syndrome ». *N. Engl. J. Med.* [En ligne]. 2015. Vol. 373, n°13, p. 1241-1249. Disponible sur : < https://doi.org/10.1056/NEJMra1411863 >

Puri A., Loomis K., Smith B., Lee J.-H., Yavlovich A., Heldman E., Blumenthal R. « Lipid-based nanoparticles as pharmaceutical drug carriers: from concepts to clinic ». *Crit. Rev. Ther. Drug Carrier Syst.* [En ligne]. 2009. Vol. 26, n°6, p. 523-580. Disponible sur : < https://www.ncbi.nlm.nih.gov/pubmed/20402623 >

Raissy H. H., Kelly H. W., Harkins M., Szefler S. J. « Inhaled corticosteroids in lung diseases ». *Am. J. Respir. Crit. Care Med.* [En ligne]. 2013. Vol. 187, n°8, p. 798-803. Disponible sur : < https://doi.org/10.1164/rccm.201210-1853PP >

Ramamoorthy S., Cidlowski J. A. « Corticosteroids: Mechanisms of Action in Health and Disease ». *Rheum. Dis. Clin. North Am.* [En ligne]. 1 février 2016. Vol. 42, n°1, p. 15-31. Disponible sur : < https://doi.org/10.1016/J.RDC.2015.08.002 > (consulté le 28 janvier 2019)

Ramsahai J. M., Wark P. A. B. « Appropriate use of oral corticosteroids for severe asthma ». *Med. J. Aust.* [En ligne]. 2018. Vol. 209, n°2 suppl, p. S18-S21. Disponible sur : < https://doi.org/10.5694/mja18.00134 >

Rigo L. A., Carvalho-Wodarz C. S., Pohlmann A. R., Guterres S. S., Schneider-Daum N., Lehr C.-M., Beck R. C. R. « Nanoencapsulation of a glucocorticoid improves barrier function and anti-inflammatory effect on monolayers of pulmonary epithelial cell lines ». *Eur. J. Pharm. Biopharm.* [En ligne]. 1 octobre 2017. Vol. 119, p. 1-10. Disponible sur : < https://doi.org/10.1016/J.EJPB.2017.05.006 > (consulté le 30 mars 2019)

Van Rijt S. H., Bein T., Meiners S. « Medical nanoparticles for next generation drug delivery to the lungs ». *Eur. Respir. J.* [En ligne]. 1 septembre 2014. Vol. 44, n°3, p. 765 LP - 774. Disponible sur : < https://doi.org/10.1183/09031936.00212813 >

Rothenberg M. E., Hogan S. P. « The Eosinophil ». *Annu. Rev. Immunol.* [En ligne]. 2006. Vol. 24, p. 147-174. Disponible sur : < https://doi.org/10.1016/S0021-9975(08)80204-6 >

Rovina N., Koutsoukou A., Koulouris N. G. « Inflammation and immune response in COPD: Where do we stand? ». *Mediators Inflamm.* [En ligne]. 2013. Vol. Article ID, p. 1-9. Disponible sur : < https://doi.org/10.1155/2013/413735 >

Rudokas M., Najlah M., Alhnan M. A., Elhissi A. « Liposome Delivery Systems for Inhalation: A Critical Review Highlighting Formulation Issues and Anticancer Applications ». *Med. Princ. Pract.* [En ligne].

juillet 2016. Vol. 25 Suppl 2, n°Suppl 2, p. 60-72. Disponible sur : < https://doi.org/10.1159/000445116 >

Ruge C. A., Hillaireau H., Grabowski N., Beck-Broichsitter M., Cañadas O., Tsapis N., Casals C., Nicolas J., Fattal E. « Pulmonary Surfactant Protein A-Mediated Enrichment of Surface-Decorated Polymeric Nanoparticles in Alveolar Macrophages ». *Mol. Pharm.* [En ligne]. 2016. Vol. 13, n°12, p. 4168-4178. Disponible sur : < https://doi.org/10.1021/acs.molpharmaceut.6b00773 >

Sahib M. N., Abdulameer S. A., Darwis Y., Peh K. K., Tan Y. T. F. « Solubilization of beclomethasone dipropionate in sterically stabilized phospholipid nanomicelles (SSMs): physicochemical and in vitro evaluations ». *Drug Des. Devel. Ther.* [En ligne]. 17 février 2012. Vol. 6, p. 29-42. Disponible sur : < https://doi.org/10.2147/DDDT.S28265 >

Sahu P. K., Mishra D. K., Jain N., Rajoriya V., Jain A. K. « Mannosylated solid lipid nanoparticles for lung-targeted delivery of Paclitaxel. » *Drug Dev. Ind. Pharm.* [En ligne]. 2014. Vol. 9045, p. 1-10. Disponible sur : < https://doi.org/10.3109/03639045.2014.891130 >

Sansores R. H., Ramírez-Venegas A. « COPD in women: Susceptibility or vulnerability ». *Eur. Respir. J.* [En ligne]. 2016. Vol. 47, n°1, p. 19-22. Disponible sur : < https://doi.org/10.1183/13993003.01781-2015 >

Schuster B. S., Suk J. S., Woodworth G. F., Hanes J. « Nanoparticle diffusion in respiratory mucus from humans without lung disease ». *Biomaterials* [En ligne]. 1 avril 2013. Vol. 34, p. 3439-3446. Disponible sur : < https://doi.org/10.1016/J.BIOMATERIALS.2013.01.064 > (consulté le 20 septembre 2017)

Sedaghat B., Stephenson R. J., Giddam A. K., Eskandari S., Apte S. H., Pattinson D. J., Doolan D. L., Toth I. « Synthesis of Mannosylated Lipopeptides with Receptor Targeting Properties ». *Bioconjug. Chem.* [En ligne]. 2016. Vol. 27, n°3, p. 533-548. Disponible sur : < https://doi.org/10.1021/acs.bioconjchem.5b00547 >

Severino P., Andreani T., Macedo A. S., Fangueiro J. F., Santana M. H. A., Silva A. M., Souto E. B. « Current State-of-Art and New Trends on Lipid Nanoparticles (SLN and NLC) for Oral Drug Delivery ». *J. Drug Deliv.* [En ligne]. 2012. Vol. 2012, p. 1-10. Disponible sur : < https://doi.org/10.1155/2012/750891 >

Shah A., Bajaj A. N., Jain D. S. « Fabrication and In Vitro Evaluation of Solid Lipid Nanoparticles of Mometasone Furoate for Pulmonary Delivery ». *J. Nanopharmaceutics Drug Deliv.* 2013. Vol. 1, n°3, p. 311-322.

Shaikh S., Nazim S., Khan T., Shaikh A., Zameeruddin M. « Recent advances in pulmonary drug delivery system : a review ». *Int. J. Appl. Pharm.* 2010. Vol. 2, n°4, p. 27-31.

Shepherd V. L., Freeze H. H., Miller A. L., Stahl P. D. « Identification of mannose 6-phosphate receptors in rabbit alveolar macrophages ». *J. Biol. Chem.* 1984. Vol. 259, n°4, p. 2257-2261.

Sims M. W., Tal-Singer R. M., Kierstein S., Musani A. I., Beers M. F., Panettieri R. A., Haczku A. « Chronic obstructive pulmonary disease and inhaled steroids alter surfactant protein D (SP-D) levels: a cross-sectional study ». *Respir. Res.* [En ligne]. 28 janvier 2008. Vol. 9, n°1, p. 13. Disponible sur : < https://doi.org/10.1186/1465-9921-9-13 >

Sin D. D., Man S. . P. « Chronic obstructive pulmonary disease: a novel risk factor for cardiovascular disease ». *Can. J. Physiol. Pharmacol.* [En ligne]. 2005. Vol. 83, n°1, p. 8-13. Disponible sur : < https://doi.org/10.1139/y04-116 >

Spies C. M., Strehl C., Van der Goes M. C., Bijlsma J. W. J., Buttgereit F. « Glucocorticoids ». *Best Pract. Res. Clin. Rheumatol.* [En ligne]. 1 décembre 2011. Vol. 25, n°6, p. 891-900. Disponible sur : < https://doi.org/10.1016/J.BERH.2011.11.002 > (consulté le 26 octobre 2018)

Spoelhof B., Ray S. D. « Corticosteroids ». *Encycl. Toxicol.* [En ligne]. 1 janvier 2014. p. 1038-1042. Disponible sur : < https://doi.org/10.1016/B978-0-12-386454-3.00293-1 > (consulté le 29 janvier 2019)

Stein S. W., Thiel C. G. « The History of Therapeutic Aerosols : A Chronological Review ». *J. Aerosol Med. Pulm. Drug Deliv.* [En ligne]. 2017. Vol. 30, n°1, p. 20-41. Disponible sur : < https://doi.org/10.1089/jamp.2016.1297 >

Stirling R. G., Van Rensen E. L. J., Barnes P. J., Chung K. F. « Interleukin-5 induces CD34+eosinophil progenitor mobilization and eosinophil CCR3 expression in asthma ». *Am. J. Respir. Crit. Care Med.* [En ligne]. 2001. Vol. 164, n°8 I, p. 1403-1409. Disponible sur : < https://doi.org/10.1164/ajrccm.164.8.2010002 >

Strehl C., Buttgereit F. « Optimized glucocorticoid therapy: Teaching old drugs new tricks ». *Mol. Cell. Endocrinol.* [En ligne]. 2013. Vol. 380, n°1-2, p. 32-40. Disponible sur : < https://doi.org/10.1016/j.mce.2013.01.026 >

Strunk R. C., Bloomberg G. R. « Omalizumab for Asthma ». *N. Engl. J. Med.* 2006. Vol. 354, p. 2689-2695.

Suntres Z. E., Shek P. N. « Prophylaxis against lipopolysaccharide-induced lung injuries by liposome-entrapped dexamethasone in rats ». *Biochem. Pharmacol.* [En ligne]. 1 mai 2000. Vol. 59, n°9, p. 1155-1161. Disponible sur : < https://doi.org/10.1016/S0006-2952(99)00411-6 > (consulté le 15 mars 2019)

Sutherland E. R., Martin R. J. « Airway inflammation in chronic obstructive pulmonary disease: Comparisons with asthma ». *J. Allergy Clin. Immunol.* [En ligne]. 1 novembre 2003. Vol. 112, n°5, p. 819-827. Disponible sur : < https://doi.org/10.1016/S0091-6749(03)02011-6 > (consulté le 28 août 2018)

Taherali F., Varum F., Basit A. W. « A slippery slope: On the origin, role and physiology of mucus ». *Adv. Drug Deliv. Rev.* [En ligne]. 15 janvier 2018. Vol. 124, p. 16-33. Disponible sur : < https://doi.org/10.1016/J.ADDR.2017.10.014 > (consulté le 25 juillet 2018)

Tam A., Morrish D., Wadsworth S., Dorscheid D., Man S. F. P., Sin D. D. « The role of female hormones on lung function in chronic lung diseases ». *BMC Womens. Health* [En ligne]. 2011. Vol. 11, n°24, p. 1-9. Disponible sur : < https://doi.org/10.1186/1472-6874-11-24 >

Tattersfield A. E., Harrison T. W., Hubbard R. B., Mortimer K. « Safety of Inhaled Corticosteroids ». *Proc. Am. Thorac. Soc.* [En ligne]. 2004. Vol. 1, p. 171-175. Disponible sur : < https://doi.org/10.1513/pats.200402-016MS >

Taylor M. E. « Structure and Function of the Macrophage Mannose Receptor ». *Mamm. Carbohydr. Recognit. Syst.* [En ligne]. 2001. Vol. 33, p. 105-121. Disponible sur : < https://doi.org/10.1007/978-3-540-46410-5_6 >

Tena A. F., Clará P. C. « Deposition of Inhaled Particles in Lungs ». *Arch. Bronconeumol. (English Ed.* [En ligne]. 2012. Vol. 48, n°7, p. 240-246. Disponible sur : < https://doi.org/10.1016/j.arbr.2012.02.006 >

Tewes F., Ehrhardt C., Healy A. M. « Superparamagnetic iron oxide nanoparticles (SPIONs)-loaded Trojan microparticles for targeted aerosol delivery to the lung ». *Eur. J. Pharm. Biopharm.* [En ligne]. 1

janvier 2014. Vol. 86, n°1, p. 98-104. Disponible sur : < https://doi.org/10.1016/J.EJPB.2013.09.004 > (consulté le 16 décembre 2018)

The American Lung Association. « Taking Her Breath Away: The rise of COPD in women ». 2013.

Triolo D., Craparo E. F., Porsio B., Fiorica C., Giammona G., Cavallaro G. « Polymeric drug delivery micelle-like nanocarriers for pulmonary administration of beclomethasone dipropionate ». *Colloids Surfaces B Biointerfaces* [En ligne]. 2017. Vol. 151, p. 206-214. Disponible sur : < https://doi.org/https://doi.org/10.1016/j.colsurfb.2016.11.025 >

Tsapis N., Bennett D., Jackson B., Weitz D. A., Edwards D. A. « Trojan particles: Large porous carriers of nanoparticles for drug delivery ». *Proc. Natl. Acad. Sci. U. S. A.* [En ligne]. 2002. Vol. 99, n°19, p. 12001-12005. Disponible sur : < https://doi.org/10.1073/pnas.182233999 >

Tunek A., Sjödin K., Hallström G. « Reversible formation of fatty acid esters of budesonide, an antiasthma glucocorticoid, in human lung and liver microsomes ». *Drug Metab. Dispos.* 1997. Vol. 25, n°11, p. 1311-1317.

Um S. J., Lam S., Coxson H., Man S. F. P., Sin D. D. « Budesonide/Formoterol Enhances the Expression of Pro Surfactant Protein-B in Lungs of COPD Patients ». *PLoS One* [En ligne]. 26 décembre 2013. Vol. 8, n°12, p. e83881. Disponible sur : < https://doi.org/10.1371/journal.pone.0083881 >

Varshosaz J., Ghaffari S., Mirshojaei S. F., Jafarian A., Atyabi F., Kobarfard F., Azarmi S. « Biodistribution of Amikacin Solid Lipid Nanoparticles after Pulmonary Delivery ». *Biomed Res. Int.* [En ligne]. 2013. Vol. 2013, p. 8 pages. Disponible sur : < https://doi.org/http://dx.doi.org/10.1155/2013/136859 >

Vatrella A., Fabozzi I., Calabrese C., Maselli R., Pelaia G. « Dupilumab: a novel treatment for asthma ». *J. Asthma Allergy* [En ligne]. 2014. Vol. 7, p. 123-130. Disponible sur : < https://doi.org/10.2147/jaa.s52387 >

Van Der Velden V. H. J. « Glucocorticoids: Mechanisms of action and anti-inflammatory potential in asthma ». *Mediators Inflamm.* [En ligne]. 1998. Vol. 7, n°4, p. 229-237. Disponible sur : < https://doi.org/10.1080/09629359890910 >

Vij N., Min T., Bodas M., Gorde A., Roy I. « Neutrophil targeted nano-drug delivery system for chronic obstructive lung diseases ». *Nanomedicine Nanotechnology, Biol. Med.* [En ligne]. 2016. Vol. 12, n°8, p. 2415-2427. Disponible sur : < https://doi.org/10.1016/j.nano.2016.06.008 >

Virchow J. C., Crompton G. K., Dal Negro R., Pedersen S., Magnan A., Seidenberg J., Barnes P. J. « Importance of inhaler devices in the management of airway disease ». *Respir. Med.* [En ligne]. 1 janvier 2008a. Vol. 102, n°1, p. 10-19. Disponible sur : < https://doi.org/10.1016/J.RMED.2007.07.031 > (consulté le 31 octobre 2018)

Vyas S. ., Katare Y. ., Mishra V., Sihorkar V. « Ligand directed macrophage targeting of amphotericin B loaded liposomes ». *Int. J. Pharm.* [En ligne]. décembre 2000. Vol. 210, n°1-2, p. 1-14. Disponible sur : < https://doi.org/10.1016/S0378-5173(00)00522-6 > (consulté le 1 juin 2016)

Vyas S. P., Sihorkar V., Jain S. « Mannosylated liposomes for bio-film targeting. » *Int. J. Pharm.* [En ligne]. 7 février 2007. Vol. 330, n°1-2, p. 6-13. Disponible sur : < https://doi.org/10.1016/j.ijpharm.2006.08.034 > (consulté le 21 avril 2016)

Waldrep J. C., Gilbert B. E., Knight C. M., Black M. B., Scherer P. W., Knight V., Eschenbacher W. « Pulmonary Delivery of Beclomethasone Liposome Aerosol in Volunteers: Tolerance and Safety ». *Chest* [En ligne]. 2008. Vol. 111, n°2, p. 316-323. Disponible sur : <

https://doi.org/10.1378/chest.111.2.316 >

Wang H., Rempel G. L. « Introduction of Polymer Nanoparticles for Drug Delivery Applications ». *J. Nanotechnol. Nanomedicine Nanobiotechnology* [En ligne]. 2015. Vol. 2, n°008, p. 1-6. Disponible sur : < https://doi.org/10.24966/NTMB-2044/100008 >

Wang Y., Lai S. K., Pace A., Cone R. « Addressing the PEG Mucoadhesivity Paradox to Engineer Nanoparticles that "Slip" through the Human Mucus Barrier ». *Angew. Chemie Int. Ed. English* [En ligne]. 2008. Vol. 47, n°50, p. 9726-9729. Disponible sur : < https://doi.org/10.1002/anie.200803526 >

Weinberger S. E., Cockrill B. A., Mandel J., Weinberger S. E., Cockrill B. A., Mandel J. « Chronic Obstructive Pulmonary Disease ». *Princ. Pulm. Med.* [En ligne]. 1 janvier 2019. p. 93-112. Disponible sur : < https://doi.org/10.1016/B978-0-323-52371-4.00009-X > (consulté le 11 juillet 2018)

Weiss S. T. « Emerging mechanisms and novel targets in allergic inflammation and asthma ». *Genome Med.* [En ligne]. 2017. Vol. 9, n°107, p. 1-3. Disponible sur : < https://doi.org/10.1186/s13073-017-0501-6 >

Von Wichert P., Seifart C. « The Lung, an Organ for Absorption? ». *Respiration* [En ligne]. 1 septembre 2005. Vol. 72, n°5, p. 552-558. Disponible sur : < https://doi.org/10.1159/000087685 >

Wijagkanalan W., Higuchi Y., Kawakami S., Teshima M., Sasaki H., Hashida M. « Enhanced anti-inflammation of inhaled dexamethasone palmitate using mannosylated liposomes in an endotoxin-induced lung inflammation model. » *Mol. Pharmacol.* [En ligne]. 2008. Vol. 74, n°5, p. 1183-1192. Disponible sur : < https://doi.org/10.1124/mol.108.050153.chemoattractant-1 >

Wijagkanalan W., Kawakami S., Takenaga M., Igarashi R., Yamashita F., Hashida M. « Efficient targeting to alveolar macrophages by intratracheal administration of mannosylated liposomes in rats. » *J. Control. release* [En ligne]. 22 janvier 2008. Vol. 125, n°2, p. 121-30. Disponible sur : < https://doi.org/10.1016/j.jconrel.2007.10.011 > (consulté le 12 avril 2016)

Wileman T., Boshans R., Stahl P. « Uptake and transport of Mannosylated ligands by alveolar macrophages ». *J. Biol. Chem.* 1985. Vol. 260, n°12, p. 7387-7393.

Winkler J., Hochhaus G., Derendorf H. « How the Lung Handles Drugs - Pharmacokinetics and Pharmacodynamics of Inhaled Corticosteroids ». *Proc. Am. Thorac. Soc.* [En ligne]. 1 décembre 2004. Vol. 1, n°4, p. 356-363. Disponible sur : < https://doi.org/10.1513/pats.200403-025MS >

Wu L., Shan W., Zhang Z., Huang Y. « Engineering nanomaterials to overcome the mucosal barrier by modulating surface properties ». *Adv. Drug Deliv. Rev.* [En ligne]. 15 janvier 2018. Vol. 124, p. 150-163. Disponible sur : < https://doi.org/10.1016/J.ADDR.2017.10.001 > (consulté le 25 juillet 2018)

Xiang Q., Wang M., Chen F., Gong T., Jian Y., Zhang Z.-R., Huang Y. « Lung-targeting delivery of dexamethasone acetate loaded solid lipid nanoparticles ». *Arch. Pharm. Res.* [En ligne]. 1 mai 2007. Vol. 30, n°4, p. 519-525. Disponible sur : < https://doi.org/10.1007/BF02980228 >

Yanagisawa S., Ichinose M. « Definition and diagnosis of asthma–COPD overlap (ACO) ». *Allergol. Int.* [En ligne]. 1 avril 2018. Vol. 67, n°2, p. 172-178. Disponible sur : < https://doi.org/10.1016/J.ALIT.2018.01.002 > (consulté le 10 juillet 2018)

Yang M., Yamamoto H., Kurashima H., Takeuchi H., Yokoyama T., Tsujimoto H., Kawashima Y. « Design and evaluation of poly (DL-lactic-co-glycolic acid) nanocomposite particles containing salmon calcitonin for inhalation ». *Eur. J. Pharm. Sci.* [En ligne]. 2012. Vol. 46, n°5, p. 374-380. Disponible sur : < https://doi.org/10.1016/j.ejps.2012.02.024 >

Yeeprae W., Kawakami S., Yamashita F., Hashida M. « Effect of mannose density on mannose receptor-mediated cellular uptake of mannosylated O/W emulsions by macrophages ». *J. Control. Release* [En ligne]. 2006. Vol. 114, n°2, p. 193-201. Disponible sur : < https://doi.org/10.1016/j.jconrel.2006.04.010 >

Yeh H.-W., Chen D.-R. « In vitro release profiles of PLGA core-shell composite particles loaded with theophylline and budesonide ». *Int. J. Pharm.* [En ligne]. 7 août 2017. Vol. 528, n°1-2, p. 637-645. Disponible sur : < https://doi.org/10.1016/J.IJPHARM.2017.06.032 > (consulté le 29 mars 2019)

Yoo D., Guk K., Kim H., Khang G., Wu D., Lee D. « Antioxidant polymeric nanoparticles as novel therapeutics for airway inflammatory diseases ». *Int. J. Pharm.* [En ligne]. 25 juin 2013. Vol. 450, n°1-2, p. 87-94. Disponible sur : < https://doi.org/10.1016/J.IJPHARM.2013.04.028 > (consulté le 11 février 2019)

Zaru M., Manca M. L., Fadda A. M., Antimisiaris S. G. « Chitosan-coated liposomes for delivery to lungs by nebulisation ». *Colloids Surfaces B Biointerfaces*. 2009. Vol. 71, n°1, p. 88-95.

Zhang J., Tachado S. D., Patel N., Zhu J., Imrich A., Manfruelli P., Cushion M., Kinane T. B., Koziel H. « Negative regulatory role of mannose receptors on human alveolar macrophage proinflammatory cytokine release in vitro cystis organisms by human AM is mediated pre- phagocytosis , release of reactive oxygen species »,. *J. Leukoc. Biol.* [En ligne]. 2005. Vol. 78, n°September, p. 665-674. Disponible sur : < https://doi.org/10.1189/jlb.1204699 >

Zhang Y., Zhang J. « Preparation of budesonide nanosuspensions for pulmonary delivery: Characterization, in vitro release and in vivo lung distribution studies ». *Artif. Cells, Nanomedicine, Biotechnol.* [En ligne]. 6 août 2016. Vol. 44, n°1, p. 285-289. Disponible sur : < https://doi.org/10.3109/21691401.2014.944645 >

Zhao C. L., Zhang Y. C., Yu Z. « Inhalable chitosan coated solid lipid nanoparticles for interventional delivery to lung cancer ». *Lat. Am. J. Pharm.* 2017. Vol. 36, n°1, p. 12-18.

TRAVAUX EXPERIMENTAUX

CHAPITRE 1

TROJAN PARTICLES OF BUDESONIDE PALMITATE NANOPRODRUGS FOR EFFICIENT ALVEOLAR MACROPHAGE TARGETING IN RATS

TROJAN PARTICLES OF BUDESONIDE PALMITATE NANOPRODRUGS FOR EFFICIENT ALVEOLAR MACROPHAGE TARGETING IN RATS

Ludmila Pinheiro do Nascimento[1], Nicolas Tsapis[1], Franceline Reynaud[1,2], Didier Desmaële[1], Catherine Cailleau[1], Juliette Vergnaud[1], Sonia Abreu[3], Pierre Chaminade[3], Elias Fattal[1]

[1] Institut Galien Paris-Sud, CNRS, Univ. Paris-Sud, Univ. Paris-Saclay, 92290 Châtenay-Malabry, France
[2] School of Pharmacy, Federal University of Rio de Janeiro, 21944-59 Rio de Janeiro, Brazil.
[3]Lip(Sys) EA7357, Lipides, systèmes analytiques et biologiques, Univ. Paris-Sud, Univ. Paris-Saclay, 92290 Châtenay-Malabry, France

Abstract

A prodrug of budesonide (Bud), budesonide palmitate (BP) was synthesized and formulated into nanoparticles by emulsion-evaporation or nanoprecipitation methods, using DSPE-mPEG as sole excipient. Spherical nanoparticles of about 200 nm were obtained, with prodrug content between 57-73 %. The anti-inflammatory effect of nanoparticles was observed 48h and 72h after incubation with RAW macrophages. To deliver nanoparticles to the lungs as dry powders, Trojan microparticles containing 5 % nanoparticles were obtained by spray drying with aerodynamic diameter around 1.3 µm, optimal to target the alveolar region. The aerodynamic evaluation also showed a good lung deposition profile with a fine particle fraction (FPF) around 67 % and an alveolar particle fraction (AF) around 41 %. Trojan microparticles were tested *in vivo* in rats to determine the pharmacokinetic and biodistribution of the prodrug and the drug after lung administration, showing very low concentrations in the plasma, for both BP and Bud. This suggests a very pronounced local delivery and a rather low passage of molecules from the lungs to the blood stream, confirmed by the high drug and prodrug concentrations found in lung tissue, epithelial lining fluid and alveolar cell pellet. These results indicate that BP Trojan microparticles present desirable characteristics for efficient alveolar targeting, improving the uptake and retention of budesonide and being a promising carrier for the treatment of respiratory diseases.

Keywords: Nanoparticles, macrophages, prodrug, targeting, Trojan microparticles

1 INTRODUCTION

Respiratory diseases such as asthma and Chronic Obstructive Pulmonary Disease (COPD) are considered a worldwide health burden, with estimated 235 million people suffering from asthma and more than 200 million people affected by COPD (European Respiratory Society, 2013). COPD represents an important public health challenge and is currently the 4th major cause of death worldwide, with projection to be the 3rd by 2020 (GOLD, 2018). Synthetic glucocorticoids (GCs) have been used clinically for decades in the treatment of respiratory chronic diseases as asthma and COPD, because of their potent anti-inflammatory and immunosuppressive effects. GCs inhibit inflammation by attenuating the proinflammatory signaling pathways and promoting the resolution of the inflammatory response through inflammatory cells. Nevertheless, their use is linked to a wide range of adverse effects such as osteoporosis, hyperglycemia, insulin resistance, disturbed fat deposition, hypertension, glaucoma and muscle atrophy, especially at high doses and for long duration of treatment (Jiang *et al.*, 2015 ; Spies *et al.*, 2011 ; Vandewalle *et al.*, 2018). Inhaled corticosteroids (ICS) have been preferred for pharmacological management of asthma and COPD, providing a rapid onset of action, releasing of the drug directly at the site of action and thus avoiding the risk of side effects caused by systemic absorption (Celli, 2018 ; Lavorini *et al*., 2015). However, the treatment of pulmonary diseases may present several challenges related to the chemical and pharmacological characteristics of the ICS (short duration of action), the anatomical characteristics of the lungs hindering the deposition of particles and the factors related to the diseases, such as mucus hypersecretion. The objective of this work is to propose strategies to reduce the risk of side effects, extend glucocorticoid retention in the lungs and favor cellular targeting, to improve treatments currently available.

Inhaled budesonide has a plasma elimination half-life around 2.8 hours, considered intermediate when compared with beclomethasone dipropionate and fluticasone propionate (0.1-0.2 h and 7.8 h, respectively) (Donnelly and Seale, 2001). Inhalation experiments in animals have showed retention of budesonide in airway tissue markedly longer than might be expected on the basis of the drug's lipophilicity alone, which can be explained by a rapid, extensive and reversible intracellular budesonide esterification with long-chain fatty acids in airway tissue (Brink *et al*., 2008 ; Miller-Larsson *et al.*, 2000). Tunek *et al.* (1997) studied the formation of lipophilic metabolites of budesonide in human liver and lung microsomes. Budesonide oleate, palmitate, linoleate, palmitoleate, and arachidonate were identified as metabolites, oleate and palmitate ester being majority species. They found that budesonide is recoverable from the conjugates through the action of lipase, and fatty acid conjugates are most likely be retained intracellularly for longer than unmodified budesonide. Lipid conjugates

therefore represent an intracellular deposit slowly releasing the active glucocorticoid. Delivering directly to the lungs lipid conjugates of budesonide might represent an interesting strategy to further extend budesonide lung retention.

Another barrier to an efficient ICS treatment is mucus hypersecretion, a pathophysiological feature of acute and chronic upper and lower airway diseases such as COPD. Mucus production is a primary defense mechanism for maintaining lung health, with ability to adsorb a wide range of molecules and particles, including drugs, and other potentially harmful entities like pathogens, toxins, and pollutants. However, the overproduction of mucin, the chief glycoprotein component of negatively-charged mucus, is a related pathological feature in respiratory diseases (Evans and Koo, 2009 ; Murgia *et al*., 2018). The protective function of the mucus also hampers the diffusion of drugs and nanomedicines, which dramatically reduces their efficiency. However, it has been shown that PEGylation of nanoparticles could favor their penetration in mucus (Huckaby and Lai, 2018 ; Lai *et al.*, 2009 ; Liu *et al.*, 2015 ; Mert *et al.*, 2012 ; Schuster *et al.*, 2013 ; Wu *et al*., 2018 ; Xu *et al.*, 2013).

Due all these considerations, we propose here to combine the strategy of delivery budesonide lipid prodrug directly to the lungs with the strategy of PEGylation to improve nanoparticle penetration in mucus. We have therefore synthesized a lipophilic derivative of budesonide, budesonide palmitate, and have formulated it into PEGylated nanoparticles using a PEGylated lipid, DSPE-mPEG. In addition, to administer these PEGylated prodrug nanoparticles efficiently to the lungs they were encapsulated into microparticles, called Trojan microparticles (Tsapis *et al*., 2002), with an aerodynamic diameter ranging from 1 to 5 µm, considered adequate size for pulmonary deposition. We have chosen the matrix excipient to quickly release PEGylated nanoparticles after deposition. By using Trojan particles we combine the efficient delivery of porous particles with the ability of nanoparticles to diffuse into mucus and internalize into cells such as macrophages, a key player in lung inflammation (Barnes, 2004 ; Gómez-Gaete *et al.*, 2008 ; Pappas *et al.*, 2013 ; Tsapis *et al*., 2002).

The purpose of this study was to optimize budesonide palmitate formulation into PEGylated nanoparticles, and then to evaluate the ability of these nanoparticles delivered as Trojan microparticles to extend lung retention of the glucocorticoid.

2 MATERIALS AND METHODS

2.1 Materials

Budesonide (Bud) and dexamethasone (DXM) were obtained from Chemos GmbH (Germany). Dexamethasone palmitate (DXP) was purchased from Interchim (France). DSPE-mPEG (1,2-Distearoyl-sn-Glycero-3-Phosphoethanolamine-N-(methoxy(polyethylene glycol)-2000) (ammonium salt)) was obtained from Avanti Polar Lipids, Inc. (USA). Palmitoyl chloride, pyridine, triethylamine, ammonium acetate, LPS (Lipopolysaccharides from Escherichia coli O55:B5), L-leucine and rhodamine were provided by Sigma-Aldrich. Chloroform HPLC-grade, methanol HPLC-grade, acetone and DMSO were purchased from Carlo Erba Reagents (France). All other chemicals were obtained commercially and were of the highest available analytical grade. Water was purified using a Milli Q Reference system (Merck Millipore, France).

2.2 Synthesis of Budesonide Palmite (BP)

Budesonide palmitate, a prodrug of budesonide, was synthesized from the esterification of the alcohol-terminus present on the C-21 carbon of budesonide by the addition of palmitoyl chloride. To carry out this synthesis, 1 mmol of budesonide was dissolved in pyridine (10.8 mL for each mmol of budesonide) and after treatment with 2 equivalents of palmitoyl chloride injected dropwise at 0°C. The solution remained at room temperature overnight under stirring and nitrogen. After 24 hours of reaction, the pyridine was distilled off.

The solution obtained was resuspended in dichloromethane (at least 10 mL) and washed successively with approximately 5 mL of HCl (0.05 M), 5 mL of distilled water and 5 mL of 5 % $NaHCO_3$ to neutralize the acid. The organic phase was dried using anhydrous magnesium sulfate ($MgSO_4$) for 30 minutes under stirring, and, after filtration, the obtained solids were abundantly solubilized in dichloromethane (Axelsson *et al.,* 1986). The product obtained was purified by silica gel column chromatography, eluted with ethyl acetate/cyclohexane 1/4 (v/v) mixture and then 1/2 (v/v) of the same mixture. The separation was performed by thin layer chromatography with the same eluent as mentioned above.

The fractions containing BP were collected in a flask, the solvent evaporated using a rotary evaporator and a 40°C bath. After weighing, the obtained products were resuspended in dichloromethane and distributed in small amber vials, remaining in laminar flow hood for 3 hours until total evaporation of the solvent. The obtained ester was analyzed by nuclear magnetic resonance (^{1}H NMR) at 300 MHz in deuterated chloroform ($CDCl_3$), with the follow results: the presence of two isomers induced the splitting of most peaks δ 7.25 (d, *J* = 10.0 Hz, 1H, H-1), 6.26 (d, *J* = 10.0 Hz, 1H, H-2), 6.00 (s, 1H, H-4),

5.17 – 5.09 (m, 1H, OC*H*O), 4.92 – 4.70 (m, 2.4H, 2H-21, 0.4H-16), 4.60 (t, *J* = 4.5 Hz, 0.6H, H-16), 4.48 (broad s, 1H, H-11), 2.52 (td, *J* = 14.5 Hz, *J* = 4.8 Hz, 1H, H-6β), 2.36 (t, *J* = 7.6 Hz, 2H, $O_2C\mathit{H}_2CH_2$), 2.36-2.28 (m, 1H, H-6α), 2.2-1.5 (m, 14H), 1.43 and 1.42 (s, 3H, H-19), 1.45-1.05 (m, 24H,), 1.00-0.83 (m, 9H, H-20, $OCH(O)CH_2CH_2\mathit{C}H_3$, palm$\mathit{C}H_3$).

2.3 PEGylated nanoparticle preparation

Nanoparticles were produced using either the emulsion-evaporation or the nanoprecipitation method to obtain 4 formulations by each method, with different BP/DSPE-mPEG weight ratios: 5/2.5, 2.5/1.25, 2.5/2.5 and 1.25/1.25 mg/mL (Table 1), using a protocol recently published (Lorscheider *et al*., 2019).

For the emulsion-evaporation process, the nanoparticles were prepared by dissolving both the lipid DSPE-mPEG and BP in 1 mL of chloroform. This organic phase was slowly injected with a 20G needle (Braun, Sterican, 0.90 by 70 mm and 20G x 2¾ ") into an aqueous phase composed of 5 or 10 mL of Milli Q water at 4°C, with subsequent vortexing. The emulsion formed was then sonicated (Branson Digital Sonifier) during 2 minutes at an amplitude of 40 % (300 W). The solvent was then evaporated under reduced pressure using a rotary evaporator (Buchi, R-124). The final volume was adjusted, when necessary, in a volumetric flask to 5 or 10 mL, according to the defined concentration.

For nanoprecipitation, BP was solubilized in 1mL of acetone (organic phase) as an organic solvent that is miscible with water. The aqueous phase was composed of DSPE-mPEG dissolved in 5 or 10 mL Milli Q water, with stirring at 60°C. The organic phase was then injected into the aqueous phase with the aid of a 20G needle as described above, the suspension being kept under moderate stirring for 5 minutes and then concentrated to a final volume of 5 or 10 mL in a rotary evaporator to remove the organic solvent and adjust the final concentration of the drug.

Table 1. Formulations composition

Code	Method*	Conc. BP (mg/mL)	Conc. DSPE-mPEG (mg/mL)	Ratio of components
BP-EE1	EE	5	2.5	2:1
BP-EE2	EE	2.5	1.25	2:1
BP-EE3	EE	2.5	2.5	1:1
BP-EE4	EE	1.25	1.25	1:1
BP-NP1	NP	5	2.5	2:1
BP-NP2	NP	2.5	1.25	2:1
BP-NP3	NP	2.5	2.5	1:1
BP-NP4	NP	1.25	1.25	1:1

* EE: emulsion-evaporation; NP: nanoprecipitation

2.4 Nanoparticle characterization

2.4.1 Size and zeta potential

Nanoparticles were characterized by their size, polydispersity index (PdI) and zeta potential, measured by dynamic light scattering with a Nano ZS (Malvern instruments, UK) at a 173° scattering angle at 25°C. Samples were diluted 1/20 in water for the size and PdI, or in 1 mM NaCl solution for the zeta potential determination. Measurements were performed in triplicate.

2.4.2 Transmission electron microscopy (TEM)

Transmission electron microscopy was performed at I2BC (CNRS, Gif-sur-Yvette, France). A volume of 5 µL of the nanoparticle suspension at 5mg/mL BP was deposited for 1 minute on 400 mesh formwar-coated copper grids. Negative staining was performed by addition of a drop of uranyl acetate at 2 % w/w for 30 seconds. Excess solution was removed and grids were left to dry before observation. Observations were carried out on a JEOL JEM-1400 microscope at an acceleration voltage of 80 KV. Images were acquired using an Orius camera (Gatan Inc, USA).

2.4.3 Encapsulation Efficiency and compound loadings

*T*o evaluate the encapsulation efficiency and the prodrug and DSPE-mPEG loadings, nanoparticle suspensions were treated with methanol for prodrug and lipids extraction, to quantify the total BP and DSPE-mPEG by HPLC. To separate the free compounds, ultracentrifugation was performed at 40.000 rpm (=109760 g) during 4 h at 4°C (Beckman Coulter Optima LE-80K ultracentrifuge, 70-1Ti rotor). After separation by ultracentrifugation, non-encapsulated BP and DSPE-mPEG in supernatant were quantified by HPLC and their amount in nanoparticles was calculated indirectly. Analyzes were performed using an Agilent chromatograph, equipped with an UV detector (785A, Applied Biosystems) coupled to an evaporative light-scattering detector (ELSD, Eurosep, Cergy, France). UV detection was performed at 244 nm wavelength and ELSD detection settings were a nebulization temperature of 35°C and an evaporation temperature of 45°C. The Waters SymmetryShield RP18 column with 5µm particles and 4.6 x 250 mm dimensions was maintained at 10°C with a cooler. The isocratic mobile phase was composed of methanol: Chloroform: Ammonium acetate pH 4,0 (95 : 3 : 2), with addition of triethylamine (104 µL/100 mL mobile phase) + acetic acid (43 µL/100 mL mobile phase). The flow rate was 1.0 mL/min. A volume of 30 µL of sample was injected and analyzed during 10 min. Retention times were 6.3 min and 8.3 min for DSPE-mPEG and BP, respectively. The concentration range of the calibration curves varied from 18.7 to 750 µg/mL for DSPE-mPEG and 10-750 µg/mL for BP. The DSPE-mPEG is detected only by ELSD, while the BP is detected by ELSD and UV. ELSD detection calibration

curves followed a power law model, equations and correlation coefficients were $y = 0.0115x^{1.3649}$, R^2=0.9974 for DSPE-mPEG and $y=0.0185x^{1.3037}$, R^2=0.997 for BP, respectively. UV calibration curve of BP followed a linear model, y=0.3137x + 4.6558, R^2=0.9943. The encapsulation efficiency was calculated as the ratio of the actual amount of the compound over the initial one. The prodrug loading was determined by the relation between the amount of prodrug encapsulated and the total weight (Prodrug+ DSPE-mPEG) added to the formulation. Similar calculation was performed for DSPE-mPEG loading.

2.5 *In vitro* tests

2.5.1 Cell culture

All *in vitro* cell culture assays were performed on murine macrophage cell line RAW 264.7 obtained from ATCC (USA), cultured in DMEM (Dulbecco's Modified Eagle's Medium) culture medium supplemented with 10 % fetal bovine serum (FBS), penicillin G (10,000 unit/mL) and streptomycin (10 mg/mL), maintained in a humidified incubator at 37°C supplied with 5 % CO_2.

2.5.2 Cellular viability

The effect of the formulations on the cellular viability was studied in the RAW 264.7 cell line using the MTT (3-(4,5-dimethylthiazol-2-yl)-2,5-diphenyltetrazolium bromide) colorimetric assay. For this test, cells were seeded in 96-well plates at the density of 1×10^4 cells/well (24 h Test) and 2×10^3 cells/well (48 h Test), and incubated for 24 h until reaching 80 % confluence. Nanoparticle formulations produced by emulsion-evaporation (2:1 and 1:1, BP:DSPE-mPEG) were added at the final concentrations 1.9×10^{-6} M, 11.7×10^{-6} M, 23.3×10^{-6} M, 46.7×10^{-6} M, 93.4×10^{-6} M and 186.8×10^{-6} M (eq Bud), with the corresponding concentrations being calculated in the case of free budesonide, solubilized in ethanol and then diluted in the culture medium. After 24 and 48 hours of incubation, 20 µL of a 5 mg/mL yellow tetrazolium MTT (3-(4,5-dimethylthiazolyl-2)-2,5-diphenyltetrazolium bromide) solution was added to each well and incubated for 1 hour until the formation of the purple formazan crystals, resulting from the MTT reduction by metabolically active cells. Afterwards, the culture medium was replaced by 200 µL of DMSO to dissolve formazan crystals and the absorbance was measured at 570 nm. The percentage of viable cells was calculated as the absorbance ratio between nanoparticle-treated and untreated control cells.

2.5.3 Cytokine release

The anti-inflammatory effect of nanoparticles was tested by inducing an inflammatory reaction in RAW 264.7 cells with the help of *Escherichia coli* lipopolysaccharides (LPS). For the cytokine quantification, RAW 264.7 cells were seeded in 24-well plates at a cellular density of 4 x 10^4 cells/well in culture medium and were incubated for 48 hours until 80 % confluency. The medium was then replaced by fresh medium alone or fresh medium with LPS at 1 µg/mL to induce inflammation, and plates were incubated another 3 hours. Afterwards, nanoparticles produced by emulsion-evaporation (2:1 BP:DSPE-mPEG) at four concentrations diluted in culture medium: 10^{-7} M, 10^{-8} M, 10^{-9} M and 10^{-10} M (eq. Bud) were added (Foillard *et al.*, 2016 ; Kis *et al.*, 2006 ; Spoelstra *et al.*, 2002 ; Wang *et al.*, 2013). Culture medium alone was used as negative control and LPS 1 µg/mL as positive control. After 24, 48 and 72 hours of incubation with the treatments, cell supernatants were collected and frozen at -20°C until analysis was performed. Cells were detached and counted. Mouse inflammatory cytokines TNFα, MCP-1, IL-10 and IL-6 were quantified using a Cytometric Beads Array (CBA) detection kit (BD Biosciences, USA). In each test tube, 50 µL of bead suspension was added, completed with either 50 µL of standards solution (20-5000 pg/mL) or 50 µL of supernatants samples. 50 µL of Phycoerythrin (PE) detection reagent was added to each tube and incubation during 2 h at room temperature was performed. Samples were washed with 1mL washing buffer provided in the kit and tubes were centrifuged (200 g, 5 min) to recover the pellet. 300 µL of washing buffer was added to resuspend the pellet and samples were quantified with the BD Accuri C6 Cytometer (BD Biosciences, USA). Cytokines results were analyzed with the FACP Array™ Software and were obtained as pg/mL concentrations. All measurements were performed in triplicate.

2.6 Formulation of nanoparticles into Trojan microparticles

Trojan microparticles were prepared by spray-drying using a BÜCHI B-290 mini-spray dryer (France), equipped with a 0.7 mm two-fluid nozzle. Aqueous suspension of PEGylated nanoparticles (BP-EE1) was spray-dried at a weight concentration of 0 %, 5 %, 10 % and 2 0% in a L-leucine solution (final solid content concentration of 4 g/L) at a solution feed rate of 12.5 mL/min. The operational conditions were as follows: aspiration rate at 100 %; atomizing air flow rate of 473 L/h; inlet temperature of 190°C; and outlet temperature of 55–65°C.

2.6.1 Particle size distribution

Particle size distribution was measured by laser diffraction using a Mastersizer 2000 equipped with a Sirocco 2000 dry dispenser unit (Malvern Instruments, France) at the dispersion pressure of 2 bars.

The refractive index used was 1.46 (corresponding to L-Leucine). Approximately 10–20 mg of powder were used for the measurements. Results were expressed in terms of particle diameter at 10 %, 50 % and 90 % of the volume of distribution (D_{10}, D_{50} and D_{90}, respectively). Measurements were performed in triplicate.

2.6.2 Tapped density

Powder tap density (ρ) was determined using a tapping apparatus (Pharma test PT-TD1). The tapped density was obtained by mechanically tapping a graduated measuring cylinder (5 mL) containing the sample. After weighing about 150 mg of powder and observing the initial powder volume, the measuring cylinder is mechanically tapped, and volume readings are taken until little further volume change is observed (N'Guessan *et al.*, 2018; Pharmacopoeia E., 2019a). Measurements were performed in duplicate.

Then the theoretical aerodynamic diameter (D_{aer}) was determined by calculation (Eq. 1):

$$D_{aer} = D_{50}\sqrt{\rho} \qquad \text{(Eq. 1)}$$

In this equation, D_{50} is the particle volume median diameter (µm) and ρ the particle density (g/cm^3) assumed to be equal to the tapped density (Hadinoto *et al.*, 2006).

2.6.3 Aerodynamic properties

The aerodynamic properties of the powders were analyzed using a multi-stage liquid impinger (MSLI, Apparatus C, Copley Scientific, Switzerland), coupled with a dry powder inhalation device (Aerolizer®, Novartis, Switzerland) containing a size 3 capsule filled with the sample. The capsule was punctured and the powder was delivered at a flow rate of 60 L/min for 4 s to simulate an inspiration. At each stage, 20 mL of a hydroalcoholic solution (ethanol 70:30 water) were added. The process was repeated at least 3 times to ensure an adequate amount of drug for dosing each stage. Particles were separated between the stages based on their aerodynamic diameters, which particles with diameters smaller than 5 µm and 3.1 were determined by interpolation from the cumulative amount of respective stages and considered as the fine particle fraction (FPF) (%), which corresponds to the fraction of powder reaching the deep lung. The alveolar fraction (AF) was calculated as a percentage of the collected dose on stage four and the filter by the initial mass in the capsule. The emitted fraction (EF) is defined as

the fraction of powder that exited the inhaler with respect to the initial dose (Cruz *et al.*, 2011 ; Liang *et al.*, 2018 ; N'Guessan *et al.,* 2018 ; Pharmacopoeia E., 2019b). BP was quantified by HPLC-UV, with the methodology previously validated above. For the powder exempt of nanoparticles, 1% of rhodamine was added to the solution prior to spray-drying for impaction studies. A UV calibration curve was obtained using rhodamine-labeled powders for quantification of impaction results.

2.6.4 Scanning electron microscopy (SEM)

Scanning electron microscopy (SEM) was performed using a LEO1530 microscope (LEO Electron Microscopy Inc., Thornwood, USA) operating between 1 and 3 kV with a filament current of about 0.5 mA. Powder samples were deposited on carbon conductive double-sided tape (Euromedex, France) and were coated with a palladium–platinum layer of about 4 nm using a Cressington sputter coater 208HR with a rotary planetary-tilt stage, equipped with a MTM-20 thickness controller.

2.7 *In vivo* tests

In vivo experiments were conducted according to the European guidelines for Animal Experiments (86/609/EEC and 2010/63/EU), with approved protocol by the ethical committee No26 and by the French Ministry of Education and Research (Accepted protocol No 14993-20180507144002162 v1). Male Sprague Dawley rats with average weight of 300 g were purchased from Janvier Labs (Le Genest-Saint-Isle, France) and let for one week after shipping for adaptation before starting experiments. They were housed 5 by cage during the study, under climate-controlled conditions and a 12 h light/dark cycle. Animals were allowed access to food and water ad libitum throughout the duration of the study.

60 rats were divided in 2 groups (treatment and control), anesthetized with an intraperitoneal injection of a mixture of ketamine (100 mg/kg) and xylazine (10 mg/kg). Once sedation as confirmed, animals were placed into a modified slant board to optimize visual placement of the insufflation cannula into the trachea. For the treatment group 3 mg of Trojan microparticles obtained with 5 % BP nanoparticles (corresponding to 90 µg of BP) was intratracheally administered using a DP-4 Microsprayer (PennCentury, Philadelphia, PA), by rapidly pushing a 2 cm^3 bolus of air through the device. The insufflator was weighed before and after the powder filling, as well as after administration to determine the exact dose delivered. For the control group, commercial micronized budesonide (Pulmicort Turbuhaler, AstraZeneca) was mixed with lactose to obtain the same final budesonide concentration as for Trojan microparticles. The same administration method was used for both groups.

2.7.1 Pharmacokinetics studies

For the pharmacokinetics studies, 30 rats by group were divided in 6 subgroups. For each time point, blood was sampled from 5 rats at 1/4, 1/2, 1, 2, 3, 4, 6, 18, 24 and 48 hours following the administration, in heparinized tubes. Before blood sampling, rats were anesthetized by isoflurane inhalation. At most two collections were performed in each rat. At collect 1, approximately 1 mL of blood from each rat was taken via tail vein or jugular vein. Rats were euthanized by intraperitoneal injection of 150 mg/Kg of sodium pentobarbital (Dolethal®), with exsanguinations by cardiac puncture (second blood collection). Plasma was separated in a mini centrifuge (Eppendorf Minispin®) at 10,000 rpm for 10 min, and subsequently frozen and stored at -80°C until analyses by liquid chromatography-tandem mass spectrometry (LC-MS/MS).

2.7.2 Bronchoalveolar lavage fluids (BALF), alveolar cell pellet (AC) and lung collection

Bronchoalveolar lavage fluids (BALF) were collected to evaluate lung lining fluid Bud/BP levels. After exsanguination, the trachea was cannulated using an 18 gauge needle adaptor for injection and retrieval of BALF. Briefly, aliquots of 1mL of PBS were instilled into lungs after intubating the trachea with a syringe coupled with tracheal cannula. The lungs were massaged and the fluid withdraws immediately in a centrifuge tube. This process was repeated 3 times, where all lavages were pooled and centrifuged (1500 rpm, 10 min, 4°C). The supernatant of lavage was then separated from the alveolar cell pellet and subsequently frozen and stored at -80°C until analyses by LC-MS/MS. Lastly, the lung was removed, washed with PBS and immediately stored at -80°C until analyses by LC-MS/MS.

2.7.3 Budesonide and BP quantification

Budesonide and budesonide palmitate were determined in plasma, BALF, AC and lung tissue by LC-MS/MS method. Chromatography was performed on a security guard cartridge (Eclipse XDB-C8, Narrow-Bore Guard Column with 5 µm particles and 2.1 x 12.5 mm, Agilent, USA) and an Eclipse XDB-C8 Narrow-Bore column with 5µm particles and 2.1 x 150 mm. The mobile phase was a linear gradient of 40–100 % (v/v) 0.1 % formic acid in acetonitrile over 14 minutes followed by isocratic elution with 100 % acetonitrile for 11 minutes, and the pump flow rate was 0.3 mL/min. The aqueous solvent was 0.1 % formic acid. The LC-MS/MS system consisted of a triple quadrupole Quattro Ultima Waters equipped with an electrospray source coupled to a HPLC Ultimate 3000 Thermoscientific and an automatic injector WPS3000PL. The mass spectrometer was operated in the positive/ion mode. Ions were analyzed by multiple reactions monitoring (MRM). Transition ions were m/z 393.48/147.16 for DXM, m/z 431.27/341.31 for Bud, and m/z 631.61/373.1 for DXP and m/z 669.59/323.23 for BP. A

volume of 5 µL of samples was injected and analyzed during 25 min. Retention times were 4.59 min and 11.48 min for Budesonide and BP, respectively, but a run for 25 min with ACN plateau was necessary to wash the column and avoid the accumulation of budesonide. DXM and DXP at 37.5 µg/mL were used as internal standards, with retention times 2.82 min and 8.11 min, respectively.

2.7.3.1 Preparation of plasma standards and samples

To quantify Bud and BP concentrations in plasma, a modified extraction method with chloroform-methanol was chosen (Lorscheider *et al.*, 2019 ; N'Guessan *et al.*, 2018), being performed as follows: in an eppendorf tube, 100 µL of plasma, 100 µL of known concentration of Bud and BP and 100 µL of known concentration of internal standard (DXM for Bud and DXP for BP) were mixed with a vortex during 30 s. Bud, BP and the internal standards were dissolved in acetonitrile. Then 3 mL of a chloroform-methanol mixture (9:1, v:v) were added in the tube. Sample was vortexed during 3 min to obtain protein precipitation and was then centrifugated at 3500 rpm (=1690 g) for 30 min (ST16R centrifuge, rotor TX-400, Thermo Scientific, France). The organic phase in the bottom was transferred into a clean glass tube and evaporated to dryness under a stream of nitrogen at 30°C. The residue was then reconstituted into 200 µL of acetonitrile and vortexed prior to analysis using LC-MS/MS conditions described above. Calibration curves were linear, respectively in the range 1-200 ng/mL (for Bud, R^2= 0.9943, y = 1.036x + 0.0679, and for BP R^2= 0.9729, y = 1.0825x + 0.2117).

2.7.3.2 Bud and BP quantification in BALF and AC

PBS was chosen as matrix for standard curves to measure Bud and BP concentrations in both BALF and AC suspensions. The same extraction processes developed for plasma analysis was used, with PBS/BALF instead of plasma. Cells from AC were resuspended in 1 mL of PBS and the suspension was sonicated at 40 % amplitude for 2 min, to lyse cells. Calibration curves were linear, respectively in the range 1-200 ng/mL (for Bud, R^2= 0.9946, y = 0.6852x + 0.044, and for BP R^2= 0.9874, y = 1.2021x + 0.0452).

2.7.3.3 Total protein quantification

Total protein content in AC was measured spectrophotometrically at 595 nm according to the Bradford method, using bovine serum albumin (BSA) as standard. Manufacturer's protocol for Bio-Rad Protein Assay (Bio-Rad Laboratories GmbH, Munich, Germany) performed on microtiter plate was followed and each sample was run in triplicate. These results were used to express the amount of drug/prodrug per gram of protein for AC.

2.7.3.4 Bud and BP quantification in lung tissue

Lung tissue was homogenized in PBS using a micro-pestle coupled with a turbine at 2000 rpm during the time needed to obtain a liquid preparation, approximately 5 min. Bud and BP were extracted from the homogenate using the same method than plasma extraction, beginning with 100 µg of homogenate lungs. 100 µL of internal standard mixture DXM and DXP at 150 ng/mL was added and vortexed 30 s, followed by the addition of 3 mL of 9/1 chloroform/methanol (v/v), vortexed for 3 min and centrifuged in the same conditions as above. Organic phase was evaporated and 200 µL acetonitrile was added and mixed during 1.5 min. This final sample was analyzed by LC-MS/MS, using the same conditions as plasma and BALF samples. Calibration curves were linear, respectively in the range 1-500 ng/mL (for Bud, R^2= 0.9925, y = 0.4612x - 0.4175, and for BP R^2= 0.989, y = 0.886x - 0.1161).

2.8 Statistical analysis

Results were reported as mean ± standard error of the mean (SEM). Statistical analysis was performed using the GraphPad Prism 7.0 software.

3 RESULTS AND DISCUSSIONS

3.1 Synthesis of Budesonide Palmite (BP)

The synthesis of budesonide palmitate was readily accomplished, with a yield of 67 % (Figure 1). The reaction was confirmed by nuclear magnetic resonance (^{1}H NMR) at 300 MHz in deuterated chloroform ($CDCl_3$).

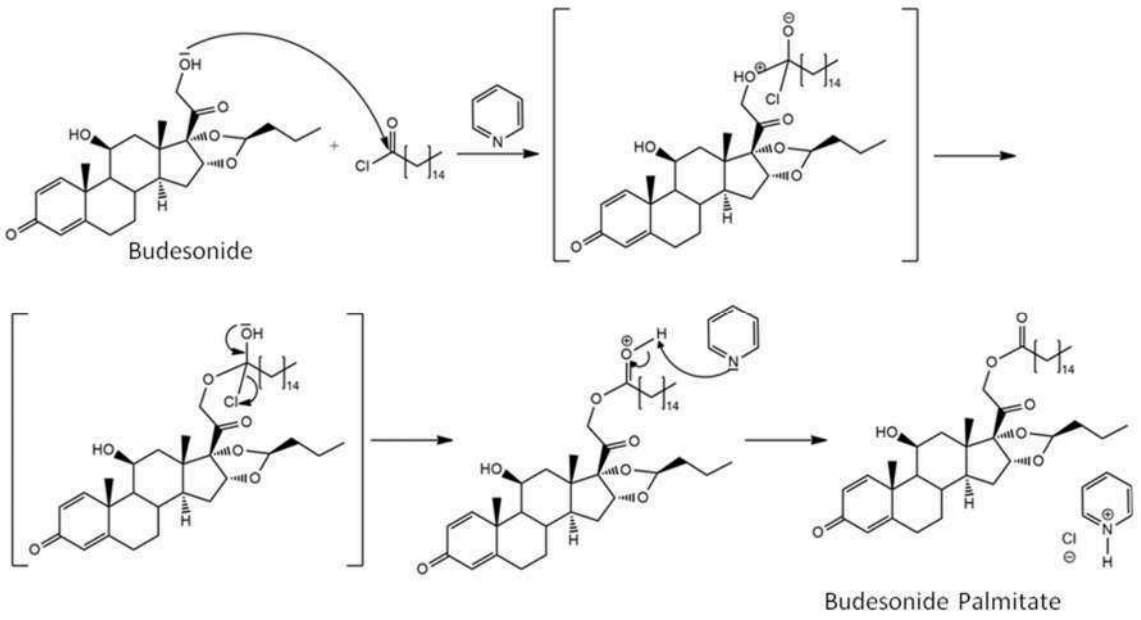

Figure 1. Reaction of budesonide's esterification, resulting in budesonide palmitate.

3.2 Formulation Process

Emulsion-evaporation and nanoprecipitation techniques were applied to prepare BP nanoparticles coated with DSPE-mPEG. Different ratios and concentrations of all the components were tested. Obtained nanoparticles were characterized and compared in terms of stability, encapsulation efficiency and loadings.

3.3 Size, zeta potential and stability over time

After preparation in triplicate, nanoparticle hydrodynamic diameter, polydispersity index (PdI) and zeta potential of all formulations were followed for 30 days to evaluate the stability of the suspension, with storage at 4°C (Figure 2). The emulsion-evaporation method yielded nanoparticles which mean diameter remained from 150 to 200 nm, polydispersity index from 0.05 to 0.25 and negative zeta potential around -30 to -50 mV. Nanoparticles characteristics were rather stable at 4°C over 30 days. Nanoprecipitation also provided nanoparticles stable at 4°C, over 30 days, with polydispersity index below 0.2 and negative zeta potential around -30 to -50 mV. Only the nanoprecipitation formulation with the highest BP concentration (BP-NP1) showed a mean hydrodynamic diameter higher than the others three formulations, with a mean hydrodynamic diameter around 250 nm. However, this diameter remained stable during 30 days. As shown previously the presence of DSPE-mPEG provides a substantial negative surface potential (Woodle *et al.*, 1992). Polydispersity index was kept around 0.2 highlighting a rather monodisperse population for both processes. As observed with

dexamethasone palmitate, the strong hydrophobic interactions between the aliphatic chains and the steric layer provide by PEG favor a good colloidal stability (Lorscheider *et al.*, 2019). The two prodrug/lipid ratios studied did not influence the formulation stability.

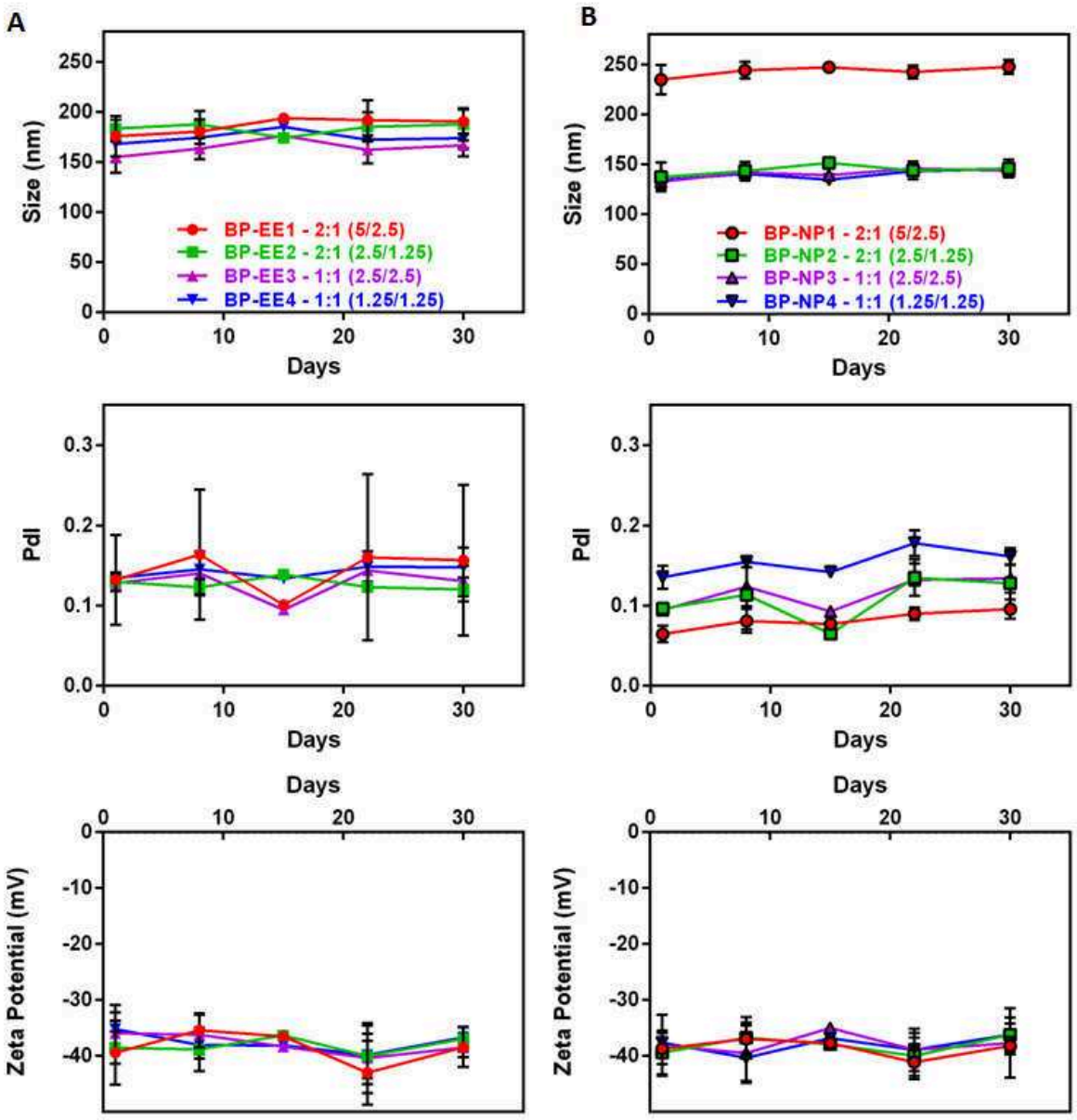

Figure 2. A) Emulsion-Evaporation method and B) Nanoprecipitation method. Size, PdI and Zeta-potential measurements of the nanoparticles at different times after the preparation, by dynamic light scattering.

TEM microscopy images were in agreement with dynamic light scattering measurements (Figure 3). At the highest concentration, nanoparticles produced by nanoprecipitation presented larger size than emulsion-evaporation, with rather spherical shape for both processes. The observed deformations for

nanoprecipitation nanoparticles were probably arising from the combination of the high nanoparticle concentration and the drying process needed for TEM observations.

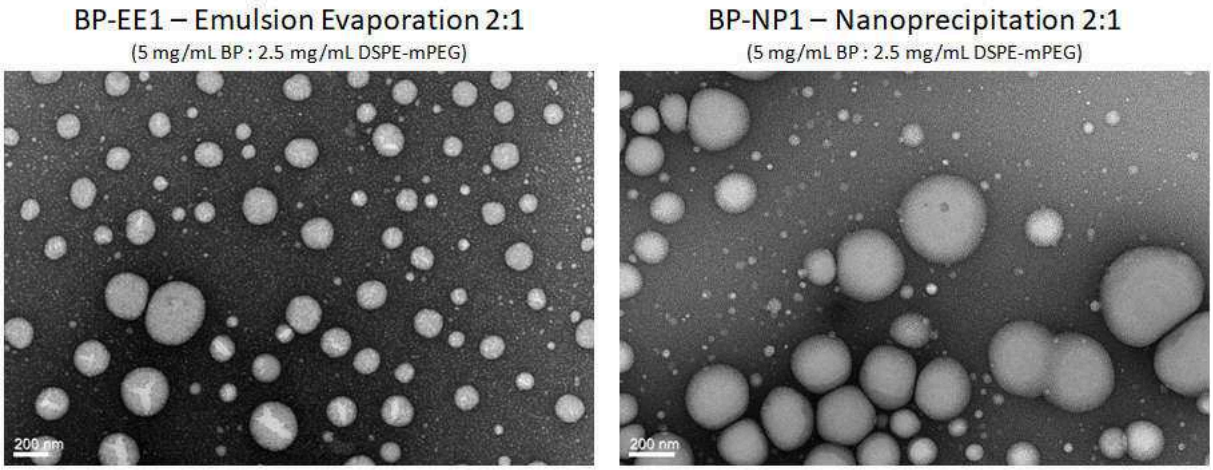

Figure 3. Transmission electron microscopy images of the BP/DSPE-mPEG nanoparticles.

3.4 Encapsulation efficiency and compound loadings

The effect of BP:DSPE-mPEG ratio and preparation method on encapsulation efficiency and loading was studied. Encapsulation efficiency was determined by quantifying the amount of BP and DSPE-mPEG associated to BP-NPs. After separation by ultracentrifugation, non-encapsulated BP and DSPE-mPEG in supernatant were determined by HPLC-ELSD and their amount in nanoparticles was calculated indirectly (Figure 4A). For emulsion-evaporation or nanoprecipitation, the encapsulation efficiency of BP was around 100 % with no significant differences proving that all the prodrug is associated to nanoparticles. The presence of palmitate chain on budesonide allows the highest possible drug encapsulation efficiency to be obtained, regardless of the formulation process used or prodrug/lipid ratio. Results were different for DSPE-mPEG encapsulation, but did not change as a function of the formulation process. One can observe a rather stable encapsulation efficiency of 33 to 44 % for nanoprecipitation and from 37 % up to 45 % for emulsion-evaporation (Figure 4A). Based on the amounts of encapsulated BP and DSPE-mPEG, BP and DSPE-mPEG loadings were calculated (Figure 4B). The loading was determined as the relative amount of compound content of nanoparticles to the whole weight of the nanoparticles. Nanoparticles prepared by emulsion-evaporation method presented a BP loading ranging from 57 to 73 % (w/w), while for nanoprecipitated nanoparticles BP loading varied from 57 to 70 %. Concerning the influence of the ratios between both components, it could be observed that formulations 2:1 showed an enhanced BP loading when compared to the ratio 1:1. Ratio 2:1 showed a BP loading going from 66 to 73 %, while ratio 1:1 presented a BP loading from

57 to 63 %. It is worth mentioning that Bud was not detected in the suspensions, proving that BP was not degraded over the formulation process.

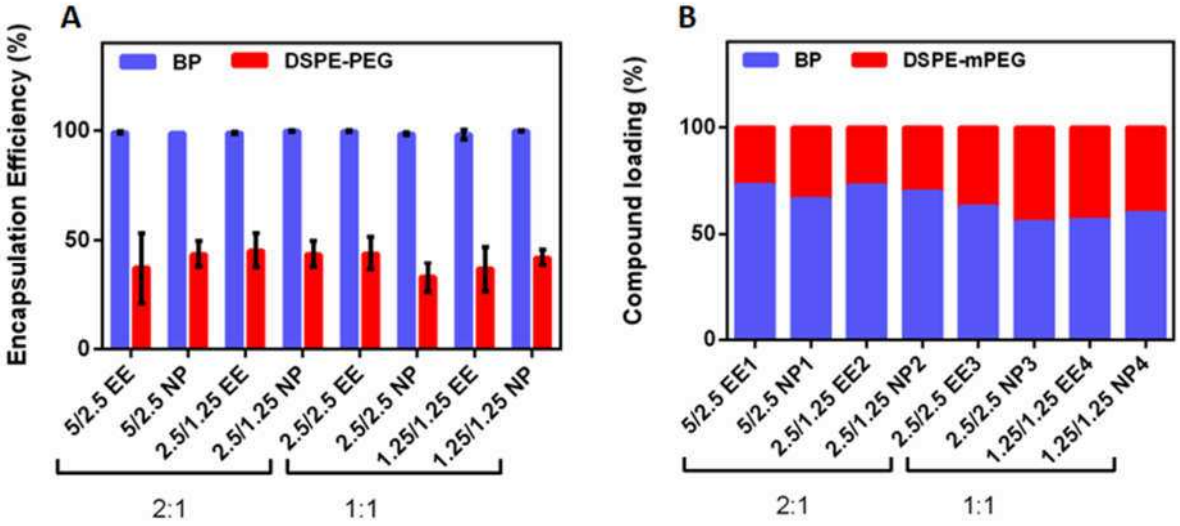

Figure 4. BP (blue) and DSPE-mPEG (red) encapsulation efficiency (A) and compound loading (B), according to ratio of components and preparation method (n=3).

Since all formulations showed excellent encapsulation efficiency and stability over the time, a choice between the methods was made considering the compound loading. Since emulsion-evaporation method showed a slightly higher BP loading than nanoprecipitation, it was chosen for all the following experiments.

3.5 *In vitro* tests

3.5.1 Cellular viability

The potential toxicity of PEGylated nanoparticles was evaluated on RAW 264.7 cells using MTT assay. According to ISO guideline for MTT assay, potential cytotoxicity is considered when cell viability decreases below 70 % of the control (International Standard Organization, 2009). Formulations prepared by emulsion-evaporation with ratios 2:1 and 1:1, in a range of concentrations from 1.9 x 10^{-6} M to 186.8 x 10^{-6} M (equivalent budesonide), were tested and compared to controls: free budesonide and free BP. After 24 hours incubation, both PEGylated nanoparticles and free BP clearly showed no cytotoxicity up to 186.8 x 10^{-6} M (eq. budesonide), while free budesonide showed cytotoxicity only at the higher concentration (Figure 5A). After 48 hours incubation, similar results to 24 hours were found to nanoparticles and free BP, but free budesonide presented cytotoxicity at all tested concentrations (Figure 5B). These results show that nanoparticles obtained at both BP/DSPE-mPEG ratios can be

considered safe. The difference in cytotoxicity between the free drug and prodrug and nanoparticles may be explained by a difference in the kinetic of cell entry.

Based on the obtained results, for the following experiments, nanoparticles obtained by emulsion-evaporation with ratio 2:1 (5mg/mL BP : 2.5 mg/mL DSPE-mPEG) were selected since they have attested absence of cytotoxicity and a higher BP loading, an important feature for further applications.

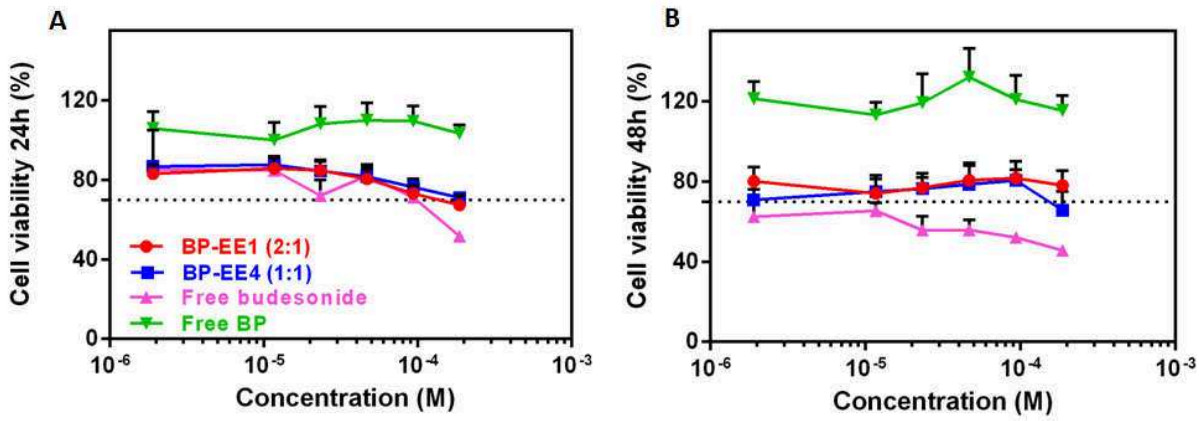

Figure 5. Cell viability after 24 h (A) and 48 h (B) of treatment (n=3).

3.5.2 Cytokine release

With the aim to verify the anti-inflammatory activity of BP PEGylated nanoparticles, the release of pro-inflammatory cytokines (IL-10, IL-6, MCP-1, TNFα) by LPS-activated macrophages RAW 264.7 into the cell culture medium was quantified after their incubation for 48 hours (Figure 6) and 72 hours (Figure 7) with nanoparticles, free budesonide or controls. Low concentrations of BP (eq budesonide) from 10^{-10} M to 10^{-7} M were chosen as therapeutically relevant concentrations (Van Den Bosch *et al.*, 1993; Spoelstra *et al.*, 2002). The release of IL-10 and IL-6 cytokines decreased when the cells were treated with PEGylated nanoparticles up to 10^{-9} M (48h) and 10^{-8} M (72h). Concerning TNFα and MCP-1 chemokines, we observed a slight decrease after treatment with free budesonide, but not with nanoparticles, at an equivalent Bud concentration. Traves *et al.* (2002) have reported MCP-1 levels significantly increased in sputum from patients with COPD compared with non-smokers and healthy smokers, confirming that MCP-1 is involved in the migration of inflammatory cells, contributing to the inflammatory process associated with COPD. In another clinical study, Giuffrida *et al.* (2014) have observed similar cytokine expression in asthmatic and non-asthmatic patients, but only chemokines (MCP-1) were significantly increased in asthmatic patients when compared with control and non-asthmatic patients. Concerning IL-10, it is a major anti-inflammatory cytokine and has been shown to suppress all the pro-inflammatory cytokines, with activity mediated by specific cell surface receptor complex. Lower IL-10 levels were reported to be associated with a higher frequency of bronchial

asthma and COPD (Huang *et al*., 2016). While IL-10 is considered an anti-inflammatory cytokine, chemokines and cytokines such as MCP-1, TNF-α and IL-6 are recognized to activate functions of inflammatory cells during acute inflammatory responses, even acting together to initiate and regulate the inflammation process. These proinflammatory cytokines have been well studied and characterized as participants in the basic inflammatory process and mediators of cellular infiltration (Elsabahy and Wooley, 2013). In our study, we have observed that a possible proinflammatory effect also could be a factor to consider in the results interpretation, improving cytokine levels as an innate response. Nevertheless, it is possible to conclude that the encapsulation and use of budesonide palmitate does not affect the anti-inflammatory activity of budesonide but probably modifies its kinetics as drug entrance in cell might be different for both forms.

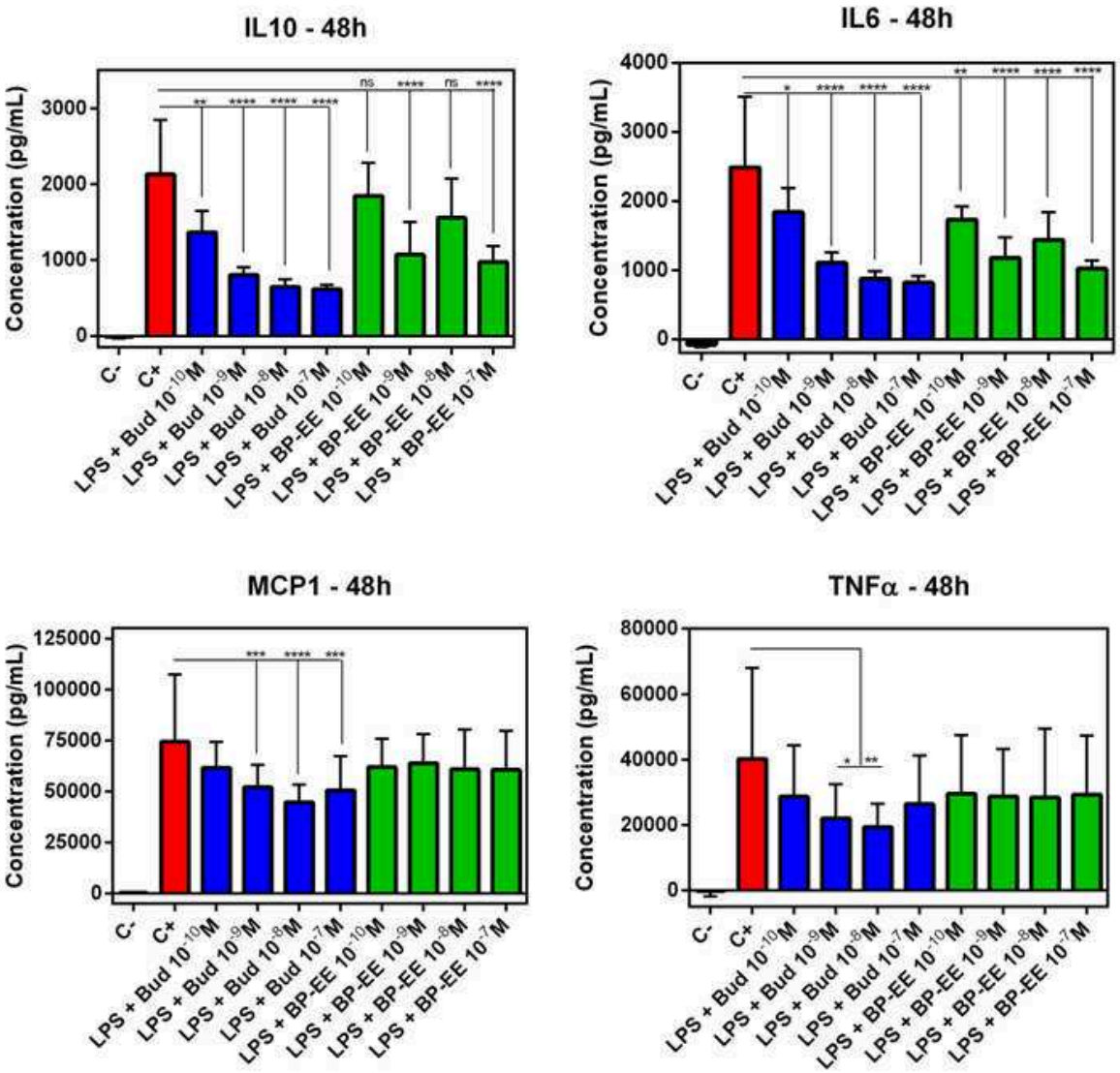

Figure 6. Quantification of cytokine release by Raw 264.7 macrophages without induction by LPS (C-), with induction by LPS 1 µg/mL (C+), after treatment for 48 hours with Budesonide (eq. BP) (blue) and PEGylated nanoparticles (green). The results are represented on average ± SD (n = 3). Statistical analysis was performed with a one-factor ANOVA followed by a Tukey post-test. ns = not significant, * $p < 0.1$, ** $p < 0.01$, *** $p < 0.001$, *** $p < 0.0001$.

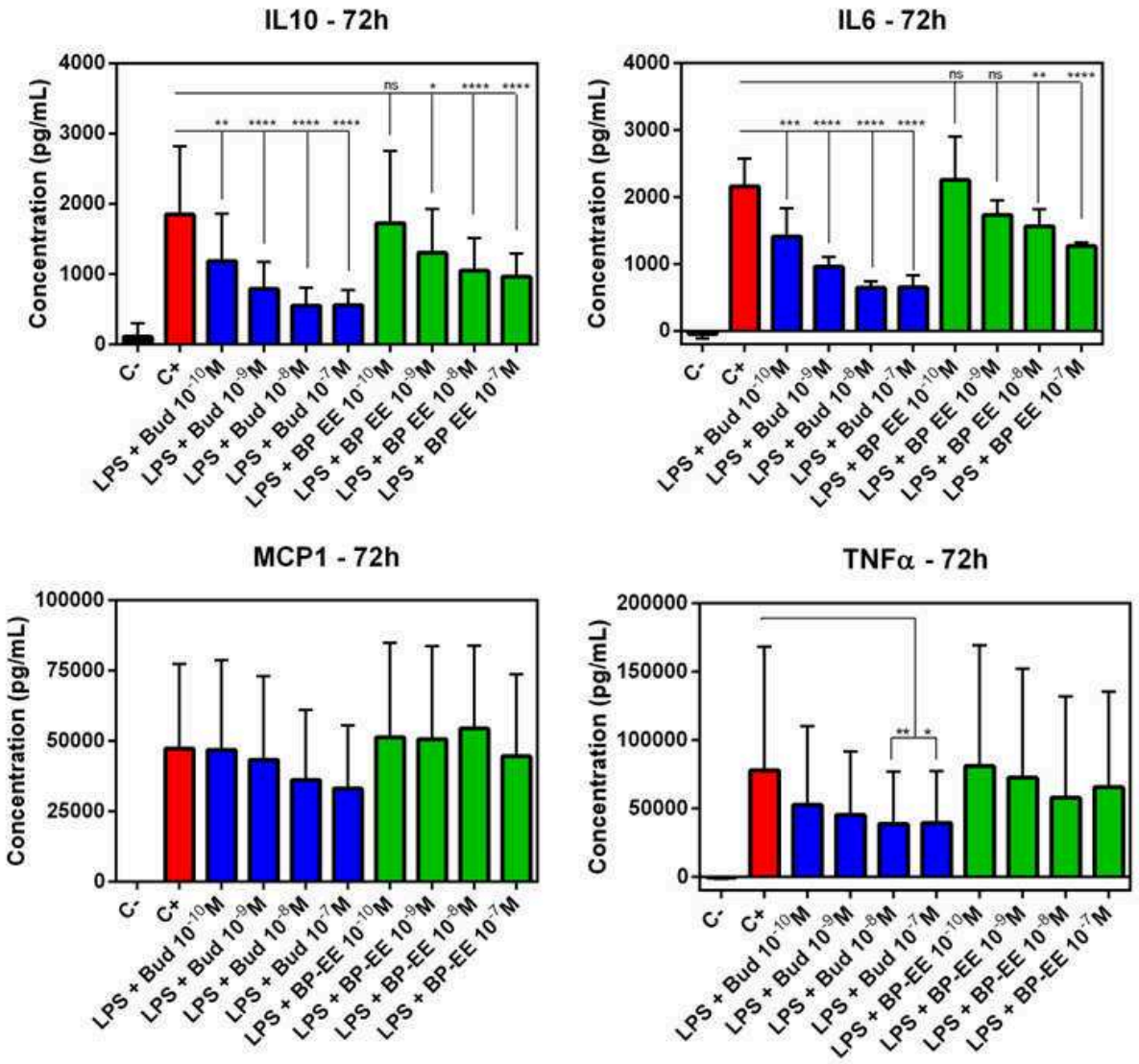

Figure 7. Quantification of cytokine release by Raw 264.7 macrophages without induction by LPS (C-), with induction by LPS 1 µg/mL (C+), after treatment for 72 hours with Budesonide (eq. BP) (blue) and PEGylated nanoparticles (green). The results are represented on average ± SD (n = 3). Statistical analysis was performed with a one-factor ANOVA followed by a Tukey post-test. ns = not significant, * $p < 0.1$, ** $p < 0.01$, *** $p < 0.001$, *** $p < 0.0001$.

3.6 Formulation of nanoparticles into Trojan microparticles

Trojan particles were then formulated by spray-drying. A white powder with a good flowability was obtained with 0, 5, 10 and 20 % of nanoparticles. L-leucine was chosen as excipient because of its recognized potential to improve the aerosolization properties and performance of dry powder formulations (Sou *et al.*, 2013). The morphology of Trojan microparticles produced by spray drying was investigated by SEM (Figure 8). Microparticles were found spherical with a slightly irregular surface

and hollow shells were observed. With the increase of nanoparticles content, particle roughness seemed to increase.

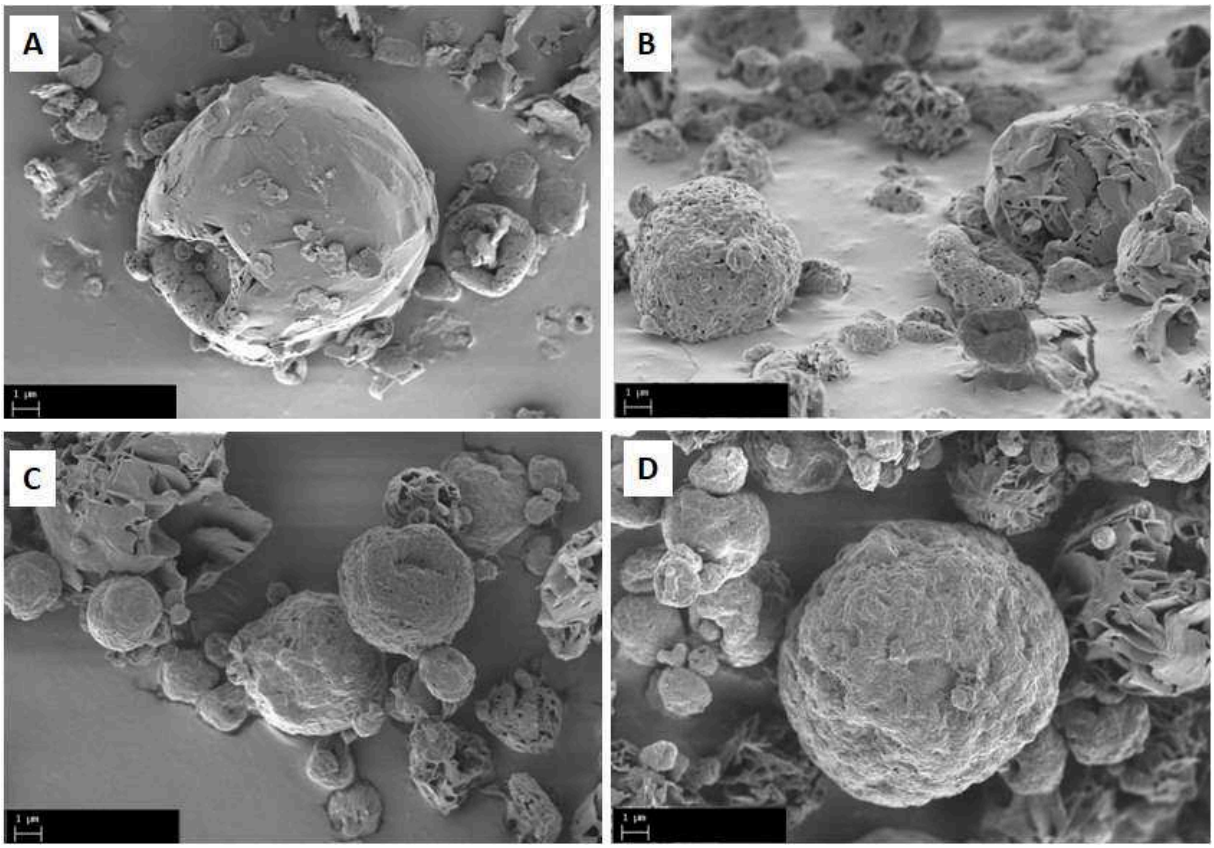

Figure 8. Typical SEM images of spray-dried powders: A) 0 %, B) 5 %, C) 10 % and D) 20 % nanoparticles. Scale bar = 1 μm.

3.6.1 Particle size distribution

The influence of nanoparticles concentration on Trojan particle size distribution was evaluated (Table 2). The volume median diameter (D_{50}) is stable around 5 μm up to 10 % of nanoparticles and then increases up to 7.2 μm when 20 % nanoparticles were added (Figure 9A). The same trend is observable for D_{10} and D_{90}, indicating a modification of particle drying process as nanoparticle content increased. The span that reflects the width of the distribution is quite stable around 1.7 ± 0.1, showing a not extensively polydisperse size distribution. These results are in agreement with Tsapis *et al.* (2002) who have observed that an increase of nanoparticles concentration leads to an increase in microparticle size, when high nanoparticle concentration is used. However, there is a controversy in the literature about the effect of nanoparticles on Trojan particle size as size decrease or size increase have been reported indicating that others factors such as excipient content could have an important impact. Gómez-Gaete *et al.* (2008) have evaluated the influence of dexamethasone acetate nanoparticles concentration on microparticle size distribution, after encapsulation in Trojan particles. When

nanoparticle concentration increased, D_{10} remain constant, but D_{50} and D_{90} showed a slight decrease although not significant ($p > 0.05$, from 6.7 to 6.4 µm and from 16.8 to 15.2 µm, respectively), indicating in this case that size distribution of microparticles is independent of the presence of nanoparticles. On the other hand, Hadinoto *et al.* (2006) have observed a reduction of microparticle size when the concentration of polyacrylate nanoparticles increase, probably attributed to an increase of fine particles.

Table 2. Microparticles size distribution as a function of nanoparticles content in the formulation

Nanoparticles concentration (%, w/w)	D_{10} (µm)	D_{50} (µm)	D_{90} (µm)	D[4.3] (µm)	Span (µm)
0	2.3 ± 0.2	5.8 ± 0.2	12.8 ± 0.4	9.9 ± 4.0	1.8 ± 0.1
5	2.1 ± 0.1	4.8 ± 0.2	10.1 ± 0.5	5.7 ± 0.5	1.7 ± 0.0
10	2.6 ± 0.0	5.3 ± 0.2	11.0 ± 0.7	7.3 ± 1.1	1.6 ± 0.1
20	3.5 ± 0.4	7.2 ± 0.8	14.9 ± 1.0	12.1 ± 0.7	1.5 ± 0.0

3.6.2 Aerodynamic properties

Aerodynamic properties of microparticles are presented in Table 3 and Figure 9. Tapped density (ρ) measurements were performed, showing an increase from 0.040 ± 0.00 g/cm^3 to 0.094 ± 0.00 g/cm^3 as nanoparticles concentration increased from 0 to 20 % (Figure 9B). These results further prove the low density/porosity of the particles, although the addition of nanoparticles makes the microparticles denser. From tapped density measurements, using equation 1, we have calculated the aerodynamic diameter. D_{aer} was around 1.3 µm up to 10 % of nanoparticles, and then increased up to 2.2 µm for 20 % nanoparticles formulation (Figure 9C).

Table 3. Aerodynamic properties of microparticles

% Nanoparticles	D_{50} (µm)	ρ (g/cm^3)	D_{aer} (µm)	EF (%)	FPF (%)	AF (%)
0	5.8 ± 0.2	0.040 ± 0.00	1.2 ± 0.0	98.6 ± 1.2	87.3 ± 0.6	69.3 ± 0.6
5	4.8 ± 0.2	0.081 ± 0.00	1.3 ± 0.0	97.9 ± 1.4	66.7 ± 9.5	41.0 ± 8.9
10	5.3 ± 0.2	0.068 ± 0.01	1.4 ± 0.0	99.3 ± 0.5	61.0 ± 3.7	34.3 ± 3.4
20	7.2 ± 0.8	0.094 ± 0.00	2.2 ± 0.3	99.8 ± 0.2	56.0 ± 4.0	28.7 ± 2.5

Particle size distribution (D_{50}), Tap density (ρ), Aerodynamic diameter (D_{aer}) and Aerosolization characterization (EF – Emitted Fraction, FPF – Fine Particle Fraction, AF – Alveolar Particle Fraction)

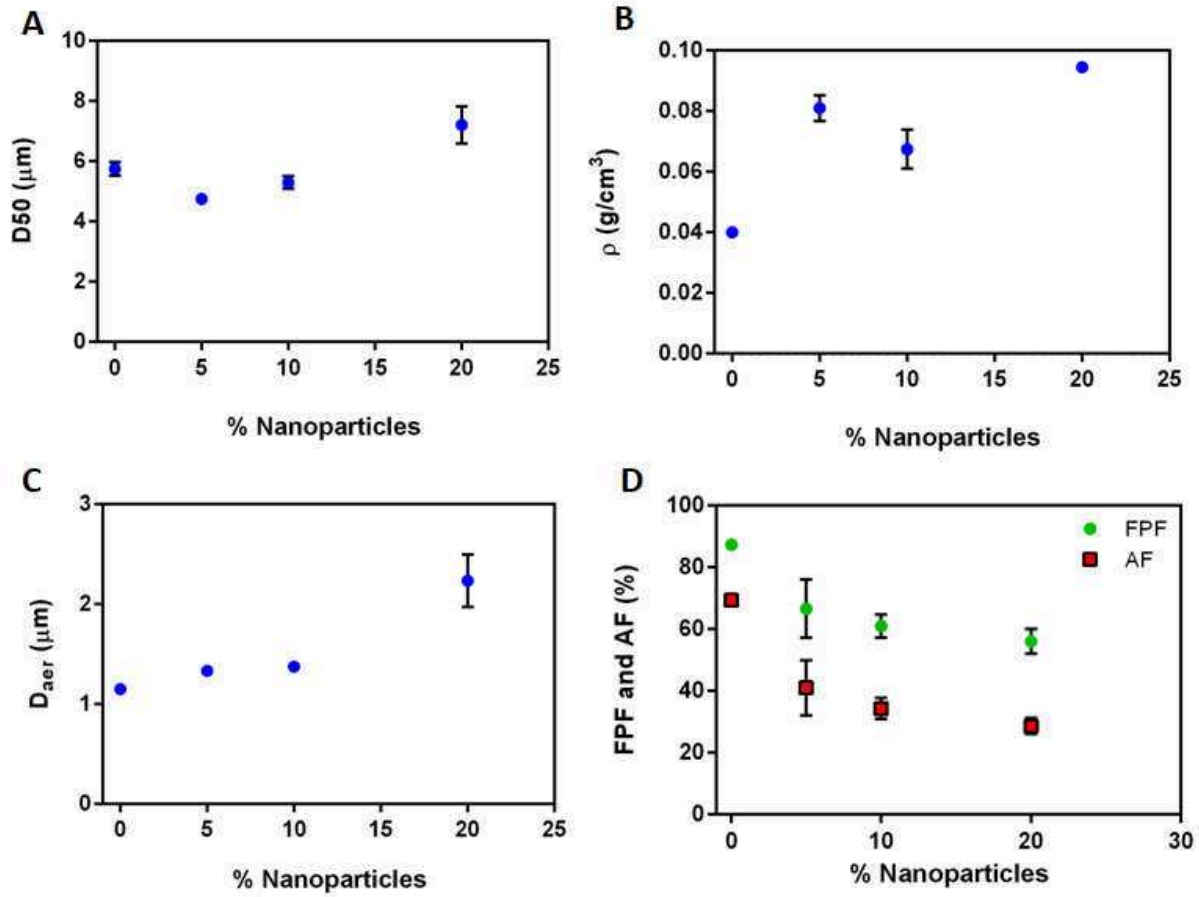

Figure 9. Aerodynamic properties of microparticles: A) Particle size distribution (D_{50}), B) Tap density (ρ), C) Aerodynamic diameter (D_{aer}), and D) Aerosolization characterization (FPF – Fine Particle Fraction (green), AF – Alveolar Particle Fraction (red)).

Aerosolization properties of the formulations were then tested using a multi-stage liquid impinger (MSLI). Impactors as MSLI are commonly used to evaluate the aerosolization efficacy of the inhaler and to predict the *in vivo* deposition of particles. This test equipment operates based on the principles of inertial impaction: deposition at each stage of the test illustrates the aerodynamic diameter of the particle. As the aerodynamic diameter is dependent on density, size and shape, it will be influenced primarily by inertial force and the role of gravitational force or diffusion will be very low (Javadzadeh and Yaqoubi, 2017). All powders presented a high emitted fraction around 100 %. The powder exempts of nanoparticles exhibited a FPF around 87 % with an AF around 70 %, proving the good aerosolization properties of the vehicle. As the nanoparticle concentration increased, a decrease of the FPF and AF was observed, down to 56 % and 28 % for 20 % nanoparticles, respectively (Table 3 and Figure 9D). This decrease is correlated to the tapped density increase. Given these results, formulations prepared with 5 % nanoparticles that lead to the highest FPF around 67 % and AF around 41 % were chosen for *in vivo* experiments.

3.7 *In vivo* tests

Biodistribution study was performed to obtain a better understanding of the behavior of BP Trojan microparticles after intratracheal administration in rats. Budesonide palmitate is a prodrug and budesonide is the active drug released from BP after ester bound hydrolysis. BP Trojan microparticles (treatment group) and budesonide (control group) were administered in a single dose after intratracheal insufflation. For the treatment group, a powder dose of around 3 mg (equivalent 90 µg BP) was delivered. For the control group, powder characteristics brought difficulties to the system delivery, resulting in a non-uniform administration (from 2.3 mg to 21.4 mg of powder). Even with the mass correction, the relationship between masse x dose was not linear, indicating a probable inhomogeneity of the drug in the powder. Due to these biases, the control group was therefore not considered here. The quantification method by LC-MS/MS was based on the use of internal standards. The limit of quantification (LOQ) in the plasma was found to be 1.0 ng for budesonide and BP. Levels below the LOQ and above the limit of detection (LOD) were arbitrarily assigned 1/3 LOQ=LOD to prevent losing the information that corticosteroid levels were low (Figure 10, dash curve=LOD).

Very low concentrations were found in the plasma, for both BP and Bud (Figure 10A). It was possible to quantify BP starting from 1 h post administration up to 24 h. BP levels remained more or less constant between 1 ng/mL (LOQ) up to 10 ng/mL. Bud levels were found lower than BP levels, remaining between the LOD and twice the LOQ at max. These data show very low passage of both the drug and prodrug in the circulation.

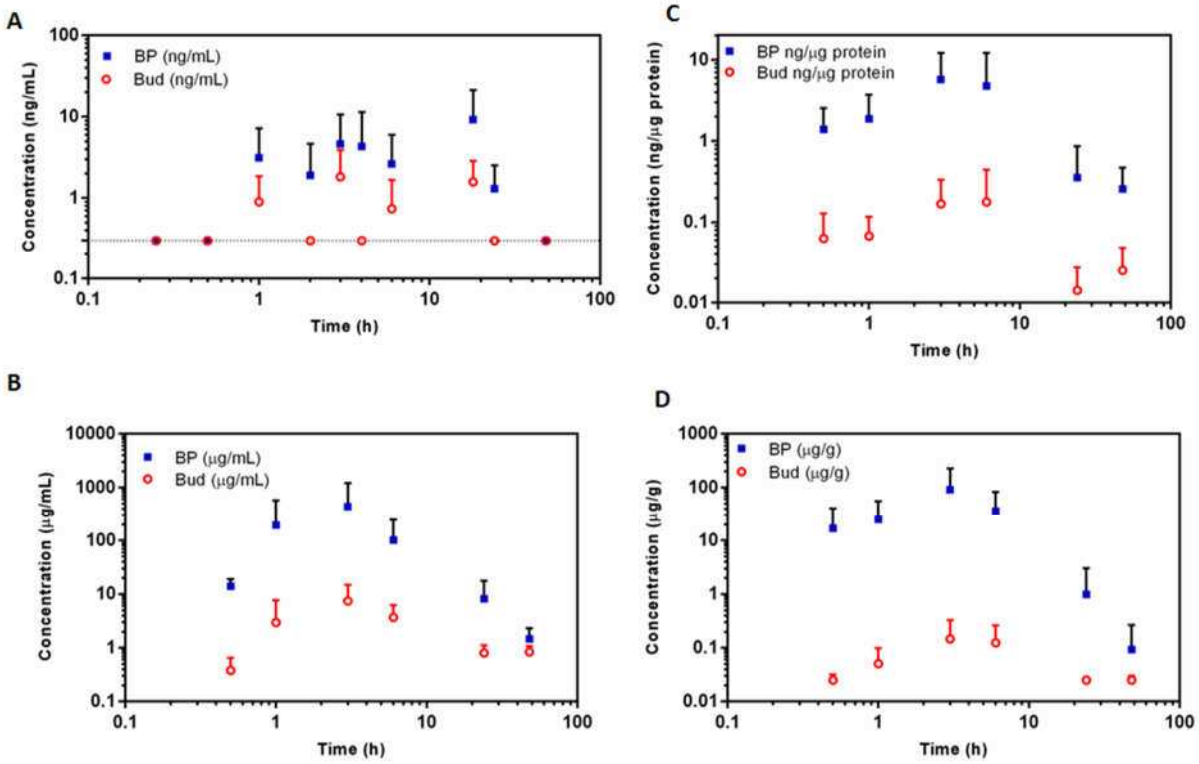

Figure 10. A) Concentration of BP and budesonide in plasma after intratracheal insufflation of ~3 mg of BP microparticles (BP dose ~90 µg), B) Concentration of BP and budesonide in ELF after intratracheal insufflation of ~3 mg of BP microparticles (BP dose ~90 µg), C) Concentration of BP and budesonide in alveolar cells after intratracheal insufflation of ~3 mg of BP microparticles (BP dose ~90 µg), expressed per µg of protein, and D) Concentration of BP and budesonide in lung tissue after intratracheal insufflation of ~3 mg of BP microparticles (BP dose ~90 µg), expressed per gram of tissue. Data are presented as mean ± SEM (Standard error of the mean), n=5.

Bronchoalveolar lavage was performed at different time points after intratracheal administration. It is a procedure used to recover cellular and non-cellular components of the ELF, the alveolar and bronchial airspaces. BALF represents a diluted form of the ELF of the lung containing cells, mainly alveolar macrophages, which can be separated by low-speed centrifugation. After centrifugation, the remaining BALF supernatant contains material that has not yet been absorbed to the systemic circulation or entered the lung tissue (Gursahani *et al.*, 2009). The amounts of BP and Bud obtained in BALF supernatant were converted to epithelial lining fluid (ELF) concentrations according to the theoretical volume of ELF reported in the literature (30 µL/kg) and to the volume of PBS used for bronchoalveolar lavage (3 x 1 mL). Thus, for a rat of 300 g, the dilution factor calculated was 333 (Gontijo *et al.*, 2014).

The results of BP and Bud concentrations obtained in ELF are presented in Figure 10B. Results show that the concentration of BP in the ELF is maximal 3 hours after administration with C_{max}= 440 µg/mL. It corresponds to about 5 % of the theoretical initial concentration given the administered dose. BP

concentration can be described by two different phases, one during which BP concentration increases and another one corresponding to BP elimination. The first phase occurs between 30min and 3h with BP concentration increasing from 14 µg/mL to 440 µg/mL. This part of the BP curve in ELF may correspond to the solubilization of particles to release BP molecules along with hydrolysis of BP into Bud occurring due to the presence of esterases in the ELF (von Deimling *et al.*, 1983). Budesonide esters are considered 500 to 10,000 times more lipophilic than free Bud and are believed to form an intracellular depot from which active drug is slowly released by the action of lipases and cholesterol esterases (Edsbäcker and Johansson, 2006). Ultimately, the second phase corresponds to elimination with BP concentration decrease between 3 h and 48 h from 440 µg/mL to 1.46 µg/mL. Bud concentration follows approximately the same trend than BP but Bud concentration remains always lower than BP concentration by at least a factor 10 to 50.

Since the cellular fraction of BALF is composed primarily by alveolar macrophages, BP and Bud concentrations in the alveolar cell pellet were determined to assess the amount of drug efficiently targeting the macrophages, key players in lung inflammation. Results are presented in Figure 10C, as concentrations calculated by µg of protein in BALF (Bradford method). BP and Bud levels remained above 1 ng/mL (LOQ) in HPLC-MS/MS quantifications (data expressed per µg of protein). Similar profiles as ELF with two phases were found, with a BP C_{max} of 5.7 ng/µg protein after 3 hours. As observed for ELF, Bud concentration was approximately 10 times lower than BP concentration. These data show that alveolar targeting was effective using Trojan microparticles.

Lung-tissue BP and Bud concentrations were quantified, up to 48 h after powder administration (Figure 10D). Similar profiles as ELF and alveolar cell pellet with two phases were found. A BP C_{max} of 90 µg/g was found after 3 hours. For lung tissue, Bud concentration was approximately 100 times lower than BP concentration. This is probably related to the difference of hydrophobicity of the prodrug compared to the drug as well as the difference of esterase concentration in the lung tissue as compared with the ELF or AC. Vatter *et al.* (1968) designed and synthesized a series of ester substrates to investigate the esterases of rabbit lung in the cytochemical and biochemical viewpoint. The results confirm that the lung is rich in hydrolytic activity, with an esterase activity most prominent in the lamellar bodies of the giant alveolar and an enzymatic profile quantitatively different from those of liver or kidney.

From PK and Biodistribution studies, pharmacokinetics parameters in plasma, ELF and lung tissue were calculated and are presented in Table 4. Very low concentrations were found in the plasma, for both BP and Bud (Figure 10A). This suggests a very pronounced local delivery and a rather low passage of

molecules from the lungs to the blood stream, confirmed by the higher AUC_{ELF}/AUC_{plasma} ratio around 18500 for BP and 2800 for Bud, and $AUC_{tissue}/AUC_{plasma}$ ratio around 4700 for BP and 84 for Bud.

Table 4. PK parameters after intratracheal insufflations of 3mg of BP powder corresponding to a BP dose of 90 μg (58 μg of Bud).

Parameters	Plasma		ELF		AC		Lung tissue	
	BP	Bud	BP	Bud	BP	Bud	BP	Bud
C_{max} (μg/mL)	0.0092	0.0018	440	7.46	0.0057	0.00018	90	0.15
t_{max} (h)	18	3	3	3	3	6	3	3
AUC (μg.h/mL)	0.140	0.031	2596	88	0.078	0.003	661	2.6
AUC/Dose (h/mL)	0.0016	0.00053	28.84	1.52	0.00087	0.00005	7.34	0.045
$T_{1/2}$ (h)	7.0	24.7	7.0	15.1	9.5	16.2	4.6	16.7
AUC_{ELF}/AUC_{plasma}			18543	2839				
AUC_{AC}/AUC_{plasma}					0.56	0.1		
$AUC_{tissue}/AUC_{plasma}$							4721	84

Since BP is a prodrug of budesonide, BP in the intrapulmonary compartment is important for supplying budesonide to ELF. Results presented by Ishizuka *et al.* (2012) in the evaluation of BAL fluid concentrations of laninamivir after a single lung administration of its prodrug, laninamivir octanoate (LO), in healthy subjects are consistent with our conclusions. They found relatively high intrapulmonary concentrations of laninamivir for 10 days after dosing 40 mg of LO, confirming previous PK studies in humans that showed a long $t_{1/2}$ of laninamivir in plasma, which is reflected by the slow release from lung tissue to plasma and by the slow hydrolysis of laninamivir from LO in ELF and alveolar macrophages (Ishizuka *et al.*, 2010). Koyama *et al.* (2013) have also evaluated intrapulmonary pharmacokinetics of LO *in vivo* and *in vitro* to investigate the potential mechanism involved in the prolonged high retention of laninamivir in mouse respiratory tissues. After intranasal administration of 0.5 mmol/kg of LO in mice, the drug was distributed from the airway space into the lungs, and laninamivir remained in the lung at 24 hours (2680 pmol/g), with a higher concentration than in the ELF. The authors have concluded that these results demonstrated that the prolonged and high retention of laninamivir in the respiratory tissues could be attributed to a consecutive series of three steps: uptake of LO by the airway epithelial cells, hydrolysis of LO into laninamivir by intracellular esterases, and limited efflux of the generated laninamivir due to its poor membrane permeability. A similar scenario probably applies to BP.

Our results confirm that BP Trojan microparticles may improve the uptake and retention of budesonide in lung tissue and alveolar cells. Experimental concentrations could be explained by the follow events: 1) powder solubilization and dispersion of PEGylated nanoparticles; 2) BP hydrolysis into Bud; 3) BP/Bud distribution in lung tissue; and 4) BP/Bud passage in the blood stream. Enhanced lipophilicity

in a glucocorticoid molecule and alveolar macrophage targeting as nanoparticles present potential advantages as increased deposition in lung tissue and consequently slow release and long retention of the drug.

4 CONCLUSIONS

In this study, a prodrug of budesonide, budesonide palmitate, was successfully synthesized and formulated as nanoparticles using DSPE-mPEG as sole excipient, using two different formulation processes. Either emulsion-evaporation or nanoprecipitation techniques provided stable spherical particles with a hydrodynamic diameter from 200 nm to 250 nm, very high encapsulation efficiency and no cytotoxicity up to 187 µM. The influence of ratio compounds was also tested (2:1 and 1:1, drug:lipids). Since nanoparticles obtained by emulsion-evaporation and ratio 2:1 have showed higher BP loading, from 66 to 73 % (w/w), they were selected for the following experiments. Cytokine release study in RAW 264.7 cells has attested that the encapsulation and use of budesonide palmitate do not affect the anti-inflammatory activity of budesonide. Trojan microparticles with 5 %, 10 % and 20 % of BP PEGylated nanoparticles were developed, characterized and evaluated *in vitro*. Microparticles containing 5 % nanoparticles were chosen for *in vivo* tests due aerodynamic diameters around 1.3 µm, optimal to target the alveolar region, and a good lung deposition profile with a fine particle fraction (FPF) around 67 % and an alveolar particle fraction (AF) around 41 %. The pharmacokinetic and biodistribution of both the prodrug and the drug were determined in healthy rats after intratracheal administration. Very low concentrations of BP and Bud were found in plasma, suggesting an excellent local retention in the lungs, with lower passage to the blood stream. These results indicate that the use of more lipophilic compounds as BP may increase tissue retention characteristics of budesonide, and Trojan microparticles could improve nanoparticle delivery and the alveolar macrophage targeting. Together, these strategies could be useful to design potential alternative treatments for lung diseases such as COPD and asthma.

5 ACKNOWLEDGMENTS

Ludmila Pinheiro do Nascimento was supported by a PhD scholarship from CNPq - National Council of Scientific and Technologic Development (Brazil) #233180/2014-1. The present work has benefited from the core facilities of Imagerie-Gif, (http://www.i2bc.paris-saclay.fr), member of IBiSA (http://www.ibisa.net), supported by “France-BioImaging” (ANR-10-INBS-04-01), and the Labex “Saclay Plant Science” (ANR-11-IDEX-0003-02) with the precious help of C. Boulogne and C. Gillet. Institut Galien Paris-Sud is a member of the Laboratory of Excellence LERMIT supported by a grant from ANR (ANR-10-LABX-33). Authors thank Institut de Chimie et des Matériaux Paris-Est (ICMPE

UMR7182, CNRS-UPEC) for access to the SEM facility and R. Pires Brazuna for technical assistance. The authors would like to acknowledge the financial support provided by COST-European Cooperation in Science and Technology, to the COST Action MP1404: Simulation and pharmaceutical technologies for advanced patient-tailored inhaled medicines (Siminhale).

6 REFERENCES

Axelsson, B. I., Brattsand, R. L., Dahlbäck, C. M. O., Källström, L. A., Trofast, J. W. « Brevet EP0170642A2 - Liposomes containing steroid esters - budesonide palmitate », 1986.

Barnes P. J. « Alveolar Macrophages as Orchestrators of COPD ». *COPD J. Chronic Obstr. Pulm. Dis.* [En ligne]. 2004. Vol. 1, n°1, p. 59-70. Disponible sur : < https://doi.org/10.1081/COPD-120028701 >

Bosch J. M. M. Van den, Westermann C. J. J., Aumann J., Edsbäcker S., Tönnesson M., Selroos O. « Relationship between lung tissue and blood plasma concentrations of inhaled budesonide ». *Biopharm. Drug Dispos.* [En ligne]. 1993. Vol. 14, n°5, p. 455-459. Disponible sur : < https://doi.org/https://doi.org/10.1002/bdd.2510140511 >

Brink K. I. M. Van den, Boorsma M., Staal-Van Den Brekel A. J., Edsbäcker S., Wouters E. F., Thorsson L. « Evidence of the in vivo esterification of budesonide in human airways ». *Br. J. Clin. Pharmacol.* [En ligne]. 2008. Vol. 66, n°1, p. 27-35. Disponible sur : < https://doi.org/10.1111/j.1365-2125.2008.03164.x >

Celli B. R. « Pharmacological Therapy of COPD: Reasons for Optimism ». *Chest* [En ligne]. 2018. Vol. 154, n°6, p. 1404-1415. Disponible sur : < https://doi.org/10.1016/j.chest.2018.07.005 >

Cruz L., Fattal E., Tasso L., Freitas G. C., Carregaro A. B., Guterres S. S., Pohlmann A. R., Tsapis N. « Formulation and in vivo evaluation of sodium alendronate spray-dried microparticles intended for lung delivery ». *J. Control. Release* [En ligne]. 30 juin 2011. Vol. 152, n°3, p. 370-375. Disponible sur : < https://doi.org/10.1016/J.JCONREL.2011.02.030 > (consulté le 22 mars 2018)

Deimling O. Von, Müller M., Eisenhardt E. « The non-specific esterases of mouse lung ». *Histochemistry*. 1983. Vol. 78, n°2, p. 271-284.

Donnelly R., Seale J. P. « Clinical pharmacokinetics of inhaled budesonide ». *Clin. Pharmacokinet.* [En ligne]. 2001. Vol. 40, n°6, p. 427-440. Disponible sur : < https://doi.org/10.2165/00003088-200140060-00004 >

Edsbäcker S., Johansson C. J. « Airway selectivity: An update of pharmacokinetic factors affecting local and systemic disposition of inhaled steroids ». *Basic Clin. Pharmacol. Toxicol.* [En ligne]. 2006. Vol. 98, n°6, p. 523-536. Disponible sur : < https://doi.org/10.1111/j.1742-7843.2006.pto_355.x >

Elsabahy M., Wooley K. L. « Cytokines as biomarkers of nanoparticle immunotoxicity ». *Chem. Soc. Rev.* [En ligne]. 2013. Vol. 42, n°12, p. 5552-5576. Disponible sur : < https://doi.org/10.1039/c3cs60064e.Cytokines >

European Respiratory Society. *Respiratory Diseases in the World. Realities of Today – Opportunities for*

Tomorrow. [En ligne]. [s.l.] : [s.n.], 2013. 1-35 p. Disponible sur : < papers3://publication/uuid/605D7CD3-0FE0-4918-8941-96F2920D09DD >ISBN : 9781849840569.

Evans C. M., Koo J. S. « Airway mucus: The good, the bad, the sticky ». *Pharmacol. Ther.* [En ligne]. 1 mars 2009. Vol. 121, n°3, p. 332-348. Disponible sur : < https://doi.org/10.1016/J.PHARMTHERA.2008.11.001 > (consulté le 17 octobre 2018)

Foillard S., Russier J., Seifert C., Dumortier H., Doris E. « Carbon nanotube-mediated delivery of budesonide to macrophages ». *RSC Adv.* [En ligne]. 2016. Vol. 6, n°58, p. 53282-53287. Disponible sur : < https://doi.org/10.1039/C6RA09809F >

Giuffrida M. J., Valero N., Mosquera J., Alvarez de Mon M., Chacín B., Espina L. M., Gotera J., Bermudez J., Mavarez A. « Increased cytokine/chemokines in serum from asthmatic and non-asthmatic patients with viral respiratory infection ». *Influenza Other Respi. Viruses* [En ligne]. 2014. Vol. 8, n°1, p. 116-122. Disponible sur : < https://doi.org/10.1111/irv.12155 >

GOLD. « Pocket guide to COPD diagnosis, management and prevention: a guide for health care professionals ». *Glob. Initiat. Chronic Obstr. Lung Dis. Inc* [En ligne]. 2018. Vol. 1, n°1, p. 3-14. Disponible sur : < https://doi.org/http://dx.doi.org/10.1164/rccm.201701-0218PP >

Gómez-Gaete C., Fattal E., Silva L., Besnard M., Tsapis N. « Dexamethasone acetate encapsulation into Trojan particles ». *J. Control. Release* [En ligne]. 2008. Vol. 128, p. 41-49. Disponible sur : < https://doi.org/10.1016/j.jconrel.2008.02.008 >

Gontijo A. V. L., Brillault J., Grégoire N., Lamarche I., Gobin P., Couet W., Marchand S. « Biopharmaceutical characterization of nebulized antimicrobial agents in rats: 1. ciprofloxacin, moxifloxacin, and grepafloxacin ». *Antimicrob. Agents Chemother.* [En ligne]. 2014. Vol. 58, n°7, p. 3942-3949. Disponible sur : < https://doi.org/10.1128/AAC.02818-14 >

Gursahani H., Riggs-sauthier J., Pfeiffer J., Lechuga-ballesteros D. « Absorption of Polyethylene Glycol (PEG) Polymers : The Effect of PEG Size on Permeability ». *J. Pharm. Sci.* [En ligne]. 2009. Vol. 98, n°8, p. 2847-2856. Disponible sur : < https://doi.org/10.1002/jps >

Hadinoto K., Phanapavudhikul P., Kewu Z., Tan R. B. H. « Novel formulation of large hollow nanoparticles aggregates as potential carriers in inhaled delivery of nanoparticulate drugs ». *Ind. Eng. Chem. Res.* [En ligne]. 2006. Vol. 45, n°10, p. 3697-3706. Disponible sur : < https://doi.org/10.1021/ie0513191 >

Huang A.-X., Lu L.-W., Liu W.-J., Huang M. « Plasma Inflammatory Cytokine IL-4, IL-8, IL-10, and TNF-α Levels Correlate with Pulmonary Function in Patients with Asthma-Chronic Obstructive Pulmonary Disease (COPD) Overlap Syndrome ». *Med. Sci. Monit.* [En ligne]. 2016. Vol. 22, p. 2800-2808. Disponible sur : < https://doi.org/10.12659/msm.896458 >

Huckaby J. T., Lai S. K. « PEGylation for enhancing nanoparticle diffusion in mucus ». *Adv. Drug Deliv. Rev.* [En ligne]. 15 janvier 2018. Vol. 124, p. 125-139. Disponible sur : < https://doi.org/10.1016/J.ADDR.2017.08.010 > (consulté le 19 mars 2019)

International Standard Organization. *ISO 10993-5 - Part 5: Tests for in vitro cytotoxicity*. [s.l.] : [s.n.], 2009. 1-34 p.ISBN : 9782832202937.

Ishizuka H., Toyama K., Yoshiba S., Okabe H., Furuie H. « Intrapulmonary distribution and pharmacokinetics of laninamivir, a neuraminidase inhibitor, after a single inhaled administration of its prodrug, laninamivir octanoate, in healthy volunteers ». *Antimicrob. Agents Chemother.* [En ligne]. 2012. Vol. 56, n°7, p. 3873-3878. Disponible sur : < https://doi.org/10.1128/AAC.06456-11 >

Ishizuka H., Yoshiba S., Okabe H., Yoshihara K. « Clinical pharmacokinetics of laninamivir, a novel long-acting neuraminidase inhibitor, after single and multiple inhaled doses of its prodrug, CS-8958, in healthy male volunteers ». *J. Clin. Pharmacol.* [En ligne]. 2010. Vol. 50, n°11, p. 1319-1329. Disponible sur : < https://doi.org/10.1177/0091270009356297 >

Javadzadeh Y., Yaqoubi S. « Therapeutic nanostructures for pulmonary drug delivery ». *Nanostructures Drug Deliv.* [En ligne]. 1 janvier 2017. p. 619-638. Disponible sur : < https://doi.org/10.1016/B978-0-323-46143-6.00020-8 > (consulté le 5 février 2019)

Jiang C.-L., Liu L., Li Z., Buttgereit F. « The novel strategy of glucocorticoid drug development via targeting nongenomic mechanisms ». *Steroids* [En ligne]. 1 octobre 2015. Vol. 102, p. 27-31. Disponible sur : < https://doi.org/10.1016/J.STEROIDS.2015.06.015 > (consulté le 26 octobre 2018)

Kis K., Bodai L., Polyanka H., Eder K., Pivarcsi A., Duda E., Soos G., Bata-Csorgo Z., Kemeny L. « Budesonide, but not tacrolimus, affects the immune functions of normal human keratinocytes ». *Int. Immunopharmacol.* [En ligne]. 1 mars 2006. Vol. 6, n°3, p. 358-368. Disponible sur : < https://doi.org/10.1016/J.INTIMP.2005.08.022 > (consulté le 23 janvier 2018)

Koyama K., Nakai D., Takahashi M., Nakai N., Kobayashi N., Imai T., Izumi T. « Pharmacokinetic Mechanism Involved in the Prolonged High Retention of Laninamivir in Mouse Respiratory Tissues after Intranasal Administration of its Prodrug Laninamivir Octanoate ». *Drug Metab. Dispos.* 2013. Vol. 41, n°January, p. 180-187.

Lai S. K., Wang Y.-Y., Hanes J. « Mucus-penetrating nanoparticles for drug and gene delivery to mucosal tissues ». *Adv. Drug Deliv. Rev.* [En ligne]. 27 février 2009. Vol. 61, n°2, p. 158-171. Disponible sur : < https://doi.org/10.1016/J.ADDR.2008.11.002 > (consulté le 20 septembre 2017)

Lavorini F., Mannini C., Chellini E. « Challenges of Inhaler Use in the Treatment of Asthma and Chronic Obstructive Pulmonary Disease ». *Eur. Med. J. Respir.* [En ligne]. 2015. Vol. 3, n°2, p. 98-105. Disponible sur : < https://pdfs.semanticscholar.org/453f/3e25be1b1f06bfb7d162c8ad16a8b53aee09.pdf >

Liang W., Chan A. Y. L., Chow M. Y. T., Lo F. F. K., Qiu Y., Kwok P. C. L., Lam J. K. W. « Spray freeze drying of small nucleic acids as inhaled powder for pulmonary delivery ». *Asian J. Pharm. Sci.* [En ligne]. 1 mars 2018. Vol. 13, n°2, p. 163-172. Disponible sur : < https://doi.org/10.1016/J.AJPS.2017.10.002 > (consulté le 24 mai 2018)

Liu M., Zhang J., Shan W., Huang Y. « Developments of mucus penetrating nanoparticles ». *Asian J. Pharm. Sci.* [En ligne]. 2015. Vol. 10, n°4, p. 275-282. Disponible sur : < https://doi.org/10.1016/j.ajps.2014.12.007 >

Lorscheider M., Tsapis N., Ur-Rehman M., Gaudin F., Stolfa I., Abreu S., Mura S., Chaminade P., Espeli M., Fattal E. « Dexamethasone palmitate nanoparticles: An efficient treatment for rheumatoid arthritis ». *J. Control. Release* [En ligne]. 2019. Vol. 296, n°28 February 2019, p. 179-189. Disponible sur : < https://doi.org/10.1016/J.JCONREL.2019.01.015 >

Mert O., Lai S. K., Ensign L., Yang M., Wang Y.-Y., Wood J., Hanes J. « A poly(ethylene glycol)-based surfactant for formulation of drug-loaded mucus penetrating particles ». *J. Control. Release* [En ligne]. 10 février 2012. Vol. 157, n°3, p. 455-460. Disponible sur : < https://doi.org/10.1016/J.JCONREL.2011.08.032 > (consulté le 20 septembre 2017)

Miller-Larsson A., Jansson P., Runstrom A., Brattsand R. « Prolonged airway activity and improved selectivity of budesonide possibly due to esterification ». *Am. J. Respir. Crit. Care Med.* [En ligne]. 2000. Vol. 162, n°4 I, p. 1455-1461. Disponible sur : < https://doi.org/10.1164/ajrccm.162.4.9806112 >

Murgia X., Loretz B., Hartwig O., Hittinger M., Lehr C.-M. « The role of mucus on drug transport and its potential to affect therapeutic outcomes ». *Adv. Drug Deliv. Rev.* [En ligne]. 15 janvier 2018. Vol. 124, p. 82-97. Disponible sur : < https://doi.org/10.1016/J.ADDR.2017.10.009 > (consulté le 25 juillet 2018)

N'Guessan A., Chapron D., Gueutin C., Koffi A., Tsapis N. « Dexamethasone palmitate large porous particles: A controlled release formulation for lung delivery of corticosteroids ». *Eur. J. Pharm. Sci.* [En ligne]. 15 février 2018. Vol. 113, p. 185-192. Disponible sur : < https://doi.org/10.1016/J.EJPS.2017.09.013 > (consulté le 24 mai 2018)

Pappas K., Papaioannou A. I., Kostikas K., Tzanakis N. « The role of macrophages in obstructive airways disease: Chronic obstructive pulmonary disease and asthma ». *Cytokine* [En ligne]. 1 décembre 2013. Vol. 64, n°3, p. 613-625. Disponible sur : < https://doi.org/10.1016/J.CYTO.2013.09.010 > (consulté le 11 juillet 2018)

Pharmacopoeia E. *Bulk density*. [s.l.] : [s.n.], 2019a.

Pharmacopoeia E. *Non enrobés inhalation: évaluation aérodynamique des particules*. [s.l.] : [s.n.], 2019b.

Schuster B. S., Suk J. S., Woodworth G. F., Hanes J. « Nanoparticle diffusion in respiratory mucus from humans without lung disease ». *Biomaterials* [En ligne]. 1 avril 2013. Vol. 34, p. 3439-3446. Disponible sur : < https://doi.org/10.1016/J.BIOMATERIALS.2013.01.064 > (consulté le 20 septembre 2017)

Sou T., Kaminskas L. M., Nguyen T.-H., Carlberg R., McIntosh M. P., Morton D. A. V. « The effect of amino acid excipients on morphology and solid-state properties of multi-component spray-dried formulations for pulmonary delivery of biomacromolecules ». *Eur. J. Pharm. Biopharm.* [En ligne]. 1 février 2013. Vol. 83, n°2, p. 234-243. Disponible sur : < https://doi.org/10.1016/J.EJPB.2012.10.015 > (consulté le 13 février 2019)

Spies C. M., Strehl C., Van der Goes M. C., Bijlsma J. W. J., Buttgereit F. « Glucocorticoids ». *Best Pract. Res. Clin. Rheumatol.* [En ligne]. 1 décembre 2011. Vol. 25, n°6, p. 891-900. Disponible sur : < https://doi.org/10.1016/J.BERH.2011.11.002 > (consulté le 26 octobre 2018)

Spoelstra F. M., Postma D. S., Hovenga H., Noordhoek J. A., Kauffman H. F. « Additive anti-inflammatory effect of formoterol and budesonide on human lung fibroblasts ». *Thorax* [En ligne]. 2002. Vol. 57, n°3, p. 237-241. Disponible sur : < https://doi.org/10.1136/thorax.57.3.237 >

Traves S. L., Culpitt S. V., Russell R. E. K., Barnes P. J., Donnelly L. E. « Increased levels of the chemokines GROα and MCP-1 in sputum samples from patients with COPD ». *Thorax* [En ligne]. 2002. Vol. 57, n°7, p. 590-595. Disponible sur : < https://doi.org/10.1136/thorax.57.7.590 >

Tsapis N., Bennett D., Jackson B., Weitz D. A., Edwards D. A. « Trojan particles: Large porous carriers of nanoparticles for drug delivery ». *Proc. Natl. Acad. Sci. U. S. A.* [En ligne]. 2002. Vol. 99, n°19, p. 12001-12005. Disponible sur : < https://doi.org/10.1073/pnas.182233999 >

Tunek A., Sjödin K., Hallström G. « Reversible formation of fatty acid esters of budesonide, an antiasthma glucocorticoid, in human lung and liver microsomes ». *Drug Metab. Dispos.* 1997. Vol. 25, n°11, p. 1311-1317.

Vandewalle J., Luypaert A., De Bosscher K., Libert C. « Therapeutic Mechanisms of Glucocorticoids ». *Trends Endocrinol. Metab.* [En ligne]. 1 janvier 2018. Vol. 29, n°1, p. 42-54. Disponible sur : < https://doi.org/10.1016/J.TEM.2017.10.010 > (consulté le 26 octobre 2018)

Vatter A. E., Reiss O. K., Newman J. K., Groeneboer E. « ENZYMES OF THE LUNG I . Detection of Esterase

with a New Cytochemical Method ». *J. Cell Biol.* 1968. Vol. 38, p. 80-98.

Wang X., Nelson A., Weiler Z. M., Patil A., Sato T., Kanaji N., Nakanishi M., Michalski J., Farid M., Basma H., Levan T. D., Miller-Larsson A., Wieslander E., Muller K.-C., Holz O., Magnussen H., Rabe K. F., Liu X., Rennard S. I. « Anti-inflammatory effects of budesonide in human lung fibroblast are independent of histone deacetylase 2 ». *J. Inflamm. Res.* [En ligne]. 20 août 2013. Vol. 6, p. 109-119. Disponible sur : < https://doi.org/10.2147/JIR.S43736 >

Woodle M. C., Martin F. J., Collins E., Sponsler N., Kossovsky N., Papahadjopoulos D., Martin F. J. « Sterically stabilized liposomes - Reduction In electrophoretic mobility but not electrostatic surface potential ». *Biophys. J.* [En ligne]. 1992. Vol. 61, n°4, p. 902-910. Disponible sur : < https://doi.org/10.1016/S0006-3495(92)81897-0 >

Wu L., Shan W., Zhang Z., Huang Y. « Engineering nanomaterials to overcome the mucosal barrier by modulating surface properties ». *Adv. Drug Deliv. Rev.* [En ligne]. 15 janvier 2018. Vol. 124, p. 150-163. Disponible sur : < https://doi.org/10.1016/J.ADDR.2017.10.001 > (consulté le 25 juillet 2018)

Xu Q., Boylan N. J., Cai S., Miao B., Patel H., Hanes J. « Scalable method to produce biodegradable nanoparticles that rapidly penetrate human mucus ». *J. Control. Release* [En ligne]. 10 septembre 2013. Vol. 170, n°2, p. 279-286. Disponible sur : < https://doi.org/10.1016/J.JCONREL.2013.05.035 > (consulté le 19 mars 2019)

CHAPITRE 2

MANNOSYLATION OF BUDESONIDE PALMITATE NANOSCALE PRODRUGS FOR IMPROVED MACROPHAGE TARGETING

MANNOSYLATION OF BUDESONIDE PALMITATE NANOSCALE PRODRUGS FOR IMPROVED MACROPHAGE TARGETING

Ludmila Pinheiro do Nascimento[1], Nicolas Tsapis[1], Franceline Reynaud[1,2], Didier Desmaële[1], Laurence Moine[1], Juliette Vergnaud[1], Sonia Abreu[3], Pierre Chaminade[3], Elias Fattal[1]

[1] Institut Galien Paris-Sud, CNRS, Univ. Paris-Sud, Univ. Paris-Saclay, 92290 Châtenay-Malabry, France
[2] School of Pharmacy, Federal University of Rio de Janeiro, 21944-59 Rio de Janeiro, Brazil.
[3]Lip(Sys) EA7357, Lipides, systèmes analytiques et biologiques, Univ. Paris-Sud, Univ. Paris-Saclay, 92290 Châtenay-Malabry, France

Abstract

To avoid side-effects and increase drug efficacy, inhaled glucocorticoids should demonstrate a high lung bioavailability and retention and a better cellular targetability. To achieve this goal, we have combined within a nanoparticulate form the prodrug approach using budesonide palmitate (BP) as well the cellular delivery functionalizing the nanomedicine by a lipid mannose derivative to better reach the alveolar macrophages. After synthesis of budesonide palmitate (BP) by esterification and mannosylated lipid (DSPE-PEG-Man) by reaction of DSPE-PEG-NH_2 and α-D-mannopyranosylphenyl isothiocyanate (MPITC), two formulation processes (emulsion-evaporation and nanoprecipitation) and different ratios of lipids DSPE-PEG-Man/DSPE-mPEG (100/0, 75/25, 50/50, 25/75, 0/100) were compared to produce nanoparticles. Nanoparticles produced by both techniques and up to 75 % of DSPE-PEG-man (75/25) were about 200nm with a low polydispersity below 0.2, a negative zeta potential from -10 to -30 mV and a one month stability at 4°C. Independently of the formulation process, the encapsulation efficiency of BP was high (89 %-107 %) proving that all the prodrug was associated to nanoparticles, leading to a final BP loading of 50-to 60 % (w/w). Lectin agglutination test was used to confirm the presence and biological activity of the mannose ligands on nanoparticles surface. Nanoparticle uptake in RAW 264.7 cells was studied by flow cytometry and confocal microscopy showing internalization after 3 hours, by an energy-dependent mechanism. After 24 hours incubation, a significantly greater internalization of mannosylated nanoparticles as compared to PEGylated nanoparticles was observed. The mannose receptor-mediated uptake was confirmed by a mannan inhibition study. After LPS-induced inflammation, the anti-inflammatory effect of mannosylated nanoparticles was assessed. After 24 hours incubation, cytokines IL-6 and IL-10 expression presented a clear reduction, with a prolonged effect up to 72 hours. MCP-1 demonstrated an effect after 48 hours and TNFα only after 72 hours.

Keywords: Nanoparticles, macrophages, prodrug, targeting, mannose receptor

1 INTRODUCTION

Respiratory diseases have been recognized in recent decades among the major causes of death worldwide, generating a large health burden. Among these diseases, asthma and chronic obstructive pulmonary disease (COPD) affect about 65 and 334 million people in the world, respectively, and these numbers are projected to increase in coming years (Forum of International Respiratory Societies, 2017 ; GOLD, 2018). In both diseases, airways are infiltrated by inflammatory cells, such as mast cells, macrophages, eosinophils, neutrophils, T lymphocytes, dendritic cells, basophils, and platelets, which release or activate *in situ* mediators and cytokines. Treatment of asthma uses inhaled corticosteroids (ICS), while for COPD it is based on bronchodilators (β-2 agonists and anticholinergics) and ICS (Fromer and Bhatia, 2011 ; GINA, 2018). For long-term control, ICS are the most effective class of drugs reducing inflammation and suppressing airway constriction and dyspnea (Corry *et al*., 2019). Indeed, ICS are selected because of their strong anti-inflammatory and immunosuppressive effects as well as their fast onset of action, especially at high doses for the treatment of severe flares and acute exacerbations (Spies *et al.,* 2011). However, corticotherapy is commonly associated with the risk of adverse events, especially when given at high doses and for long time (Spies *et al.*, 2011). Adverse effects such as obesity, pneumonia, osteoporosis/fractures, voice problems, pulmonary embolism, ophthalmic effects (cataract or/and glaucoma) and reduced grown velocity have been reported (Cho and Sin, 2018 ; Finney *et al.*, 2014 ; Gonzalez *et al*., 2018 ; Heffler *et al.*, 2018 ; Sneeboer *et al*., 2016 ; Spantideas *et al.*, 2017). To improve the efficacy of ICS and reduce their effective dose, several strategies have been proposed in the last decades. The ideal ICS with optimal therapeutic index should have high lung bioavailability, negligible oral bioavailability, low systemic absorption, high systemic clearance and high protein binding (Derendorf, 2005).

Many GCs, among which budesonide, are naturally and partially esterified by fatty acids in the lungs supporting their prolonged duration of action (Edsbäcker and Brattsand, 2002). This is the reason why molecules such as Ciclesonide, an inactive prodrug, that is activated by esterases in the lung to an active metabolite has been developed (Derendorf, 2007). Our strategy what to use a biomimetic approach through the synthesis of the Budesonide palmitate (BP) prodrug to improve lung bioavailability. Moreover, we recently demonstrated that fatty acid derivative of CS can be turned to nanoparticles when associated to 1,2-distearoyl-sn-glycero-3-phosphoethanolamine-N [amino (polyethylene glycol)-2000] (DSPE-PEG) (Lorscheider *et al.*, 2019).

Because of their high affinity to phagocytic cells, nanoparticles can deliver drugs to macrophages increasing the pool of delivered drugs within these cells. As a matter of fact, alveolar macrophages are

important targets for CS since they are key effector in the defense system and pulmonary homeostasis (Pappas *et al.*, 2013). Our group has recently shown that polymeric NPs bearing mannose on their surface produce an increase uptake by alveolar macrophages after intratracheal instillation in mice. Because of the high presence of mannose receptors exclusively expressed on the surface of alveolar macrophages, that can recognize mannose terminal molecules with high affinity, the development of macrophages targeting systems using a variety of carriers would improve the therapeutic efficiency and minimize drug side effects (Wijagkanalan *et al.*, 2008). While mannose was coupled to different carriers made of polymers and lipids, it was never associated to lipid prodrugs despite the large interest of using and combining both strategies.

In the present report, lipophilic derivative of budesonide, budesonide palmitate (BP) was synthesized and formulated into nanoparticles by using solely, DSPE-PEG and a mannosylated lipid, DPSE-PEG-Man to efficiently deliver the corticosteroids to alveolar macrophages. The formulation process was optimized, nanoparticles were characterized and their ability to target macrophages and reduce inflammation was evaluated on RAW 264.7 macrophages.

2 MATERIALS AND METHODS

2.1 Materials

Budesonide (Bud) was obtained from Chemos GmbH & Co (Germany). DSPE-PEG-NH_2 (1,2-Distearoyl-sn-Glycero-3-Phosphoethanolamine-N-(methoxy(polyethylene glycol)-2000) (ammonium salt), DSPE-mPEG (1,2-Distearoyl-sn-Glycero-3-Phosphoethanolamine-N-(amino(polyethylene glycol)-2000) (ammonium salt) and lissamine-rhodamine B sulfonyl were purchased from Avanti Polar Lipids, Inc. (USA). Palmitoyl chloride, pyridine, triethylamine, ammonium acetate, α-D-Mannopyranosylphenyl isothiocyanate (MPITC), Methyl α-D-mannopyranoside, Concanavalin A type IV, Mannan (isolated from Saccharomyces cerevisiae) and LPS (Lipopolysaccharides from Escherichia coli O55:B5) were provided by Sigma-Aldrich. Dialysis membrane Spectra/Por 6 Dialysis Tubing 1 kD MWCO was purchased from Spectrum labs. Chloroform HPLC-grade, methanol HPLC-grade, acetone and DMSO were purchased from Carlo Erba Reagents (France). All other chemicals were obtained commercially and were of the highest available analytical grade. Water was purified using a Milli Q Reference system (Merck Millipore, France).

2.2 Synthesis of Budesonide Palmite (BP)

Budesonide palmitate, a prodrug of budesonide, was synthesized from the esterification of the alcohol-terminus present on the C-21 carbon of budesonide by the addition of palmitoyl chloride (Figure 1).

Briefly, 1 mmol of budesonide was dissolved in pyridine (10.8 mL for each mmol of budesonide) and after treatment with 2 equivalents of palmitoyl chloride injected dropwise at 0°C. The solution remained at room temperature overnight under stirring and nitrogen. After 24 hours of reaction, the pyridine was distilled off.

The solution obtained was resuspended in dichloromethane (at least 10 mL) and washed successively with approximately 5 mL of HCl (0.05 M), 5mL of distilled water and 5 mL of 5 % $NaHCO_3$ to neutralize the acid. The organic phase was dried using anhydrous magnesium sulfate ($MgSO_4$) for 30 minutes under stirring, and, after filtration, the obtained solids were abundantly solubilized in dichloromethane (Axelsson *et al.*, 1986). The product obtained was purified by silica gel column chromatography, eluted with ethyl acetate/cyclohexane 1/4 (v/v) mixture and then 1/2 (v/v) mixture. The separation was performed by thin layer chromatography with the same eluent as mentioned above.

The fractions containing the product were collected in a flask, the solvent evaporated using a rotary evaporator and a 40°C bath. After weighing, the obtained products were resuspended in dichloromethane and distributed in small amber vials, remaining in laminar flow hood for 3 hours until total evaporation of the solvent. The obtained ester was analyzed by nuclear magnetic resonance (^{1}H NMR) at 300MHz in deuterated chloroform ($CDCl_3$), with the following results: the presence of two isomers induced the splitting of most peaks δ 7.25 (d, *J* = 10.0 Hz, 1H, H-1), 6.26 (d, *J* = 10.0 Hz, 1H, H-2), 6.00 (s, 1H, H-4), 5.17 – 5.09 (m, 1H, OC*H*O), 4.92 – 4.70 (m, 2.4H, 2H-21, 0.4H-16), 4.60 (t, *J* = 4.5 Hz, 0.6H, H-16), 4.48 (broad s, 1H, H-11), 2.52 (td, *J* = 14.5 Hz, *J* = 4.8 Hz, 1H, H-6β), 2.36 (t, *J* = 7.6 Hz, 2H, O_2C*H*$_2CH_2$), 2.36-2.28 (m, 1H, H-6α), 2.2-1.5 (m, 14H), 1.43 and 1.42 (s, 3H, H-19), 1.45-1.05 (m, 24H,), 1.00-0.83 (m, 9H, H-20, OCH(O)CH_2CH_2*C*H_3, palm*C*H_3).

2.3 Synthesis of DSPE-PEG-Man

The synthesis of DSPE-PEG-Mannose (DSPE-PEG-Man) was performed by chemical reaction between DSPE-PEG-NH_2 and MPITC (Chen, 2013 ; Kim *et al.*, 2012 ; Wang *et al.*, 2014). DSPE-PEG-NH_2 (Mw = 2790.486 g.mol^{-1}) and MPITC (Mw = 313.33 g.mol^{-1}) were dissolved in DMSO in the 1:3 ratio, with the reaction being kept under stirring at 25°C for 16 h. The product obtained, DSPE-PEG-Man, was then mixed with Milli Q water (1:10) and dialyzed for 48 h to remove free mannose (distilled water, 1 kDa membrane) and lyophilized at the end. The chemical structure of DSPE-PEG-Man was characterized with ^{1}H NMR (Figure 2).

2.4 Nanoparticles formulation

Nanoparticles were formulated using either emulsion-evaporation or nanoprecipitation methods to obtain 5 formulations by each method, with final BP concentration 1.25 mg/mL and different DSPE-PEG-Man/DSPE-mPEG ratios to a final lipid concentration 1.25mg/mL: 100/0, 75/25, 50/50, 25/75 and 0/100, respectively (Table 1), using a protocol recently published (Lorscheider *et al.*, 2019).

For the emulsion-evaporation, nanoparticles were prepared by solubilizing the lipids DSPE-PEG-Man/DSPE-mPEG and BP in 1 mL of chloroform. This organic phase was slowly injected with a 20G needle (Braun, Sterican, 0.90 by 70 mm and 20G x 2¾ ") into an aqueous phase composed of 5 or 10 mL of Milli Q water at 4°C, with subsequent vortexing. The emulsion formed was then sonicated (Branson Digital Sonifier) during 2 minutes at an amplitude of 40 % (300W). The solvent was then evaporated under reduced pressure using a rotary evaporator (Buchi, R-124). The final volume was adjusted, when necessary, in a volumetric flask to 5 or 10 mL, according to the defined concentration.

For nanoprecipitation, BP was solubilized in 1mL of acetone (organic phase) as an organic solvent that is miscible with water. The aqueous phase was composed of the lipids dissolved in 5 or 10 mL Milli Q water, with stirring at 60°C. The organic phase was then injected into the aqueous phase with the help of a 20G needle, the suspension being kept under moderate stirring for 5 minutes and then concentrated to a final volume of 5 or 10 mL in a rotary evaporator to remove the organic solvent and adjust the final drug concentration.

Table 1. Mannosylated (M) and PEGylated nanoparticles composition

Code	Method*	Conc. BP (mg/mL)	Conc. DSPE-PEG-Man (mg/mL)	Conc. DSPE-mPEG (mg/mL)	Ratio DSPE-PEG-Man/DSPE-mPEG
EE 100/0	EE	1.25	1.25	0	100/0
EE 75/25	EE	1.25	0.937	0.313	75/25
EE 50/50	EE	1.25	0.625	0.625	50/50
EE 25/75	EE	1.25	0.313	0.937	25/75
EE 0/100	EE	1.25	0	1.25	0/100
NP 100/0	NP	1.25	1.25	0	100/0
NP 75/25	NP	1.25	0.937	0.313	75/25
NP 50/50	NP	1.25	0.625	0.625	50/50
NP 25/75	NP	1.25	0.313	0.937	25/75
NP 0/100	NP	1.25	0	1.25	0/100

* EE: emulsion-evaporation; NP: nanoprecipitation

2.5 Nanoparticle characterization

2.5.1 Size and zeta potential

Nanoparticles were characterized by their size, polydispersity index (PdI) and zeta potential, measured by dynamic light scattering with a Nano ZS (Malvern instruments, UK) at a 173° scattering angle at 25°C. Samples were diluted 1/20 in water for the size and PdI, or in 1 mM NaCl solution for the zeta potential determination. Measurements were performed in triplicate.

2.5.2 Encapsulation Efficiency (EE) and Drug Loading

To evaluate the encapsulation efficiency and the prodrug loading, nanoparticle suspensions were treated with methanol to extract the prodrug and lipids and further quantify the total BP and DSPE-PEG-Man by HPLC. To separate the free compounds from the nanoparticles, ultracentrifugation was performed at 40.000 rpm (= 109760 g) during 4 h at 4°C (Beckman Coulter Optima LE-80K ultracentrifuge, 70-1Ti rotor). After separation by ultracentrifugation, non-encapsulated BP and DSPE-PEG-Man in supernatant were quantified by HPLC-UV and their amount in nanoparticles was calculated indirectly. Analyzes were performed using an Agilent chromatograph, equipped with an UV detector (785A, Applied Biosystems) coupled to an evaporative light-scattering detector (ELSD, Eurosep, Cergy, France). UV detection was performed at 244 nm wavelength and ELSD detection settings were a nebulization temperature of 35°C and an evaporation temperature of 45°C. The Waters SymmetryShield RP18 column with 5µm particles and 4.6 x 250 mm dimensions was maintained at 10°C with a cooler. The isocratic mobile phase was composed of methanol: Chloroform: Ammonium acetate pH 4,0 (95 : 3 : 2, v : v : v), with addition of triethylamine 25 µL % + acetic acid 30 µL %. The flow rate was 1.0 mL/min. A volume of 30µL of samples was injected and analyzed during 12 min. UV Retention times were 6.5 min and 9.7 min for DSPE-PEG-Man and BP, respectively. The concentration ranges of the calibration curves were 0.1-3 mg/mL for DSPE-PEG-Man and 10-750 µg/mL for BP. UV calibration curve followed a linear model, y=2185x-42.883, R^2=0.9838 (DSPE-PEG-Man) and y=27.359x+54.682, R^2=0.9994 (BP). ELSD Retention times were 6 min and 6.5 min for DSPE-mPEG and DSPE-PEG-NH_2, respectively. The concentration ranges of the calibration curves were 18.7-750 µg/mL for DSPE-mPEG and 18.7-500 µg/mL for DSPE-PEG-NH_2. ELSD detection calibration curves followed a power law model, equations and correlation coefficients were $y = 0.0039x^{1.4907}$, R^2=0.9959 for DSPE-mPEG and $y=0.6532x^{1.4494}$, R^2=0.998 for DSPE-PEG-NH_2. The Encapsulation Efficiency was calculated as a percentage of the ratio of the actual amount of the compound over the initial one. The prodrug loading was determined as a weight percentage of the weight of prodrug encapsulated over the total

weight of nanoparticle compounds (Prodrug + DSPE-PEG-Man + DSPE-mPEG) added to the formulation. Similar calculations were performed for DSPE-PEG-Man.

2.5.3 Lectin Agglutination Test (ConA Test)

The presence of mannose particles on the surface of the nanoparticles was evaluated by the agglutination assay with the Concanavalin A (ConA) lectin. Lectins are proteins that specifically and reversibly interact with carbohydrates, forming precipitates. Among the commonly available lectins, Concanavalin A (ConA) is a tetrameric protein with four binding sites for specific interaction with terminal D-mannose residues (Muller and Schuber, 1989). It is known to bind specifically to molecules containing α-D-mannosyl and α-D-glucosyl residues, this binding being reversible with the use of Methyl α- mannopyranoside (Agrawal and Goldstein, 1965 ; Fontaniella *et al.*, 2004 ; Kitano *et al.,* 2001). It has been used to characterize the presence of sugars on the surface of colloidal carriers, with the binding of the ConA to the nanoparticle surface monitored by dynamic light scattering (DLS). Mannosylated nanoparticles were diluted in ConA buffer (5 mM HEPES, 150 mM NaCl, 1 mM $CaCl_2$, 1 mM $MnCl_2$, pH 6.5) to the final concentration of 100 µg/mL. After 5 minutes of size measurement at 25°C (Zetasizer Nano ZS), 80 µL of a 100 µM ConA in the above described buffer was added to the nanoparticle suspensions (ConA final concentration of 2 µM), the particle size being measured for a further 35 minutes (Ruge *et al.*, 2016). After 40 minutes a solution of Methyl α-D-mannopyranoside (10 mM) was added as a desorption agent of ConA (Pan and Chien, 2003) and the size of the suspension was measured by DLS.

2.6 *In vitro* tests

2.6.1 Cell culture

All *in vitro* cell culture assays were performed on murine macrophage cell line RAW 264.7 obtained from ATCC (USA), cultured in DMEM (Dulbecco's Modified Eagle's Medium) culture medium supplemented with 10 % fetal bovine serum (FBS), penicillin G (10,000 unit/mL) and streptomycin (10 mg/mL), maintained in a humidified incubator at 37°C supplied with 5% CO_2.

2.6.2 Cellular viability

The effect of the formulations on the cellular viability was studied on the RAW 264.7 cell line using the MTT (3-(4,5-dimethylthiazolyl-2)-2,5-diphenyltetrazolium bromide) colorimetric assay. Cells were seeded in 96-well plates at the density of 1 x 10^4 cells/well (24 h Test) and 2 x 10^3 cells/well (48 h Test) and incubated for 24 h until 80 % confluence. PEGylated and mannosylated nanoparticles were added

at the final concentrations 1.9 x 10^{-6} M, 11.7 x 10^{-6} M, 23.3 x 10^{-6} M, 46.7 x 10^{-6} M, 93.4 x 10^{-6} M and 186.8 x 10^{-6} M (eq. Bud), with the corresponding concentrations being equivalent to free budesonide, solubilized in ethanol and then diluted in the culture medium. After 24 hours and 48 hours of incubation, 20 µL of a 5 mg/mL yellow tetrazolium MTT (3-(4,5-dimethylthiazolyl-2)-2,5-diphenyltetrazolium bromide) solution was added to each well and incubated for 1 additional hour or until the formation of the purple formazan crystals, resulting from the MTT reduction by metabolically active cells. Afterwards, the culture medium was replaced by 200 µL of DMSO to dissolve formazan crystals and the absorbance was measured at 570 nm. The percentage of viable cells was calculated as the absorbance ratio between nanoparticle-treated and untreated control cells.

2.6.3 Cytokine release

The anti-inflammatory effect of mannosylated nanoparticles was tested by inducing an inflammatory reaction in RAW 264.7 cells with the help of E. coli lipopolysaccharides (LPS). For the cytokine quantification, RAW 264.7 cells were seeded in 24-well plates at a cellular density of 4 x 10^4 cells/well in culture medium and were incubated for 48 hours until 80 % confluency. Then, the medium was replaced by fresh medium alone or fresh medium with LPS at 1 µg/mL to induce inflammation, and plates were incubated another 3 hours. Afterwards, mannosylated nanoparticles EE 75/25 and free budesonide at four concentrations diluted in culture medium: 10^{-7} M, 10^{-8} M, 10^{-9} M and 10^{-10} M (eq. Bud) were added (Foillard *et al.*, 2016 ; Kis *et al.,* 2006 ; Spoelstra *et al.*, 2002 ; Wang *et al.*, 2013). Culture medium alone was used as negative control and LPS 1 µg/mL as positive control. After 24, 48 and 72 hours of incubation with the treatments, cell supernatants were collected and frozen at -20°C until analysis was performed. Cells were detached and counted. Mouse inflammatory cytokines TNFα, MCP-1, IL-10 and IL-6 were quantified using a Cytometric Beads Array (CBA) detection kit (BD Biosciences, USA). In each test tube, 50 µL of mouse inflammation capture bead suspension was added, completed with either 50 µL of standards solution (20-5000 pg/mL) or 50µL of supernatants samples. Phycoerythrin (PE) detection reagent was added 50 µL to each tube and incubation during 2 h at room temperature was performed. Samples were washed with 1 mL wash buffer provided in the kit and tubes were centrifuged (200 g, 5 min) to recover the pellet. 300 µL of wash buffer was added to resuspend the pellet and samples were quantified with the BD Accuri C6 Cytometer (BD Biosciences, USA). Cytokines results were analyzed with the FACP Array™ Software and were obtained as pg/mL concentrations. All measurements were performed in triplicate.

2.6.4 Nanoparticle uptake

The internalization/uptake of nanoparticles in RAW 264.7 cells was analyzed by Confocal Laser Scanning Microscopy (CLSM) and quantified by Flow Cytometry, using Rhodamine labeled nanoparticles (labeled with 1 % lissamine-rhodamine).

For the microscopic analysis, RAW 264.7 cells were seeded in culture medium in a 6-well plate containing a 0.17 mm diameter coverslip, at a cell density of 4 x 10^4 cells/well (24 h treatment) and 2 x 10^4 cells/well for 48 h), remaining in the incubator for 24 h until reaching 80 % of confluence. After this period, the culture medium was replaced by fresh medium in the control case or medium containing 25 µg/mL BP nanoparticles (PEGylated and mannosylated nanoparticles containing budesonide palmitate), these plates being incubated for another 24 h and 48 h. Observations were performed with a LSM 510 (Zeiss – Meta) confocal microscope equipped Helium-Neon (543 nm, 5 mW) laser and a plan-apochromat 63X objective. Red fluorescence was observed with a long-pass 560 nm emission filter under 543 nm laser illumination.

For flow cytometry measures, cells were seeded in 12-well plates at the density of 4 x 10^4 cells/well and incubated for 24 h until 80 % confluence. PEGylated and mannosylated nanoparticle formulations were added at the final concentration of 25 µg/mL and incubated for 1, 3, 5, 7, 24 and 48 hours, at 4°C and 37°C. Cells were then washed with PBS, centrifuged at 300 g at 4°C for 5 minutes, and resuspended in 200µL PBS (Agnoletti *et al*., 2017 ; Zeng *et al.*, 2014). Samples were analyzed using a flow cytometer (Accuri C6, BD Biosciences, USA) at the excitation and emission wavelengths of 570 and 590 nm, respectively. For the quantification of the fluorescence intensity relative to the entry of the nanoparticles into the cells, the mean fluorescence intensity (MFI) was calculated by the fluorescence ratio between untreated cells (control) and treated cells.

To verify the uptake mechanism of mannosylated nanoparticles was arising from binding to the mannose receptor, an inhibition study was performed with mannan, a known mannose receptor antagonist. Cells were seeded in 12-well plates at the density of 4 x 10^4 cells/well and incubated for 24 h until 80 % confluence, cultured in DMEM culture medium supplemented with FBS and Penicilin-streptomycin. After 24 h, the medium was replaced for a fresh medium DMEM containing 1 % bovine serum albumin (BSA), 25 mM HEPES, 3 mM $CaCl_2$ and mannan 1 %, and the cells were incubated for 2 h. PEGylated and mannosylated nanoparticles were added at the final BP concentration of 25 µg/mL and incubated for 24 and 48 hours at 37°C. DMEM medium was used for negative control (He *et al.*, 2018 ; Sedaghat *et al*., 2016 ; Szolnoky *et al.*, 2001 ; Yeeprae *et al.*, 2006). Flow cytometry experiments were performed as described above.

2.7 Statistical analysis

Results were reported as mean ± standard error of the mean (SEM). Statistical analysis was performed using the GraphPad Prism 7.0 software.

3 RESULTS AND DISCUSSIONS

3.1 Synthesis of Budesonide Palmitate (BP)

The synthesis of budesonide palmitate was readily accomplished, with a yield of 67 % (Figure 1). The reaction was confirmed by nuclear magnetic resonance (^{1}H NMR) at 300 MHz in deuterated chloroform ($CDCl_3$).

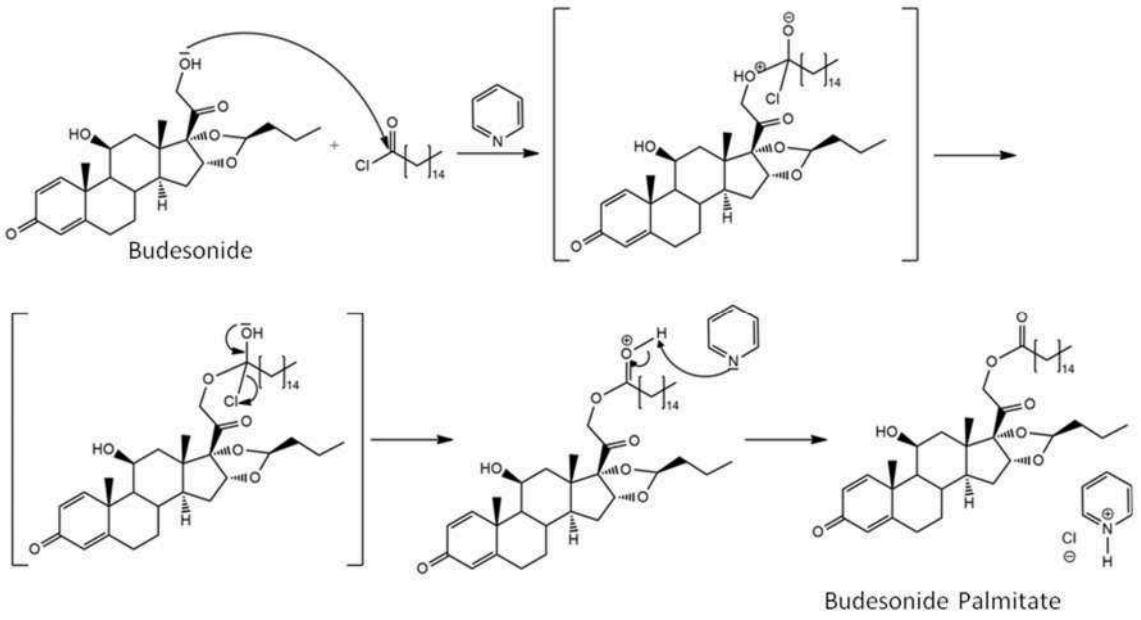

Figure 1. Reaction of esterification of budesonide, resulting in budesonide palmitate.

3.2 Synthesis of DSPE-PEG-Man

The synthesis of DSPE-PEG-Man was successfully performed, with a yield between 50-75 %. Initially, around 80 % of the product was lost owed to the presence of DMSO at the time of the dialysis. Indeed DSPE-PEG-Man was detected in the dialysis liquid, suggesting a membrane pore opening caused by DMSO. After a 10x dilution with water of the synthesis solvent, the yield was improved from 22 % (first

synthesis) to 50-75 %. DSPE-PEG-man NMR analysis exhibited two peaks at δ 7.0-7.2 (MPITC phenyl-H), indicating successful incorporation of DSPE-PEG and mannose in the final product (Figure 2).

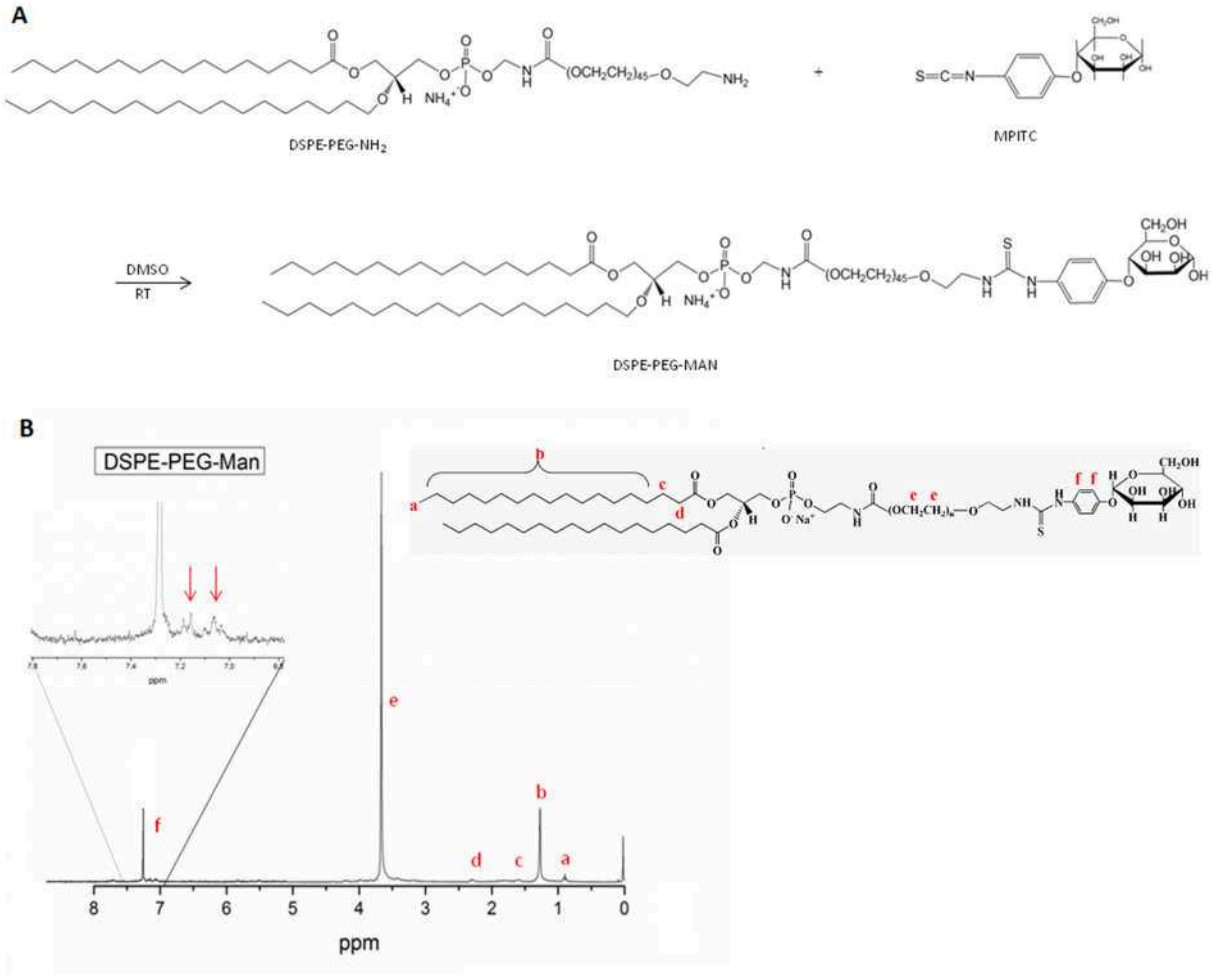

Figure 2. A) DSPE-PEG-Man synthesis and B) ^{1}H RMN spectrum of DSPE-PEG-Man

However, when DSPE-PEG-Man is analyzed by HPLC-ELSD-UV, it is possible to detect and quantify DSPE-PEG-NH_2 by HPLC-ELSD, indicating a small quantity of unreacted DSPE-PEG-NH_2 (around 12 %, n=8). Figure 3A presents a DSPE-PEG-Man chromatogram, analyzed by HPLC-ELSD-UV. In red, DSPE-PEG-Man (UV detector) presents a retention time of 6.5 min, identical to the retention time of DSPE-PEG-NH_2 in black (ELSD detector).

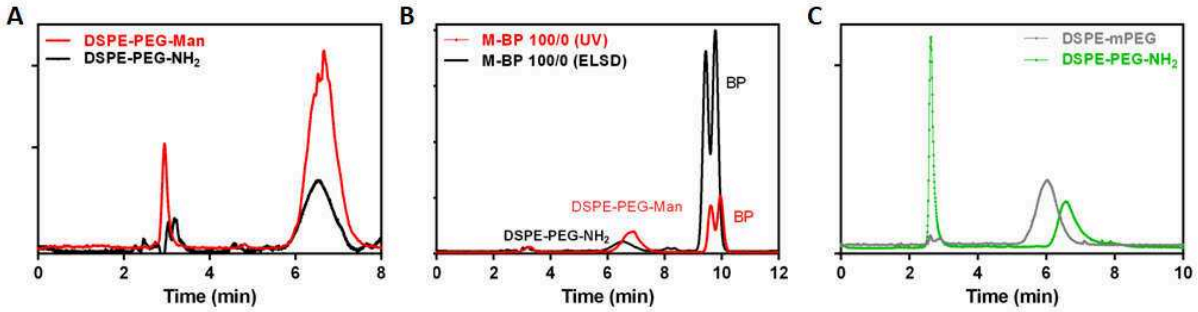

Figure 3. HPLC-ELSD-UV chromatograms of DSPE-PEG-Man and mannosylated formulations. A) DSPE-PEG-Man chromatogram: DSPE-PEG-Man (red, UV detector) and DSPE-PEG-NH_2 (black, ELSD detector); B) mannosylated nanoparticles 100/0 (red: UV detection, and black: ELSD detection); C) ELSD chromatogram, showing the overlap between DSPE-mPEG (gray) and DSPE-PEG-NH_2 (green).

3.3 Nanoparticle characterization and budesonide palmitate loading

Nanoparticles were obtained using various ratios of DSPE-PEG-man/DSPE-mPEG and prepared either by emulsion-evaporation or nanoprecipitation. An initial BP concentration of 1.25 mg/mL was fixed, using the ratio 1/1 for BP/total lipids (PEGylated and Mannosylated). For emulsion-evaporation, small nanoparticles of 180-200 nm were obtained, except for the formulation 100/0 (100 % DSPE-PEG-Man), which showed a hydrodynamic diameter around 400 nm (Figure 4A). For nanoprecipitation, all nanoparticle suspensions display a diameter of 150-200 nm (Figure 4B). On one hand, from 0/100 to 75/25 ratios, PdI remained below 0.2 indicating rather monodisperse suspensions. On the other hand, however, the PdI of 100/0 formulations was around 0.5 suggesting very polydisperse suspensions, independently of the formulation process. This can be explained by the zeta potential values. Indeed, as the amount of mannosylated lipid is increasing the zeta potential increases from -30 mV up to almost 0. This increase arises from the unreacted DSPE-PEG-NH_2 that could not be separated from the DSPE-PEG-Man after synthesis and represents 12 % of lipids (Figure 3B). Since DSPE-PEG-NH_2 is positively charged, as its proportion increases in the formulations, the zeta potential progressively becomes neutral for 100/0 formulations. The neutral zeta potential leads to aggregation since nanoparticles are not electrostatically stabilized anymore explaining large sizes and high polydispersity.

The stability of the nanoparticles stored at 4 °C was monitored for one month by measuring the size, PdI and zeta potential (Figure 4). All formulations were stable until 30 days, except for the 100/0 formulations for the reasons explained above.

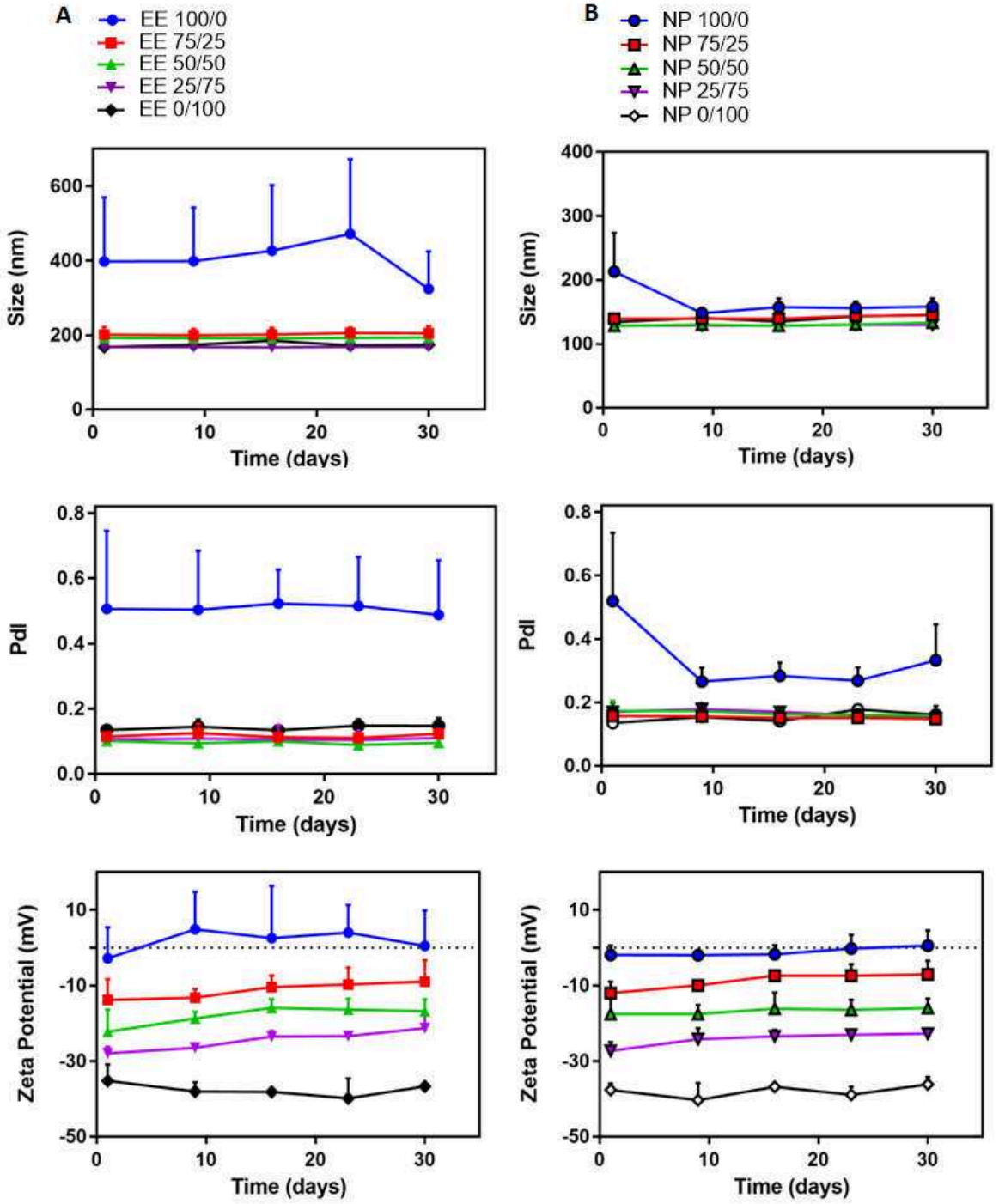

Figure 4. A) Emulsion-Evaporation method: Size, PdI and Z-potential (Z); and B) Nanoprecipitation method: Size, PdI and Z-potential (Z) measurements of the mannosylated nanoparticles at different times after the preparation, by dynamic light scattering (n=3).

The encapsulation efficiency and drug loading of the mannosylated nanoparticles were measured by HPLC-UV and HPLC-ELSD. Encapsulation efficiency was determined by quantifying the amount of DSPE-PEG-Man associated to BP-nanoparticles. After separation by ultracentrifugation, non-encapsulated BP and DSPE-PEG-Man in supernatant were quantified and their amount in nanoparticles was

calculated indirectly (Figure 5A). For emulsion-evaporation or nanoprecipitation, the encapsulation efficiency of BP was ranging from 8 9% up to 107 % with no significant differences proving that all the prodrug is associated to nanoparticles. Results were different for DSPE-PEG-Man encapsulation with variations according to the formulation process. One can observe a rather stable encapsulation efficiency of 27 to 42 % with no obvious trend for nanoprecipitation while for emulsion-evaporation, the encapsulation efficiency increased as the DSPE-PEG-Man ratio increased from 14 % up to 37 %. These differences result from the differences of formulation process: lipids were solubilized with the prodrug for the emulsion-evaporation process, whereas they were solubilized in water for nanoprecipitation. In addition, the partition coefficient of lipids between water and solvent (chloroform or acetone) may differ.

Based on the amounts of encapsulated BP and DSPE-PEG-Man, BP, DSPE-PEG-Man, DSPE-PEG-NH_2 and DSPE-mPEG loadings were calculated (Figure 5B). Nanoparticles prepared by emulsion-evaporation method presented a BP loading from 50 to 57 % (w/w). For nanoprecipitated particles, BP loading varied from 48 to 60 %.

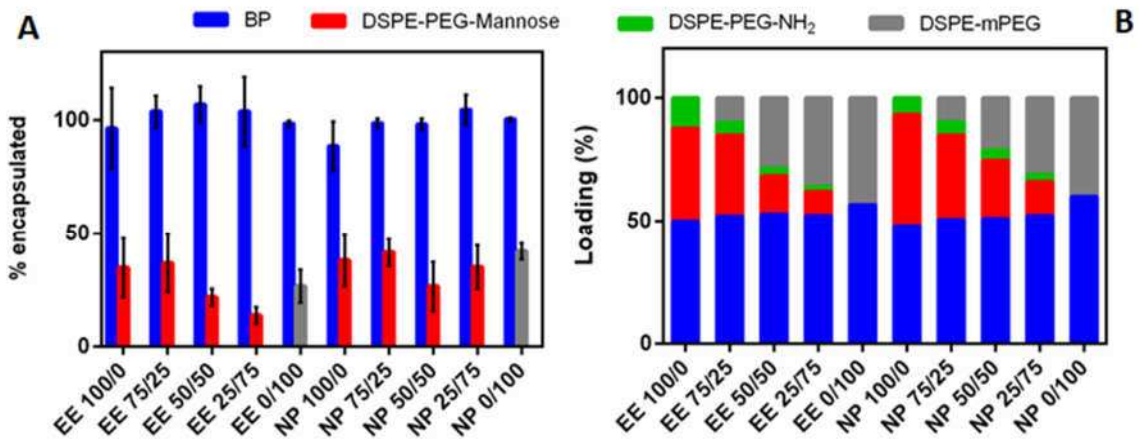

Figure 5. BP (blue) and DSPE-PEG-Man (red) encapsulation efficiency (A) and loading (B), according to preparation method and proportion of components (n=3).

The quantification of DSPE-PEG-NH_2 and DSPE-mPEG was performed by HPLC-ELSD detection method. However, when these compounds are present at the same formulation, as ratios 75/25, 50/50 and 25/75, they showed similar retention times (Figure 3C), making it impossible to separate them. For this reason, we first quantified the amount of unreacted DSPE-PEG-NH_2 present in several synthesis batches of DSPE-PEG-Man, around 12 %. Then, to calculate the compound loading, we use the following data: 1) quantification of DSPE-PEG-Man in each formulation (HPLC-UV); 2) theoretic total lipids in each formulation (1.25 mg/mL); 3) lipid ratio in each formulation; 4) the difference between

theoretic total lipids and quantified DSPE-PEG-Man = other lipids; 5) quantity obtained as other lipids = DSPE-PEG-Meth and/or DSPE-PEG-NH_2, which we calculated each one considering the ratio used and DSPE-PEG-NH_2 as 12 % of dosed DSPE-PEG-Man. Formulations 100/0 (100 % DSPE-PEG-Man) and 0/100 (100% DSPE-mPEG) (Figure 3B), were calculated by direct dosing of DSPE-PEG-NH_2 and DSPE-mPEG, respectively, since these were the only other lipids present.

3.4 Lectin Agglutination Test

Lectin agglutination test was used to verify the presence and biological activity of the mannose ligands on the surface of nanoparticles (Figure 6). On one hand, controls obtained using PEGylated nanoparticles (EE 0/100 and NP 0/100) and amine terminated nanoparticles (EE-NH_2 and NP-NH_2) did not show any change regarding their size distribution in the presence of ConA, indicating no interactions with the protein, for both formulation processes. On the other hand, mannosylated nanoparticles exhibited a size increase when ConA was added. The higher the mannosylated lipid content, the stronger the size increase for both formulation processes. This confirms that the extent of agglomeration depended on the amount of mannose present on nanoparticle surface. When methyl α-D-mannopyranoside was added to compete with mannosylated nanoparticles, aggregation was reversed, and the initial nanoparticle size was recovered as ConA desorbed from nanoparticle surface and interacted with methyl α-D-mannopyranoside.

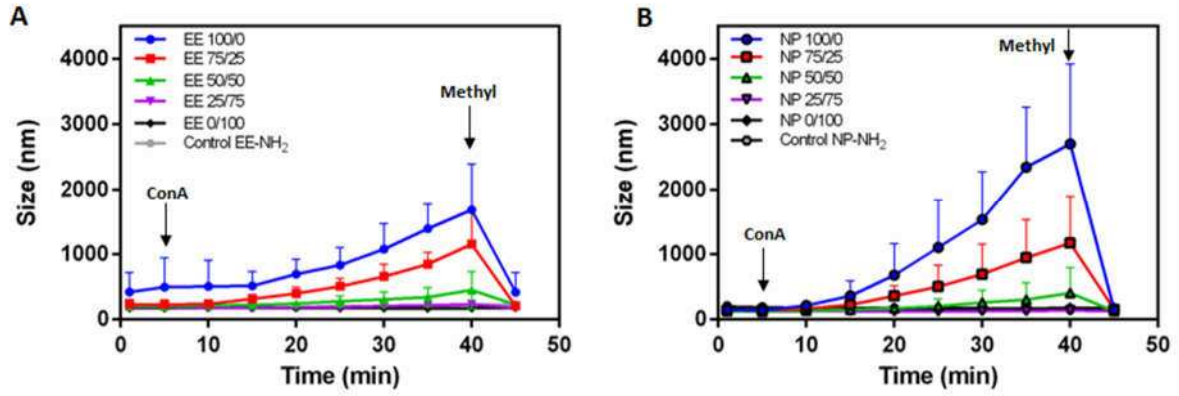

Figure 6. Reaction of mannosylated nanoparticles to the addition of 100 µM ConA (time = 5 min) and 10 mM Methyl α-D-mannopyranoside (time = 40 min) (n = 3). A) Emulsion-Evaporation method; B) Nanoprecipitation method.

For the following experiments, nanoparticles obtained by emulsion-evaporation were selected since they presented a higher BP loading, an important feature for further applications. Nanoparticles obtained with 100/0 Mannosylated lipid ratio were discarded due to their instability.

3.5 *In vitro* tests

3.5.1 Cellular viability

Before conducting targeting experiments, the potential toxicity of mannosylated nanoparticles was evaluated on RAW 264.7 cells using MTT assay. According to ISO guideline for MTT assay, potential cytotoxicity is considered when cell viability decreases below 70 % of the control (International Standard Organization, 2009). A range of concentrations from 1.9 x 10^{-6} M to 186.8 x 10^{-6} M (equivalent budesonide) was tested and compared to controls: budesonide and PEGylated nanoparticles. After 24 hours incubation, mannosylated and PEGylated nanoparticles clearly showed no cytotoxicity up to 186.8 x 10^{-6} M (eq. budesonide), while free budesonide showed cytotoxicity only at the higher concentration (Figure 7A). After 48 hours incubation, EE3 75/25 also demonstrated no cytotoxicity up to 186.8 x 10^{-6} M, whereas a slight cytotoxicity was observed for the other nanoparticles, which showed safety up to 93.4 x 10^{-6} M. Free budesonide presented cytotoxicity that started to be cytotoxic at concentration higher than 50 x 10^{-6} M (Figure 7B) which correlates to previous data demonstrating a relative safety of budesonide versus macrophages at micromolar concentration (Zetterlund *et al.*, 1998). Moreover, this cytotoxicity is not changed by the nanoscale prodrug formulation and might be reduced due to a slow release process by esterases of bud.

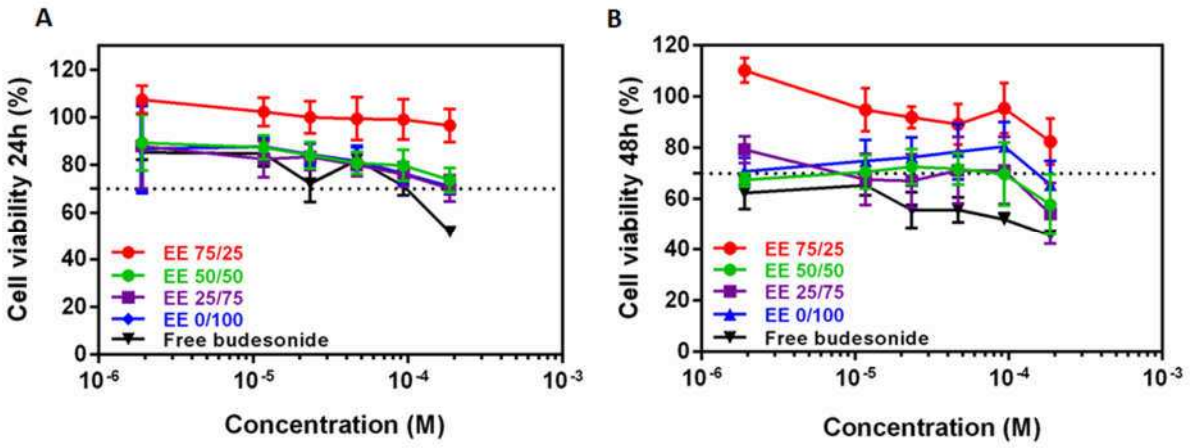

Figure 7. Cell viability of the RAW 264.7 cell line incubated with nanoparticles at different ratios and eq. budesonide, after 24 h (A) and 48 h (B) of treatment (n=3).

Given these results, formulation EE 75/25 (mannosylated nanoparticles) was chosen to test the targeting efficacy and anti-inflammatory effect of the nanoparticles. They do present the highest BP loading and the highest amount of mannose at their surface with good stability.

3.5.2 Nanoparticle uptake

The internalization of the nanoparticles in the RAW 264.7 cell line was studied by means of flow cytometry using nanoparticles labelled with a 1 % lissamine-rhodamine. Tests were performed comparing mannosylated nanoparticles (EE 75/25), PEGylated nanoparticles (EE 0/100) and control (non-treated cells). Figure 8A shows that the internalization of nanoparticles either PEGylated or mannosylated can be already detected after 3 hours. After 24 hours incubation, it is possible to verify a significant greater internalization of mannosylated nanoparticles as compared to PEGylated nanoparticles. This finding holds true also for 48 h incubation. To truly compare the extent of mannosylated nanoparticles and PEGylated nanoparticle uptake, the mean fluorescence intensity increase (MFI, nanoparticle-treated cells versus non-treated cells) was corrected by the fluorescence intensity ratios accordingly. The internalization of the nanoparticles at 37°C was fast, with a clear increase in the fluorescence detected after 1 hour of nanoparticles incubation with the cells (Figure 8B). The fluorescence increased almost four-fold after 7 hours of incubation and it was high after 24 and 48 hours, with a MFI about 4 to 8 times higher than the initial fluorescence. Results reveal also a significant difference between the formulations after 24 hours, with the mannosylated nanoparticles presenting an uptake twice higher than PEGylated nanoparticles. To evaluate if nanoparticle uptake was energy dependent, the same experiment was performed at 4°C (Figure 8C). Results show no uptake at this temperature for either PEGylated or mannosylated nanoparticles confirming the uptake observed at 37°C occurs by an energy-dependent uptake mechanism. The higher uptake of mannosylated nanoparticles as compared to PEGylated nanoparticles support our targeting strategy as already observed by Chono *et al.* (2007) on another macrophage cell line or on peritoneal macrophages and Kupffer cells (Barratt *et al.*, 1986 ; Kawakami *et al.*, 2000).

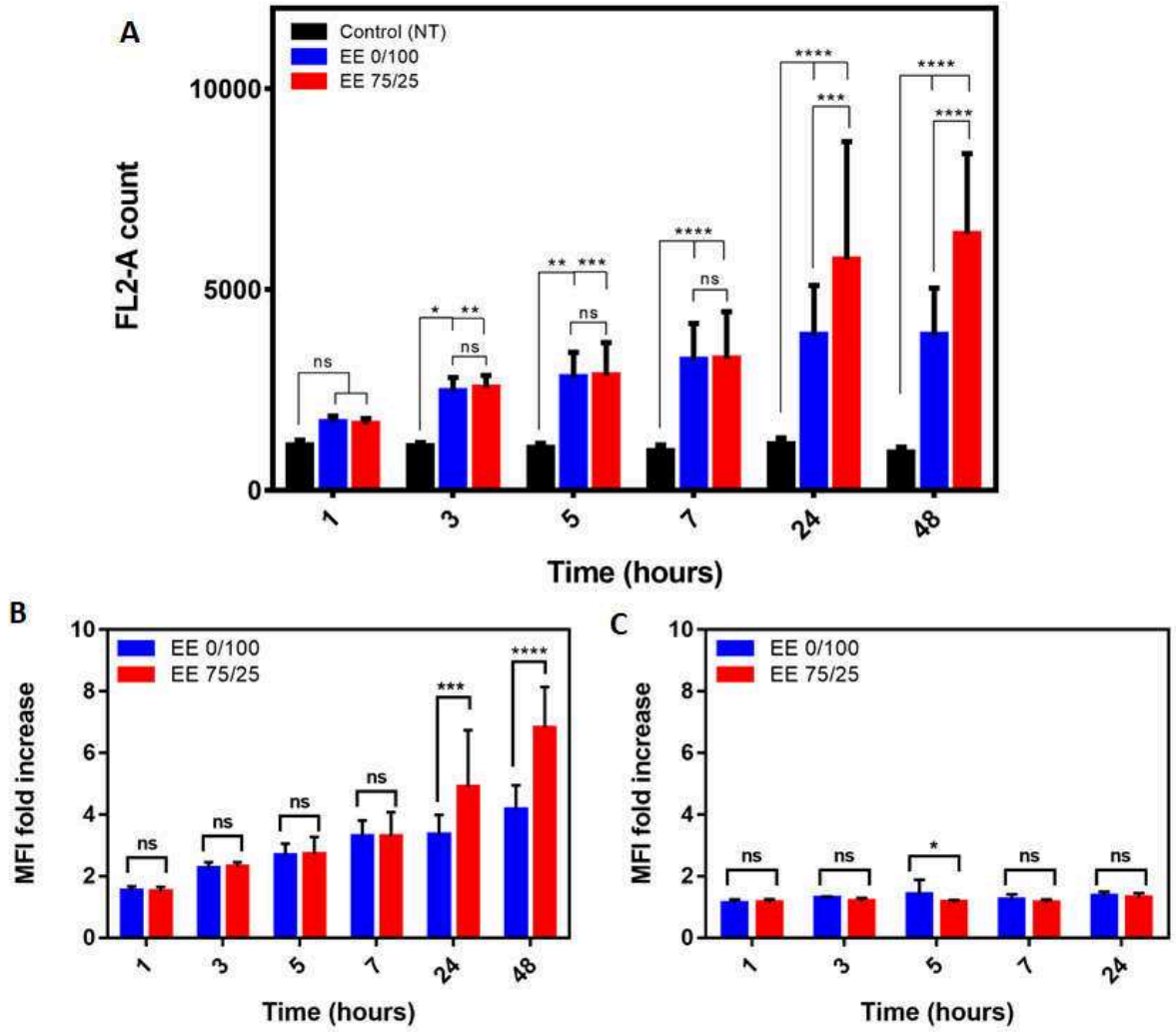

Figure 8. A) Uptake kinetics of PEGylated nanoparticles (EE 0/100, blue) and mannosylated nanoparticles (EE 75/25, red) by RAW 264.7 cells after 1, 3, 5, 7, 24 and 48 h incubation at 37°C, compared to non-treated (NT, gray) cells, evaluated by flow cytometry (FL-2 channel), B) uptake after 1, 3, 5, 7, 24 and 48 h incubation at 37°C, evaluated by the mean fluorescence intensity (MFI) in flow cytometry, and C) uptake after 1, 3, 5, 7, 24 and 48 h incubation at 4°C, evaluated by the mean fluorescence intensity (MFI) in flow cytometry. Statistical analysis was performed with two-way ANOVA followed by Tukey's multiple comparisons test (n=9). ns: not significant, * $p < 0.05$, ** $p < 0.01$, *** $p < 0.001$, **** $p < 0.0001$.

With the aim to confirm a mannose receptor-mediated uptake, a mannan inhibition study was performed, since mannan is a known ligand of the mannose receptor (MR). RAW 264.7 cells were incubated with mannan at 1 mg/mL (+ Mannan) or medium (- Mannan), and then treated with PEGylated or mannosylated nanoparticles (Figure 9). After 24 hours incubation, PEGylated nanoparticles did not show significant differences when the cells were incubated with mannan, while a statistically significant decrease in cellular uptake was observed in the case of mannosylated nanoparticles. Similar results were found after 48 hours incubation. The results suggest that the pre-

incubation of cells with mannan probably leads to the saturation of mannose receptors on cell surface, confirming mannose receptor-mediated uptake of mannosylated nanoparticles. Our results are in agreement with a mannose receptor mediated mechanisms as shown by other (Sedaghat *et al*. 2016).

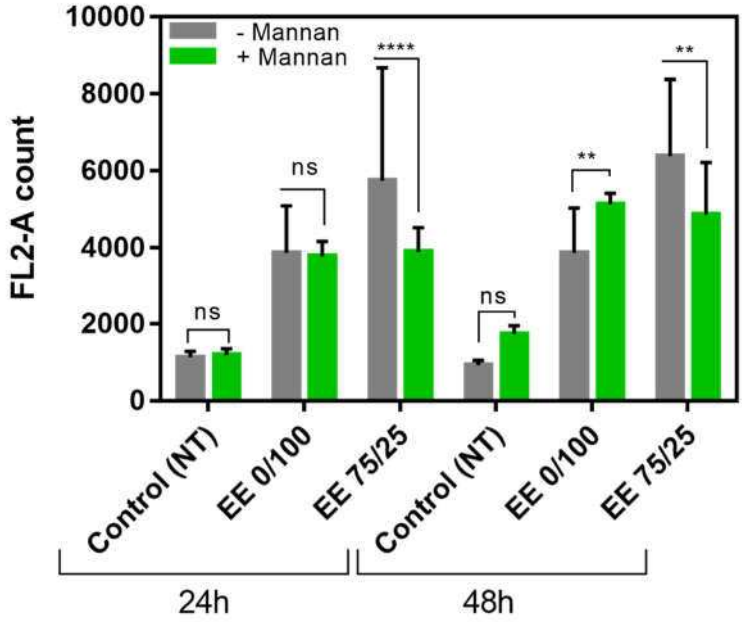

Figure 9. Mannose receptor inhibition test. In green (+ Mannan): RAW 264.7 cells incubated with mannan 1mg/mL, and then treated with PEGylated (EE 0/100) and mannosylated (EE 75/25) nanoparticles, comparing with a control (medium). In gray (- Mannan): cells without mannan incubation, treated with PEGylated and mannosylated nanoparticles. The uptake was analyzed after 24 and 48 h, by flow cytometry. Statistical analysis was performed with two-way ANOVA followed by Sidak's multiple comparisons test. ns: not significant, * $p < 0.05$, ** $p < 0.01$, *** $p < 0.001$, **** $p < 0.0001$.

Finally, confocal laser scanning microscopy (CLSM) experiments were carried out to confirm the internalization of mannosylated and PEGylated nanoparticles. Figure 10 shows the internalization of nanoparticles by RAW 264.7 cells. After 48 hours incubation, it was possible to identify a clearly enhanced uptake for mannosylated nanoparticles (Figure 10B), when compared to PEGylated nanoparticles (Figure 10A). These findings confirm the results previously presented in the uptake study by flow cytometry. In addition, both PEGylated and mannosylated nanoparticles were found in the cytoplasm of macrophages.

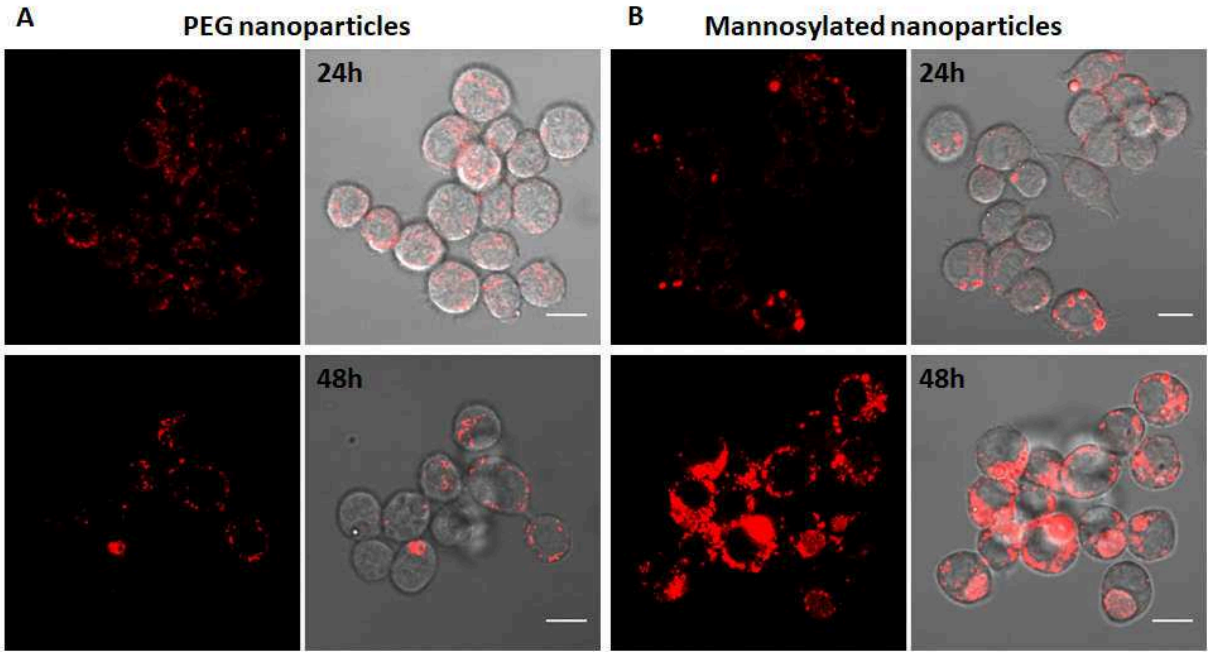

Figure 10. Confocal Microscopy to evaluate the uptake of (A) PEGylated nanoparticles and (B) mannosylated nanoparticles after 24 h and 48 h incubation. Scale bar = 10 µm.

In conclusion, these studies provided the evidence that mannosylated nanoparticles can be used to target delivery to mannose receptors on macrophages. Macrophages have substantial amounts of mannose receptors on the cell surface, suggesting that the delivery occurs by receptor-mediated endocytosis via surface-bound mannose receptors. Indeed, previous studies showing enhanced cellular uptake of mannose-conjugated nanoparticulate systems are available (Asthana *et al.,* 2014 ; Chaubey and Mishra, 2014 ; Jiang *et al.*, 2008 ; Viswanathan *et al.*, 2018).

3.5.3 Cytokine release

Anti-inflammatory activity of mannosylated nanoparticles was evaluated by flow cytometry. The release of pro-inflammatory cytokines (IL-10, IL-6, MCP-1, TNFα) by LPS-activated macrophages RAW 264.7 into the cell culture medium was quantified after their incubation for 24, 48 and 72 hours with mannosylated nanoparticles, free budesonide or controls (Figure 11). Low concentrations of BP (eq. budesonide) from 10^{-10} M to 10^{-7} M were chosen as therapeutically relevant concentrations (Bosch *et al.*, 1993 ; Spoelstra *et al.*, 2002). For MCP-1, no significant reduction was detected for mannosylated nanoparticles and free budesonide until 24 hours, but a significant decrease was observed after 48 hours for both treatments. However, MCP-1 reduction did not persist after 72 hours, except for the more concentrated mannosylated nanoparticles. Concerning TNFα, mannosylated nanoparticles showed a strong and significant reduction only after 72 hours, with no dose-effect observed, meaning that the lower concentration of nanoparticles (10^{-10} M) was sufficient to reach the expected anti-

inflammatory effect. IL-6 and IL-10 cytokines showed similar results, presenting a prolonged activity from 24 hours up to 72 hours.

This late anti-inflammatory effect observed in MCP-1 and TNFα could be explained by a difference of kinetics between cytokine secretion and nanoparticles internalization. Cytokines are regulators of host responses to inflammation, which some cytokines act to make disease worse (proinflammatory), whereas others serve to reduce inflammation and promote healing (anti-inflammatory). MCP-1 (chemokine), TNFα and IL-6 are considered pro-inflammatory modulators, participating in acute and chronic inflammation, while IL-10 is considered an anti-inflammatory modulator (Dinarello, 2000 ; Hanada and Yoshimura, 2002). With this study, it is possible to conclude that the nanoparticle mannosylation and use of budesonide palmitate does not affect the anti-inflammatory activity of budesonide.

However, it is also important to emphasize two biases that must be considered in the analysis, which could explain unexpected results: first, free budesonide and mannosylated nanoparticles effect was evaluated with different cells at different passages; and second, because a technical issue, mannosylated nanoparticles CBA analysis was performed using a different cytometer. For these reasons, anti-inflammatory study will be repeated respecting the same conditions for all formulations, and with PEGylated nanoparticles (EE 0/100) inclusion as control to compare with free budesonide and mannosylated nanoparticles (EE 75/25).

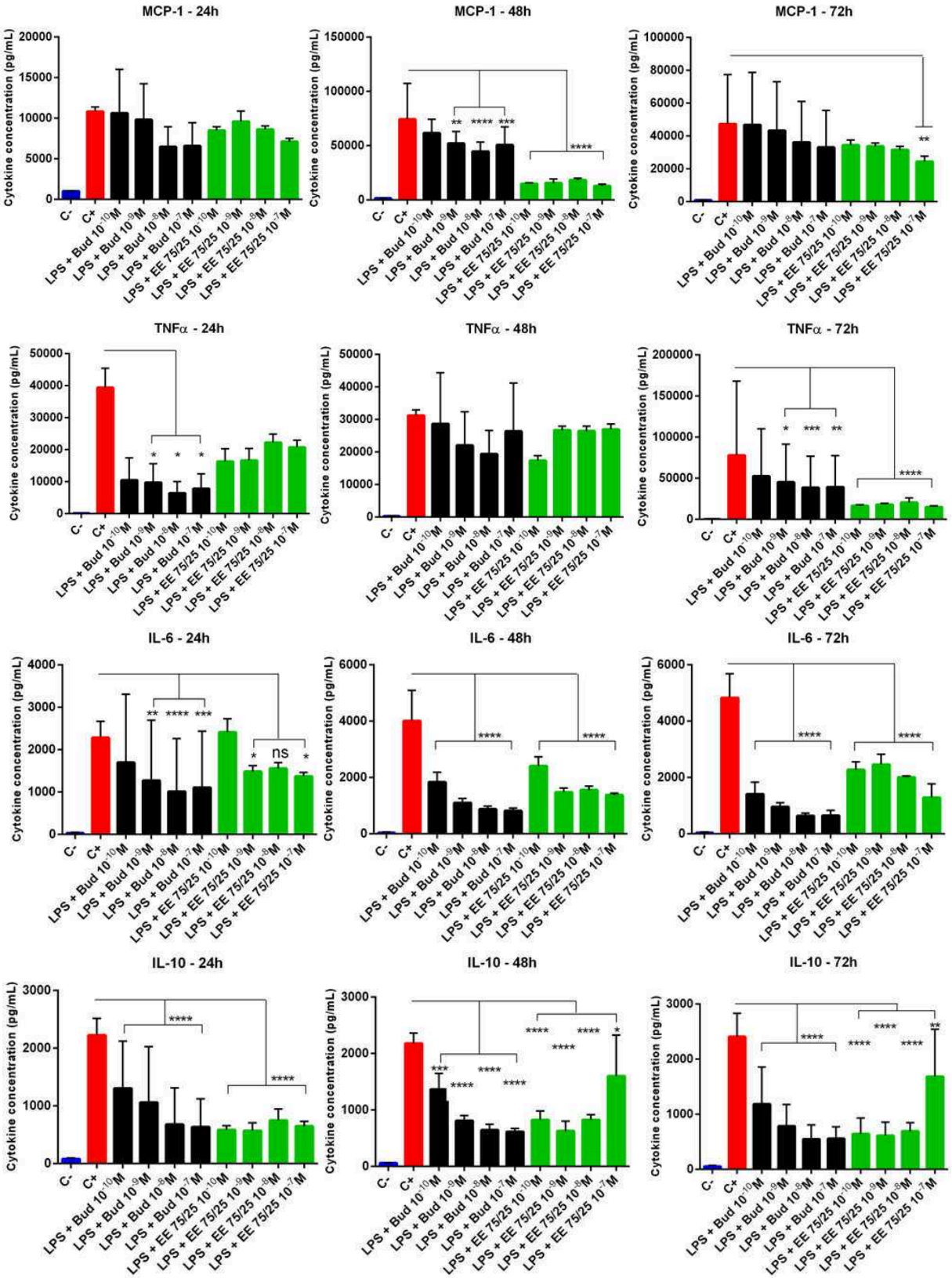

Figure 11. Quantification of cytokine release by Raw 264.7 macrophages without induction by LPS (C-, blue), with induction by LPS 1 µg/mL (C+, red), after treatment for 24, 48 and 72 hours with Budesonide (eq. BP) (dark) and mannosylated nanoparticles (green). The results are represented on average ± SD (n = 3). Statistical analysis was performed with a one-factor ANOVA followed by a Tukey post-test. ns = not significant, * $p < 0.1$, ** $p < 0.01$, *** $p < 0.001$, *** $p < 0.0001$.

4 CONCLUSION

The present study demonstrates the possibility of mannosylated nanoparticles of budesonide palmitate to improve macrophage targeting and uptake. We have synthesized a lipophilic derivative of budesonide, budesonide palmitate (BP), and a mannosylated lipid, DSPE-PEG-Man. Two formulation processes (emulsion-evaporation and nanoprecipitation) and different ratios of lipids DSPE-PEG-Man/DSPE-mPEG were compared to produce mannosylated nanoparticles (ratios 100/0, 75/25, 50/50, 25/75) and PEGylated nanoparticles (ratio 0/100). Only mannosylated nanoparticles prepared with ratio 100/0 presented undesired instability characteristics, probably because the zeta potential around zero. All other formulations, produced by both techniques, resulted in stable nanoparticles of about 200 nm, low PdI below 0.2, negative zeta potential from -10 to -30 mV, and excellent encapsulation efficiency and BP loading. The presence and biological activity of mannose ligands on nanoparticles surface was confirmed by lectin agglutination test. *In vitro* studies demonstrated the safety of mannosylated nanoparticles, as well as the nanoparticle uptake characteristics, showing that surface mannosylation may be an interesting way to target alveolar macrophages and improve drug selectivity. Cytokine release study confirmed their anti-inflammatory activity even in very low concentrations.

5 ACKNOWLEDGMENTS

Ludmila Pinheiro do Nascimento was supported by a PhD scholarship from CNPq - National Council of Scientific and Technologic Development (Brazil) #233180/2014-1. Authors would like to acknowledge the help of S. Denis for cell culture and V. Nicolas (MIPSIT, SFR-UMS-IPSIT, Univ. Paris-Sud, Université Paris-Saclay) for confocal microscopy. Institut Galien Paris-Sud is a member of the Laboratory of Excellence LERMIT supported by a grant from ANR (ANR-10-LABX-33). The authors would like to acknowledge the financial support provided by COST-European Cooperation in Science and Technology, to the COST Action MP1404: Simulation and pharmaceutical technologies for advanced patient-tailored inhaled medicines (Siminhale).

6 REFERENCES

Agnoletti M., Bohr A., Thanki K., Wan F., Zeng X., Boetker J. P., Yang M., Foged C. « Inhalable siRNA-loaded nano-embedded microparticles engineered using microfluidics and spray drying ». *Eur. J. Pharm. Biopharm.* [En ligne]. 1 novembre 2017. Vol. 120, p. 9-21. Disponible sur : < http://dx.doi.org/10.1016/J.EJPB.2017.08.001 > (consulté le 14 mars 2018)

Agrawal B. B., Goldstein I. J. « Specific binding of concanavalin A to cross-linked dextran gels. » *Biochem. J.* [En ligne]. 1965. Vol. 96, n°3, p. 23c-25c. Disponible sur : < http://www.pubmedcentral.nih.gov/articlerender.fcgi?artid=1207236&tool=pmcentrez&rendertype=abstract >

Asthana G. S., Asthana A., Kohli D. V., Vyas S. P. « Mannosylated Chitosan Nanoparticles for Delivery of Antisense Oligonucleotides for Macrophage Targeting ». *Biomed Res. Int.* [En ligne]. 2014. p. 1-17. Disponible sur : < http://dx.doi.org/10.1155/2014/526391 >

Axelsson, B. I., Brattsand, R. L., Dahlbäck, C. M. O., Källström, L. A., Trofast, J. W. « Brevet EP0170642A2 - Liposomes containing steroid esters - budesonide palmitate », 1986.

Barratt G., Tenu J., Yapo A., Petit J. « Preparation and characterisation of liposomes containing mannosylated phospholipids capable of targetting drugs to macrophages ». *Biochim. Biopttvsica Acta*. 1986. Vol. 862, p. 153-164.

Bosch J. M. M. Van den, Westermann C. J. J., Aumann J., Edsbäcker S., Tönnesson M., Selroos O. « Relationship between lung tissue and blood plasma concentrations of inhaled budesonide ». *Biopharm. Drug Dispos.* [En ligne]. 1993. Vol. 14, n°5, p. 455-459. Disponible sur : < http://dx.doi.org/https://doi.org/10.1002/bdd.2510140511 >

Chaubey P., Mishra B. « Mannose-conjugated chitosan nanoparticles loaded with rifampicin for the treatment of visceral leishmaniasis ». *Carbohydr. Polym.* [En ligne]. 30 janvier 2014. Vol. 101, p. 1101-1108. Disponible sur : < http://dx.doi.org/10.1016/J.CARBPOL.2013.10.044 > (consulté le 4 février 2019)

Chen D. « Targeted siRNA Delivery Methods for RNAi- Based Therapies ». *Electron. Thesis Diss. Repos. Pap. 1245.* [En ligne]. 2013. n°May,. Disponible sur : < http://ir.lib.uwo.ca/etd >

Cho Y. J., Sin D. D. « Inhaled Corticosteroids and Fractures in COPD: Can We Finally Put This to Bed? ». *Chest* [En ligne]. 2018. Vol. 153, n°2, p. 293-294. Disponible sur : < http://dx.doi.org/10.1016/j.chest.2017.08.027 >

Chono S., Tanino T., Seki T., Morimoto K. « Uptake characteristics of liposomes by rat alveolar macrophages: influence of particle size and surface mannose modification ». *J. Pharm. Pharmacol.* [En ligne]. 2007. Vol. 59, n°1, p. 75-80. Disponible sur : < http://dx.doi.org/10.1211/jpp.59.1.0010 >

Corry D. B., Kheradmand F., Luong A., Pandit L. « Immunological Mechanisms of Airway Diseases and Pathways to Therapy ». *Clin. Immunol.* [En ligne]. 1 janvier 2019. p. 571-584.e1. Disponible sur : < http://dx.doi.org/10.1016/B978-0-7020-6896-6.00041-7 > (consulté le 11 juillet 2018)

Derendorf H. « Corticosteroid pharmacokinetic/pharmacodynamic parameters and their relationship to safety and efficacy ». *Allergy Asthma Proc.* 2005. Vol. 26, n°5, p. 327-335.

Derendorf H. « Pharmacokinetic and pharmacodynamic properties of inhaled ciclesonide ». *J. Clin. Pharmacol.* [En ligne]. 2007. Vol. 47, n°6, p. 782-789. Disponible sur : <

http://dx.doi.org/10.1177/0091270007299763 >

Dinarello C. A. « Proinflammatory cytokines ». *Chest* [En ligne]. 2000. Vol. 118, n°2, p. 503-508. Disponible sur : < http://dx.doi.org/10.1378/chest.118.2.503 >

Edsbäcker S., Brattsand R. « Budesonide fatty-acid esterification: a novel mechanism prolonging binding to airway tissue. Review of available data ». *Ann. Allergy, Asthma Immunol.* [En ligne]. 1 juin 2002. Vol. 88, n°6, p. 609-616. Disponible sur : < http://dx.doi.org/10.1016/S1081-1206(10)61893-5 > (consulté le 11 octobre 2017)

Finney L., Berry M., Singanayagam A., Elkin S. L., Johnston S. L., Mallia P. « Inhaled corticosteroids and pneumonia in chronic obstructive pulmonary disease ». *Lancet Respir. Med.* [En ligne]. 1 novembre 2014. Vol. 2, n°11, p. 919-932. Disponible sur : < http://dx.doi.org/10.1016/S2213-2600(14)70169-9 > (consulté le 24 octobre 2018)

Foillard S., Russier J., Seifert C., Dumortier H., Doris E. « Carbon nanotube-mediated delivery of budesonide to macrophages ». *RSC Adv.* [En ligne]. 2016. Vol. 6, n°58, p. 53282-53287. Disponible sur : < http://dx.doi.org/10.1039/C6RA09809F >

Fontaniella B., Millanes A.-M., Vicente C., Legaz M.-E. « Concanavalin A binds to a mannose-containing ligand in the cell wall of some lichen phycobionts. » *Plant Physiol. Biochem. PPB / Société Fr. Physiol. végétale* [En ligne]. décembre 2004. Vol. 42, n°10, p. 773-9. Disponible sur : < http://dx.doi.org/10.1016/j.plaphy.2004.09.003 > (consulté le 5 avril 2016)

Forum of International Respiratory Societies. *The Global Impact of Respiratory Disease* [En ligne]. [s.l.] : [s.n.], 2017. 1-43 p. Disponible sur : < http://www.who.int/gard/publications/The_Global_Impact_of_Respiratory_Disease.pdf >ISBN : 9781849840873.

Fromer L., Bhatia R. « Diagnosing and treating COPD: understanding the challenges and finding solutions ». *Int. J. Gen. Med.* [En ligne]. 2011. Vol. 4, p. 729-739. Disponible sur : < http://dx.doi.org/10.2147/IJGM.S21387 >

GINA. « GLOBAL STRATEGY FOR Global Strategy for Asthma Management and Prevention ». 2018.

GOLD. « Pocket guide to COPD diagnosis, management and prevention: a guide for health care professionals ». *Glob. Initiat. Chronic Obstr. Lung Dis. Inc* [En ligne]. 2018. Vol. 1, n°1, p. 3-14. Disponible sur : < http://dx.doi.org/http://dx.doi.org/10.1164/rccm.201701-0218PP >

Gonzalez A. V., Coulombe J., Ernst P., Suissa S. « Long-term Use of Inhaled Corticosteroids in COPD and the Risk of Fracture ». *Chest* [En ligne]. 1 février 2018. Vol. 153, n°2, p. 321-328. Disponible sur : < http://dx.doi.org/10.1016/J.CHEST.2017.07.002 > (consulté le 18 septembre 2018)

Hanada T., Yoshimura A. « Regulation of cytokine signaling and inflammation ». *Cytokine Growth Factor Rev.* [En ligne]. 2002. Vol. 13, n°4-5, p. 413-421. Disponible sur : < http://dx.doi.org/10.1016/S1359-6101(02)00026-6 >

He H., Yuan Q., Bie J., Wallace R. L., Yannie P. J., Wang J., Lancina M. G., Zolotarskaya O. Y., Korzun W., Yang H., Ghosh S. « Development of mannose functionalized dendrimeric nanoparticles for targeted delivery to macrophages: use of this platform to modulate atherosclerosis ». *Transl. Res.* [En ligne]. 2018. Vol. 193, p. 13-30. Disponible sur : < http://dx.doi.org/10.1016/j.trsl.2017.10.008 >

Heffler E., Madeira L. N. G., Ferrando M., Puggioni F., Racca F., Malvezzi L., Passalacqua G., Canonica G. W. « Inhaled Corticosteroids Safety and Adverse Effects in Patients with Asthma ». *J. Allergy Clin.*

Immunol. Pract. [En ligne]. 1 mai 2018. Vol. 6, n°3, p. 776-781. Disponible sur : < http://dx.doi.org/10.1016/J.JAIP.2018.01.025 > (consulté le 29 janvier 2019)

International Standard Organization. *ISO 10993-5 - Part 5: Tests for in vitro cytotoxicity*. [s.l.] : [s.n.], 2009. 1-34 p.ISBN : 9782832202937.

Jiang H.-L., Kang M. L., Quan J.-S., Kang S. G., Akaike T., Yoo H. S., Cho C.-S. « The potential of mannosylated chitosan microspheres to target macrophage mannose receptors in an adjuvant-delivery system for intranasal immunization ». *Biomaterials* [En ligne]. 2008. Vol. 29, n°12, p. 1931-1939. Disponible sur : < http://dx.doi.org/10.1016/j.biomaterials.2007.12.025 >

Kawakami S., Wong J., Sato A., Hattori Y., Yamashita F., Hashida M. « Biodistribution characteristics of mannosylated, fucosylated, and galactosylated liposomes in mice ». *Biochim. Biophys. Acta - Gen. Subj.* [En ligne]. 15 décembre 2000. Vol. 1524, n°2-3, p. 258-265. Disponible sur : < http://dx.doi.org/10.1016/S0304-4165(00)00163-X > (consulté le 3 février 2019)

Kim N., Jiang D., Jacobi A. M., Lennox K. A., Rose S. D., Behlke M. A., Salem A. K. « Synthesis and characterization of mannosylated pegylated polyethylenimine as a carrier for siRNA ». *Int. J. Pharm.* [En ligne]. 2012. Vol. 427, n°1, p. 123-133. Disponible sur : < http://dx.doi.org/10.1016/j.ijpharm.2011.08.014 >

Kis K., Bodai L., Polyanka H., Eder K., Pivarcsi A., Duda E., Soos G., Bata-Csorgo Z., Kemeny L. « Budesonide, but not tacrolimus, affects the immune functions of normal human keratinocytes ». *Int. Immunopharmacol.* [En ligne]. 1 mars 2006. Vol. 6, n°3, p. 358-368. Disponible sur : < http://dx.doi.org/10.1016/J.INTIMP.2005.08.022 > (consulté le 23 janvier 2018)

Kitano H., Ishino Y., Yabe K. « Dehydration effect on the recognition of amphiphiles with many pendent mannose residues by Concanavalin A ». *Langmuir* [En ligne]. 2001. Vol. 17, n°8, p. 2312-2316. Disponible sur : < http://dx.doi.org/10.1021/la000910u >

Lorscheider M., Tsapis N., Ur-Rehman M., Gaudin F., Stolfa I., Abreu S., Mura S., Chaminade P., Espeli M., Fattal E. « Dexamethasone palmitate nanoparticles: An efficient treatment for rheumatoid arthritis ». *J. Control. Release* [En ligne]. 2019. Vol. 296, n°28 February 2019, p. 179-189. Disponible sur : < http://dx.doi.org/10.1016/J.JCONREL.2019.01.015 >

Muller C. D., Schuber F. « Neo-mannosylated liposomes: Synthesis and interaction with mouse Kupffer cells and resident peritoneal macrophages ». *Biochim. Biophys. Acta - Biomembr.* [En ligne]. novembre 1989. Vol. 986, n°1, p. 97-105. Disponible sur : < http://dx.doi.org/10.1016/0005-2736(89)90277-0 > (consulté le 1 juin 2016)

Pan L.-C., Chien C.-C. « A novel application of thermo-responsive polymer to affinity precipitation of polysaccharide ». *J. Biochem. Biophys. Methods* [En ligne]. janvier 2003. Vol. 55, n°1, p. 87-94. Disponible sur : < http://dx.doi.org/10.1016/S0165-022X(02)00180-X > (consulté le 2 juin 2016)

Pappas K., Papaioannou A. I., Kostikas K., Tzanakis N. « The role of macrophages in obstructive airways disease: Chronic obstructive pulmonary disease and asthma ». *Cytokine* [En ligne]. 2013. Vol. 64, n°3, p. 613-625. Disponible sur : < http://dx.doi.org/10.1016/j.cyto.2013.09.010 >

Ruge C. A., Hillaireau H., Grabowski N., Beck-Broichsitter M., Cañadas O., Tsapis N., Casals C., Nicolas J., Fattal E. « Pulmonary Surfactant Protein A-Mediated Enrichment of Surface-Decorated Polymeric Nanoparticles in Alveolar Macrophages ». *Mol. Pharm.* [En ligne]. 2016. Vol. 13, n°12, p. 4168-4178. Disponible sur : < http://dx.doi.org/10.1021/acs.molpharmaceut.6b00773 >

Sedaghat B., Stephenson R. J., Giddam A. K., Eskandari S., Apte S. H., Pattinson D. J., Doolan D. L., Toth

I. « Synthesis of Mannosylated Lipopeptides with Receptor Targeting Properties ». *Bioconjug. Chem.* [En ligne]. 2016. Vol. 27, n°3, p. 533-548. Disponible sur : < http://dx.doi.org/10.1021/acs.bioconjchem.5b00547 >

Sneeboer M. M. S., Hutten B. A., Majoor C. J., Bel E. H. D., Kamphuisen P. W. « Oral and inhaled corticosteroid use and risk of recurrent pulmonary embolism ». *Thromb. Res.* [En ligne]. 1 avril 2016. Vol. 140, p. 46-50. Disponible sur : < http://dx.doi.org/10.1016/J.THROMRES.2016.02.010 > (consulté le 25 octobre 2018)

Spantideas N., Drosou E., Bougea A., Assimakopoulos D. « Inhaled Corticosteroids and Voice Problems. What Is New? ». *J. Voice* [En ligne]. 1 mai 2017. Vol. 31, n°3, p. 384.e1-384.e7. Disponible sur : < http://dx.doi.org/10.1016/J.JVOICE.2016.09.002 > (consulté le 24 octobre 2018)

Spies C. M., Strehl C., Van der Goes M. C., Bijlsma J. W. J., Buttgereit F. « Glucocorticoids ». *Best Pract. Res. Clin. Rheumatol.* [En ligne]. 1 décembre 2011. Vol. 25, n°6, p. 891-900. Disponible sur : < http://dx.doi.org/10.1016/J.BERH.2011.11.002 > (consulté le 26 octobre 2018)

Spoelstra F. M., Postma D. S., Hovenga H., Noordhoek J. A., Kauffman H. F. « Additive anti-inflammatory effect of formoterol and budesonide on human lung fibroblasts ». *Thorax* [En ligne]. 2002. Vol. 57, n°3, p. 237-241. Disponible sur : < http://dx.doi.org/10.1136/thorax.57.3.237 >

Szolnoky G., Bata-Csörgö Z., Kenderessy A. S., Kiss M., Pivarcsi A., Novák Z., Newman K. N., Michel G., Ruzicka T., Maródi L., Dobozy A., Kemény L. « A mannose-binding receptor is expressed on human keratinocytes and mediates killing of Candida albicans ». *J. Invest. Dermatol.* [En ligne]. 2001. Vol. 117, n°2, p. 205-213. Disponible sur : < http://dx.doi.org/10.1046/j.1523-1747.2001.14071.x >

Viswanathan V., Mehta H., Pharande R., Bannalikar A., Gupta P., Gupta U., Mukne A. « Mannosylated gelatin nanoparticles of licorice for use in tuberculosis: Formulation, in vitro evaluation, in vitro cell uptake, in vivo pharmacokinetics and in vivo anti-tubercular efficacy ». *J. Drug Deliv. Sci. Technol.* [En ligne]. 1 juin 2018. Vol. 45, p. 255-263. Disponible sur : < http://dx.doi.org/10.1016/J.JDDST.2018.01.017 > (consulté le 4 février 2019)

Wang C., Liu P., Zhuang Y., Li P., Jiang B., Pan H., Liu L., Cai L., Ma Y. « Lymphatic-targeted cationic liposomes: A robust vaccine adjuvant for promoting long-term immunological memory ». *Vaccine*. 2014. Vol. 32, p. 5475-5483.

Wang X., Nelson A., Patil A., Sato T., Kanaji N., Nakanishi M., Michalski J., Farid M., Basma H., Miller-Larsson A., Weislander E., Muller K.-C., Holz O., Magnussen H., Rabe K., Liu X., Rennard S. « Anti-inflammatory effects of budesonide in human lung fibroblasts are independent of HDAC2 ». *Am. J. Respir. Crit. Care Med.* [En ligne]. 2013. Vol. 6, p. 109-119. Disponible sur : < http://www.embase.com/search/results?subaction=viewrecord&from=export&id=L70846499%5Cnhttp://ajrccm.atsjournals.org/cgi/reprint/183/1_MeetingAbstracts/A2135?sid=a5c0f1e8-420b-48f2-b77e-4c78a826a66a%5Cnhttp://sfx.library.uu.nl/utrecht?sid=EMBASE&issn=10734 >

Wijagkanalan W., Kawakami S., Takenaga M., Igarashi R., Yamashita F., Hashida M. « Efficient targeting to alveolar macrophages by intratracheal administration of mannosylated liposomes in rats. » *J. Control. release* [En ligne]. 22 janvier 2008. Vol. 125, n°2, p. 121-30. Disponible sur : < http://dx.doi.org/10.1016/j.jconrel.2007.10.011 > (consulté le 12 avril 2016)

Yeeprae W., Kawakami S., Yamashita F., Hashida M. « Effect of mannose density on mannose receptor-mediated cellular uptake of mannosylated O/W emulsions by macrophages ». *J. Control. Release* [En ligne]. 2006. Vol. 114, n°2, p. 193-201. Disponible sur : < http://dx.doi.org/10.1016/j.jconrel.2006.04.010 >

Zeng X., Morgenstern R., Nyström A. M. « Nanoparticle-directed sub-cellular localization of doxorubicin and the sensitization breast cancer cells by circumventing GST-Mediated drug resistance ». *Biomaterials* [En ligne]. 1 janvier 2014. Vol. 35, n°4, p. 1227-1239. Disponible sur : < http://dx.doi.org/10.1016/J.BIOMATERIALS.2013.10.042 > (consulté le 13 mars 2018)

Zetterlund A., Larsson P. H., Müller-Suur C., Palmberg L., Larsson K. « Budesonide but not terbutaline decreases phagocytosis in alveolar macrophages ». *Respir. Med.* [En ligne]. 1 février 1998. Vol. 92, n°2, p. 162-166. Disponible sur : < http://dx.doi.org/10.1016/S0954-6111(98)90089-0 > (consulté le 13 octobre 2017)

CONCLUSION ET PERSPECTIVES

Conclusion et perspectives

Ce travail de thèse nous a permis de démontrer l'importance de l'élaboration de nouvelles stratégies pour la vectorisation de substances actives utilisées dans le traitement de l'asthme et de la BPCO. Nous avons d'abord synthétisé une prodrogue de budésonide, le palmitate de budésonide, augmentant ainsi le caractère hydrophobe de cette molécule et, par conséquent, son temps de résidence dans les poumons. Deux formulations différentes de nanoparticules contenant la prodrogue ont été développées, l'une recouverte de polyéthylène glycol (PEGylée) et l'autre de molécules de mannose (mannosylée).

Dans le premier chapitre, les nanoparticules PEGylées ont été formulées pour faciliter leur pénétration à travers la couche de mucus présente dans les voies respiratoires et améliorer le ciblage des macrophages alvéolaires. De plus, nous avons développé des microparticules Troyennes, dans lesquelles les nanoparticules ont été encapsulées. Cette stratégie permet de formuler des microparticules de taille adéquate pour le dépôt pulmonaire dans les régions les plus profondes du poumon, tout en empêchant les nanoparticules d'être exhalées en raison de leur taille réduite. Les études *in vitro* et *in vivo* ont démontré que les microparticules ont un diamètre aérodynamique approprié pour le dépôt dans la région alvéolaire et une biodistribution qui permet la rétention du budésonide et de la prodrogue dans les poumons.

Dans le deuxième chapitre, des nanoparticules mannosylées ont été formulées pour encore améliorer le ciblage des macrophages alvéolaires, cellules clés du processus inflammatoire. Les résultats *in vitro* ont confirmé la présence du mannose à la surface des nanoparticules et l'augmentation de l'internalisation cellulaire des nanoparticules mannosylées par rapport aux nanoparticules PEGylées.

Le budésonide est un glucocorticoïde couramment utilisé pour le traitement des maladies respiratoires notamment par voie inhalée. Cette dernière voie offre une meilleure biodisponibilité et une action plus ciblée au niveau du site d'action. Le budésonide présente cependant des effets indésirables tels que l'obésité, le glaucome, l'ostéoporose, ou induit un déficit de croissance chez l'enfant (Kiri *et al.*, 2009; Finney *et al.*, 2014; Sneeboer *et al.*, 2016; Spantideas *et al.*, 2017; Cho and Sin, 2018; Gonzalez *et al.*, 2018; Heffler *et al.*, 2018). Ces effets indésirables pourraient être encore réduits par une diminution des doses administrées tout en maintenant une bonne efficacité *via* un meilleur ciblage du budésonide, notamment vers les macrophages alvéolaires, cellules clés du processus inflammatoire. Les difficultés d'utilisation correcte des dispositifs d'inhalation peuvent également être un facteur de

perte d'efficacité (Murphy, 2010; Price *et al.*, 2013; Chorão, Pereira and Fonseca, 2014; Lavorini, Mannini and Chellini, 2015; Sanchis *et al.*, 2016; Luczak-Wozniak *et al.*, 2018). Un autre inconvénient consiste en la nécessité d'une administration continue et au moins deux fois par jour de la substance active, en raison de sa courte durée d'action. Le budésonide possède en effet une demi-vie d'élimination plasmatique relativement courte après inhalation. Les expériences d'inhalation chez l'animal ont cependant montré une rétention du budésonide dans le tissu pulmonaire nettement plus longue que ce à quoi on pourrait s'attendre compte tenu de la seule lipophilie de la substance active, ce qui peut s'expliquer par une estérification intracellulaire rapide et réversible du budésonide (Brattsand and Miller-Larsson, 2003; Brink *et al.*, 2008; Miller-Larsson *et al.*, 2000; Edsbäcker and Brattsand, 2002). Compte tenu de ces problèmes identifiés et de l'estérification *in situ* du budésonide dans les poumons, il nous a semblé intéressant d'envisager l'utilisation directe d'un ester de budésonide comme prodrogue afin de prolonger l'effet, ce qui permettrait également une réduction de la dose et du nombre d'administrations quotidiennes et par conséquent une diminution des effets secondaires.

Dans ce qui suit, nous avons fait le choix très personnel d'aborder les éléments complémentaires à mettre en perspectives de travaux futurs. Ainsi, nous proposons une série d'expériences qui pourrait être envisagée pour une meilleure compréhension des mécanismes impliqués dans la libération de la substance active et son efficacité biologique.

Etudes de libération in vitro

La solubilité d'une substance active dans le liquide pulmonaire est un facteur déterminant pour les études de libération *in vitro*, et il est souhaitable d'effectuer cette évaluation dans un milieu représentatif du liquide pulmonaire (ELF, epithelial lining fluid). Contrairement au liquide intestinal, qui a fait l'objet de nombreuses études, les travaux sur le liquide pulmonaire sont moins abondants dans la littérature. Initialement, des fluides tels que l'eau et des solutions salines physiologiques ont été utilisées, souvent complétées de phospholipides et de substances tensioactives telles que le dodécyl sulfate de sodium (SDS). Des données concernant la composition du liquide de la muqueuse du poumon humain sain à différents niveaux de l'arbre pulmonaire sont maintenant disponibles, permettant le développement de milieux synthétiques présentant une plus grande similitude et biocompatibilité avec les milieux physiologiques (Kumar *et al.*, 2017).

Au cours de nos études, il aurait été intéressant d'obtenir le profil de libération de la substance active à partir des nanoparticules et des microparticules Troyennes. Cela sera plus complexe pour ces dernières du fait de leur faible densité qui rend difficile une dispersion homogène dans un milieu de

libération. Pour ce faire, de nombreux modèles de liquide pulmonaire sont décrits dans la littérature, tels que la solution Gamble (un type de fluide pulmonaire simulé ou une solution imitant les fluides tensioactifs libérés par les cellules alvéolaires de type II, avec ou sans dipalmitoylphosphatidylcholine (DPPC), principal phospholipide du surfactant pulmonaire) ou le fluide artificiel lysosomal (Calas *et al.*, 2017). D'autres modèles synthétiques basés sur la composition du fluide pulmonaire humain ont été développés ces dernières années pour l'obtention de fluides plus pratiques, économiques et avec conditions de stockage et d'utilisation bien définies (Spitler *et al.*, 2015; Kumar *et al.*, 2016; Dean *et al.*, 2017; Hassoun *et al.*, 2018).

Etudes de mucopénétration

Dans les pathologies pulmonaires inflammatoires, on observe souvent une hypersécrétion de mucus (Martin *et al.*, 2014). Le mucus est un milieu extrêmement complexe qui s'oppose à la délivrance des substances actives, formant une barrière stérique avec une charge négative et des domaines hydrophobes, qui limitent la diffusion libre de composants (Boegh and Nielsen, 2015). Il est donc important d'évaluer la capacité d'une formulation à franchir cette barrière. Dans nos travaux, nous proposons l'utilisation de lipides PEGylés à la surface des nanoparticules, afin de minimiser la mucoadhésion et de faciliter la pénétration des particules à travers une sécrétion muqueuse dense, caractéristique des patients atteints de BPCO. Il aurait été intéressant de valider expérimentalement cette approche.

Les méthodes les plus utilisées pour étudier la diffusion de particules vers le mucus incluent le suivi de particules par microscopie (MPT, multiple particle tracking), la chambre de Ussing ou la chambre de diffusion Transwell-Snapwell (Liu *et al.*, 2015). Parmi ces méthodes, le transport des nanoparticules dans le mucus proposé par Suh *et al.* (2005) pourrait être appliquée pour analyser la pénétration de nos formulations à travers le mucus, notamment des nanoparticules PEGylées et mannosylées. Cette méthode enregistre la trajectoire de chaque particule par microscopie de fluorescence. Si la littérature sur la mucopénétration des particules PEGylées est importante, nous n'avons, en revanche, rien trouvé sur l'influence des groupements mannose en bout de chaîne de PEG. Cependant comme le mannose n'est pas chargé, on peut au moins espérer que les particules mannosylées ne soient pas piégées dans le mucus par interactions électrostatiques.

Les systèmes *in vitro* typiques modélisant un organe tel que le poumon peuvent inclure l'utilisation de lignées cellulaires continues établies, de cellules primaires et de tissus (tels que des coupes d'organes). Pour modéliser les voies respiratoires trachéo-bronchiques on peut utiliser des cellules épithéliales bronchiques humaines primaires (HBEC), des lignées cellulaires bronchiques Calu-3, des lignées

cellulaires épithéliales bronchiques dérivées d'un carcinome mucoépidermoïde (NCI-H292), des cellules provenant d'une lignée cellulaire normale épithéliale bronchique humaine qui a été transformée par l'antigène T SV40 (16HBE14σ) et des lignées de cellules épithéliales bronchiques humaines normales transformées en utilisant le virus hybride adénovirus 12 simian virus 40 (BEAS-2B). D'autre part, pour modéliser la région alvéolaire, des lignées cellulaires d'adénocarcinome A549 sont les plus utilisées. Cependant, des études démontrent que les co-cultures cellulaires peuvent être plus efficaces que des cultures séparées pour reproduire un système complexe tel que la BPCO (Adamson *et al.*, 2011; Boegh and Nielsen, 2015).

En perspective de notre travail de thèse, nous pourrions réaliser une étude sur des lignées cellulaires bronchiques Calu-3, qui produisent du mucus lorsqu'elles sont cultivées à l'interface air-liquide. Calu-3 est un mélange de cellules ciliées et sécrétoires qui sont capables de sécréter la mucine (MUC5AC) à une interface air-liquide, où les cils sont plus courts et plus épais que les cellules cultivées dans l'air. A la suite de la culture des cellules Calu-3 sur des inserts de culture cellulaire, une interface air-liquide est mise en œuvre, avec un milieu dans la chambre basolatérale et aucun liquide dans la chambre apicale. Les substances actives ou les nanoparticules sont ajoutées dans la chambre apicale et le milieu basolatéral est collecté au bout de quelques heures pour quantifier la concentration de la substance active ce qui reflète la capacité à diffuser à travers le mucus (Lock *et al.*, 2018). Les cellules Calu-3 peuvent aussi servir à étudier la diffusion de nanoparticules au travers du mucus et leur internalisation cellulaire, en les marquant avec un fluorophore (Mura *et al.*, 2011). Cela permettrait d'évaluer la capacité des nanoparticules PEGylées ou mannosylés à traverser la muqueuse.

Etudes *in vivo* et modèles animaux

Les études de pharmacocinétique et de biodistribution ont été réalisées sur des rats sains par administration intratrachéale des formulations avec un insufflateur Penn-Century® DPI modèle DP-4. L'utilisation de rats sains est une des limites de notre étude.

Il est évident que les études de pharmacocinétique et de biodistribution pourraient être menées sur des modèles animaux d'asthme ou de BPCO, étant donné que les modifications morphologiques des voies respiratoires causées par la maladie ont un impact important sur le dépôt de la substance active, de même que la présence abondante de mucus peut empêcher son passage. Le métabolisme d'absorption et d'élimination est encore souvent altéré dans la pathologie. On pourrait réitérer l'administration de particules Troyennes sur ce type de modèles animaux. Des études d'efficacité pourraient aussi être conduites en faisant varier la dose de budésonide administrée. Nous pensons enfin qu'il serait également intéressant d'évaluer la pharmacocinétique et l'efficacité d'une

formulation de microparticules Troyennes obtenues avec des nanoparticules mannosylées, en comparaison avec les microparticules Troyennes détaillées dans cette thèse. Cela permettrait de confirmer l'intérêt de la mannosylation pour le traitement de ces pathologies.

Alors que les modèles animaux d'asthme sont bien décrits, les modèles de BPCO sont plus complexes. En effet, diverses approches ont été utilisées pour modéliser les caractéristiques histopathologiques de la BPCO. On peut exposer des animaux à la fumée de cigarette (CS, cigarette smoke) ou à des stimuli inflammatoires, comme des infections virales et bactériennes ou des instillation d'enzymes protéolytiques. Il est aussi possible d'utiliser des modèles génétiquement modifiés. En règle générale, ces études ont abordé des aspects spécifiques de la BPCO, tels que l'inflammation, l'emphysème ou la production de mucus, mais n'ont pas permis de modéliser l'intégralité du syndrome de la BPCO (Gaschler *et al.*, 2007).

L'utilisation de substances exogènes pour développer l'emphysème *in vivo* a été largement rapportée en raison de sa similitude avec les facteurs responsables de l'étiologie de la BPCO. À titre d'exemple, nous discuterons de modèles d'exposition aux cigarettes, au dioxyde de soufre, au dioxyde d'azote, au chlorure de cadmium, mais aussi des stimulants oxydants et des particules polluantes.

- **Modèle d'emphysème induit par la fumée de cigarette**

L'exposition à la fumée de cigarette est devenue l'un des modèles les plus utilisés d'emphysème et de BPCO (Vandivier and Ghosh, 2017). Il est principalement choisi pour étudier les mécanismes pathogènes de la maladie et de la susceptibilité au développement et à sa progression (Pérez-Rial *et al.*, 2015). L'exposition des souris à la fumée de cigarette augmente l'inflammation pulmonaire, l'activité des protéases, le stress oxydant et l'apoptose, et dans certaines souches entraîne le développement de petites quantités d'emphysème et de légers degrés de remodelage des voies respiratoires et des poumons. Cependant, les souris exposées à la fumée de cigarette ne développent ni la production excessive de mucus, ni la métaplasie des cellules muqueuses, ni les exacerbations périodiques caractérisant la BPCO chez l'homme, probablement à cause des différences entre les souris et les humains en termes de développement pulmonaire. Malgré ces différences, ce modèle murin est le modèle de BPCO le plus utilisé car relativement facile, les réactifs immunologiques sont disponibles et les coûts sont faibles (Vandivier and Ghosh, 2017).

- **Autres modèles d'emphysème induit par inhalation**

Outre l'exposition à la fumée de cigarette, d'autres modèles d'exposition existent : exposition au dioxyde de souffre (Bell and Davis, 2001; Groneberg and Chung, 2004; Wagner *et al.*, 2006), au dioxyde

d'azote (Gong *et al.*, 2005; Andersen *et al.*, 2011; Geravandi *et al.*, 2015; Lamichhane *et al.*, 2018; Zhang *et al.*, 2018) ou au chlorure de cadmium (Mahadeva and Shapiro, 2002; Hassan *et al.*, 2014; Lindén *et al.*, 2016; Ganguly *et al.*, 2018; Hutchinson, 2018), qui sont soit des gaz retrouvés dans la pollution urbaine soit des composants de la fumée de cigarette.

- **Modèles d'exacerbation**

Les exacerbations sont une caractéristique de la BPCO qui détermine l'évolution clinique du patient. Elles sont associées à une progression plus importante de la maladie, à une baisse qualité de vie et à un risque de mortalité plus élevé (Pérez-Rial *et al.*, 2015). Les modèles animaux d'exacerbation les plus utilisés sont les modèles bactériens et les modèles viraux, mais d'autres facteurs sont cités dans la littérature, tels que les agents protéolytiques (Groneberg and Chung, 2004; Meng *et al.*, 2006; Gaschler *et al.*, 2007; Brass *et al.*, 2008; Wright, Cosio and Churg, 2008; Rittirsch *et al.*, 2008; Stevenson and Birrell, 2011; Vlahos and Bozinovski, 2014; Oliveira *et al.*, 2016; Ghorani *et al.*, 2017; Shu *et al.*, 2017; Lee *et al.*, 2018).

- **Modèles génétiquement modifiés**

Des modèles génétiquement modifiés qui miment la BPCO ont été développés ces dernières années et pourraient être utilisés pour la reconnaissance des fonctions physiologiques de différents gènes ainsi que des mécanismes possibles de la BPCO (Ghorani *et al.*, 2017). Deux approches principales existent : le gain de fonction ou la perte de fonction. Le gain de fonction est obtenu par surexpression de gène chez des souris transgéniques ou par expression d'un gène humain ou d'un variant de ce gène. La perte de fonction est obtenue en ciblant spécifiquement la perte d'expression d'un gène, par mutagenèse directe ou chimique. Ces manipulations géniques peuvent être ciblées dans tout le corps ou dans des tissus ou cellules spécifiques. Une autre possibilité est l'introduction d'un gène humain dans une souris pour entraîner le développement de la BPCO sans exposition environnementale (Chow *et al.*, 2017). Il est également important de noter que certaines espèces de souris C57BL/6 ont naturellement des mutations génétiques qui favorisent le développement de l'emphysème (Dawkins and Stockley, 2001).

- **Modèles combinant les différents aspects de la pathologie**

Plusieurs possibilités de modèles combinés, qui essaient de reproduire différents aspects des réponses inflammatoires dans la BPCO par l'utilisation concomitante de différents inducteurs tels que la fumée

de cigarette, le LPS, l'élastase, les bactéries et les virus ont été décrits (Meng *et al.*, 2006; Gaschler *et al.*, 2007; Stevenson and Birrell, 2011; Ghorani *et al.*, 2017). Les modèles combinés peuvent également surmonter les limitations individuelles de chaque méthode, augmentant ainsi les chances d'un effet inflammatoire plus compatible avec celui rencontré couramment chez les patients atteints de BPCO.

Malgré la forte augmentation du nombre de publications et de nouveaux modèles animaux pour la BPCO mis au point ces dernières années, il n'est toujours pas possible d'affirmer l'existence d'un modèle qui mime tous les symptômes de la maladie. Parmi les modèles présentés, le modèle combiné de développement de la BPCO pourrait être le plus fiable en ce qui concerne les symptômes présentés par les patients. Cependant, le temps de traitement nécessaire pour obtenir toute la symptomatologie souhaitée chez les animaux et les coûts impliqués dans ce développement doivent être pris en compte.

REFERENCES

Adamson, J., Haswell, L. E., Phillips, G., Gaça, M. D. (2011) 'In Vitro Models of Chronic Obstructive Pulmonary Disease (COPD)'*, in Haswell, L. E. (ed.) Bronchitis. Rijeka: IntechOpen,* p. Chapter 3, 41-66. doi: 10.5772/18247.

Andersen, Z., Hvidberg, M., Jensen, S., Ketzel, M., Loft, S., Sørensen, M., Tjønneland, A., Overvad, K., Raaschou-Nielsen, O. (2011) 'Chronic Obstructive Pulmonary Disease and Long-Term Exposure to Traffic-Related Air Pollution: A Cohort Study'*, American journal of respiratory and critical care medicine.* doi: 10.1164/rccm.201006-0937OC.

Bell, M. L. and Davis, D. L. (2001) *'Reassessment of the lethal London fog of 1952: novel indicators of* acute and chronic consequences of acute exposure to air pollution', *Environmental health perspectives*, 109 Suppl(Suppl 3), pp. 389–394. doi: 10.1289/ehp.01109s3389.

Boegh, M. and Nielsen, H. M. (2015) 'Mucus as a Barrier to Drug Delivery – Understanding and Mimicking the Barrier Properties', *Basic & Clinical Pharmacology & Toxicology*. John Wiley & Sons, Ltd (10.1111), 116(3), pp. 179–186. doi: 10.1111/bcpt.12342.

Brass, D. M., Hollingsworth, J. W., Cinque, M., Li, Z., Potts, E., Toloza, E., Foster, W. M., Schwartz, D. A. (2008) 'Chronic LPS inhalation causes emphysema-like changes in mouse lung that are associated with apoptosis', *American journal of respiratory cell and molecular biology*. 2008/06/06. American Thoracic Society, 39(5), pp. 584–590. doi: 10.1165/rcmb.2007-0448OC.

Brattsand, R. and Miller-Larsson, A. (2003) 'The Role of Intracellular Esterification in Budesonide Once-Daily Dosing and Airway Selectivity', *Clinical Therapeutics*, 25(SUPPL. C), pp. 28–41. doi: 10.1016/S0149-2918(03)80304-1.

Brink, K. I. M. Van den, Boorsma, M., Staal-Van Den Brekel, A. J., Edsbäcker, S., Wouters, E. F., Thorsson, L. (2008) 'Evidence of the in vivo esterification of budesonide in human airways', *British Journal of Clinical Pharmacology*, 66(1), pp. 27–35. doi: 10.1111/j.1365-2125.2008.03164.x.

Calas, A. Uzu, G., Martins, J. M. F., Voisin, D., Spadini, L., Lacroix, T., Jaffrezo, J-L. (2017) 'The importance of simulated lung fluid (SLF) extractions for a more relevant evaluation of the oxidative potential of particulate matter', *Scientific Reports*, 7(1), p. 11617. doi: 10.1038/s41598-017-11979-3.

Cho, Y. J. and Sin, D. D. (2018) 'Inhaled Corticosteroids and Fractures in COPD: Can We Finally Put This to Bed?', *Chest*. *American College of Chest Physicians*, 153(2), pp. 293–294. doi: 10.1016/j.chest.2017.08.027.

Chorão, P., Pereira, A. M., Fonseca, J. A. (2014) 'Inhaler devices in asthma and COPD – An assessment of inhaler technique and patient preferences', *Respiratory Medicine*. W.B. Saunders, 108(7), pp. 968–975. doi: 10.1016/J.RMED.2014.04.019.

Chow, L., Smith, D., Chokshi, K., Ezegbunam, W., Charoenpong, P., Foley, K., Cargill, A., Geraghty, P. (2017) 'Animal Models of Chronic Obstructive Pulmonary Disease', in Smith, D. (ed.) *COPD - An Update in Pathogenesis and Clinical Management*. Rijeka: IntechOpen, p. Ch. 1. doi: 10.5772/intechopen.70262.

Dawkins, P. A. and Stockley, R. A. (2001) 'Animal models of chronic obstructive pulmonary disease', *Thorax*, 56(12), pp. 972 LP – 977. doi: 10.1136/thorax.56.12.972.

Dean, J., I. Elom, N., Entwistle, J. (2017) 'Use of simulated epithelial lung fluid in assessing the human health risk of Pb in urban street dust', *Science of The Total Environment*, 579(February), pp. 387–395. doi: 10.1016/j.scitotenv.2016.11.085.

Edsbäcker, S. and Brattsand, R. (2002) 'Budesonide fatty-acid esterification: a novel mechanism prolonging binding to airway tissue. Review of available data', *Annals of Allergy, Asthma & Immunology*. Elsevier, 88(6), pp. 609–616. doi: 10.1016/S1081-1206(10)61893-5.

Finney, L., Berry, M., Singanayagam, A., Elkin, S. L., Johnston, S. L., Mallia, P. (2014) 'Inhaled corticosteroids and pneumonia in chronic obstructive pulmonary disease', *The Lancet Respiratory Medicine*. Elsevier, 2(11), pp. 919–932. doi: 10.1016/S2213-2600(14)70169-9.

Ganguly, K., Levänen, B., Palmberg, L., Åkesson, A., Lindén, A. (2018) 'Cadmium in tobacco smokers: a neglected link to lung disease?', *European Respiratory Review*, 27(147), p. 170122. doi: 10.1183/16000617.0122-2017.

Geravandi, S., Goudarzi, G., Javad Mohammadi, M., Sadat Taghavirad, S., Salmanzadeh, S. (2015) 'Sulfur and Nitrogen Dioxide Exposure and the Incidence of Health Endpoints in Ahvaz, Iran', *Health Scope,* 4(2) 6 p. doi: 10.17795/jhealthscope-24318.

Ghorani, V., Boskabady, M. H., Khazdair, M., Kianmeher, M. (2017) 'Experimental animal models for COPD: a methodological review', *Tobacco Induced Diseases*, 15, pp. 1-13. doi: 10.1186/s12971-017-0130-2.

Gong, H. J., Linn, W. S., Clark, K. W., Anderson, K. R., Geller, M. D., Sioutas, C. (2005) 'Respiratory Responses to Exposures With Fine Particulates and Nitrogen Dioxide in the Elderly With and Without COPD', *Inhalation Toxicology*. Taylor & Francis, 17(3), pp. 123–132. doi: 10.1080/08958370590904481.

Gonzalez, A. V., Coulombe, J., Ernst, P., Suissa, S. (2018) 'Long-term Use of Inhaled Corticosteroids in COPD and the Risk of Fracture', *Chest*. Elsevier, 153(2), pp. 321–328. doi: 10.1016/J.CHEST.2017.07.002.

Groneberg, D. A. and Chung, K. F. (2004) 'Models of chronic obstructive pulmonary disease', *Respiratory Research*, 5(1), p. 18. doi: 10.1186/1465-9921-5-18.

Hassan, F., Xu, X., Nuovo, G., Killilea, D. W., Tyrrell, J., Da Tan, C., Tarran, R., Diaz, P., Jee, J., Knoell, D., Boyaka, P. N., Cormet-Boyaka, E. (2014) 'Accumulation of metals in GOLD4 COPD lungs is associated with decreased CFTR levels', *Respiratory research*. BioMed Central, 15(1), p. 69. doi: 10.1186/1465-9921-15-69.

Hassoun, M., Royall, P. G., Parry, M., Harvey, R. D., Forbes, B. (2018) 'Design and development of a biorelevant simulated human lung fluid', *Journal of Drug Delivery Science and Technology*, 47, pp. 485–491. doi: 10.1016/j.jddst.2018.08.006.

Heffler, E., Madeira, L. N. G., Ferrando, M., Puggioni, F., Racca, F., Malvezzi, L., Passalacqua, G., Canonica, G. W. (2018) 'Inhaled Corticosteroids Safety and Adverse Effects in Patients with Asthma', *The Journal of Allergy and Clinical Immunology: In Practice*. Elsevier, 6(3), pp. 776–781. doi: 10.1016/J.JAIP.2018.01.025.

Hutchinson, D. (2018) 'Cadmium lung adsorption, citrullination and an enhanced risk of COPD', *European Respiratory Review*, 27(149), p. 180054. doi: 10.1183/16000617.0054-2018.

Gaschler, G. J., Bauer, C. M. T., Zavitz, C. C. J., Stämpfli, M. R. (2007) 'Animal Models of Chronic Obstructive Pulmonary Disease Exacerbations', *Contributions to microbiology,* 14, pp. 126-141. doi: 10.1159/0000107059.

Kiri, V. A., Fabbri, L. M., Davis, K. J., Soriano, J. B. (2009) 'Inhaled corticosteroids and risk of lung cancer among COPD patients who quit smoking', *Respiratory Medicine*. W.B. Saunders, 103(1), pp. 85–90. doi: 10.1016/J.RMED.2008.07.024.

Kumar, A., Bicer, E., Morgan, A., Pfeffer, P. E., Monopoli, M., Dawson, K., Eriksson, J., Edwards, K., Lynham, S., Arno, M., Behndig, A., Blomberg, A., Somers, G., Hassall, D., Dailey, L., Forbes, B., Mudway, I. (2016) 'Enrichment of immunoregulatory proteins in the biomolecular corona of nanoparticles within human respiratory tract lining fluid', *Nanomedicine: Nanotechnology, Biology and Medicine*, 12(4), pp. 1033–1043. doi: 10.1016/j.nano.2015.12.369.

Kumar, A., Terakosolphan, W., Hassoun, M., Vandera, K-K., Novicky, A., Harvey, R., Royall, P. G., Bicer, E. M., Eriksson, J., Edwards, K., Valkenborg, D., Nelissen, I., Hassall, D., Mudway, I. S., Forbes, B. (2017) 'A Biocompatible Synthetic Lung Fluid Based on Human Respiratory Tract Lining Fluid Composition', *Pharmaceutical research*. 2017/05/30. Springer US, 34(12), pp. 2454–2465. doi: 10.1007/s11095-017-2169-4.

Lamichhane, D. K., Han Leem, J., Kim, H. (2018) 'Associations between Ambient Particulate Matter and Nitrogen Dioxide and Chronic Obstructive Pulmonary Diseases in Adults and Effect Modification by Demographic and Lifestyle Factors', *International Journal of Environmental Research and Public Health*, 15, 363. doi: 10.3390/ijerph15020363.

Lavorini, F., Mannini, C., Chellini, E. (2015) 'Challenges of Inhaler Use in the Treatment of Asthma and Chronic Obstructive Pulmonary Disease', *European Medical Journal Respiratory*, 3(2), pp. 98–105. Available at: https://pdfs.semanticscholar.org/453f/3e25be1b1f06bfb7d162c8ad16a8b53aee09.pdf.

Lee, S.-Y., Cho, J.-H., Cho, S. S., Bae, C.-S., Kim, G.-Y., Park, D.-H. (2018) 'Establishment of a chronic obstructive pulmonary disease mouse model based on the elapsed time after LPS intranasal instillation', *Laboratory animal research*. 2018/03/22. Korean Association for Laboratory Animal Science, 34(1), pp. 1–10. doi: 10.5625/lar.2018.34.1.1.

Lindén, A., Sundblad, B.-M., Ji, J., Levänen, B., Midander, K., Julander, A., Larsson, K., Palmberg, L. (2016) 'Extracellular cadmium in the bronchoalveolar space of long-term tobacco smokers with and without COPD and its association with inflammation', *International Journal of Chronic Obstructive Pulmonary Disease,* 11, p. 1005. doi: 10.2147/COPD.S105234.

Liu, M., Zhang, J., Shan, W., Huang, Y. (2015) 'Developments of mucus penetrating nanoparticles', *Asian Journal of Pharmaceutical Sciences*. Elsevier Ltd, 10(4), pp. 275–282. doi: 10.1016/j.ajps.2014.12.007.

Lock, J. Y., Carlson, T. L., Carrier, R. L. (2018) 'Mucus models to evaluate the diffusion of drugs and particles', *Advanced Drug Delivery Reviews*. Elsevier, 124, pp. 34–49. doi: 10.1016/J.ADDR.2017.11.001.

Luczak-Wozniak, K., Dabrowska, M., Domagala, I., Miszczuk, M., Lubanski, W., Leszczynski, A., Krenke, R. (2018) 'Mishandling of pMDI and DPI inhalers in asthma and COPD – Repetitive and non-repetitive errors', *Pulmonary Pharmacology and Therapeutics*. Elsevier Ltd, 51, pp. 65–72. doi: 10.1016/j.pupt.2018.06.002.

Mahadeva, R. and Shapiro, S. D. (2002) 'Chronic obstructive pulmonary disease • 3: Experimental animal models of pulmonary emphysema', *Thorax*, 57(10), pp. 908 LP – 914. doi:

10.1136/thorax.57.10.908.

Martin, C., Frija-Masson, J., Burgel, P.-R. (2014) 'Targeting Mucus Hypersecretion: New Therapeutic Opportunities for COPD?', *Drugs*, 74(10), pp. 1073–1089. doi: 10.1007/s40265-014-0235-3.

Meng, Q. R., Gideon, K. M., Harbo, S. J., Renne, R. A., Lee, M. K., Brys, A. M., Jones, R. (2006) 'Gene Expression Profiling in Lung Tissues from Mice Exposed to Cigarette Smoke, Lipopolysaccharide, or Smoke Plus Lipopolysaccharide by Inhalation', *Inhalation Toxicology*. Taylor & Francis, 18(8), pp. 555–568. doi: 10.1080/08958370600686226.

Miller-Larsson, A., Jansson, P., Runstrom, A., Brattsand, R. (2000) 'Prolonged airway activity and improved selectivity of budesonide possibly due to esterification', *American Journal of Respiratory and Critical Care Medicine*, 162(4 I), pp. 1455–1461. doi: 10.1164/ajrccm.162.4.9806112.

Mura, S., Hillaireau, H., Nicolas, J., Kerdine-Römer, S., Le Droumaguet, B., Deloménie, C., Nicolas, V., Pallardy, M., Tsapis, N., Fattal, E. (2011) 'Biodegradable nanoparticles meet the bronchial airway barrier: How surface properties affect their interaction with mucus and epithelial cells', *Biomacromolecules*, 12, pp. 4136–4143. doi: 10.1021/bm201226x.

Murphy, K. R. (2010) 'Adherence to inhaled corticosteroids: Comparison of available therapies', *Pulmonary Pharmacology and Therapeutics*. Elsevier Ltd, 23(5), pp. 384–388. doi: 10.1016/j.pupt.2010.06.001.

Oliveira, M. V. de, Silva, P. L., Rocco, P. R. M. (2016) 'Animal Models of Chronic Obstructive Pulmonary Disease Exacerbations: A Review of the Current Status', *Journal of Biomedical Sciencies*, 5(1), pp. 1–14. doi: 10.4172/2254-609X.100022.

Pérez-Rial, S., Girón-Martínez, Á., Peces-Barba, G. (2015) 'Animal Models of Chronic Obstructive Pulmonary Disease', *Archivos de Bronconeumología (English Edition)*, 51(3), pp. 121–127. doi: 10.1016/j.arbr.2014.12.023.

Price, D., Bosnic-Anticevich, S., Briggs, A., Chrystyn, H., Rand, C., Scheuch, G., Bousquet, J. (2013) 'Inhaler competence in asthma: Common errors, barriers to use and recommended solutions', *Respiratory Medicine*. W.B. Saunders, 107(1), pp. 37–46. doi: 10.1016/J.RMED.2012.09.017.

Rittirsch, D., Flierl, M. A., Day, D. E., Nadeau, B., McGuire, S. R., Hoesel, L. M., Ipaktchi, K., Zetoune, F. S., Vidya Sarma, J., Leng, L., Huber-Lang, M. S., Neff, T. A., Bucala, R., Ward, P. A. (2008) 'Acute Lung Injury Induced by Lipopolysaccharide Is Independent of Complement Activation', *Journal of immunology (Baltimore, Md. : 1950)*, 180, pp. 7664–7672. doi: 10.4049/jimmunol.180.11.7664.

Sanchis, J., Gich, I., Pedersen, S. (2016) 'Systematic Review of Errors in Inhaler Use: Has Patient Technique Improved Over Time?', *Chest*. Elsevier, 150(2), pp. 394–406. doi: 10.1016/J.CHEST.2016.03.041.

Shu, J., Li, D., Ouyang, H., Huang, J., Long, Z., Liang, Z., Chen, Y., Chen, Y., Zheng, Q., Kuang, M., Tang, H., Wang, J., Lu, W. (2017) 'Comparison and evaluation of two different methods to establish the cigarette smoke exposure mouse model of COPD', *Scientific Reports*, 7(1), p. 15454. doi: 10.1038/s41598-017-15685-y.

Sneeboer, M. M. S., Hutten, B. A., Majoor, C. J., Bel, E. H.D., Kamphuisen, P. W. (2016) 'Oral and inhaled corticosteroid use and risk of recurrent pulmonary embolism', *Thrombosis Research*. Pergamon, 140, pp. 46–50. doi: 10.1016/J.THROMRES.2016.02.010.

Spantideas, N., Drosou, E., Bougea, A., Assimakopoulos, D. (2017) 'Inhaled Corticosteroids and Voice Problems. What Is New?', *Journal of Voice*. Mosby, 31(3), pp. 384.e1-384.e7. doi: 10.1016/J.JVOICE.2016.09.002.

Spitler, G., Spitz, H., Glasser, S., Kathryn Hoffman, M., Bowen, J. (2015) 'In Vitro Dissolution of Uranium-contaminated Soil in Simulated Lung Fluid Containing a Pulmonary Surfactant', *Health physics*, 108, pp. 336–343. doi: 10.1097/HP.0000000000000211.

Stevenson, C. S. and Birrell, M. A. (2011) 'Moving towards a new generation of animal models for asthma and COPD with improved clinical relevance', *Pharmacology & Therapeutics*, 130(2), pp. 93–105. doi: 10.1016/j.pharmthera.2010.10.008.

Suh, J., Dawson, M., Hanes, J. (2005) 'Real-time multiple-particle tracking: applications to drug and gene delivery', *Advanced Drug Delivery Reviews*. Elsevier, 57(1), pp. 63–78. doi: 10.1016/J.ADDR.2004.06.001.

Vandivier, R. W. and Ghosh, M. (2017) 'Understanding the Relevance of the Mouse Cigarette Smoke Model of COPD: Peering through the Smoke', *American Journal of Respiratory Cell and Molecular Biology*. American Thoracic Society - AJRCMB, 57(1), pp. 3–4. doi: 10.1165/rcmb.2017-0110ED.

Vlahos, R. and Bozinovski, S. (2014) 'Recent advances in pre-clinical mouse models of COPD', *Clinical science (London, England : 1979)*. 2013/10/14. Portland Press Ltd., 126(4), pp. 253–265. doi: 10.1042/CS20130182.

Wagner, U., Staats, P., Fehmann, H.-C., Fischer, A., Welte, T., Groneberg, D. (2006) 'Analysis of airway secretions in a model of sulfur dioxide induced chronic obstructive pulmonary disease (COPD)', *Journal of occupational medicine and toxicology (London, England)*, 1, p. 12. doi: 10.1186/1745-6673-1-12.

Wright, J. L., Cosio, M., Churg, A. (2008) 'Animal models of chronic obstructive pulmonary disease', *American journal of physiology. Lung cellular and molecular physiology*. 2008/05/02. American Physiological Society, 295(1), pp. L1–L15. doi: 10.1152/ajplung.90200.2008.

Zhang, Z., Wang, J., Lu, W. (2018) 'Exposure to nitrogen dioxide and chronic obstructive pulmonary disease (COPD) in adults: a systematic review and meta-analysis', *Environmental Science and Pollution Research*, 25, pp. 1–13. doi: 10.1007/s11356-018-1629-7.

université PARIS-SACLAY | ÉCOLE DOCTORALE Innovation thérapeutique : du fondamental à l'appliqué

Titre : Stratégies de ciblage des macrophages alvéolaires pour l'administration de glucocorticoïdes.

Mots clés : Nanoparticules, microparticules Troyennes, macrophages, prodrogue, ciblage, glucocorticoïdes.

Résumé : Au cours de ce travail de thèse nous avons proposé une stratégie de ciblage des macrophages alvéolaires afin d'y vectoriser des glucocorticoïdes. Une prodrogue de budésonide, le palmitate de budésonide (BP) a été synthétisée dans le but de prolonger sa demi-vie dans les poumons après inhalation. Des nanoparticules PEGylées de BP ont été développées et étudiées pour obtenir une formulation stable avec des caractéristiques physico-chimiques appropriées et un taux de charge élevé pour pénétrer dans les macrophages alvéolaires, cellules centrales dans l'inflammation pulmonaire. Des tests *in vitro* sur les macrophages RAW 264.7 ont confirmé l'activité anti-inflammatoire et l'absence de cytotoxicité des nanoparticules. Celles-ci ont ensuite été séchée au sein de microparticules Troyennes obtenues par atomisation-séchage afin de faciliter leur administration pulmonaire sous forme de poudres et libérer les nanoparticules à proximité des alvéoles pulmonaires. Les microparticules sphériques creuses contenant de 0 % à 20 % de nanoparticules de BP présentent des diamètres aérodynamiques et une fraction de particules fines appropriés pour la délivrance pulmonaire. Les études pharmacocinétiques *in vivo* montrent des concentrations élevées et prolongées de budésonide dans les poumons, avec de faibles concentrations plasmatiques. Dans la deuxième partie de cette thèse, une autre stratégie de ciblage des macrophages a été évaluée par la décoration de la surface des nanoparticules avec du mannose. Après la synthèse d'un lipide mannosylé, des nanoparticules ont été formulées et caractérisées, démontrant un taux de charge élevé et une bonne stabilité jusqu'à 30 jours. Des tests *in vitro* sur les macrophages RAW 264.7 ont montré que la présence du mannose à la surface augmente l'internalisation des nanoparticules d'un facteur 2 après 48 h d'incubation, par rapport aux nanoparticules PEGylées.

Title : Targeting strategies for glucocorticoid administration to alveolar macrophages.

Keywords : Nanoparticles, Trojan microparticles, macrophages, prodrug, targeting, glucocorticoids.

Abstract : This work focuses on innovative strategies to target glucocorticoids to alveolar macrophages. We have synthesized a budesonide prodrug, budesonide palmitate (BP), increasing its lipophilicity to extend drug half-life in the lungs. BP PEGylated nanoparticles were developed and studied to obtain a stable formulation with suitable physicochemical characteristics and high drug loading to enter alveolar macrophages, key players in lung inflammation. *In vitro* tests on RAW 264.7 macrophages confirmed the anti-inflammatory activity and the absence of cytotoxicity of nanoparticles. Nanoparticles were then encapsulated into Trojan microparticles obtained by spray-drying to facilitate their delivery to the lung as dry powders and release nanoparticles directly to the pulmonary alveoli. Spherical hollow microparticles containing from 0 % to 20 % of BP nanoparticles presented suitable aerodynamic diameters and fine particle fraction for lung delivery. *In vivo* pharmacokinetic studies demonstrated high and extended budesonide concentrations in the lungs, with low plasma concentrations. In the second part of this thesis, another macrophage targeting strategy was assessed by decoration of nanoparticle surface with mannose. After synthesis of a mannosylated lipid, nanoparticles were formulated and characterized, demonstrating high drug loading and stability up to 30 days. *In vitro* tests on RAW 264.7 macrophages showed that the presence of mannose on the surface increases nanoparticles internalization 2 fold after 48 h incubation, as compared with PEGylated nanoparticles.

Université Paris-Saclay
Espace Technologique / Immeuble Discovery
Route de l'Orme aux Merisiers RD 128 / 91190 Saint-Aubin, France